Ledgewood

Geologic Traverse Across the Precambrian Rocks of the New Jersey Highlands

Field Guide and Proceedings

Edited by
John H. Puffer
Department of Geology
Rutgers University
Newark, New Jersey 07101

Tenth Annual Meeting of the
Geological Association of New Jersey

October 29 - 30, 1993

Days Inn
Ledgewood, New Jersey
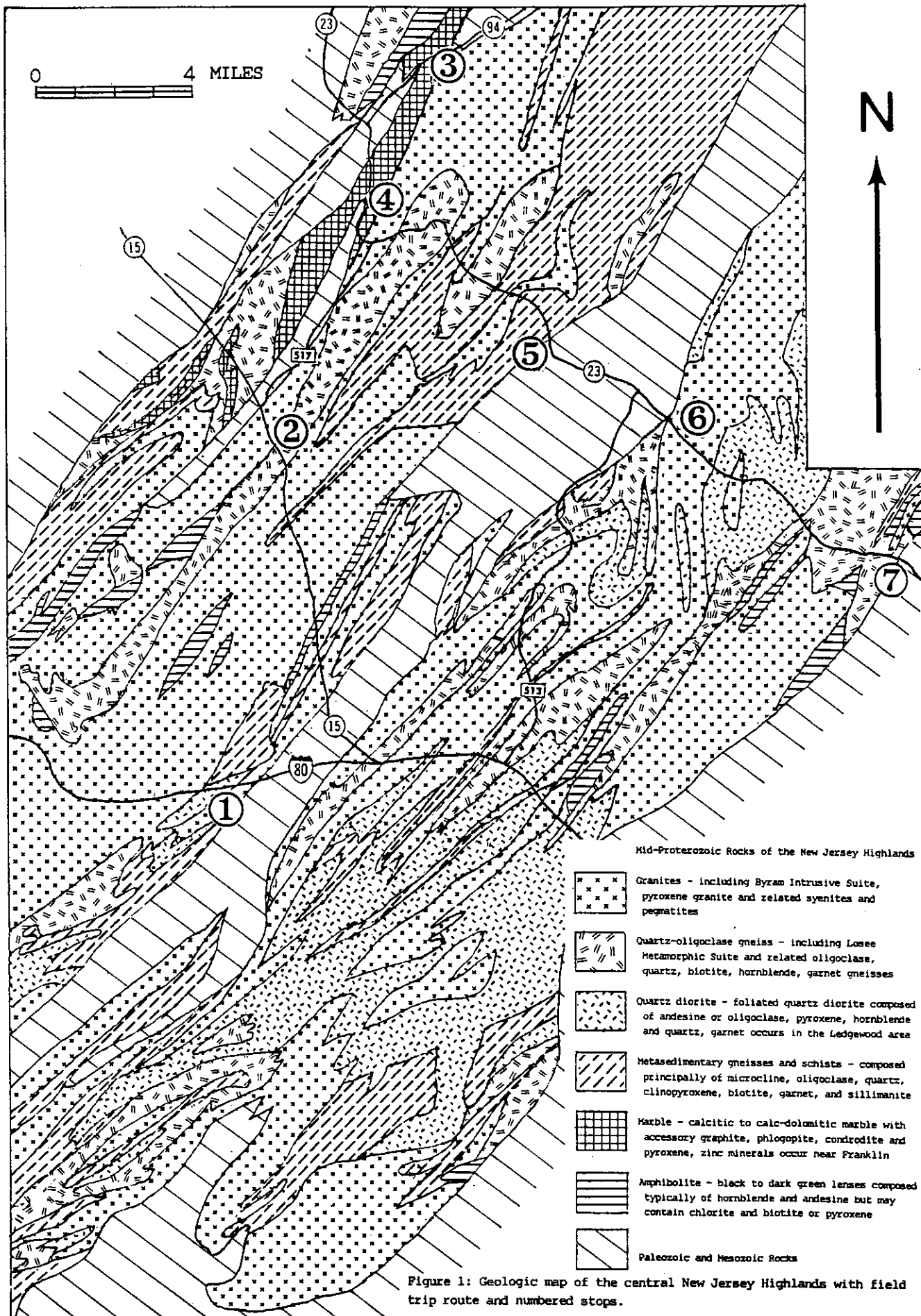
TABLE OF CONTENTS

CHAPTER 1

FIELD GUIDE TO A GEOLOGIC TRAVERSE ACROSS THE PRECAMBRIAN OF THE NEW JERSEY HIGHLANDS

John H. Puffer, Alexander E. Gates, and Ralph E. Costa,
Geology Department, Rutgers Univ. Newark, NJ 07102;
Richard A. Volkert, New Jersey Geological Survey, CN-427,
Trenton, New Jersey 08625; and Thomas D. Gillespie Langan
Engineering Environmental Services, Inc. Doylestown, PA 18901.

INTRODUCTION

As soon as the anxiously awaited new geologic map of New
Jersey is published our understanding of the Precambrian rocks
of New Jersey is expected to undergo a major enhancement.
Until then we must rely on the status of existing quadrangle
map coverage as our geologic base. The ongoing research
currently being conducted by the authors of this guidebook
also draws heavily on classic coverage of the Precambrian of
New Jersey by Bayley (1910, 1941), Baker and Buddington
(1970), Buddington and Leonard (1962), Collins (1969), Sims
(1958), Dallmeyer (1974), Hague and others (1956), Hotz
(1953), and Young (1971, 1978) and on more recent work by
Ratcliffe (1980), Drake (1984), Hull and others (1986),
Volkert and Drake (1986), and Puffer and Volkert (1991).
Ongoing active research in the New Jersey Highlands by the
United States Geological Survey personnel, particularly Drake,
and by the New Jersey Geological Survey, particularly Volkert,
is also acknowledged.

Just as was the case with most of the previously pub-
lished work on the Precambrian of New Jersey, this field guide
will also focus on iron mineralization, the petrology of some
of the rock units, and the structural development of the New
Jersey Highlands. Iron mineralization will be described at
STOP 1 where John Puffer will present some new ideas based
largely on chemical analyses of several magnetite concentra-
tions; also see Chapter 3 of this guide book. Some new
interpretations of the petrology of Precambrian amphibolites
will be proposed by Puffer at STOP 2 (also see Chapter 4).
Some radical new ideas about the origin of a marble and gneiss
breccia will be presented by Thomas Gillespie at STOP 3
(Chapter 5). Then the geochemistry and petrogenesis of some
of the Precambrian granitic suites will be discussed by
Richard Volkert at STOP 6 (also see Chapter 2). Structural

0   4 MILES

N

Mid-Proterozoic Rocks of the New Jersey Highlands

Granites – including Byram Intrusive Suite, pyroxene granite and related syenites and pegmatites

Quartz-oligoclase gneiss – including Losee Metamorphic Suite and related oligoclase, quartz, biotite, hornblende, garnet gneisses

Quartz diorite – foliated quartz diorite composed of andesine or oligoclase, pyroxene, hornblende and quartz, garnet occurs in the Ledgewood area

Metasedimentary gneisses and schists – composed principally of microcline, oligoclase, quartz, clinopyroxene, biotite, garnet, and sillimanite

Marble – calcitic to calc-dolomitic marble with accessory graphite, phlogopite, condrodite and pyroxene, zinc minerals occur near Franklin

Amphibolite – black to dark green lenses composed typically of hornblende and andesine but may contain chlorite and biotite or pyroxene

Paleozoic and Mesozoic Rocks

Figure 1: Geologic map of the central New Jersey Highlands with field trip route and numbered stops.

and tectonic aspects of the major fault zones in the New Jersey Highlands will be discussed at STOPS 4, 5 and 7 where Alex Gates, and Ralph Costa and will present some new data and some new interpretations (also see Chapters 6 and 7).

FIELD TRIP ROAD LOG WITH MILEAGE FROM THE DAYS INN, LEDGEWOOD, NEW JERSEY.

0.0 Leave Days Inn parking lot (8:00 AM) turn left onto Route 46 East.

0.2 Bear to the right and continue onto Rt. 46 E.

0.7 Turn right onto Main Street.

1.0 Turn right onto Emmans Road.

1.1 Turn into Morris Canal Park.

STOP 1: HIGH-LEDGE IRON MINE

As we walk through the park gate, Ledgewood pond is to our left with a section of the Morris Canal located in front of us. A brief description of the historic significance of the canal is posted on the park bulletin board located along the park trail and a review of the canal, particularly its use by the iron mining industry is found on Chapter 8 of this guide book by Ralph Costa. We will proceed past the bulletin board and turn left (west) onto a nature trail that leads to the abandoned High-ledge Iron Mine (Figure 2) located about 1/3 mile from the trail-head.

The High-ledge Iron Mine is one of the very few New Jersey iron mines of the approximately 80 examined by Puffer (Chapter 3) that is not either heavily posted and fenced, accessible only by traversing long distances across difficult terrain, comple-tely filled or flooded with no surface expression, or completely buried under commercial develop-ments. It, therefore, offers us an opportunity to examine one of few remaining accessible members of the New Jersey High-lands mining district that included about 300 active mines and prospects during the late 1800s and early 1990s. The under-ground workings of the High-ledge Mine, including two shafts, are fenced off for our protection but the rock exposures near the shafts are representative of the subsurface rock and some high grade ore has been dumped near one of the shafts. A few
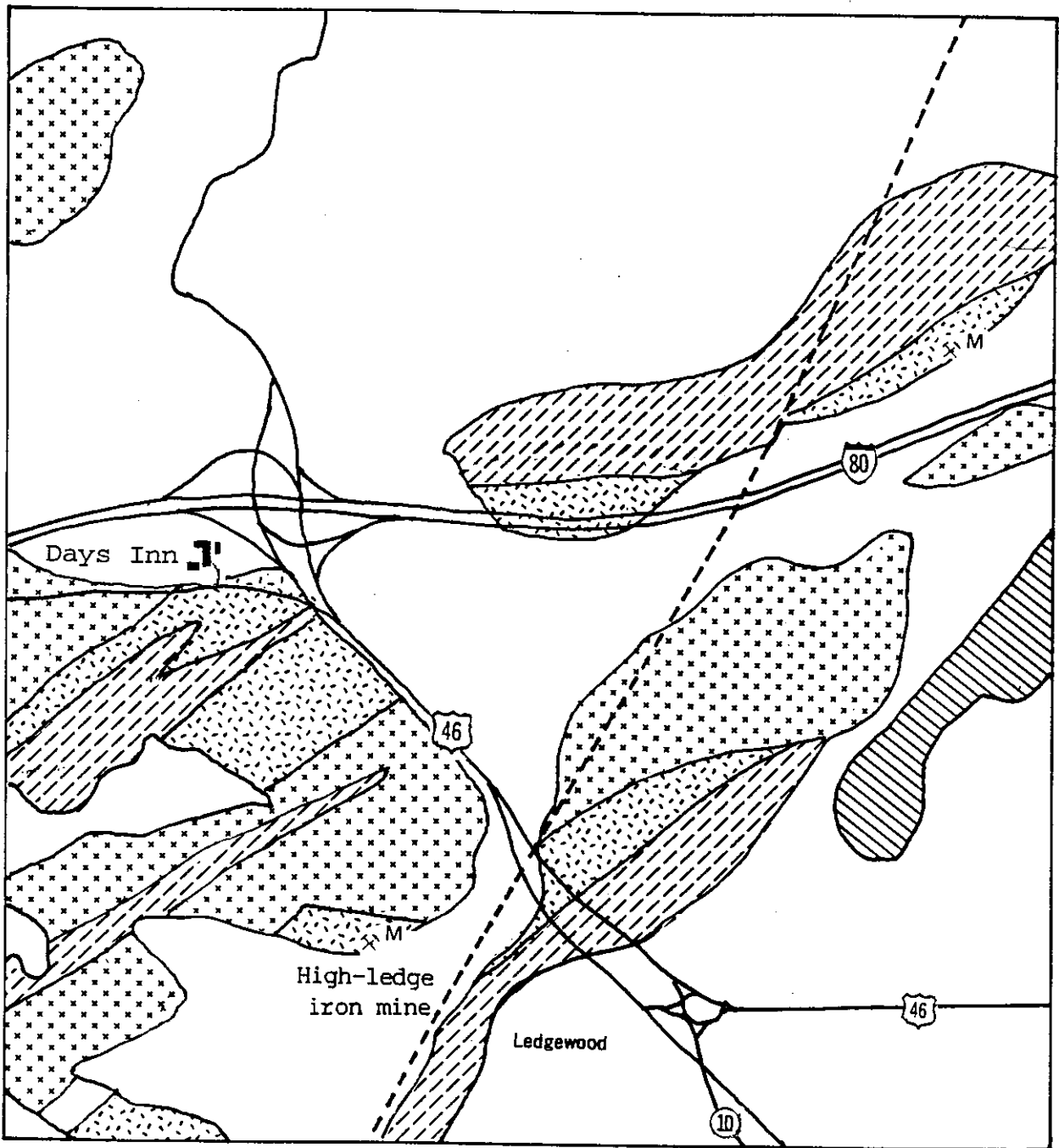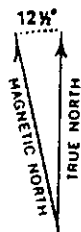
Figure 2: Geologic map of the Ledgewood, New Jersey area with iron mine locations based on a modified portion of the New Jersey Geological Survey Stanhope Quad. by Volkert and others (1989).

4

typical ore samples collected from the underground workings by Puffer will be displayed.

The High-ledge Mine is located on the Stanhope Quad. that has been recently mapped by Volkert and others (1992). The mine is surrounded by quartz diorite which is described by Volkert and others (1992) as a medium grained, massive to moderately foliated, greenish-gray to brownish-gray rock composed of andesine or oligoclase, clinopyroxene, hornblende, hypersthene, and quartz, with garnet occurring in the Ledgewoood area. Amphibolite and biotite amphibolite layers in the quartz diorite are common. The quartz diorite is listed by Volkert and others (1992) together with the Losee Gneiss under the heading "metamorphic rocks of uncertain origin". The quartz diorite is similar in most respects to the Losee Gneiss but differs in that the quartz diorite is darker and contains pyroxene. Quartz diorite is also less likely to be associated with magnetite deposits than Losee Gneiss but does host at least 5 additional magnetite deposits.

The quartz diorite exposed along the path to the mine contains amphibolite layers that are particularly common close to the mine and contain magnetite ore. The richest ore is found in biotite-amphibolite as lenses of magnetite and coexisting hemo-ilmenite. The close association of magnetite with potassium bearing minerals such as biotite is an important characteristic of most New Jersey Highlands type magnetite deposits. Puffer in Chapter 3 of this guidebook suggests that iron, and potassium minerals precipitated from an aqueous phase driven out of hydrous phases in adjacent rocks during prograde metamorphism.

1.1   Turn left onto Emmans Road.

1.2   Turn left onto Main Street.

1.4   Turn right onto Route 10 South.

1.9   At trafic circle follow signs to Route 46 West.

3.0   Bear right onto Interstate 80 East.

7.7   Take exit 34 to Route 15 North.

16.1   Exit Route 15 at Sparta.

16.4   Park in the lot along Route 181 N.

STOP 2: AMPHIBOLITE

The amphibolite exposed at Stop 2 is a typical example of one of three genetic types of amphibolite (Chapter 4) found within the New Jersey Highlands. The amphibolite is the dark green to black rock that contrasts with the light gray to white leucocratic Losee Gneiss host rock exposed at the north and south contacts of the amphibolite layer. Each of the amphibolite types described in Chapter 4 are characterized by large concentrations of both amphibole and plagioclase in roughly equal proportions but with highly variable concentrations of pyroxene, biotite, magnetite, garnet, chlorite, K-spar, and quartz. The amphibolite exposed at Stop 2 is composed of about 40 percent plagioclase, 45 percent hornblende, 5 percent biotite, 10 percent chlorite and minor magnetite, pyrite, and apatite.

This amphibolite layer is interpreted as a meta-basalt largely on the basis of it's chemical composition, particularly trace-element concentrations (Chapter 4). Other genetic types of basalt found within the New Jersey Highlands include meta-sedimentary varieties, mafic refractory residues left from partial fusion processes, and amphibole mineralized shear-zones (see Gates, Chapter 6).

16.4   Turn left onto Route 181 N.

18.4   Bear to the left onto Route 517 North.

24.2   Turn left onto Route 23.

27.9   Turn right onto Route 94.

30.8   Turn left into the parking lot behind the Ski Shop.

STOP 3: MCAFEE BRECCIA DIKES

The McAfee breccia dikes are exposed in a conspicuous outcrop (Figure 3) which rises approximately 20 meters above a sediment filled valley in the village of McAfee. The outcrop is an erosional remnant of the footwall (west) block of the northeast-trending East Fault (N25E-N30E). The fault separates the Franklin Band of Marbles (Grenville) on the west, from Proterozoic gneisses (Drake, 1984) and overlying Cambrian shelf corbonates, to the east.

Figure 3:

**McAfee Breccia Dike - View Shows Angular, White Clasts of
Microcline Gneiss in Brown Dolomite Matrix**

The Breccia Dike Complex occurs within a microcline gneiss host, which is one of a series of strike parallel, lenticular gneiss bodies included within the Franklin Band, as described by Hague and others (1956). The complex consists of an apparently disparate series of clastic dikes which are composed of white to light gray, angular clasts of microcline gneiss, set in a brown dolomite matrix (Figure 3). Dike widths range from 1-2 cm up to 3 meters, and lengths range up to 50 meters. Clasts are nearly all sharpley angular and range up to 0.5 m^2.

Dikes occur either as small, non-clast-bearing veins, typically less than 5 cm thick, or as clast bearing dikes. There is extreem variability in the appearance of the carbon-ate matrix, mostly in the color and style of crystallization. Typically, however, the narrow veins are formed by a dark brown, coarsely crystalline carbonate, with elongate, parallel crystals of calcite of low magnesian dolomite, all of which tend to be aligned with long axes normal to the veins. The large, clast-bearing dikes tend to be composed of a coarse grained variety of dolomite, which is a lighter brown, and displays no particular crystallization characteristics. Apart from this compositional difference there is a distinct distribution of the clasts: clasts are present in the large-scale dikes composed of fine-grained dolomite, but are absent in the coarse-grained veins. Veins tend to occur either as offshoots of the main trunks of the dikes, or at the fringes of the complex. The breccia dikes form a network aligned along two general orientations: between 020-84E and 045-80E, and between 085-70S and 110-80S. These orientations correspond to two joint sets, which are common near the large dikes, but are not pervasive on the outcrop scale, or throughout the region.

The breccia dikes and the host gneisse are crosscut by an isolated dike of lamprophyre at the southwest end of the outcrop. The lamprophyre cross-cuts the breccia dike, but intermingling of the two types along the contacts sugests that the breccia dikes were intruded at approximately the same time.

Intrusion of the breccia dikes was caused by seismic pumping related to activity along the adjacent East Fault, which occurred in at least two separate pulses. During the first pulse, a high-pressure, low viscosity, CO_2-rich fault-plane fluid was injected into an incipient conjugate joint set in the adjacent gneiss body. Both the joints and the fluid pressure along the fault plane were the result of a regional,

8

compressional stress field. The presence of the gneiss along the fault plane created an asperity and locked movement along the section of the fault. The resultant elastic strain in the gneiss, which formed an inclusion within the more ductile Franklin Formation, compressed the rock in a direction subparallel to the fault. The increased strain along the fault zone also resulted in abnormally high fluid pressure in the CO_2-rich fluid.

When brittle failure occurred, the confining pressure on the gneiss was released, and the fluid was injected into the incipient joints, which dilated in the relaxed local strain field. The high pressure fluid intruded the gneiss along the two joint orientations, causing in-situ brecciation by hydrofracturing. This initial hydrofracturing was followed by a second stage intrusion (time interval not known), which was composed of a granular, crystal-plastic, CO2-rich-fluid cataclasite. This later stage of intrusion accompanied dilation of the gneiss in nearly all horizontal directions, which was accommodated by instantaneous relaxation of elastic strain in the gneiss following fault slip. The cataclasite consisted of crushed grains of Franklin Marble with some microcline gneiss. The semi-solid material intruded the gneiss body along the previously hydrofractured planes, entrained the brecciated blocks which were separated by the initial carbonate fluid, and transported them down a pressure gradient, away from the fault plane.

For additional descriptions and interpretations of McAfee breccia dikes see Chapter 5 of this guidebook.

30.8 Turn right onto Route 94.

33.7 Turn left onto Route 23.

36.4 Turn left into the shopping center parking lot.

STOP 4: RUTHERFORD CROSS-FAULT

The cross-fault quarry cut is behind the shopping center with restaurants, grocery store and rest-room facilities. Box lunches will be served.

The Rutherford cross-fault, approximately 1400 meters in length, is a crossover between two normal faults: the Zero Fault and the East Fault (Figure 4). The Zero and East faults justapose down-dropped Cambro-Ordovician Allentown Dolomite with Proterozoic Franklin Marble (Hague and others, 1956).
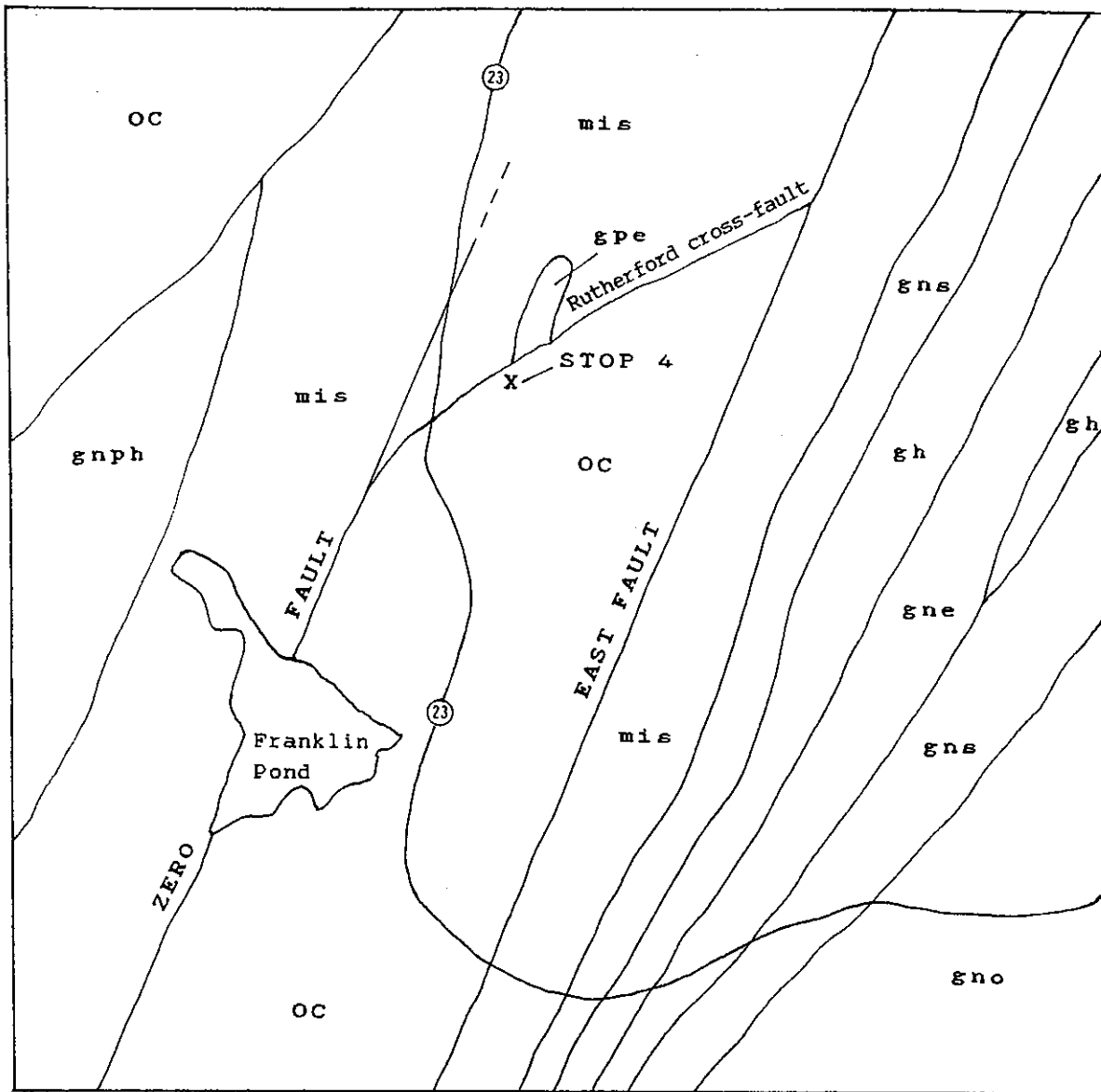
OC Cambrian and Ordovician sandstone and limestone undivided.

gpe Granite pegmatite, pink to white, coarse grained and massive.

gh Byram granite composed of mesoperthite, quartz, and hornblende.

gnph Belts of gneiss that are "heterogeneous and cannot clearly be mapped".

gns Hornblende and pyroxene syenite orthogneiss, green and granoblastic.

gne Epidote-scapolite-quartz gneiss and associated metasedimentary rocks.

gno Losee Gneiss composed of quartz, oligoclase, and biotite.

mis Franklin Marble that varies from impure calcite to almost pure dolmite.

Figure 4: Geologic map of the Franklin, New Jersey area near STOP 4 based on a slightly modified portion of a geologic map by Baker and Buddington (1970).

Kinematic evidence indicate that the cross-fault had a complex reactivation history which involved reverse, strike-slip and normal mavement at different times.

Figure 4 is a slightly modified portion of a USGS geologic map by Baker and Buddington (1970) that includes the Stop 4 site area. The geology of Figure 4 including the faults and the pegmatites also appears on a map by Hague and others (1956) and on the USGS Franklin Furnace Quadrangle mapped by Spencer and others (1908).

The nearly vertical cross-fault forms a mylonite zone within the Franklin Marble on the northwest side of the exposure. On the southeast side of the fault the Allentown Dolomite is exposed. The two formations are separated by a light gray clay gouge zone which is oriented 060, 81°SE. The thickness of the gouge zone is typically 6.5 cm to 7.0 cm but reaches a maxi-mum thickness of approximately 17 cm. The Allentown Dolomite is light to dark blue-gray and massive with minor small black chert nodules and common tension gashes.

The Franklin Marble is white and coarse-grained and varies from impure calcite to almost pure dolomite with minor disseminated graphite, phlogopite, pyroxene, tremolite, chondrodite, pyrrhotite, scapolite, quartz, and secondary euhedral (<1.0 mm) pyrite crystals. Baker and Buddington (1970) describe lenses of granite and pegmatite within the marble and a few lenses of quartz-rich gneiss that they inferred to have been originally sandy beds. The grain size range of undeformed Franklin Marble is 8 to 30 mm (Stephens and others, 1988) but decreases toward the fault. Styolites approximately 4 to 5 m from the gouge zone accompany the decrease in grain size and indicate volume loss. The mylonitic Franklin Marble is enriched in insolubles such as graphite, tremolite, muscovite (phlogopite?) and talc which have been concentrated into dark seams.

The mylonite zone is approximately 3 to 4 m thick with foliation oriented 072,56°SE. Mesoscopic dolomite porphyro-clasts are present within the strong SE-dipping mylonite and indicate top to the northwest reverse faulting. The ductile fabric is cross-cut by moderately - to steeply - dipping younger brittle fault planes and narrow cataclasite zones. The cata-clasite zones are approximately 0.5 to 2 cm thick and contain carbonate clasts which range from about 1 mm to 1.7 cm. The brittle fault planes contain slickensides that indicate a predominant left lateral strike-slip movement. In addition, several slickensides indicate dip-slip movement (normal and reverse) of the fault. Several brittle fault

planes contain two distinct sets of slickensides.

The earliest of the three episodes of movement on the Rutherford cross-fault resulted in the top to the northwest reverse mylonite zone, and may be synchronous with proposed mid- to late-Paleozoic activation of the Zero fault (Stephens and others, 1988). The next two episodes were brittle reactivations that are poorly constrained. The first reactivation resulted in brittle fault planes with slickensides (predominantly left-lateral strike-slip) and narrow cataclasite seams. The second reactivation resulted in the fault gouge zone.

The pegmatites of the Franklin area are described by Baker and Buddington (1970) as "Granite pegmatite - Pink to white, coarse grained and massive. Composed principally of microcline microperthite, quartz, and sodic plagioclase". Pegmatites are found in each of the Precambrian units of the New Jersey Highlands and typically assume the approximate mineralogy of their host rocks. The principal exceptions to this generalization are the pegmatites of the Franklin Marble which as in the case of the pegmatites at Stop 4 are composed principally of sodic plagioclase, graphic granite and quartz with minor scapolite and tremolite. The tremolite component of the pegmatite at Stop 4 is quite fiberous particularly when crushed as is typical of tremolite within Franklin Marble (Germine, 1986).

36.4 Turn left onto Route 23 South.

44.4 Make a U-turn at Oak Ridge Road onto 23 North.

44.8 Park along the road.

STOP 5: RESERVOIR FAULT

This stop illustrates how hydrothermal chemical and resulting mineralogical changes in a fault zone can change deformation style from brittle to ductile. We will observe undeformed protolith (granitic gneiss), hydrothermally mineralized cataclasite (brittle), and mylonite (ductile) of the mineralized zone in two outcrops.

Walk 300 meters south from Route 23 along the shore of the reservoir. The first outcrop shows the western margin of the Reservoir fault zone. The undeformed to slightly deformed rock to the west is mapped as pyroxene gneiss and interpreted as a metasedimentary sequence. The rock consists of diopside-amphibole- and rarely scapolite- bearing granitic to quartz

dioritic gneiss with sparse interlayered amphibolite gneiss and pegmatite veins. The fault rock to the east is cataclasite and breccia with mainly rounded blocks and clasts of granitic- quartz dioritic gneiss. The blocks range from 1 meter to microscopic with size frequency inversely proportional to size. The matrix material is composed of 95% randomly oriented actino-lite with minor epidote, albite, chlorite, and sulphides although finely ground xenocrystic phases from the gneiss are locally abundant. Thin ductile shear zones can be found in this outcrop but the structures observed are primarily the result of brittle deformation coupled with hydrothermal activity that produced the amphibole-sulphide mineralization.

The second outcrop is 200 meters farther south along the shore. Although still against the western margin of the fault zone, this outcrop contains rocks typical of the center of the zone. After formation through hydrothermal alteration, the amphibole-rich matrix underwent ductile deformation forming an S-C mylonite. The ductile deformation produced a strong foliation with significantly reduced grainsize from the randomly oriented fabric of the first outcrop. Kinematic indicators including dragged foliation, S and C bands, rotated porphyroclasts and offset markers show a consistent dextral strike-slip sense.

44.6 Continue north on Route 23.

45.7 Make a U-turn at Canistear Road onto Rt. 23 South.

51.8 Make a U-turn onto Route 23 North.

52.0 Park along the road.

STOP 6: HORNBLENDE GRANITE

At this stop we will see continuous exposures approximately 1,300 feet thick of typical Middle Proterozoic hornblende granite. The rock here is massive-textured, medium-grained, and composed principally of microcline microperthite, quartz, oligoclase, and hornblende. Locally occurring accessories include biotite, allanite, and opaque minerals. The reader is referred to Chapter 2 (this volume) for a more complete discussion of the geochemistry and petrogenesis of hornblende granite and related rocks of the Byram Intrusive Suite.
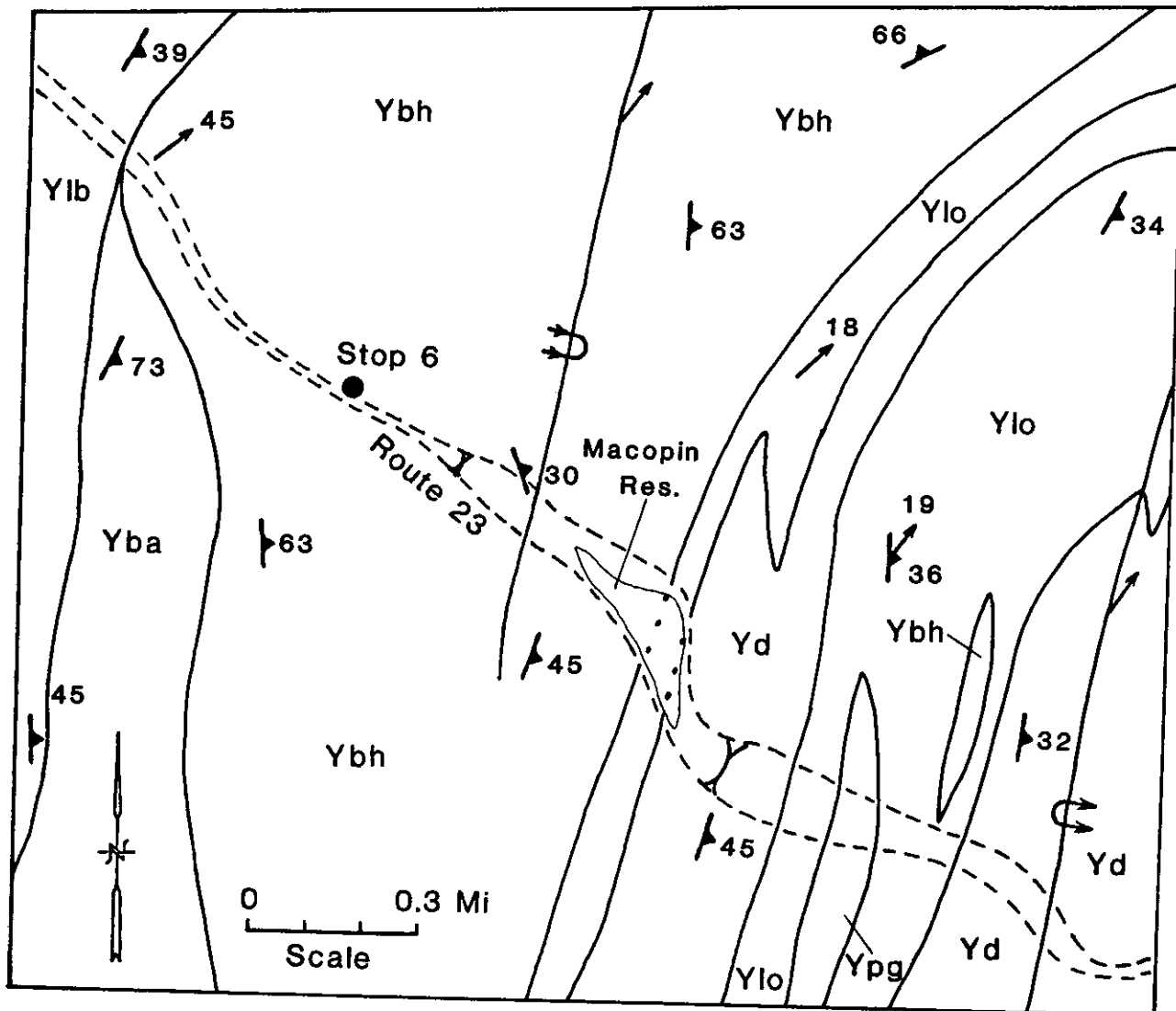
Figure 5:

Geologic map of the Macopin Reservoir area, Newfoundland 7.5-minute quadrangle (Volkert, unpublished data). Map unit and symbol explanations shown on adjacent page.

EXPLANATION OF MAP UNITS AND SYMBOLS

Ybh   Hornblende granite

Yba   Microperthite alaskite

Ypg   Pyroxene granite

Ylb   Biotite-quartz-oligoclase gneiss

Ylo   Quartz-oligoclase gneiss

Yd   Diorite

Middle
Proterozoic

———— ··· Contact - Dotted where concealed

Overturned antiform - Showing trace of axial
surface, direction and dip of limbs, and
direction of plunge

Overturned synform - Showing trace of axial
surface, direction and dip of limbs, and
direction of plunge

66

Strike and dip of crystallization foliation

18◄—

Bearing and plunge of mineral lineation

●   Field trip stop location

Regional geologic mapping (Figure 5) shows that these rocks are on the west limb of a northwest-overturned, northeast-plunging synform. The foliation conforms to the regional trend and here averages N22E 54° SE. A moderately developed mineral lineation visible on foliation surfaces plunges about 30° N75E.

Thin to thick seams of pegmatite, conformable to foliation in the granite, occur throughout the outcrop. They are simple and largely unzoned, although some have a quartz core enclosed by feldspar, which is then bounded by a thin mafic rim. Pegma-tites here are interpreted to be the result of partial melting of the host rock. The mineralogy of the pegmatites is identical that of the granite, and the contact between them is gradational.

Several small undigested enclaves of biotite amphibolite are enclosed within the granite toward the northern end of the exposure. They probably represent fragments ripped free from the country rock during intrusion of the granite.

Four sets of joints are present, as well as variants of these sets. The dominant set trends N34W 68° SW; subordinate sets trend N54E 45° NW, N76E 54° NW, and N22E 49° SE. Many of the northwest-dipping joints are coated with epidote and have smoothly polished tool-and-groove type slickensides. Gently dipping, curvilinear sheeting joints are locally well developed and are oriented appproximately N73W 31° SW.

52.0   Continue north on Route 23.

52.6   Make a U-turn at Echo Lake Road onto Route 23 South.

60.2   Turn onto Interstate 287 (under construction) and park.

STOP 7A: RAMAPO FAULT ZONE, RIVERDALE, NEW JERSEY

This exposure is located at the interchange of I-287 and Route 23 in Riverdale, New Jersey. The entire interchange is a spectacular and nearly continuous exposure with three dimensional views of Proterozoic Y rocks. We will concentrate only on the exposure south of the Route 23 overpass and on the south-bound side of I-287. This exposure is within the large and complex Ramapo Fault Zone (RFZ). The northeast-trending RFZ is the major border fault which juxtaposes the Proterozoic Y gneisses of the New Jersey Highlands with the Mesozoic sedimentary and igneous rocks of the Newark Basin. Width of the RFZ varies from approximately 5 km to 10 km (Ratcliffe,

1980). Abundant moderate to steep southeast-dipping zones up
to 25 m thick are developed within the granitic gneisses of
the RFZ and exhibit mesoscopic S-C mylonite fabric. The RFZ
is intruded by mafic dikes which have been subsequently
sheared during brittle reactivation of the zone. The RFZ
originally developed as a reverse right-lateral strike-slip
fault during the Grenville orogeny (Ratcliffe, 1980) and has a
long and complex kinematic history which included four to five
recognizable episodes of fault movement. Despite the long
history of reactivation of the RFZ there is no strong evidence
of any post-Mesozoic or neotectonic movement. Exposures
found throughout the interchange contain evidence for three
episodes of fault reactivation.

    This exposure is predominantly medium to coarse grained
Losee Gneiss and coarse grained (almost pegmatitic) Protero-
zoic unakite gneiss, which contains epidote, orthoclase ,
quartz and minor amphiboles and oxides. Abundant slickenside
fault planes are commonly coated with secondary fine-grained
chlorite, calcite, tremolite-actinolite, limonite and lesser
amounts of quartz and epidote. Additional secondary mineral-
ization found throughout the interchange and to the northeast
throughout the RFZ include pyrite, fluorite, datolite and,
rarely, molybdenite. Narrow (typically less than 2 m thick)
moderate to steeply southeast-dipping S-C mylonite zones found
throughout the exposure contain a dominant foliation, or C
planes, defined by aligned micas, type B2a and B2b quartz
ribbons, and tails on s-type quartz and feldspar
porphyroclasts. Moderately southeast-dipping S planes are
defined by chlorite ìfishî and the core of s-type quartz and
feldspar porphyroclasts. Within zones of the highest strain,
C' planes developed and dip toward the southeast at an angle
20° - 30° shallower than the C planes. Ductile behavior of
feldspar indicates the temperature of deformation must be in
excess of 450±50° C. The mylonites within the RFZ consis-
tently indicate top to the northwest reverse faulting. These
zones, in addition to the proposed initiation during the
Grenville orogeny , were reactivated under mid- to upper
greenschist facies conditions during the Taconic orogeny
approximately 450 - 460 Ma (Ratcliffe, 1980).

    Several east-striking mafic dikes intrude the New Jersey
Highland gneisses and were subsequently severely sheared and
retrograded. The dikes are unaffected by northwest directed
reverse Taconic ductile shearing. The dark green dikes
consist predominantly of chlorite and minor calcite and
pyrite. The silica content of the dikes has been depleted and

original igneous textures are difficult to recognize. The dikes vary in thickness from less than 1 cm to approximately 2 m. The different episodes of shearing recorded in these dikes are the result of different episodes of reactivation of the RFZ. Although the orientation of these dikes is consistent with Ordovician Cortlandt-Beemerville dikes, the dikes have not been radiometrically dated and their chemistry is enigmatic. These dikes are cut by early brittle north-northeast dipping normal faults. Offset along these faults in on the order of centimeters. Assuming that the normal faults commonly developed parallel to the maximum stress direction, these faults are a record of a response to the Alleghanian approximate west-northwest-trending maximum compression direction. In addition, portions of the mafic dikes have developed south-southwest-dipping S-C mylonite fabrics which are visible on the mesoscopic and microscopic scale. Angle between the C and S plane vary from approximately 10°-30° and indicate ductile top to the north-northeast reverse shearing of the mafic dikes. Because the dikes had been retrograded, their ductility was enhanced. Therefore, although the granitic gneisses of the country rock within the RFZ deformed by brittle processes, the mafic dikes were deformed by ductile processes. The north-northeast reverse shearing of the dikes is a record of the response to the approximate Triassic north-south-trending maximum compression direction. In the mafic dikes subsequent folding of the reverse sheared fabric is visible. The vergence of these folds indicates top to the south-southwest normal faulting and may represent post-Triassic relaxation.

STOP 7B: RAMAPO FAULT ZONE, RIVERDALE, NEW JERSEY.

This exposure is located in the town park at the end of West Parkway in Riverdale, New Jersey. The entire exposure consists of ultramylonites of the Ramapo Fault Zone (RFZ). Glacial striations oriented essentially north-south have polished the surface of the exposure. The alternating black and white/gray bands of foliation dip moderately to the southeast. The black bands are composed of fine grained foliated chlorite, whereas the white/gray bands are quartzo-feldspathic. Both quartz and feldspar deformed in a ductile manner, and are extensively dynamically recrystallized. Small grains of pyrite are present within the foliation. This exposure contains evidence for four episodes of post-Grenvillian reactivation of the RFZ. Evidence for Taconic, Alleghanian and Mesozoic reactivation of the RFZ supports that

which was seen in stop 7A. In addition, because the RFZ is a
major zone of crustal weakness with a long and complex history
of reactivation, it is suspected to have been activated during
Proterozoic Z crustal extension associated with the opening
of the Iapetus ocean. Microstructural analysis of mylonites
and ultramylonites from several areas of the RFZ revealed
textures which support the southeast directed normal faulting
of the RFZ during Proterozoic Z crustal attenuation. Relicts
of the early normal faulting are seen through the pervasive
Taconic fabric. The Proterozoic Z fabric has been sheared in
approximtely a parallel but opposite direction during the
Taconic. The resulting microstructures from this exposure
include mylonite layers originally developed during the normal
faulting which were subsequently folded during the oppositely
directed Taconic orogeny. Also, tails of quartz
porphyroclasts, originally developed during the Proterozoic Z
normal faulting, were dragged in the opposite direction and
back under the cores of the porphyroclasts.

The fourth episode of faulting of within the RFZ took
place during the Alleghanian orogeny. Semi-brittle overprint-
ing of the Taconic southeast-dipping ultramylonite with a
reverse (locally with a slightly right-lateral component)
confirms this reactivation. Because of the lower temperature
of deformation at the brittle-ductile transition, quartz
commonly deformed in a ductile manner, whereas feldspar
deformed in a brittle manner. Feldspars typically have
plucked grain boundaries and antithetic extensional shears.
At many exposures along the RFZ a complex set of britttle
faults have developed. This set includes: east-southeast- and
west-northwest-dipping reverse faults, northest- and south-
west-dipping normal faults and a conjugate set of north-
northwest- and south-southeast-dipping right-lateral strike-
slip and east- and west-dipping left-lateral strike-slip
faults.

A second set of complex brittle faults overprints the RFZ
during the fifth episode of faulting. This complex set of
faults includes: south-southeast- and north-northwest-dipping
reverse faults, southeast- and northwest-dipping normal faults
(this includes the development of the Newark basin) and the
development of conjugate strike-slip faults which offset the
ultramylonite foliation. In this exposure strain within the
RFZ is concentrated on the right-lateral component of the
conjugate pair. A total of 223.8 cm of right-lateral dis-
placement along northwest-striking faults and 112.3 cm of
left-lateral displacement along north-northeast-striking

faults was measured over a distance of 914.4 cm. Quartz
filled extension fractures, which bisect the acute angle of
the conjugate pair, are also visible. Overprinting relation-
ships indicate that this brittle reactivation post-dates the
Alleghanian reactivation and indicate that it is Mesozoic. For
this Mesozoic reactivation of the RFZ, a north-northeast
trending maximum compression direction is approximately
parallel to the orientation of these extension fractures.

REFERENCES:

Baker, D.R., and Buddington, A.F., 1970, Geology and magnetite
    deposits of the Franklin Quadrangle and part of the
    Hamburg Quadrangle, New Jersey: USGS Prof.Paper 638,73 pp.

Bayley, W.S., 1910, Iron mines and mining in New Jersey: New
    Jersey Geol. Survey Final Rept, v. 7, 512 pp.

Bayley, W.S., 1941, Precambrian geology and mineral resources
    of the Delaware Water Gap and Easton quadrangles, New
    Jersey and Pennsylvania:U.S. Geol. Survey Bull. 930. 98 pp.

Buddington, A.F., and Leonard, B.F., 1962, Regional geology of
    the St. Lawrence County magnetite district, Northwest
    Adirondacks, New   York: USGS Prof. Paper 376, 145 pp.

Collins, L.G., 1969, Regional recrystallization and the
    formation of magnetite concentrations, Dover magnetite
    district, New Jersey: Econ. Geol., v. 64, p. 17-33.

Dallmeyer, R.D., 1974, Tectonic setting of the Northeastern
    Reading Prong: Geol. Soc. Amer. Bull., v. 85, p. 131-134.

Drake, A.A., Jr., 1984, The Reading Prong of New Jersey and
    eastern Pennsylvania: An appraisal of rock relations and
    chemistry of a major Proterozoic terrane in the Appala-
    chians, in Bartholomew, M.J., ed., The Grenville event
    in the Appalachians and related   topics: GSA Special
    Paper 94, p. 75-109.

Germine, M, 1986, Asbestiform and non-asbestiform amphiboles,
    cadmium, and zinc in quarry samples of marble from
    Franklin and Sparta, Sussex County, New Jersey:
    Geologic Report 15, New Jersey Geological Survey, 30 pp.

Hague, J.M., Baum, J.L., Herrman, L.A., and Pickering, R.J., 1956, Geology and structure of the Franklin-Sterling area, New Jersey, Geol. Soc. Am. Bull., v. 67, p. 434-474.

Hotz, P.E., 1953, Magnetite deposits of the Sterling Lake,NY & Ringwood, NJ area: USGS Bull. 982-F.

Hull,J., Koto, R., and Bizub, R., 1986, Deformation zones in the Highlands of New Jersey: Geological Association of New Jersey, in Husch J.M. and Goldstein F.R., (Editors), Geology of the New Jersey Highlands and Radon in New Jersey. Field Guide and Proceedings of the Geological Association of New Jersey, part 1, p. 19-66.

Puffer, J.H., and Volkert, R.A., 1991, Generation of trondhjemite from partial melting of dacite under granulite facies conditions: an example from the New Jersey Highlands, USA: Precambrian Research, v. 51, p. 115-125.

Ratcliffe, N.M., 1980, Brittle faults (Ramapo fault) and phyllonitic ductile shear zones in the basement rocks of the Ramapo seismic zones, New York and New Jersey, and their relationship to current seismicity: in Manspeizer, W. (Editor) Field studies of New Jersey geology and guide to field trips: Newark, N.J.,Rutgers Univ., p. 278-312.

Sims P. K., 1958, Geology and magnetite diposits of Dover District, Morris County, New Jersey: US Geol. Survey Prof. Paper 287, 162 pp.

Spencer, A.C., Kummel, H.B., Wolff, J.E., Salisbury, R.D., and Palache, C., 1908, Description of the Franklin Furnace Quadrangle (New Jersey): U.S. Geol. Surv., Geologic Atlas, Folio 161, 27 pp.

Stephens, G.C., Metsger, R.W., and Yang, Q., 1988, Shear zone development in the Franklin marble: Observations on the Zero fault at the Sterling Hill mine, Sussex County, New Jersey: Geological Society of America Abstracts with Programs: v. 20, p. 180.

Volkert, R.A., and Drake, A.A., Jr., 1986, Some Middle Proterozoic rocks of the New Jersey Highlands: in Husch J.M. and Goldstein F.R., (Editors), Geology of the New Jersey Highlands and Radon in New Jersey. Field Guide and Proceedings of the Geological Association of New Jersey, p. 1-17,

Volkert, R.A., Monteverde, D.H., and Drake, A. A., Bedrock
    Geologic Map of the Stanhope Quadrangle, Sussex and
    Morris Coundies, New   Jersey, 1989, New Jersey
    Geological Survey, Geologic Quadrangle Map GQ-1671.
Young, D.A., 1971, Precambrian rocks of the Lake Hopatcong area,
    New Jersey: Geol. Soc. Amer. Bull., v. 82, p. 141-158.

Young, D.A., 1978, Precambrian salic intrusive rocks of the
    Reading Prong: Geol. Soc. Amer. Bull., v. 89, p. 1502-1514.

GEOLOGY OF THE MIDDLE PROTEROZOIC ROCKS OF THE
NEW JERSEY HIGHLANDS

Richard A. Volkert, New Jersey Geological Survey, CN-427, Trenton, New Jersey 08625-0029

INTRODUCTION

The geology of the Middle Proterozoic rocks of the New Jersey Highlands has been a subject of study for over a century. The pioneering work of early geologists resulted in a subdivision of the crystallines into the Byram, Pochuck, and Losee Gneiss, and the Franklin Limestone. This generic breakdown was refined by geologists from the N.J. Zinc Company (e.g. Hague and others, 1956) and the U.S. Geological Survey (e.g. Sims and Leonard, 1952; Hotz, 1953; Sims, 1958; Drake, 1969) into a more practical breakdown based on mineralogy. Recent detailed geologic mapping of the Highlands by the New Jersey Geological Survey and the U.S. Geological Survey since 1984, undertaken for the new geologic map of New Jersey, has led to further lithologic refinement and a more complete understanding of the geologic and stratigraphic relations of the various Middle Proterozoic rocks. Currently, more than 30 different units are recognized and most are shown on the new State geologic map. These units were mapped on the basis of distinctive mineralogy and/or geochemistry.

The purpose of this paper is to discuss the nomenclature and lithology of the various Middle Proterozoic units shown on the new State geologic map of New Jersey and to discuss new information and interpretations that have developed out of the recent work in these complex and interesting rocks. In this paper, lithologic names are accompanied by their respective map symbols. These are prefixed by the capital letter Y, denoting the age of the units as Proterozoic Y, or Middle Proterozoic. While rocks in the Highlands are still appropriately referred to as Precambrian, the designation of Middle Proterozoic enables their age to be placed more accurately within a geochronologic framework that encompasses everything from the earliest Archean to the Cambrian.

Rocks of Middle Proterozoic age in the New Jersey Highlands, along with the physically continuous Hudson Highlands in New York and Reading Prong in Pennsylvania, constitute one of the largest of the numerous Grenville-age massifs that extend northeastward along the eastern United States from Alabama to Vermont. These massifs are the exposed roots of the Appalachian Mountains and contain rocks greater than 1 billion years old. The Highlands occupies slightly over 1,000 square miles in northern New Jersey. It is divided into two subequal parts by sedimentary rocks of Cambrian through Devonian age of the Green Pond Mountain region. The Highlands is in fault contact on the southeast with sedimentary and igneous rocks of Mesozoic age of the Newark Basin and locally with sedimentary rocks of Cambrian and Ordovician age. On the northwest, the Middle Proterozoic rocks are unconformably overlain by, or in fault contact with, sedimentary continental margin clastic and carbonate rocks of Cambrian and Ordovician age. A generalized version of these geologic relations is shown in figure 1.

Losee Metamorphic Suite

The name Losee was first introduced by Wolff and Brooks (1898) for the light-colored rocks exposed at Losee Pond (currently known as Beaver Lake) in the Franklin quadrangle. These rocks were named the Losee Pond granite by them. Spencer and others (1908) changed the name to Losee Gneiss, the name shown on the old State geologic map of New Jersey (Lewis and Kummel, 1912). Drake (1984) renamed these rocks the Losee Metamorphic Suite.

Rocks of the Losee Suite occur throughout the Highlands in New Jersey, but are most abundant in the Greenwood Lake, Franklin, Hamburg, Boonton, Califon, High Bridge, and Belvidere quadrangles (fig. 1). These rocks exhibit textural variations that range from well layered gneiss and granofels to indistinctly foliated granite and pegmatite. The layered and granofels phases are mapped as quartz-oligoclase gneiss (Ylo), and, where they contain appreciable amounts of hornblende or biotite, as hornblende-quartz-oligoclase gneiss (Ylh), or biotite-quartz-oligoclase gneiss (Ylb) respectively. The granitic phase is mapped as albite-oligoclase granite (Yla). Pegmatite occurs very locally and commonly is mapped with the granite. One small exposure of albite-oligoclase syenite (Yls) was mapped by Volkert and others (1990) near the abandoned Gulick iron mine in the Chester quadrangle. Similar quartz-poor rocks associated with the Losee have not been recognized elsewhere in the Highlands.

The Losee Suite is characterized by highly sodic rocks that are typically white weathering, light-greenish-gray on fresh surface, and medium- to coarse-grained. The essential minerals are quartz and plagioclase (oligoclase to andesine). Accessory minerals include biotite, hornblende, clinopyroxene, garnet, and magnetite. Interlayered amphibolite is often associated with all of the textural phases of the Losee.

Offield (1967) was among the first to advance the idea that Losee-type rocks and charnockitic gneiss in the New York Hudson Highlands were basement to the overlying metasedimentary rocks, and he suggested the possibility of an unconformity between them. Drake (1984) and Volkert and Drake (1990) have proposed that the Losee in New Jersey also is basement to the rest of the Middle Proterozoic rocks. Recent mapping in the Wanaque quadrangle by Volkert (unpublished data) supports this as an exposure was found of feldspathic quartzite resting in angular discordance on amphibolite and charnockitic gneiss. The basal layers of metaquartzite contain clasts of the underlying amphibolite.

Samples of Losee plot into either the field of tonalite or trondhjemite on a normative feldspar diagram (fig. 2). The geochemistry of the Losee is fairly distinctive as these rocks typically contain >60 weight percent SiO_2, 12 to 18 weight percent Al_2O_3, and 3 to 7 weight percent Na_2O. Puffer and Volkert (1991) proposed that rocks of the Losee Suite originated in a continental margin magmatic arc setting dominated by calc-alka-
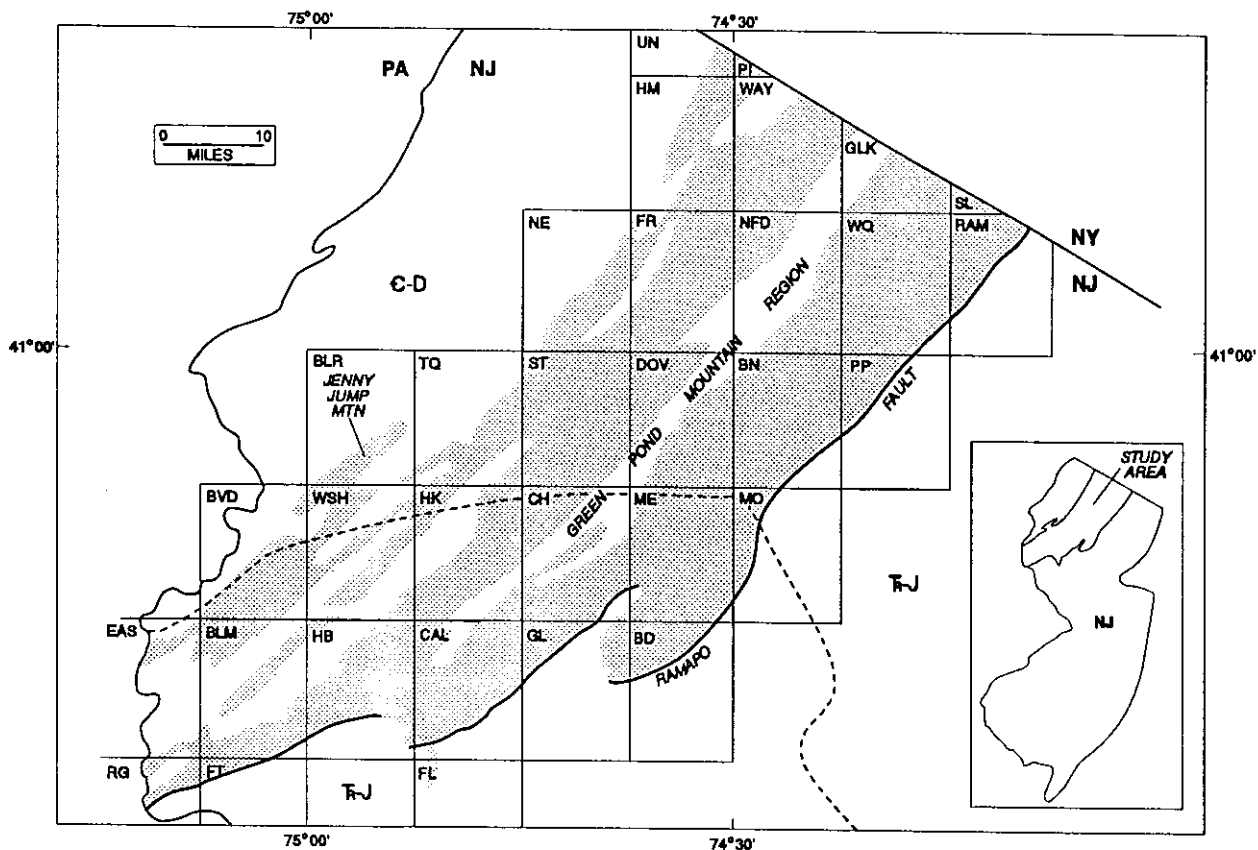
Figure 1. Generalized geologic map of northern New Jersey showing Middle Proterozoic rocks of the Highlands (shaded), Mesozoic rocks of the Newark Basin (Tr-J), and Paleozoic rocks of the Valley and Ridge (C-D). Dashed line marks limit of Wisconsinan terminal moraine. Small inset map locates study area shown in geologic map. Abbreviations of 7.5' quadrangles are: UN, Unionville; PI, Pine Island; HM, Hamburg; WAY, Wawayanda; GLK, Greenwood Lake; SL, Sloatsburg; NE, Newton East; FR, Franklin; NFD, Newfoundland; WQ, Wanaque; RAM, Ramsey; BLR, Blairstown; TQ, Tranquility; ST, Stanhope; DOV, Dover; BN, Boonton; PP, Pompton Plains; BVD, Belvidere; WSH, Washington; HK, Hackettstown; CH, Chester; ME, Mendham; MO, Morristown; EAS, Easton; BLM, Bloomsbury; HB, High Bridge; CAL, Califon; GL, Gladstone; BD, Bernardsville; RG, Riegelsville; FT, Frenchtown; and FL, Flemington.

line magmatism. The enrichment in SiO_2, Al_2O_3, and Na_2O, and the MgO/FeO ratio of Losee rocks is consistent with this interpretation. Therefore, the Losee likely represents a metamorphosed sequence of dacitic metavolcanic rocks and associated metabasalt (amphibolite). Partial melting of basaltic source rock produced the Losee metadacite and metatonalite, whereas the more massive phases of the Losee are interpreted by Puffer and Volkert (1991) to be intrusions of trondhjemitic magma resulting from partial melting of Losee metadacite and metatonalite.

Isotopic dating of the Losee is in process, but the results are not yet available. Similar rocks in Vermont have yielded ages of about 1308 to 1357 Ma (Aleinikoff and others, 1990) and in the Adirondacks of New York of about 1300 to 1330 Ma (McLelland and Chiarenzelli, 1991). There is little reason to believe that the age of the Losee in New Jersey is much different.

Charnockitic rocks

Charnockitic rocks (rocks that contain hypersthene) in the New Jersey Highlands are of two distinct types: quartz-rich, layered gneiss mapped as hypersthene-quartz-plagioclase gneiss (Yh), and massive-textured, generally quartz-poor rock mapped as diorite (Yd). Both types are spatially associated with rocks of the Losee Suite, but are less areally extensive. The layered, quartz-rich gneiss has been mapped throughout the Highlands, but is most abundant in the Franklin, Greenwood Lake, and Wanaque quadrangles. Quartz-poor diorite is rare west of the Green Pond Mountain region with exception of a few small exposures mapped by Volkert and others (1989) in the southeastern part of the Stanhope quadrangle. It is abundantly exposed in the Greenwood Lake, Wanaque, Dover, Morristown, and Mendham quadrangles.

The layered charnockitic rocks typically weather gray to tan, are greenish-gray to brownish-gray, greasy-lustered, and medium to medium-coarse-grained. They are composed of plagioclase (oligoclase to andesine), quartz, clinopyroxene, hornblende, biotite, hypersthene, minor potassic feldspar, and opaque minerals. Graphite is a very local accessory in a few exposures in the Franklin and Newfoundland quadrangles. Layered charnockitic gneiss is commonly interlayered with amphibolite and mafic-rich quartz-plagioclase gneiss lacking hypersthene and of Losee affinity. Exposures of quartz-oligoclase gneiss, quartz-rich charnockitic gneiss, and amphibolite are repetitiously layered on a scale of a few feet in the Newfoundland quadrangle and less abundantly in the Wanaque quadrangle.

On the basis of major and trace element abundances, the layered charnockitic rocks may be subdivided into rocks having the composition of meta-andesite and also of metadacite. Charnockitic metadacite overlaps virtually all major and trace element abundances in the Losee metadacite. The only difference is a very slight enrichment in K_2O in charnockitic metadacite. Charnockitic meta-andesite has somewhat lower SiO_2 and higher Fe_2O_3, FeO, CaO, TiO_2, P_2O_5, and Cr than charnockitic metadacite or the Losee Suite. While charnockitic metadacites are widespread, char-

nockitic meta-andesite appears to be confined to the Highlands west of the Green Pond Mountain region.

The massive-textured charnockitic rocks also weather gray to tan, are greenish-gray to brownish-gray, greasy-lustered, and medium- to coarse-grained. They are composed of plagioclase (oligoclase to andesine), clinopyroxene, hornblende, biotite, hypersthene, minor quartz, and opaque minerals. Garnet is a very local accessory in an exposure in the Stanhope quadrangle. The massive charnockites are also commonly associated with amphibolite. Cognate inclusions of noritic composition are locally preserved in an exposure of diorite in the Boonton quadrangle. The principal differences seen in the field between diorite and the layered charnockitic rocks are the massive, indistinctly foliated texture, the quartz-poor composition, and the absence of associated mafic quartz-plagioclase gneiss in the diorite.

The layered and massive charnockitic rocks are also distinguishable by their geochemistry. On a normative Q-A-P diagram (fig. 3), the two rock types fall into separate but overlapping fields. The more siliceous and slightly more potassic composition of the layered charnockites is clearly seen on this diagram. Layered charnockites characteristically contain >60 weight percent SiO_2. By comparison, massive charnockites contain <60 weight percent SiO_2, although a few contain from 60 to 65 percent and are more properly termed quartz diorite. The massive charnockites have a more mafic composition that is enriched in Al_2O_3, Fe_2O_3, FeO, MgO, and CaO. The remainder of major oxides and trace elements overlap the range of elements in the layered charnockites.

Using a variety of tectonic discrimination methods based on immobile elements (e.g. Jakes and White, 1972; Bailey, 1981), charnockitic meta-andesites are consistently found to be orogenic andesites and to have a continental margin arc affinity. Rocks of rhyodacitic to rhyolitic composition are often associated with basalt, andesite, and dacite in orogenic settings. To date, rocks definitively identified as metarhyolite have not been recognized in the Highlands. It is possible that not all of the massive-textured, foliated rock mapped as microperthite alaskite belongs in the Byram Intrusive Suite; some may, in fact, be metarhyolite. Further work is necessary to test the merit of this speculation.

The origin of charnockitic rocks in New Jersey has been problematic. More recently, Drake (1984) and Volkert and Drake (1990) have interpreted the layered rocks to be a sequence of metavolcanics including associated metabasalt and the massive phases mapped as diorite to be intrusive rocks. Both layered and massive phases have a distinct calc-alkaline chemistry readily seen on peacock (fig. 4) and AFM (fig. 5) diagrams. It is interesting to note that the layered and massive charnockites fall along the same trend on figure 4. This strongly suggests a petrogenetic relationship between both rock types. It is also interesting to note the overlap of massive and layered charnockites and the Losee on figure 5. All three rock types follow the same strong calc-alkaline trend from slight Fe-enrichment in diorite and quartz diorite, to Fe-depletion in the layered charnockites and the Losee. A similar relationship is seen on a $CaO-Al_2O_3-$ (FeO+MgO) diagram (fig. 6) with both charnockitic rock types and
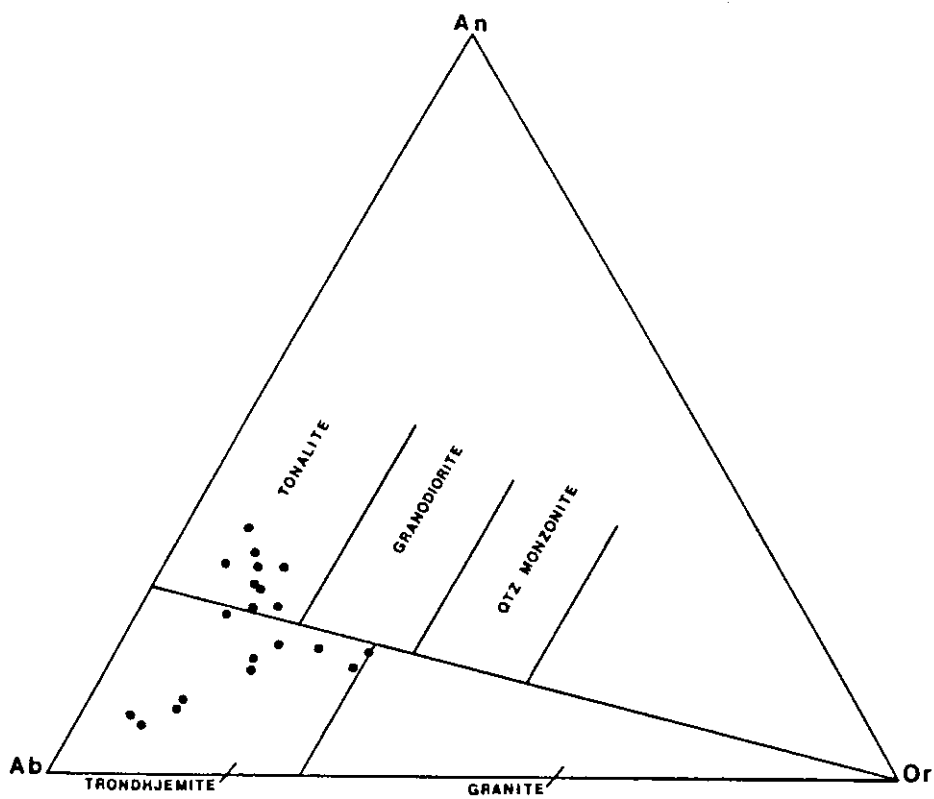
Figure 2. Rocks of the Losee Metamorphic Suite plotted on a normative feldspar diagram.
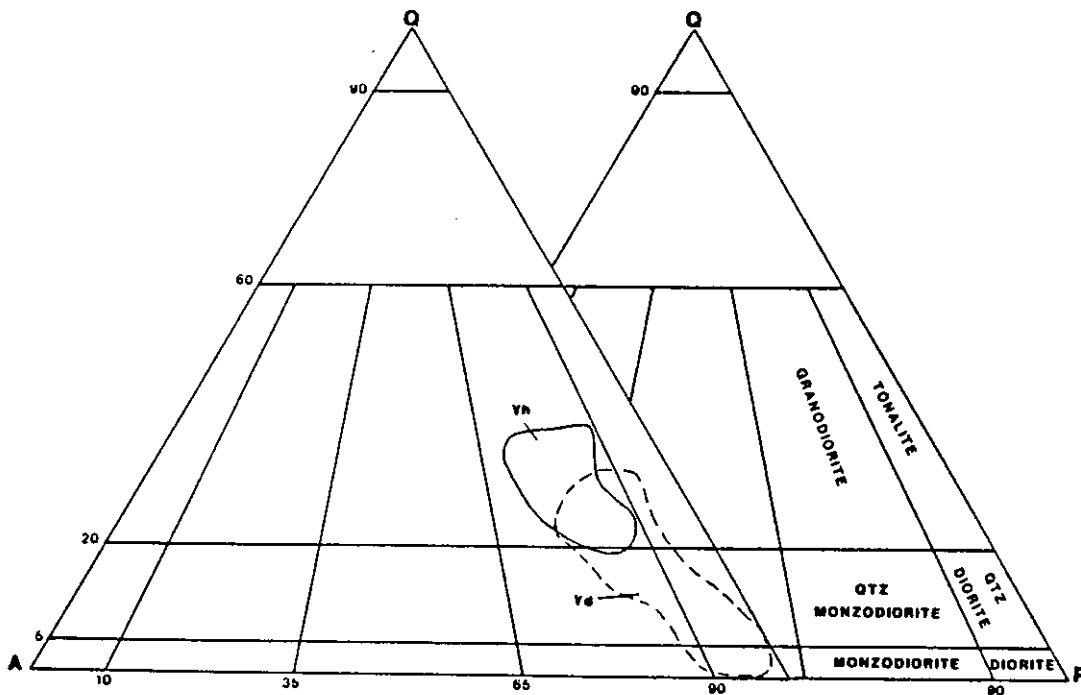
Figure 3. Normative quartz-alkali feldspar-plagioclase diagram of New Jersey Highlands layered (solid field) and massive (dashed field) charnockitic rocks. Compositional fields for plutonic rocks after Streckeisen (1976) shown alongside for comparison.
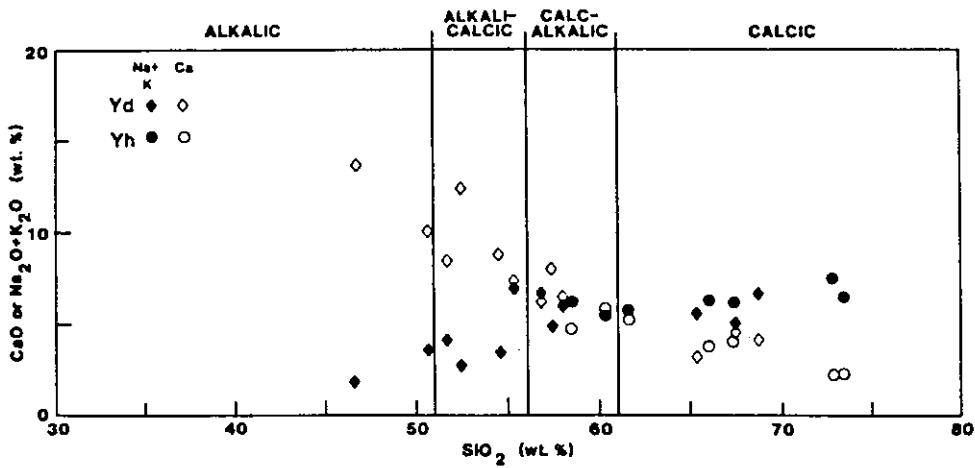
Figure 4. Peacock plot of layered charnockites (filled and open circles) and massive charnockites (filled and open diamonds). Note the well defined trends and their intersection in the calc-alkaline field.
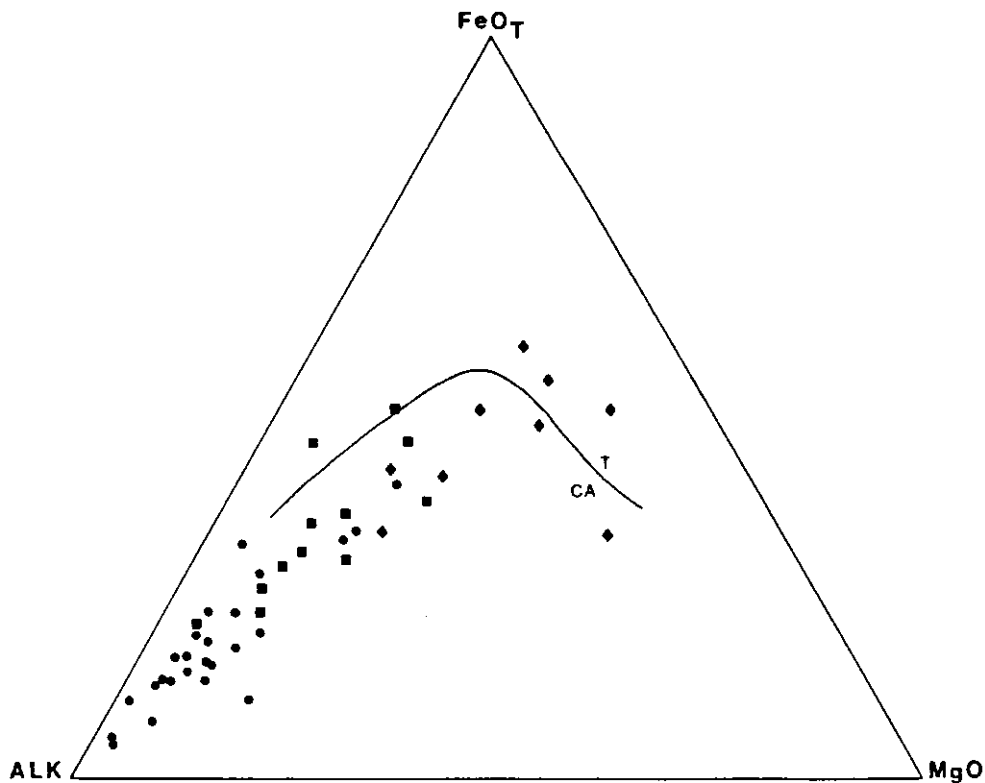
Figure 5. Plot of Losee rocks (circles), layered charnockites (squares), and massive charnockites (diamonds) on AFM diagram. Line shows boundary between tholeiitic (T) and calc-alkaline (CA) rocks from Irvine and Baragar (1971).

29
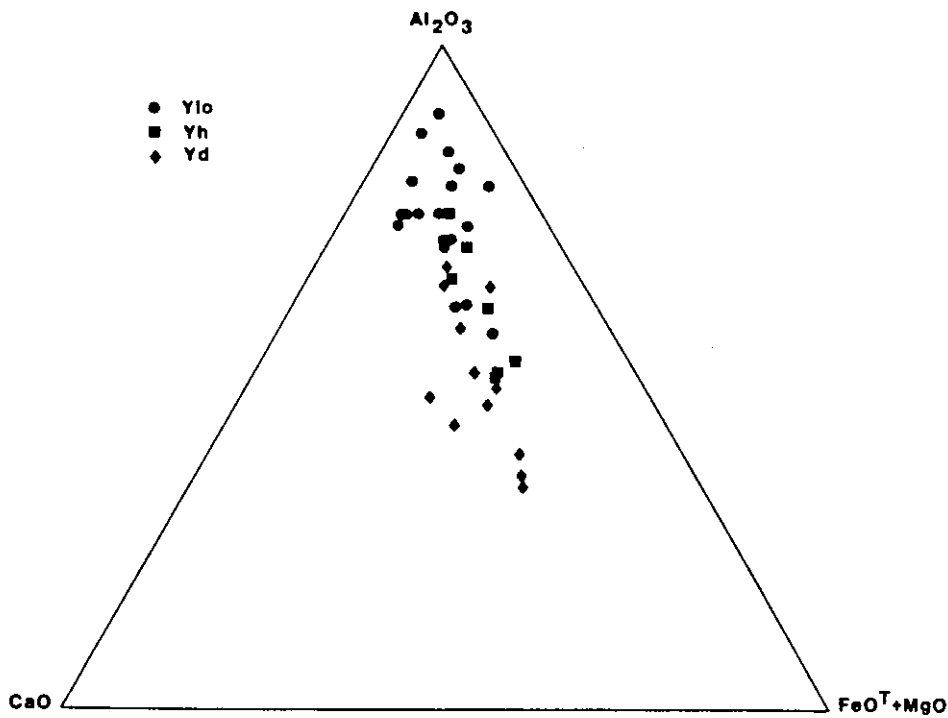
Figure 6. Plot of Losee rocks, layered charnockites, and massive charnockites on CaO-Al₂O₃-(FeO+MgO) diagram. Note the single trend defined by all three rock types. Symbols as in figure 5.

the Losee defining a single, continuous trend.

Because of the intimate field relationship between the Losee and charnockitic rocks, especially in the Newfoundland and Wanaque quadrangles, and because of the similarities in the chemistry of both charnockitic rock types, I interpret them to be a product of the same continental magmatic arc setting that generated the Losee. Partial melting of a basaltic source at lower crustal depths would produce magma having the composition of diorite. Whether the Losee fractionated from this dioritic magma, or whether the Losee and charnockitic rocks are descendents of separate magmas produced by different amounts of partial melting of a parental basalt is difficult to say without further work. At this time, I prefer an interpretation involving fractionation of diorite to produce charnockitic meta-andesite, charnockitic metadacite, and the Losee metadacite. This is particularly supported by the relationships seen on figures 5 and 6 and by the abundant occurrence in the Highlands of rocks of intermediate composition. Therefore, the charnockitic rocks and the Losee would be comagmatic. Regardless, the Losee and charnockitic rocks are here interpreted to be cogenetic and part of the same suite that is composed of both intrusive and metavolcanic rocks.

30

Unconformably overlying the Losee and associated charnockitic rocks in the Highlands is a thick sequence of layered metasediments that are quartzofeldspathic gneiss, quartzite, calcsilicate gneiss, and marble. Metasedimentary rocks are widespread and abundant in the Highlands both east and west of the Green Pond Mountain region.

Quartzofeldspathic gneiss

Gneiss and granofels having a quartzofeldspathic composition encompasses a wide range of rock types that are mapped as potassic feldspar gneiss (Yk), microcline gneiss (Ym), biotite-quartz-feldspar gneiss (Yb), and hornblende-quartz-feldspar gneiss (Ymh).

Potassic feldspar gneiss has been mapped in virtually every quadrangle, but it appears to be most abundant in the southwest half of the Highlands. It is a light-pinkish-white or buff, medium- to medium-coarse-grained, moderately foliated gneiss and lesser granofels containing quartz, microcline, oligoclase and local accessory biotite, garnet, sillimanite, and magnetite. Potassic feldspar predominates over plagioclase.

Potassic feldspar gneiss characteristically contains >70 weight percent SiO_2 and >5 weight percent K_2O. The iron content is variable but typically low, as is CaO and MgO. Samples analyzed by Drake (1984) from the southwest Highlands contain slightly less CaO and Na_2O, but otherwise the chemistry of this unit is reasonably uniform throughout the Highlands. On a diagram of molar Si/Si+Al versus molar Na+Ca/Na+Ca+K (fig. 7), potassic feldspar gneiss dominantly falls within the fields of arkose and lithic arenite. The chemistry of potassic feldspar gneiss is very close to that of rhyolite. However, several things argue against a metavolcanic protolith for this unit. These include the presence of interlayered quartzite, lithologic association with rocks of known sedimentary parentage, highly variable trace element contents, especially Zr and Nb, and the lack of correlation between Niggli mg and Cr, which Van De Kamp and others (1976) consider diagnostic of sedimentary rock. Therefore, a sandstone of mainly arkosic composition is the most likely protolith for potassic feldspar gneiss.

Microcline gneiss, as first recognized by New Jersey Zinc Company geologists (Hague and others, 1956), occurs sporadically throughout the northern Highlands, but is most abundant in the Unionville, Hamburg, Newton East, Stanhope, and Tranquility quadrangles. It is a pinkish-white, fine- to medium-grained, well layered and foliated gneiss composed of quartz, microcline, and oligoclase. Common accessory minerals are biotite, garnet, sillimanite, and magnetite. Potassic feldspar predominates over plagioclase.

Microcline gneiss is characterized by the same enrichment in SiO_2 and K_2O as potassic feldspar gneiss, but contains slightly

less CaO. Other major and trace element abundances are similar to those in potassic feldspar gneiss. On figure 7, microcline gneiss falls almost completely within the arkose field. It is interesting to note that while microcline gneiss is most abundant in the northwest Highlands and potassic feldspar gneiss in the southwest Highlands, the two units occur along strike. They are in direct contact in the Tranquility quadrangle where, perhaps not by coincidence, microcline gneiss ends and potassic feldspar gneiss begins. It is entirely possible that both units are related and are sedimentary facies equivalents that differ mainly in texture. However, for the time being they are mapped separately. The protolith of microcline gneiss is interpreted to be an arkosic sandstone rather than rhyolite for the same reasons as were outlined above for potassic feldspar gneiss.

Biotite-quartz-feldspar gneiss occurs throughout the Highlands and is equally abundant east and west of the Green Pond Mountain region. This unit is variable in texture and composition. It typically weathers pinkish-gray, although some phases are locally rusty, and is a medium to coarse-grained, moderately layered and foliated rock. The rusty coloration is distinctive in phases that contain abundant sulfide. Biotite-quartz-feldspar gneiss is composed principally of quartz, oligoclase, microcline, and biotite. Feldspar proportions are variable, but plagioclase typically predominates over potassic feldspar. Garnet, sillimanite, and magnetite are common accessory minerals, but graphite is confined to the rusty weathering, sulfidic phase. Volkert (unpublished data) has mapped locally hornblende-bearing phases of this unit in the Newfoundland, Ramsey, and Blairstown quadrangles. Amphibolite layers are present in both the rusty weathering and pinkish-gray weathering phases of this unit, but are much more common in the former. Interlayered, locally graphitic metaquartzite has been mapped within the rusty weathering phase in the Hackettstown quadrangle (Volkert and others, in press). Thin, graphitic scapolite-bearing gneiss layers have been mapped within it in the High Bridge quadrangle (Volkert, unpublished data). In the 19th and early 20th century, biotite-quartz-feldspar gneiss was locally exploited for graphite from small quarries throughout the Highlands.

Biotite-quartz-feldspar gneiss has a variable SiO_2 content that ranges from 53 to 88 weight percent and equally variable Al_2O_3 that ranges from about 5 to 23 weight percent. This unit contains higher Fe_2O_3, FeO, Na_2O, and lower K_2O than potassic feldspar gneiss or microcline gneiss. There is very little difference overall in the major element composition of the pinkish-gray or the rusty weathering phases of this unit. On figure 7, biotite-quartz-feldspar gneiss falls mainly in the field of graywacke and, to a lesser extent, lithic arenite. A few samples fall close to, or within, the field of pelitic rocks (mudrocks). This is consistent with their low SiO_2 and high Al_2O_3 contents. A few more fall in, or close to, the field of carbonate rocks and are probably calcareous shale. The scatter seen on figure 7 clearly reflects the heterogeneous composition of the sedimentary protoliths that comprise this unit.

Hornblende-quartz-feldspar gneiss is best exposed in the

Wawayanda and Ramsey quadrangles where thick layers are in conformable contact with calcareous metasedimentary rocks. This unit is pinkish-gray, medium-grained, moderately layered and foliated and composed of quartz, microcline, lesser oligoclase, and hornblende. Biotite, garnet, and magnetite are minor accessories; titanite is rare.

Compared to potassic feldspar gneiss, hornblende-quartz-feldspar gneiss is characterized by slightly lower SiO_2 and higher Al_2O_3 and FeO. Most of the major elements overlap those in biotite-quartz-feldspar gneiss, suggesting that this unit is likely a metamorphosed sedimentary rock also. The layered texture and lithologic associations of hornblende-quartz-feldspar gneiss also support this interpretation. The few analyses of this unit fall in the fields of arkose and graywacke on figure 7.

Quartzite

Metaquartzite (Yq) occurs as lenses and thin layers scattered throughout the Highlands, but is most abundant in the Wanaque quadrangle. It is a sparsely exposed, but lithologically significant unit that provides an excellent stratigraphic and structural marker. The quartzite is typically a light gray, vitreous, medium-grained, massive to well layered rock. Thin layers of metaquartzite are associated with potassic feldspar gneiss, biotite-quartz-feldspar gneiss, pyroxene gneiss, epidote gneiss, and marble. Quartzite associated with biotite-quartz-feldspar gneiss, calc-silicate gneiss, and marble often contains graphite. Minor amounts of biotite, scapolite, and clinopyroxene have also been observed. Quartzite associated with potassic feldspar gneiss contains locally abundant garnet. At other locations quartzite associated with potassic feldspar gneiss contains magnetite and tourmaline-bearing layers. The tourmaline is black and probably Fe-rich schorl. This quartzite has been noted in the Blairstown and Belvidere quadrangles (Volkert, unpublished data).

There is little question that the bulk of metaquartzite represents metamorphosed pure and impure quartz sandstone. Some of the metaquartzite that is associated with calc-silicate gneiss and marble as pods, lenses, and thin layers may be metamorphosed chert.

Calc-silicate gneiss

Rocks having a calc-silicate affinity, like quartzofeldspathic gneiss, encompass a wide range of rock types that are mapped as clinopyroxene-quartz-feldspar gneiss (Ymp), pyroxene gneiss (Yp), pyroxene-epidote gneiss (Ype), and epidote-bearing gneiss (Ye). Other phases of calc-silicate rock, such as epidote-scapolite-quartz gneiss and hornblende-pyroxene skarn, are recognized but are not extensive enough to be mapped separately. They are minor phases of the calc-silicate units shown on the new State geologic map.

Clinopyroxene-quartz-feldspar gneiss occurs throughout the

Highlands, but is most abundant in the Wawayanda, Wanaque, Dover, Stanhope, and Chester quadrangles. At least some of the rock in the southwest Highlands mapped as potassic feldspar gneiss by earlier workers actually is clinopyroxene-quartz-feldspar gneiss. This unit is important as it represents a transitional lithology that bridges the gap between the quartzofeldspathic and calc-silicate gneisses. It could easily be grouped with the former, but, because of its lithologic associations, it is more appropriately included with the calc-silicate gneisses. Clinopyroxene-quartz-feldspar gneiss is a pinkish-gray, medium-grained, moderately layered and foliated rock containing quartz, microcline, oligoclase, and clinopyroxene. Local accessories include titanite, biotite, epidote, and opaque minerals. Amphibolite or pyroxene amphibolite is commonly layered with this unit. Clinopyroxene-quartz-feldspar gneiss is often spatially associated with a quartz-rich phase of pyroxene gneiss (Yp), and the two units may have a sedimentary facies relationship. Both units contain thin, conformable lenses or layers of green, medium-grained rock composed wholly of clinopyroxene. I have observed these very locally occurring and unusual rocks within clinopyroxene-quartz-feldspar gneiss in the Stanhope and Wanaque quadrangles and within pyroxene gneiss in the Tranquility quadrangle. Kastelic (1979) observed the same rock within calc-silicate gneiss near the Washington mine in the Washington quadrangle. A chemical analysis of the rock from Tranquility has about 50 weight percent SiO_2, 13 weight percent MgO, and 23 weight percent CaO. All other major oxides are low, including Al_2O_3. These rocks likely are metamorphosed lenses and layers of cherty dolomite.

The chemistry of clinopyroxene-quartz-feldspar gneiss overlaps that of hornblende-quartz-feldspar gneiss, but is slightly higher in CaO. The former typically contains 60 to 78 weight percent SiO_2, 10 to 14 weight percent Al_2O_3, 1 to 6 weight percent CaO, and is enriched in both Na_2O and K_2O. On figure 7, clinopyroxene-quartz-feldspar gneiss spans the fields of arkose, lithic arenite, and graywacke, reflecting variability in the original sedimentary protoliths.

Pyroxene gneiss occurs throughout the Highlands, but is most abundant west of the Green Pond Mountain region in the Wawayanda, Newfoundland, Franklin, and Hackettstown quadrangles. It is a white to tan weathering, greenish-gray, medium-grained, well layered rock composed of oligoclase, clinopyroxene, and variable amounts of quartz. Titanite and magnetite occur as accessory minerals. Some phases of this unit are extremely quartz-poor and some are quartz-rich. Despite this variability, both phases are clearly the same rock and are shown together on the new State geologic map. In the Newfoundland and Wawayanda quadrangles, some phases contain local accessory biotite and/or hornblende. Graphite has been observed as an occasional accessory in the biotite-bearing phase. Amphibolite or pyroxene amphibolite is commonly layered with all phases of pyroxene gneiss. Throughout the Highlands, pyroxene gneiss and biotite-quartz-feldspar gneiss are in conformable contact and are closely associated. While the latter sometimes occurs alone, it is rare to find exposures of pyroxene gneiss unassociated with at least minor amounts of biotite-
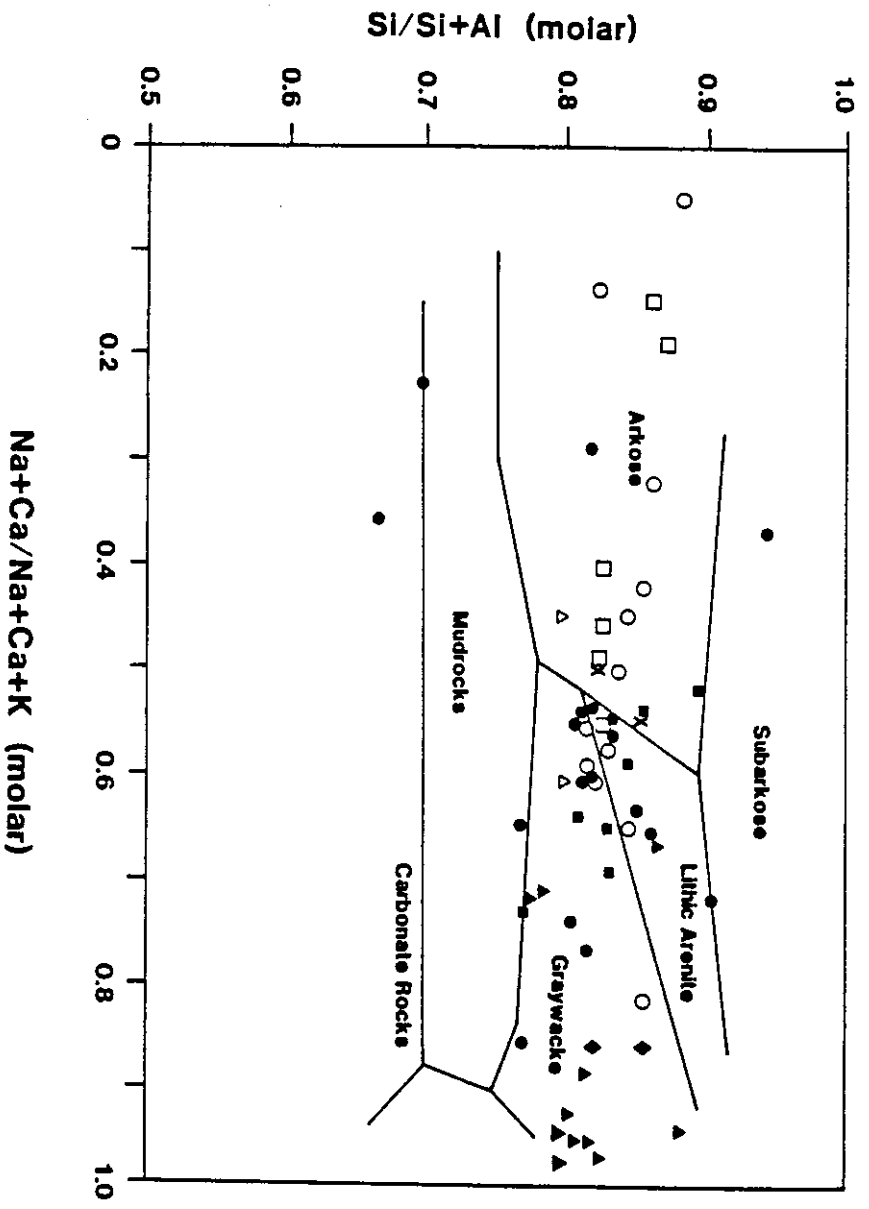
Figure 7. Si/Si+Al versus Na+Ca/Na+Ca+K (mole %) diagram after Garrels and McKenzie (1971) showing distribution of metasedimentary rocks from the New Jersey Highlands. Symbols are: open circle, potassic feldspar gneiss; open square, microcline gneiss; solid circle, biotite-quartz-feldspar gneiss; open triangle, hornblende-quartz-feldspar gneiss; solid square, open triangle, quartz-feldspar gneiss; solid triangle, pyroxene gneiss; solid diamond, pyroxene-epidote gneiss; and letter x, monazite gneiss.

quartz-feldspar gneiss.

Pyroxene gneiss has greater variability in its chemistry than in its mineralogy. On the basis of major element abundances and selected ratios, particularly K_2O/Na_2O and $Fe_2O_3^t+MgO$, pyroxene gneiss is divisible into two main types, alkali-poor and alkali-rich. The alkali-poor group is characterized by a K_2O/Na_2O ratio of ≤ 0.3, <1.0 weight percent K_2O, and an enrichment in Na_2O and $Fe_2O_3^t+MgO$. The alkali-poor group may be further divided into a SiO_2-poor subgroup that contains <60 weight percent SiO_2 and a SiO_2-rich subgroup that contains >65 weight percent SiO_2. The SiO_2-poor subgroup is readily distinguishable by its higher $Fe_2O_3^t+MgO$ and lower Al_2O_3 content. The second main type, the alkali-rich group, is characterized by a K_2O/Na_2O ratio of about 1.0, >2.5 weight percent K_2O, and much lower Na_2O than the alkali-poor group. The alkali-rich group has higher Al_2O_3 and lower $Fe_2O_3^t+MgO$ than either of the alkali-poor subgroups. On figure 7 practically all pyroxene gneiss falls within the graywacke field. This is not surprising given the typically high Na_2O content and the ubiquitous association and interlayered nature of biotite-quartz-feldspar gneiss and pyroxene gneiss. The latter probably is a more calcareous facies of these two units.

Epidote-bearing gneiss occurs only west of the Green Pond Mountain region and is most abundant in the Franklin, Tranquility, and Washington quadrangles. Pyroxene-epidote gneiss is a light-greenish-gray, fine- to medium-grained, well layered rock composed principally of quartz, oligoclase, microcline, clinopyroxene, epidote, and sparse titanite. Some phases of this unit are quartz-rich. Pyroxene-epidote gneiss in the Tranquility quadrangle is locally migmatized by veins and layers of quartz and feldspar. Pyroxene-epidote gneiss is probably related to pyroxene gneiss with which it is spatially associated. Both have very similar major element compositions and fall in the graywacke field on figure 7. Epidote gneiss is a similar rock but is not as well layered. It consists dominantly of quartz, microcline, epidote, and magnetite. It may be related to potassic feldspar gneiss and/or clinopyroxene-quartz-feldspar gneiss, both of which it is often spatially associated with.

Most calc-silicate gneiss represents some gradation between metamorphosed calcareous sandstone and shale to quartzose and argillaceous carbonate rocks, with the latter being less abundant.

Marble

The name Franklin Limestone was originally introduced by Wolff and Brooks (1898) for the marble occurring in the Franklin belt in Sussex County. Because all marble in the Highlands was correlated with that at the type locality in Franklin, this is the name shown on the old State geologic map.

Marble is widespread in its distribution, but is best exposed west of the Green Pond Mountain region. It is especially abundant in the Wawayanda, Hamburg, Franklin, Blairstown, and Belvidere quadrangles. Most marble is a white to light gray,

medium- to coarse-crystalline, massive to moderately layered, calcitic to locally dolomitic rock. Principal accessory minerals in the Franklin area are graphite, phlogopite, chondrodite, and clinopyroxene. Marble in the Franklin-Ogdensburg area is host to the renowned zinc ore bodies and has been extensively studied by New Jersey Zinc Company geologists (e.g. Hague and others, 1956; Metsger and others, 1958).

Other pods, lenses, and layers of marble in the Highlands east of the Green Pond Mountain region are well layered, contain characteristic serpentine minerals, and are associated with talc and tremolite-bearing rocks. Most of these small bodies were locally quarried for serpentine and/or crushed lime. They occur in the Wanaque, Pompton Plains, Mendham, and Belvidere quadrangles. Similar occurrences in the Easton quadrangle were commercially exploited for talc and serpentine minerals (Peck, 1904). All of these bodies of marble are spatially associated with the same lithologies as marble in the Franklin area. Therefore, at this time, all marble is tentatively correlated with the Franklin, although it is recognized that not all marble in the Highlands occurs at the same stratigraphic level.

All workers in the Highlands are in agreement that the marble is a metamorphosed limestone and lesser dolomitic limestone that contains pods, lenses, and layers of calcareous and quartzose metasedimentary rocks, amphibolite, and metaquartzite.

Some constraint on a minimum age for the Franklin Marble is provided by an age obtained from galena in a marble "dike" from a gneiss fragment. This was collected in the core of the ore body at the Sterling Hill zinc mine in Ogdensburg. According to Metsger (1977) the galena, unquestionably younger than the enclosing gneiss or marble, yielded a lead age of 1100 Ma.

Stratigraphic relations and tectonic setting

Interpreting the stratigraphic relationships among the Middle Proterozoic metasedimentary rocks is a vexing problem owing to the obliteration of primary sedimentary features and masking of the original sedimentary parentage during Grenvillian, high-grade metamorphism, the obscuring of stratigraphic relations by large volumes of intrusive rock, and the lack of geochronologic data to constrain the overall sequence of sedimentation. Bounding ages for the metasedimentary sequence are provided by rocks dated elsewhere that are analagous to the Losee and, as discussed in the next section, the younger Byram Intrusive Suite. However, age relations within the metasediments are unknown. Past and present sedimentary basinal analogs may instead be used for comparison. In the previous section detailed geochemistry was used to identify reasonable protoliths. These allow an appropriate speculative sedimentary framework to be developed.

Assuming that the Losee and charnockitic rocks are basement to the other Middle Proterozoic rocks, then unconformable quartzite and associated potassic feldspar gneiss in the Wanaque quadrangle suggest that they may be among the oldest, if not the oldest metasedimentary rocks in the Highlands. These arkosic

rocks, which include potassic feldspar gneiss, microcline gneiss, and possibly monazite gneiss, likely collected in a block faulted or downwarped basin within the craton in an extensional tectonic setting. This is supported by the tectonic discrimination diagrams of Blatt and others (1972) (fig. 8) and Roser and Korsch (1986) (fig. 9). Sediments supplying these rocks were largely derived from a granitic or rhyolitic source. Since the basement substrate is interpreted as having been dominantly calc-alkaline and plagioclase-rich, this raises the question of an available potassic source. As stated previously, rhyolite is commonly associated with basalt and dacite in orogenic settings. Erosion of a rhyolitic source would have provided detritus of the appropriate composition for an arkose and would explain the apparent absence of rhyolites in the Highlands at the present level of erosion. In this basinal interpretation, continued erosion of the craton altered the character of the sediment deposited to that of lithic arenite, reflecting deposition of different source material in a fluvial to shallow marine environment. This was followed by deposition of quartzite, limestone, and quartzofeldspathic and calc-silicate gneiss of graywacke composition all in a marine environment (figs. 8 and 9).

The depositional environment of pyroxene gneiss is reasonably constrained by the geochemical data. The SiO_2-poor subgroup of the alkali-poor group has the composition of volcanic graywacke suggesting an oceanic island arc as a likely sediment source. This is further supported by the tectonic discriminants of Bhatia (1983), especially $Fe_2O_3^t$, MgO, and $Al_2O_3/(Na_2O+CaO)$, and also of Roser and Korsch (1986) (fig. 9). Using the same discriminants, the SiO_2-rich subgroup of the alkali-poor group has characteristics that are transitional between sedimentation in an oceanic island arc setting and an active continental margin setting. The SiO_2- and alkali-rich group has characteristics that consistently reflect sedimentation in an active continental margin setting. Taken together, the compositions of both pyroxene gneiss groups show a clear transition from source rocks that were calc-alkaline to tholeiitic and derived from a magmatic arc, to more siliceous source rocks closer in composition to granite and derived from a continental crustal source. Considering the smooth transition in composition of the pyroxene gneiss groups, it is doubtful that sedimentation occurred in separate basin settings. The difference is mainly one of varying source material that was shed into the basin. While admittedly speculative, it is not unreasonable to interpret the sequence of sedimentation to have progressed from alkali-rich to alkali-poor rocks. The SiO_2- and alkali-rich group of continental affinity would have been deposited in the same extensional tectonic setting as quartzite, marble, and some of the quartzofeldspathic gneisses, whereas the alkali-poor group would reflect a transition to a later compressional tectonic setting and the concomitant development of an oceanic island arc.

The occurrence of carbonaceous, sulfidic phases within biotite-quartz-feldspar gneiss and some calc-silicate gneisses indicates that locally stagnant and reducing conditions existed in this marine basin. These rocks represent organic-rich sands
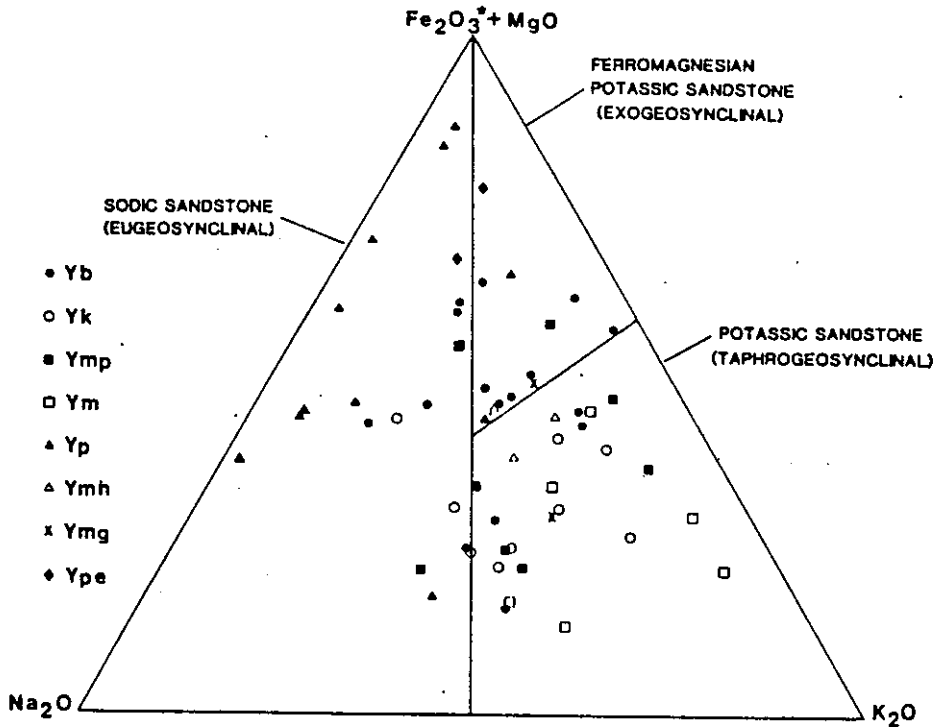
Figure 8. $Na_2O-Fe_2O_3+MgO-K_2O$ diagram after Blatt and others (1972) showing chemical composition of Highlands metasedimentary rocks in relation to tectonic setting. Symbols as in figure 7.
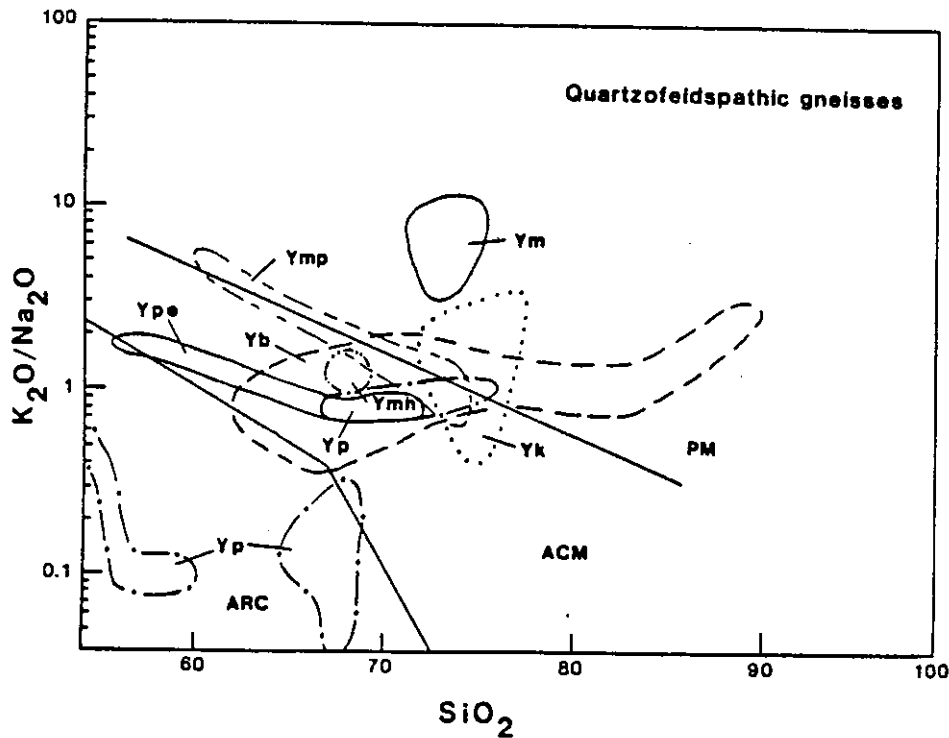
Figure 9. Diagram of log K_2O/Na_2O versus SiO_2 after Roser and Korsch (1986) for Highlands metasedimentary rocks. Fields are: PM, passive margin; ACM, active continental margin; and ARC, ocean island arc margin. Symbols are: Ym, microcline gneiss; Yk, potassic feldspar gneiss; Ymh, hornblende-quartz-feldspar gneiss; Ymp, clinopyroxene-quartz-feldspar gneiss; Yb, biotite-quartz-feldspar gneiss; Ype, pyroxene-epidote gneiss; Yp, pyroxene gneiss.

and lesser muds that grade into non carbonaceous and non sulfidic phases of the same units. Perhaps the euxinic sediments are the result of an oceanward structural high that obstructed circulation and created a less oxygenated environment.

The overall stratigraphy of the marine sequence is ambiguous, but reconstruction of partial successions from different parts of the Highlands suggests a generalized stratigraphic order upward of biotite-quartz-feldspar gneiss, quartzite, pyroxene gneiss, marble, and then more biotite-quartz-feldspar gneiss and pyroxene gneiss. Conformable amphibolite occurs throughout the marine sequence. However, the units in this proposed stratigraphy are not always present. In the western Highlands it appears that marble was deposited directly on the arkosic quartzofeldspathic gneisses.

Intrusive Rocks

Three suites of syn- to post-tectonic granite intrude the Losee Suite, the charnockitic rocks, and the overlying metasedimentary rocks. These were initially named the Byram Gneiss by Spencer and others (1908) for exposures at Byram (currently Byram Township) in Sussex County, and included all granite and gneiss having a potassic composition. Subsequent workers (e.g. Hotz, 1952; Sims, 1958) abandoned the name Byram and mapped granitic rocks according to their constituent mineralogy. Thereby, all granite previously included in the Byram Gneiss became mainly hornblende granite (and related rocks) and pyroxene granite (and related rocks). Drake (1984) renamed hornblende granite and related rocks the Byram Intrusive Suite. Pyroxene granite and related rocks were named the Lake Hopatcong Intrusive Suite by Drake and Volkert (1991) for excellent exposures in the Lake Hopatcong area. These exposures were recognized and mapped by Chapman (1966), Young (1969), Baker and Buddington (1970), and Volkert and others (1989). The third suite is the Mount Eve Granite, recognized and mapped by Hague and others (1956), and later formally named and discussed by Drake and others (1991a).

Byram Intrusive Suite

Rocks of the Byram Intrusive Suite are more or less evenly distributed throughout the Highlands, but are probably most abundant in the Greenwood Lake, Newfoundland, Dover, Mendham, Bernardsville, Gladstone, Califon, Stanhope, Tranquility, and Washington quadrangles. The Byram is variable in texture and ranges from gneissoid granite and lesser granite gneiss to indistinctly foliated granite and pegmatite.

The Byram dominantly consists of hornblende granite (Ybh), biotite granite (Ybb), microperthite alaskite (Yba), hornblende quartz syenite, and hornblende syenite (Ybs). Hornblende quartz syenite is usually mapped with granite or syenite depending on the quartz content. Other phases have also been recognized. While

these are volumetrically insignificant and are not normally mapped separately, they are important for geologic interpretation and merit mention here. Hornblende granite in several areas, most notably the Blairstown quadrangle (Volkert, unpublished data) contains appreciable biotite in nearly equal proportion to hornblende. Elsewhere, hornblende syenite contains sufficient plagioclase that these rocks are more properly termed hornblende monzonite or monzodiorite. This has been noted especially in the Tranquility quadrangle (Volkert, unpublished data).

Byram rocks are characteristically pinkish-gray and medium- to coarse-grained. They contain hornblende or biotite as their dominant mafic mineral. The alaskitic phase contains <5 percent mafic minerals by definition. Quartz is present in varying amounts, and the feldspars are mainly microperthite, oligoclase, and minor microcline. Magnetite is ubiquitous in all phases of the Byram. Sparse amounts of local accessory radioactive minerals are confined to the more differentiated parts of the Byram, namely granite, pegmatite, and alaskite. Most phases of the Byram contain small bodies of amphibolite. However, these are rare or absent in the biotite-bearing phases.

U-Pb data from zircons in a sample of hornblende granite from the Greenwood Lake quadrangle yields an age range of 1122 ± 53 Ma to 1088 ± 41 Ma (Drake and others, 1991b).

Lake Hopatcong Intrusive Suite

Rocks of the Lake Hopatcong Intrusive Suite are found throughout the Highlands, but primarily west of the Green Pond Mountain region. They are most abundant in the Wawayanda, Franklin, Dover, Stanhope, Hackettstown, and High Bridge quadrangles. These rocks are less variable in texture than the Byram and consist mainly of massive, gneissoid to indistinctly foliated rocks. Pegmatite is present, usually as small, discrete bodies, but is much rarer than the abundant pegmatite developed in the Byram rocks.

Lake Hopatcong rocks dominantly consist of granite (Ypg), quartz syenite, syenite (Yps), and alaskite (Ypa). Quartz syenite is usually mapped with the granite or syenite. Less abundant phases of these rocks not mapped separately are quartz monzonite, monzonite, monzodiorite, and granodiorite.

Lake Hopatcong Intrusive Suite rocks are characteristically greenish-gray to greenish-buff and medium- to coarse-grained. They contain clinopyroxene as their dominant mafic mineral. Quartz is present in varying amounts, and the feldspars are mainly mesoperthite to microantiperthite with minor amounts of free oligoclase. Magnetite and titanite are ubiquitous accessory minerals. Amphibolite commonly occurs as small bodies associated with all phases of the Lake Hopatcong Suite.

Comparison of Byram and Lake Hopatcong rocks

The relationship of Byram and Lake Hopatcong rocks poses

another dilemma in deciphering rock relations in the Highlands. Cross cutting relationships and chilled margins are absent between rocks of these two suites and all contacts appear to be conformable. Where Byram and Lake Hopatcong rocks are in contact, a hybrid border phase containing both amphibole and clinopyroxene is occasionally observed. In terms of their respective mineralogy, Byram and Lake Hopatcong rocks define two distinct suites. Despite this difference, it is now clear that striking similarities exist in their chemistry. In order to characterize the overall composition of these rocks and compare them with granites from various tectonic settings, major and trace element analyses were obtained on about 40 samples covering both suites from throughout the Highlands.

Byram and Lake Hopatcong rocks overlap in nearly all concentrations of major oxides. However, Lake Hopatcong rocks contain slightly more Fe_2O_3 and Na_2O and slightly less MgO, CaO, and K_2O (table 1). Trace element concentrations also overlap, although Ba, Rb, Sr, U, and Th tend to be slightly higher in Byram rocks. Both suites are moderately enriched in Y, Nb, and Zr, (table 1) and display similar patterns on chondrite-normalized incompatible element diagrams. Total rare earth element concentrations for both suites overlap and display similar enrichments and depletions. Byram rocks are enriched in light rare earth elements 100 to 500 times relative to chondrite and Lake Hopatcong rocks 70 to 400 times chondrite. On a diagram of molar A/NK versus molar A/CNK (fig. 10), all of the Lake Hopatcong and most of the Byram samples are metaluminous. A few Byram samples are marginally peraluminous.

Byram and Lake Hopatcong rocks fall within the A-type granite compositional field (fig. 11). As defined by Collins and others (1982), White and Chappell (1983), and Whalen and others (1987), A-type granite characteristically contains high SiO_2, Na_2O + K_2O, Nb, Zr, Y, and light rare earth elements and low Al_2O_3, MgO, and CaO. High Nb, Zr, Y, and REE contents are diagnostic of A-type granite and help distinguish it from compositionally similar I-type granite. A-type magma also typically contains fluorine (Collins and others, 1982; Whalen and others, 1987). It is interesting to note that sparse amounts of fluorite occur in Byram rocks in the Hamburg, Pompton Plains, Wanaque, and Franklin quadrangles. Hotz (1953) reports its occurrence in Byram rocks in the Sterling Lake, New York area. The A-type granite geochemical signature was previously interpreted to mean that such rocks were post-tectonic, anorogenic, and had intruded in a within-plate, extensional tectonic setting. This is inconsistent with the known geologic relations in the Highlands which suggest that Byram and Lake Hopatcong rocks are syn-tectonic and were emplaced during a compressional tectonic regime. More recent work involving A-type granite (e.g. Whalen and others, 1987; Sylvester, 1989; and Whalen and Currie, 1990) shows that it may be generated in a variety of tectonic environments unrelated to anorogenic rifting. These may include subduction zone settings.

As stated, Byram and Lake Hopatcong rocks consistently display few discernible differences on plots of various major and trace element combinations. When taken with the above, this leads

Table 1. Average chemical analyses of granite of the Byram and
Lake Hopatcong Intrusive Suites*

	Byram	Lake Hopatcong
No. of samples	16	15
SiO_2	70.32	70.64
TiO_2	0.45	0.45
Al_2O_3	13.61	13.01
Fe_2O_3	1.60	2.66
FeO	2.51	1.71
MgO	0.42	0.27
CaO	1.88	1.50
Na_2O	3.31	4.19
K_2O	5.09	4.58
P_2O_5	0.09	0.07
MnO	0.04	0.08
Ba	1035	929
Rb	141	100
Sr	168	139
Zr	658	813
Nb	31	35
Y	98	87

* Major oxides, weight percent; trace elements, parts per million

inescapably to the question as to whether these rocks do actually
define two distinct and separate intrusive suites. Recent geo-
chemical work suggests that they do not, and permits the follow-
ing interpretation offered here in a rather brief and simplified
fashion. Partial melting of relatively anhydrous lower crustal
source rocks of felsic composition generated magma that was
mainly alkaline (fig. 12), metaluminous, and initially dry.
Hypersolvus Lake Hopatcong rocks were the first to crystallize
from this magma under what Young (1972) and Rhett (1975) propose
were conditions of low water pressure and high temperature. Young
(1972) estimates the temperature was well in excess of $800^{\circ}C$ at
the time of intrusion, whereas Rhett (1975) estimates the temper-
ature to have been closer to $770^{\circ}C$. As the melt became more
hydrous in response to changes in temperature and pressure,
amphibole formed at the expense of clinopyroxene and the meso-
perthitic to microantiperthitic feldspars unmixed to form micro-
perthite and free plagioclase characteristic of subsolvus Byram
rocks.
    Following this scheme, I interpret the Byram and Lake Hopat-
cong rocks to be cogenetic and comagmatic. The principal differ-
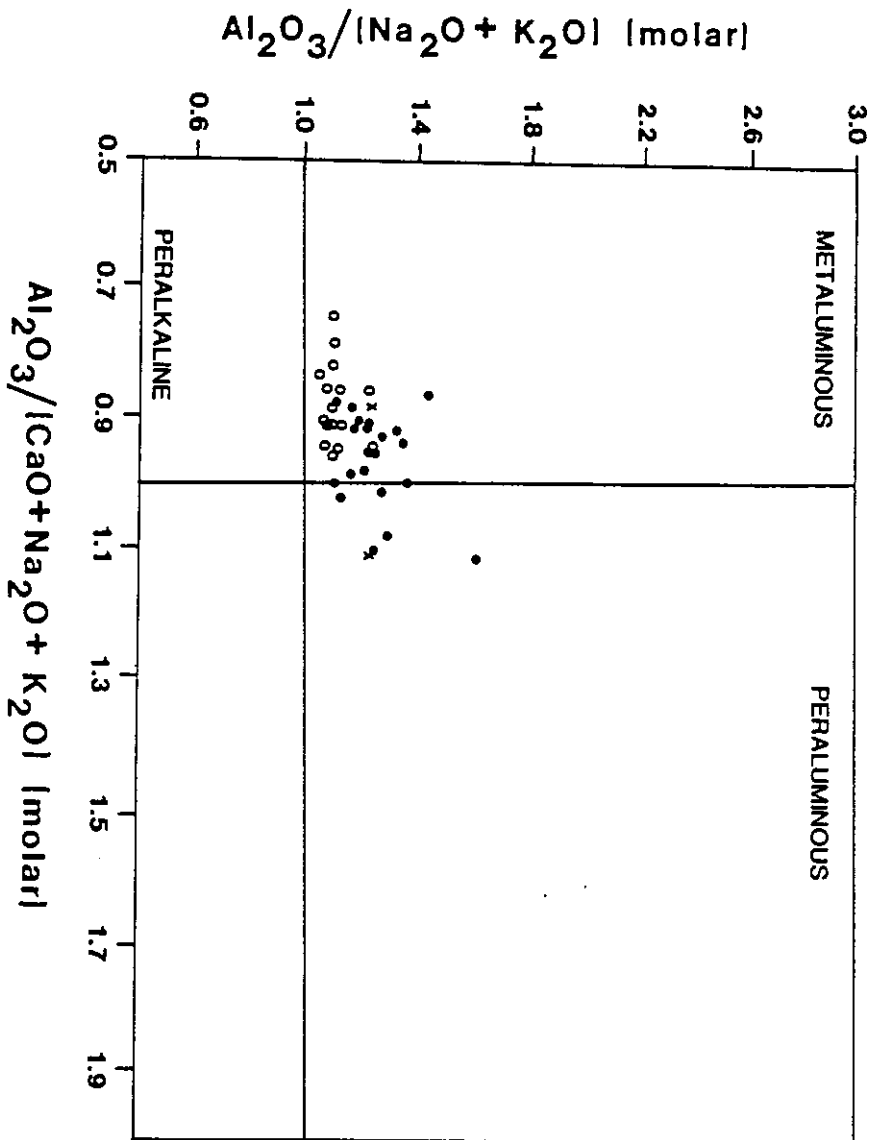
Figure 10. Shand's index showing chemical classification of granitic rocks. Metaluminous, A/NK >1 and A/CNK <1; peraluminous, A/CNK >1. Symbols are: solid circle, Byram Intrusive Suite; open circle, Lake Hopatcong Intrusive Suite; and letter x, Mount Eve Granite.
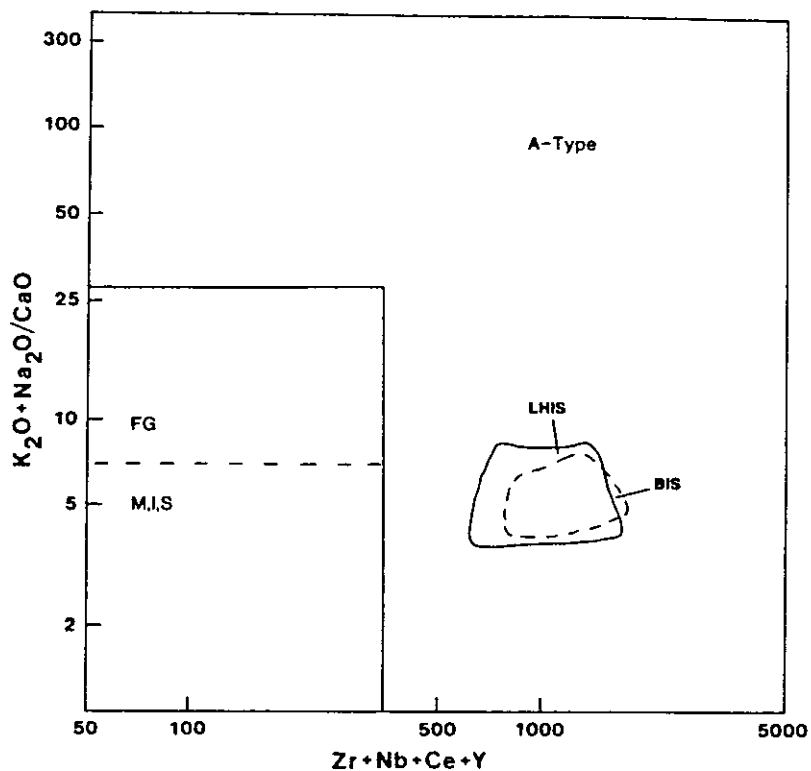
Figure 11. (K$_2$O+Na$_2$O)/CaO versus Zr+Nb+Y discrimination diagram of granitic rocks after Whalen and others (1987). Note overlap of Byram rocks (dashed field) and Lake Hopatcong rocks (solid field) and their restriction to A-type granite field. Other fields are for fractionated granite (FG) and M-, I-, and S-type granites.
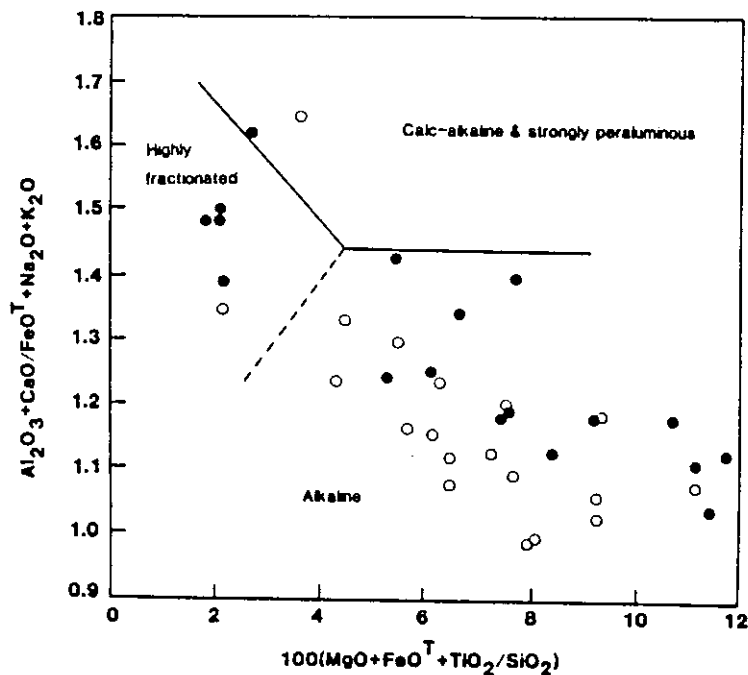
Figure 12. Major element discrimination diagram of granitic rocks after Sylvester (1988) showing plot of Byram and Lake Hopatcong rocks. Symbols as in figure 10.

ences between them are in the mineralogy and the slightly more evolved composition of the Byram. The relatively anhydrous conditions under which the Lake Hopatcong rocks formed favored the development of clinopyroxene and suppressed the formation of pegmatites, which are rare in Lake Hopatcong granite.

Mount Eve Granite

Rocks mapped as Mount Eve Granite (Ygm) occur in the extreme northern Highlands, where they straddle the New Jersey-New York border. They are confined in New Jersey to the Pine Island, Unionville, Wawayanda, and Hamburg quadrangles. They are massive, moderately to indistinctly foliated granite that is light gray to pinkish-gray and medium- to coarse-grained. The Mount Eve contains biotite and subordinate hornblende as its mafic minerals. Quartz is always an important constituent. The feldspars are microperthite and oligoclase. Common accessory minerals include magnetite and allanite.

The Mount Eve is clearly a late synorogenic to postorogenic granite. Geologic mapping by the author in the Hamburg and Wawayanda quadrangles, and by A.A. Drake, Jr. in the Unionville and Pine Island quadrangles, shows that the Mount Eve is discordant to lithologic contacts in adjacent units, contains inclusions of local metasedimentary rock, and has produced contact aureoles where intrusive into the Franklin Marble. U-Pb data from zircons in a sample of Mount Eve from the Pine Island quadrangle provide an age of 1020 ± 4 Ma (Drake and others, 1991a), confirming the late orogenic age. A limited amount of chemical data obtained on the Mount Eve shows the range of major oxides to overlap those of both the Byram and Lake Hopatcong rocks. As defined by the two samples on figure 10, the Mount Eve is metaluminous to marginally peraluminous.

Other Rocks

Amphibolite

The name Pochuck Gneiss was introduced by Spencer and others (1908) for all dark colored gneiss containing hornblende, clinopyroxene, and biotite that is exposed on Pochuck Mountain. The name Pochuck Gneiss was used on the old State geologic map for amphibolite in the Hamburg and Wawayanda quadrangles, but has since been abandoned because the rocks classified as Pochuck are neither lithologically nor stratigraphically distinctive.

Rocks mapped as amphibolite (Ya) are widespread throughout the Highlands, where they occur in virtually every quadrangle. They are associated with nearly all other Middle Proterozoic rock types. Amphibolite is a grayish-black, medium-grained, moderately foliated rock that contains hornblende and plagioclase (andesine). Some phases interlayered with calcareous metasedimentary rocks contain clinopyroxene and some interlayered with

quartzofeldspathic gneiss contain biotite. Hypersthene is a local accessory where amphibolite is associated with more mafic lithologies such as charnockitic rocks. Magnetite is a ubiquitous accessory in practically all phases of amphibolite. In the southwestern Highlands, some amphibolite is locally migmatized by veins and layers of quartz and feldspar (potassic feldspar or plagioclase). Migmatitic amphibolite (Yam) in this part of the Highlands is described by Drake (1984).

Amphibolite is mapped as a single unit in the Highlands, although it clearly has different protoliths. Drake (1984) interprets much of the amphibolite in the southwestern Highlands to be metasedimentary, perhaps originally calcareous shale, since it is conformably interlayered with calc-silicate gneiss and marble. Other amphibolite is metavolcanic. Hague and others (1956) identified pillow structures in amphibolite from Sussex County. A geochemical study by Volkert (Volkert and others, 1986) on a sample from one of the pillow localities showed the protolith to be a tholeiitic basalt closely resembling basalt from a mid-ocean ridge setting. Maxey (1971) chemically analyzed 56 samples of Highlands amphibolites and concluded that all were metabasalt. Still other amphibolite appears to be metagabbro. Baker and Buddington (1970) describe a Sussex County amphibolite with a locally preserved relict primary igneous texture. Hull and others (1986) identified a similar occurrence in the Tranquility quadrangle. A fourth, very distinctive type of amphibolite is a metaporphyry containing rectangular phenocrysts of plagioclase up to an inch or more in length in a matrix of medium-grained hornblende and plagioclase. This type of amphibolite was identified by the author in exposures of limited areal extent in the Stanhope, Tranquility, and Blairstown quadrangles. A similar exposure was identified recently in the Riegelsville quadrangle (D.H. Monteverde, oral communication, 1993). In the Blairstown quadrangle, this rock is completely enclosed in a large body of biotite-hornblende granite. In the Tranquility quadrangle it is intimately layered with charnockitic gneiss and grades along strike into biotite amphibolite. In the Stanhope quadrangle it appears to be spatially associated with Losee, but the stratigraphic relations are masked by exposures of intrusive rocks. Lithologic associations of the Riegelsville amphibolite are unknown. It is likely that this type of amphibolite is metavolcanic based on the known lithologic associations, and also on a geochemical analysis of the rock from Tranquility.

Because amphibolite is derived from different protoliths, it logically follows that not all amphibolite in the Highlands is the same age. That associated with the Losee and charnockitic rocks is obviously the oldest. It very likely is metabasalt, although some may well be metagabbro. Amphibolite interlayered with metasedimentary rocks may be older than amphibolite associated with the Byram and Lake Hopatcong intrusive rocks.

Monazite gneiss

Quartzofeldspathic gneiss containing abundant monazite, as

first recognized by Markewicz (ca. 1965), is very restricted in occurrence. It is discussed here because of its scientific importance and its uniqueness. Monazite gneiss (Ymg) is confined to two exposures. The larger is a single, poorly exposed layer that was mapped in the Chester quadrangle (Volkert and others, 1990) and the Hackettstown quadrangle (Volkert and others, in press), largely on the basis of float and the strong signature of this unit on aeroradiometric maps. A small lens of monazite gneiss was also mapped in the Bernardsville quadrangle (Volkert, unpublished data).

Monazite gneiss is a light-greenish-gray to greenish-buff, medium-grained, massive, moderately foliated rock composed of microperthite, quartz, oligoclase, biotite, and monazite. Accessory minerals include hornblende and magnetite. Monazite occurs as small, reddish-brown, resinous grains.

In the Chester and Hackettstown quadrangles, monazite gneiss is in conformable contact with biotite-quartz-feldspar gneiss and quartz-oligoclase gneiss. Monazite gneiss in the Bernardsville quadrangle is in conformable contact with garnetiferous hornblende-quartz-feldspar gneiss and hornblende granite. At both locations it occurs with rocks of known metasedimentary parentage. Chemical analyses obtained on samples from the Chester and Bernardsville quadrangles are very similar and confirm that these rocks can be placed in the same map unit. Both analyses overlap the chemistry of potassic feldspar gneiss. In addition, the monazite gneiss has a similar mineralogy to potassic feldspar gneiss. Therefore, monazite gneiss is similarly interpreted to be a metasedimentary rock. On figure 7, both samples of monazite gneiss fall in the field of arkose. The monazite in this unit may be detrital and represent a small placer of eroded material from an uplifted continental source that, at least locally, was monazite-rich.

Proterozoic tectonic synthesis of the Highlands

A simplified version of rock relations in the Highlands is shown schematically in figure 13. If rocks of the Losee Suite and the charnockitic rocks are the oldest exposed rocks in the Highlands, then they record an episode of early compressional tectonics at about 1350 to 1300 Ma, resulting from the subduction of a crustal slab beneath the Laurentian continental margin of what is now the eastern United States. Partial melting of the subducting slab generated a series of continental magmatic arcs similar to the present Andes Mountains. Magmatism at this time was mainly calc-alkaline and tholeiitic in composition. Final suturing of these plates occurred sometime after 1300 Ma and produced an uplifted continental block.

This was followed by a period of quiescence and erosion of the continental terrane sometime after 1300 Ma and until about 1122 Ma. Early sedimentation may have occurred in a cratonic basin setting with the deposition of some quartzite and arkosic material that is now potassic feldspar gneiss, microcline gneiss,
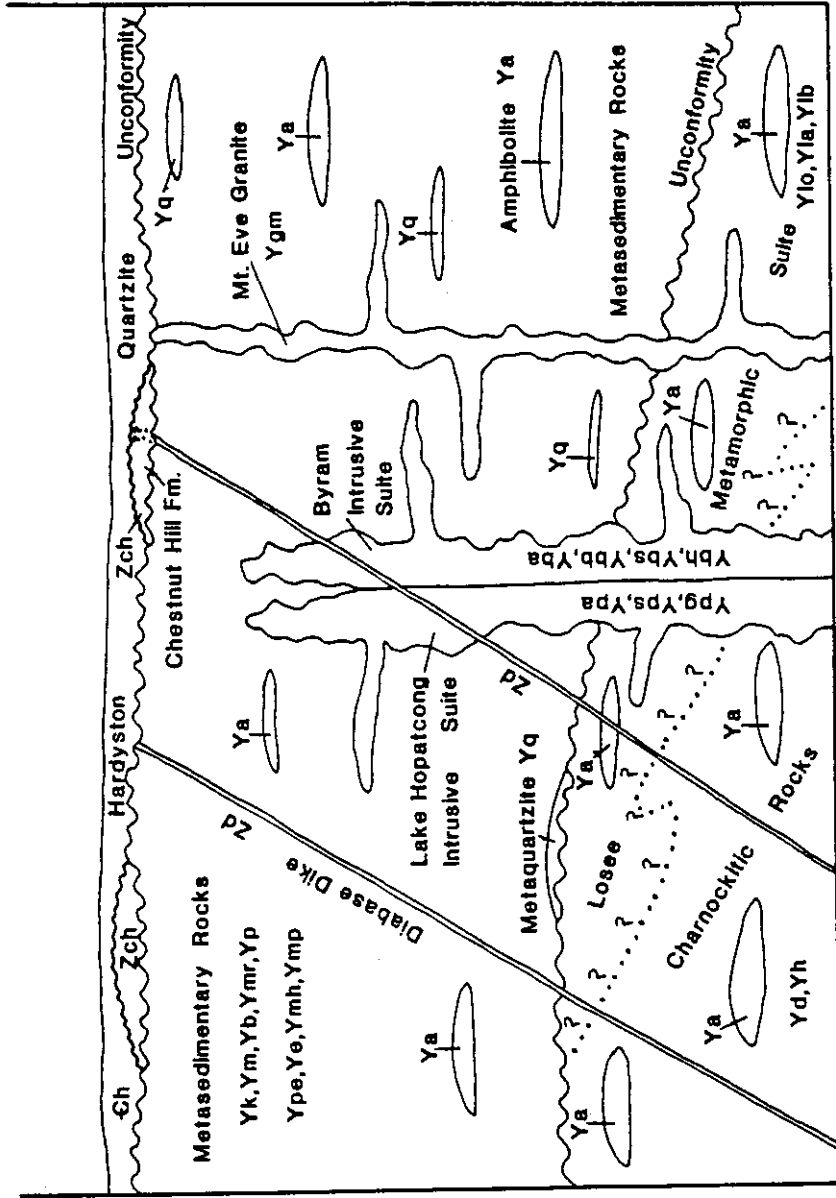
Figure 13. Schematic diagram showing inferred stratigraphic relations of major Middle and Late Proterozoic rock units of the New Jersey Highlands

49

and perhaps monazite gneiss. A subsequent change in the composition of material shed from the source area led to an increase in the amount of lithic fragments over feldspar and deposition of the lithic arenites. Perhaps this marked a transition from sedimentation in a largely terrestrial environment to a shallow marine one. Continued erosion of the continental source and the onset of an extensional tectonic regime resulted in marine transgression. This led to the deposition of a mixed sequence of quartz sandstone, calcareous rocks, limestone, and graywacke in a marine environment. Some sedimentation was probably associated with tholeiitic basalt from a small spreading center in this basin. This is consistent with the close spatial association of amphibolite containing relict pillow structures and marble along the eastern margin of Pochuck Mountain.

Sedimentation was interrupted by the eventual destruction of this basin during the onset of compressional tectonics occurring at about 1122 Ma and lasting until 900 Ma. The onset of this interval likely was marked by the development of an oceanic island arc. During the interval between 1122 Ma and about 1000 Ma, magma of dominantly alkaline, metaluminous composition was generated and the granites and related rocks of the Lake Hopatcong and Byram Intrusive Suites were emplaced. This was followed by the full intensity of Grenville orogenesis during which all Middle Proterozoic rocks of the New Jersey Highlands were metamorphosed at upper amphibolite to granulite facies. The Mount Eve Granite was emplaced at about 1020 Ma during the waning stages of Grenville orogenesis and some late pegmatites were intruded.

Between about 900 Ma and 760 Ma another period of quiescence occurred. This was followed at about 760 Ma by the onset of extensional tectonics and rifting of the proto-North American continent. Continental rift basins were the setting for the deposition of the Late Proterozoic Chestnut Hill Formation (Drake, 1984), a weakly metamorphosed sequence of interbedded clastic and metavolcanic rocks and metasaprolite. These rocks are currently very locally preserved as erosional remnants and as small slices along faults mainly in the southwest Highlands. Continued rifting produced fissures in the crust that acted as conduits allowing diabase dikes of Late Proterozoic age (Puffer and others, 1991; Volkert and Puffer, in press) to intrude Middle Proterozoic rocks throughout the Highlands. Cessation of Late Proterozoic sedimentation and magmatism in the Highlands was followed by further quiescence, erosion, and deposition of the Hardyston Quartzite during the early Cambrian.

Acknowledgements

References Cited

Aleinikoff, J.N., Ratcliffe, N.M., Burton, W.C., and Karabinos, P., 1990, U-Pb ages of Middle Proterozoic igneous and metamorphic events, Green Mountains, Vermont: Geological Society of America Abstracts with Programs, v. 22, p. 1.

Bailey, J.C., 1981, Geochemical criteria for a refined tectonic discrimination of orogenic andesites: Chemical Geology, v. 32, p. 139-154.

Baker, D.R., and Buddington, A.F., 1970, Geology and magnetite deposits of the Franklin quadrangle and part of the Hamburg quadrangle, New Jersey: U.S. Geological Survey Professional Paper 638, 73 p.

Bhatia, M.R., 1983, Plate tectonics and geochemical compositions of sandstones: Journal of Geology, v. 91, p. 611-627.

Blatt, Harvey, Middleton, Gerard, and Murray, Raymond, 1972, Origin of sedimentary rocks: Englewood Cliffs, New Jersey, Prentice-Hall, Inc., 634 p.

Chapman, D.F., 1966, Petrology and structure of the Byram Cove synform, Precambrian Highlands, New Jersey: New Brunswick, New Jersey, Rutgers University, unpublished M.S. thesis, 116 p.

Collins, W.J., Beams, S.D., White, A.J.R., and Chappell, B.W., 1982, Nature and origin of A-type granites with particular reference to southeastern Australia: Contributions to Mineralogy and Petrology, v. 80, p. 189-200.

Drake, A.A., Jr., 1969, Precambrian and Lower Paleozoic geology of the Delaware Valley, New Jersey-Pennsylvania, in Subitzky, S., ed., Geology of selected areas in New Jersey and eastern Pennsylvania and Guidebook of Excursions: New Brunswick, New Jersey, Rutgers University Press, p. 51-131.

------, 1984, The Reading Prong of New Jersey and eastern Pennsylvania: An appraisal of rock relations and chemistry of a major Proterozoic terrane in the Appalachians, in Bartholomew, M.J., ed., The Grenville event in the Appalachians and related topics: Geological Society of America Special Paper 194, p. 75-109.

Drake, A.A., Jr., Aleinikoff, J.N., and Volkert, R.A., 1991a, The Mount Eve Granite (Middle Proterozoic) of northern New Jersey and southeastern New York, in Drake, A.A., Jr., ed., Contributions to New Jersey Geology: U.S. Geological Survey Bulletin 1952, p. C1-C10.

------, 1991b, The Byram Intrusive Suite of the Reading Prong-

Age and tectonic environment, in Drake, A.A., Jr., ed.,
Contributions to New Jersey Geology: U.S. Geological Survey
Bulletin 1952, p. D1-D14.

Drake, A.A., Jr., and Volkert, R.A., 1991, The Lake Hopatcong
Intrusive Suite (Middle Proterozoic) of the New Jersey
Highlands, in Drake, A.A., Jr., ed., Contributions to
New Jersey Geology: U.S. Geological Survey Bulletin 1952,
p. A1-A9.

Garrels, R.M., and McKenzie, F.T., 1971, Evolution of sedimentary
rocks: New York, Norton, 397 p.

Hague, J.M., Baum, J.L., Hermann, L.A., and Pickering, R.J.,
1956, Geology and structure of the Franklin-Sterling area,
New Jersey: Geological Society of America Bulletin, v. 67,
p. 435-474.

Hotz, P.E., 1953, Magnetite deposits of the Sterling Lake, N.Y.-
Ringwood, N.J. area: U.S. Geological Survey Bulletin 982-F,
p. 153-244.

Hull, J.M., Koto, R.Y., and Bizub, R., 1986, Deformation zones
in the Highlands of New Jersey, in Husch, J.M., and
Goldstein, F.R., eds., Geology of the New Jersey Highlands
and radon in New Jersey: Field guide and proceedings of the
third annual meeting of the Geological Association of New
Jersey, p. 19-66.

Irvine, N.T., and Baragar, W.A.R., 1971, A guide to the chemical
classification of common volcanic rocks: Canadian Journal of
Earth Science, v. 8, p. 523-543.

Jakes, P., and White, A.J.R., 1972, Major and trace element abun-
dances in volcanic rocks of orogenic areas: Geological
Society of America Bulletin, v. 83, p. 29-40.

Kastelic, R.L., Jr., 1979, Precambrian geology and magnetite
deposits of the New Jersey Highlands in Warren County, New
Jersey: Bethlehem, Pennsylvania, Lehigh University, unpub-
lished M.S. thesis, 148 p.

Lewis, J.L., and Kummel, H.B., 1912, Geologic map of New Jersey:
New Jersey Department of Conservation and Development, Atlas
Sheet no. 40, scale 1:250,000.

Markewicz, F.J., ca. 1965, Chester monazite belt: Unpublished
report on file in the office of the New Jersey Geological
Survey, Trenton, New Jersey, 6 p.

Maxey, L.R., 1971, Metamorphism and origin of Precambrian amphi-
bolite of the New Jersey Highlands: New Brunswick, New
Jersey, Rutgers University, unpublished PhD dissertation,
156 p.

McLelland, J.M., and Chiarenzelli, J.R., 1991, Geochronological studies in the Adirondack Mountains and the implications of a Middle Proterozoic tonalitic suite, in Gower, C.F., Rivers, T., and Ryan, B., eds., Mid-Proterozoic Laurentia-Baltica: Geological Association of Canada Special Paper 38, p. 175-194.

Metsger, R.W., 1977, Notes on the Precambrian metalimestones of northern New Jersey, in Stratigraphy and applied geology of the Lower Paleozoic carbonates in northwestern New Jersey: Guidebook for the 42nd Annual Field Conference of Pennsylvania Geologists, p. 48-54.

Metsger, R.W., Tennant, C.B., and Rodda, J.L., 1958, Geochemistry of the Sterling Hill zinc deposit, Sussex Co., N.J.: Geological Society of America Bulletin, v. 69, p. 775-788.

Offield, T.W., 1967, Bedrock geology of the Goshen-Greenwood Lake area, N.Y.: New York State Museum and Science Service Map and Chart Series, no. 9, 78 p.

Peck, F.B., 1904, The talc deposits of Phillipsburg, N.J. and Easton, Pa.: Geological Survey of New Jersey, Annual Report of the State Geologist for the year 1904, p. 161-185.

Puffer, J.H., and Volkert, R.A., 1991, Generation of trondhjemite from partial melting of dacite under granulite facies conditions: An example from the New Jersey Highlands, USA: Precambrian Research, v. 51, p. 115-125.

Puffer, J.H., Volkert, R.A., and Hozik, M.J., 1991, Probable Late Proterozoic mafic dikes in the New Jersey Highlands: Geological Society of America Abstracts with Programs, v. 23, p. 118.

Rhett, D.W., 1975, Phase relationships and petrogenetic environment of Precambrian granites of the New Jersey Highlands: New Brunswick, New Jersey, Rutgers University, unpublished PhD dissertation, 157 p.

Roser, B.P., and Korsch, R.J., 1986, Determination of tectonic setting of sandstone-mudstone suite using SiO_2 content and K_2O/Na_2O ratio: Journal of Geology, v. 94, p. 635-650.

Sims, P.K., 1958, Geology and magnetite deposits of the Dover district, Morris County, New Jersey: U.S. Geological Survey Professional Paper 287, 162 p.

Sims, P.K., and Leonard, B.F., 1952, Geology of the Andover mining district, Sussex County, New Jersey: New Jersey Department of Conservation and Economic Development, Bulletin 62, 46 p.

Spencer, A.C., Kummel, H.B., Wolff, J.E., Salisbury, R.D., and

Palache, C., 1908, Franklin Furnace, New Jersey: U.S. Geological Survey Geologic Atlas, Folio 161, 27 p.

Streckeisen, A., 1976, To each plutonic rock its proper name: Earth Science Reviews, v. 12, p. 1-33.

Sylvester, P.J., 1988, Post-collisional alkaline granites: Journal of Geology, v. 97, p. 261-280.

Van De Kamp, P.C., Leake, B.E., and Senior, A., 1976, The petrography and geochemistry of some Californian arkoses with application to identifying gneisses of metasedimentary origin: Journal of Geology, v. 84, p. 195-212.

Volkert, R.A., and Drake, A.A., Jr., 1990, New geologic map of the New Jersey Highlands: Geological Society of America Abstracts with Programs, v. 22, p. 76-77.

Volkert, R.A., Drake, A.A., Jr., Hull, J.M., and Koto, R.Y., 1986, Road log for the field trip on the geology of the New Jersey Highlands, in Husch, J.M., and Goldstein, F.R., eds., Geology of the New Jersey Highlands and radon in New Jersey: Field guide and proceedings of the third annual meeting of the Geological Association of New Jersey, p. 67-116.

Volkert, R.A., Markewicz, F.J., and Drake, A.A., Jr., 1990, Bedrock geologic map of the Chester quadrangle, Morris County, New Jersey: New Jersey Geological Survey Geologic Map Series GMS 90-1, scale 1:24,000.

Volkert, R.A., Monteverde, D.H., and Drake, A.A., Jr., 1989, Geologic map of the Stanhope quadrangle, Morris and Sussex Counties, New Jersey: U.S. Geological Survey Geologic Quadrangle Map GQ-1671, scale 1:24,000.

------, Bedrock geologic map of the Hackettstown quadrangle, Morris, Warren, and Hunterdon Counties, New Jersey: New Jersey Geological Survey Geologic Map Series GMS 93-3, scale 1:24,000, in press.

Volkert, R.A., and Puffer, J.H., Late Proterozoic diabase dikes of the New Jersey Highlands: A remnant of Iapetan rifting in the north-central Appalachians, in Drake, A.A., Jr., ed., Geologic Studies in New Jersey and eastern Pennsylvania: U.S. Geological Survey Professional Paper, in press.

Whalen, J.B., and Currie, K.L., 1990, The Topsails igneous suite, western Newfoundland; Fractionation and magma mixing in an "orogenic" A-type granite suite, in Stein, H.J., and Hannah, J.L., eds., Ore-bearing granite systems; Petrogenesis and mineralizing processes: Geological Society of America Special Paper 246, p. 287- 299.

Whalen, J.B., Currie, K.L., and Chappell, B.W., 1987, A-type
    granites: geochemical characteristics, discrimination and
    petrogenesis: Contributions to Mineralogy and Petrology,
    v. 95, p. 407-419.

White, A.J.R., and Chappell, B.W., 1983, Granitoid types and
    their distribution in the Lachlan fold belt, southeastern
    Australia: Geological Society of America Memoir 159,
    p. 21-34.

Wolff, J.E., and Brooks, A.H., 1898, The age of the Franklin
    white limestone of Sussex County, New Jersey: U.S. Geologi-
    cal Survey 18th Annual Report, part 2, p. 425-457.

Young, D.A., 1969, Petrology and structure of the west-central
    New Jersey Highlands: Providence, Rhode Island, Brown
    University, unpublished PhD dissertation, 194 p.

-----, 1972, A quartz syenite intrusion in the New Jersey
    Highlands: Journal of Petrology, v. 13, p. 511-528.

CHAPTER 3

PRECAMBRIAN IRON DEPOSITS OF THE NEW JERSEY HIGHLANDS

Puffer, John H.; Pamganamamula, Rao V.; and Davin, Mark T.,
Department of Geological Sciences, Rutgers, The State
University of New Jersey, Newark, New Jersey 07102

INTRODUCTION

Several excellent studies of iron mineralization in the
Proterozoic rocks of the New Jersey Highlands have been
published during the last 40 years including major efforts by
Buddington (1966), Buddington and Leonard (1962), Baker and
Buddington (1970), Collins (1970), Hotz (1970), Sims (1970),
and Sims and Leonard (1952). These publications include
detailed descriptions of the mineralogy, lithology, and
geologic setting of most iron deposits in New Jersey together
with speculation regarding their origin. Speculation was
divided between proposals that the iron concentrations were
precipitated from hydrothermal solutions and proposals that
most of the iron was contained in sedimentary rocks that were
subsequently metamorphosed. The debate continues and includes
some recent and quite radical modifications of earlier
hydrothermal (Puffer, 1980) and syngenetic arguments
(Kastelic, 1980; Gunderson, 1986).

A problem faced by the authors of these earlier studies
was the lack of chemical data other than some major element
analyses of host rocks and some iron and a few titanium
analyses of ore samples published by Bayley (1910). The
conclusions that we offer in this report are based on some of
the first trace element analyses of both iron ore and mineral
concentrates sampled from most of the larger ore deposits
located throughout the New Jersey Highlands. Our data
suggests that a few of the Highlands deposits are probably
syngenetic but that most of the magnetite concentrations were
precipitated out of hydrothermal fluids generated by dehydra-
tion reactions during granulite facies metamorphism.

GEOLOGIC SETTING

Figure 1, based on a compilation of USGS and NJGS
geologic mapping as of 1992, groups the Precambrian rocks of
the New Jersey Highlands into 6 types: 1) Granites including
the Hornblende granites, syenites and alaskites of the Byram
intrusive suite and the Pyroxene granites, syenites and
alaskites; 2) Diorite and related orthogneises; 3) The Losee
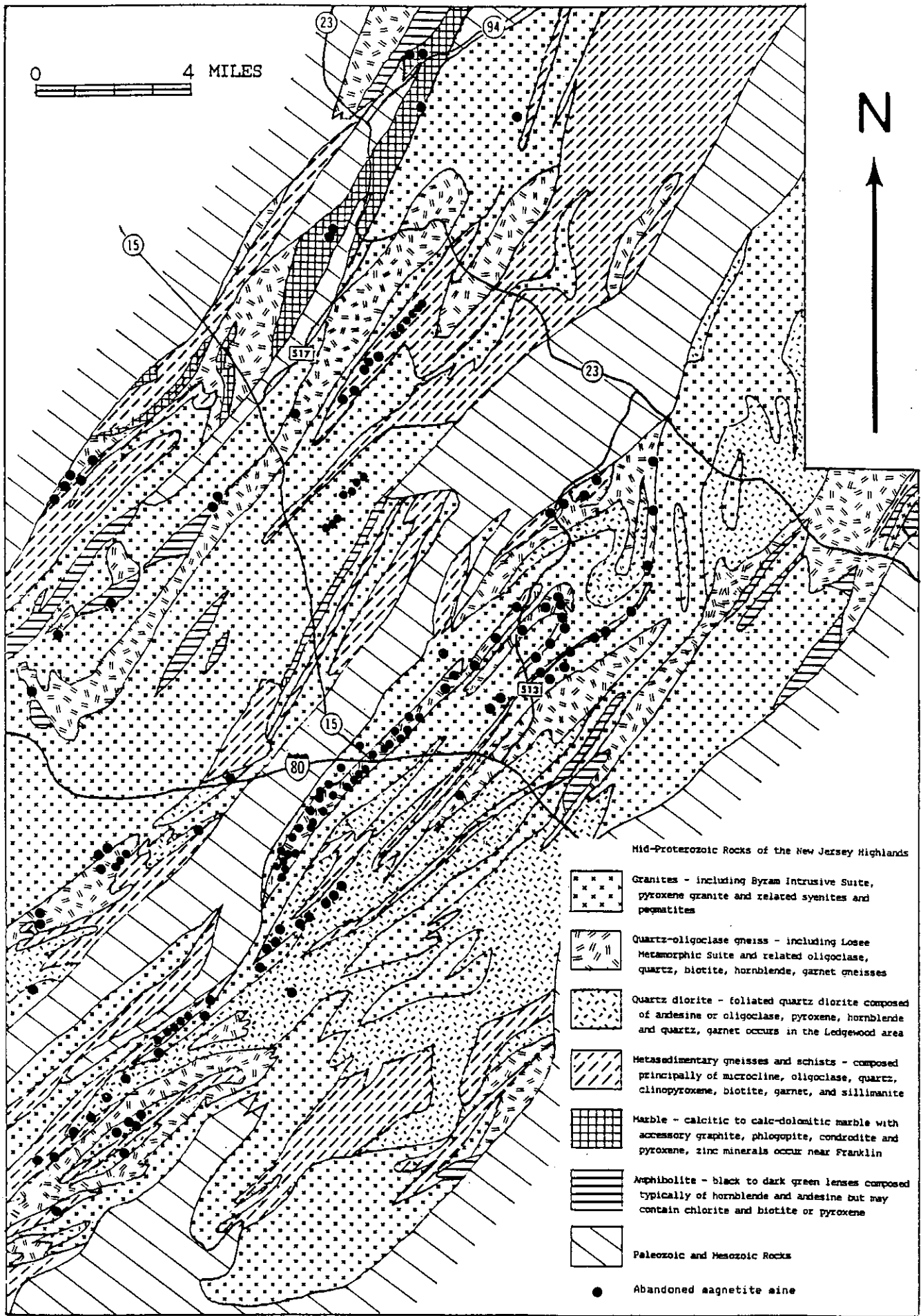
Figure 1: Geologic map of the central New Jersey Highlands with iron mine locations.

The map includes the following elements:

- Scale bar: 0 to 4 MILES
- North arrow (N)
- Highway markers: 23, 94, 15, 517, 80, 513

Mid-Proterozoic Rocks of the New Jersey Highlands

Granites - including Byram Intrusive Suite, pyroxene granite and related syenites and pegmatites

Quartz-oligoclase gneiss - including Losee Metamorphic Suite and related oligoclase, quartz, biotite, hornblende, garnet gneisses

Quartz diorite - foliated quartz diorite composed of andesine or oligoclase, pyroxene, hornblende and quartz, garnet occurs in the Ledgewood area

Metasedimentary gneisses and schists - composed principally of microcline, oligoclase, quartz, clinopyroxene, biotite, garnet, and sillimanite

Marble - calcitic to calc-dolomitic marble with accessory graphite, phlogopite, condrodite and pyroxene, zinc minerals occur near Franklin

Amphibolite - black to dark green lenses composed typically of hornblende and andesine but may contain chlorite and biotite or pyroxene

Paleozoic and Mesozoic Rocks

● Abandoned magnetite mine

Gneiss and related meta-volcanic quartz-oligoclase gneisses; 4) Meta-sedimentary rock types other than marble and amphibolite; 5) The Franklin and Wildcat Marbles; and 6) amphibolites. Although most of the iron deposits occur within or close to the margins of leucocratic oligoclase enriched rocks particularly the Losee Gneiss, iron deposits are found within each of these 6 diverse and genetically unrelated rock types (Table 1). Virtually all of the iron deposits occur as either disseminated magnetite concentrations or veins oriented subparallel and conformable to the regional north-east strike of the Highlands rocks (Fig. 1).

Figure 2 illustrates AKF and ACF diagrams that represent the Granulite metamorphic facies. Several mineral assemblages found in the rocks of the New Jersey Highlands are represented in Figure 2 and there is little doubt that Granulite facies conditions or at least upper Amphibolite facies conditions prevailed during metamorphic equilibration of Highlands rocks. Figure 3 illustrates the approximate 700 to 900 C° temperature and 3 to 10 kbars pressure range represented by upper Amphibolite facies to middle Granulite facies environments.

METHODS

Of the approximately 300 magnetite mines and prospects that are hosted by Precambrian rocks in New Jersey approximately 190 occur within the central New Jersey Highlands area (Figure 1). During the last 20 years, and particularly during 1993, Dr. Puffer has attempted to examine each of the Precambrian iron mines in New Jersey. Over half of these mines, however, are no longer exposed and have been completely relandscaped typically under housing developments or farms. Many of the mines that can be located are poorly exposed and are represented by only a small cut or a few ore samples in a small tailings pile. About 36 mines, however, are still exposed enough or are represented by a large enough tailings or abandoned drill core pile to gain some insight into the geology of the mine. Wherever possible ore samples were collected at such mines typically consisting of five or six three pound samples. The ore samples judged to be the most representative were then cut, crushed and split into separates to be analyzed for whole rock chemistry, petrology (hand specimen, thin section and polished section analyses), and oxide content. Each ore sample chosen for analysis would be considered high grade on the basis of an oxide content ranging from 25 to 95 volume percent. Samples containing in excess of

Amphibolite Hosted

	Daven GP	MtHope	Dodge	Ford	Blue	Hibernia	H. Ledge	Fairview
SiO2	1.42	2.11	2.01	1.21	1.85	1.35	1.39	1
TiO2	1.35	1.33	3.04	2.52	0.94	1.75	3.78	1.85
MnO	0.41	0.35	0.33	0.21	0.19	0.07	0.33	0.05
FeOt	88.95	89.31	92.45	79.38	86.35	89.74	91.59	91.31

Pyroxenite Hosted

	Cogill	DeHart	George
SiO2	0.98	1.23	1.38
TiO2	5.32	5.21	3.19
MnO	0.53	0.46	0.24
FeOt	79.72	83.05	82.06

Quartz-Oligoclase Gneiss Hosted

	Dickers.	L.Baker	Scrub O.	Wawayu.	Byrant	Righter	Gulick	Baker
SiO2	1.23	0.86	0.74	0.98	0.89	0.73	0.86	1.73
TiO2	1.59	1.22	0.71	0.92	1.97	1.64	1.22	2.98
MnO	0.32	0.31	0.06	0.35	0.37	0.35	0.36	0.07
FeOt	92.32	93.04	88.52	91.42	91.46	91.28	87.31	94.39

	Allen	Randall	Richard	Leonard	Elizabeth	Evers
SiO2	1.91	0.97	0.87	0.99	1.62	0.94
TiO2	1.46	3.16	1.35	1.26	1.18	1.76
MnO	0.07	0.08	0.13	0.07	0.06	0.09
FeOt	95.31	89.26	87.79	93.21	94.22	88.73

Meta-sedimentary K-spar Gneiss Hosted

	Edison	ShermanB	DavenBV	Bunker	McKean	Beach Gl
SiO2	1.32	1.21	1.21	1.42	1.32	1.72
TiO2	1.28	1.03	4.87	3.99	4.38	1.15
MnO	0.39	0.41	0.55	0.36	0.45	0.26
FeOt	94.01	93.16	86.32	88.93	94.95	94.21

Marble Hosted

	Rossville	Sulfur Hill	Andover	Ahles	PikePeak
SiO2	2.01	0.41	0.62	0.25	0.41
TiO2	0.27	0.06	0.09	0.08	0.11
MnO	0.45	0.36	0.49	0.73	0.68
FeOt	88.92	85.31	84.64	85.22	86.41

Table 1: Chemical composition of magnetite concentrates separated from high grade ore samples at most of the larger iron mines within the New Jersey Highlands. SiO2 values are related to the purity of the magnetite concentrate; FeOt values are deminished by the magnitude of included Fe2O3 and Fe(OH)3 caused by low temperature oxidation.
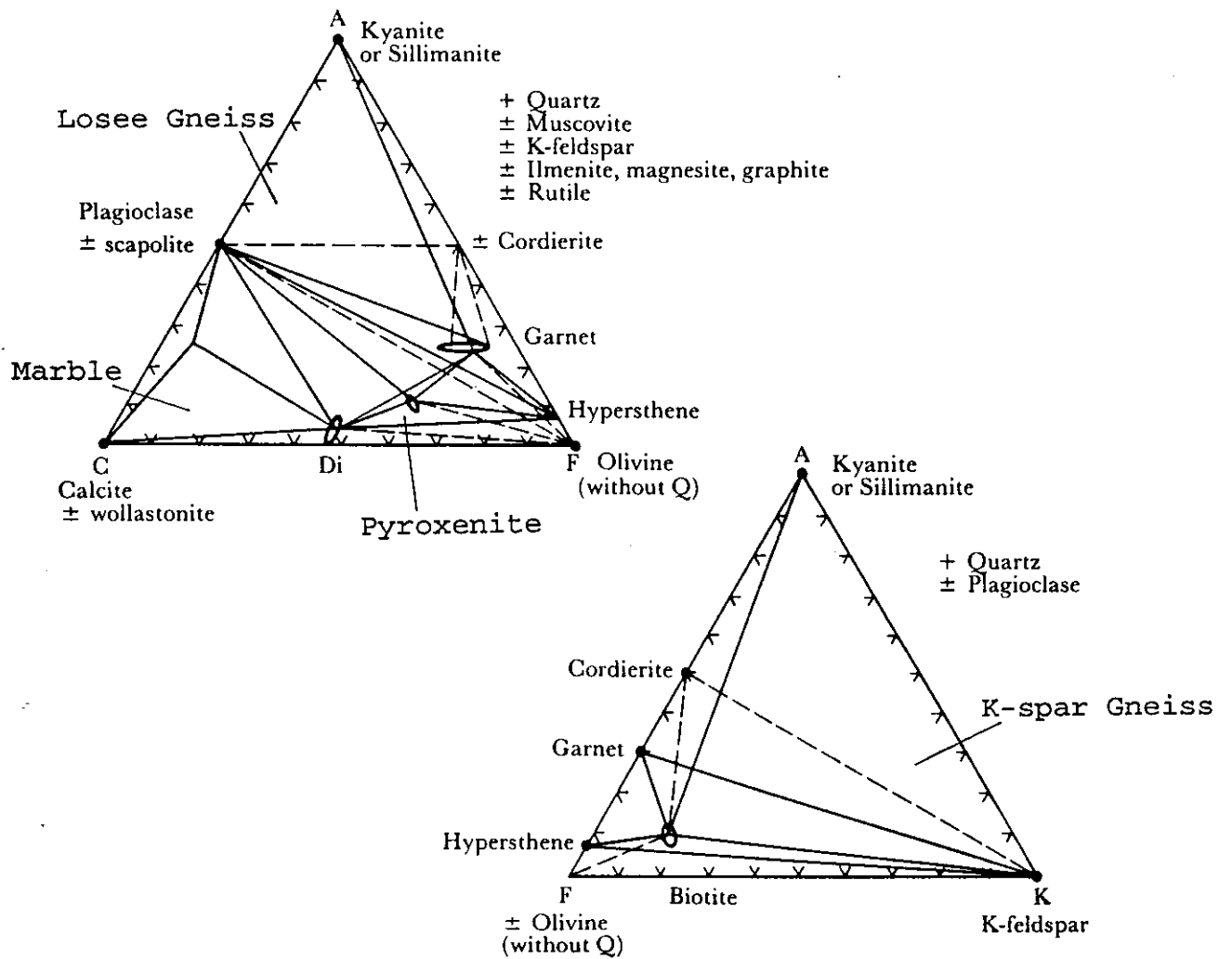
Figure 2: AKF and ACF diagrams pertaining to granulite facies conditions after Hyndman (1985). Note several mineral assemblages found in metamorphic rocks of the New Jersey Highlands.
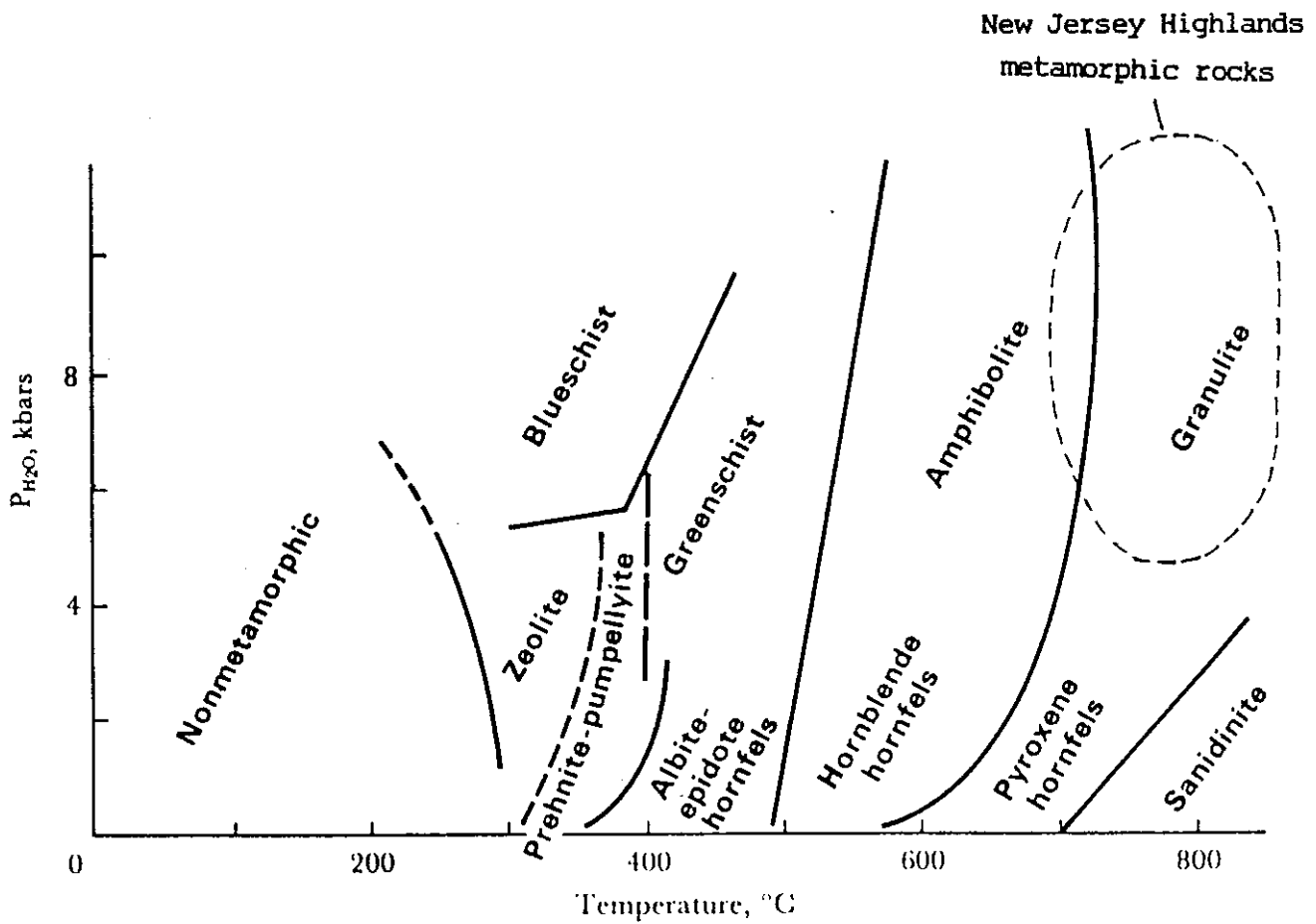
Figure 3: Metamorphic facies with boundaries based on experimental data
reviewed by Hyndman (1985). Note the probable 700 to 800 C° and 3 to 12
kb environment of New Jersey Highlands metamorphism based on upper
amphibolite to granulite facies mineral assemblages.

61

95 percent oxide content were not chosen so that the influence of the gangue minerals on the chemistry of the ore could be assessed.

Magnetite, biotite and in a few cases some other minerals were separated from splits of crushed ore using magnetic and heavy-liquid separation methods. Mineral separates were further purified of contamination by hand picking under a binocular microscope. Ore samples and mineral concentrates were chemically analyzed with a Rigaku wavelength dispersive x-ray fluorescence spectroscope. Microprobe techniques were rejected as an alternative method for magnetite analysis because of the presence of fine exsolution/oxidation lamellae of ilmenite that have depleted the titanium content of the host magnetite below solidus or primary hydrothermal precipitation levels. Microprobe analyses would have, therefore, yielded erroneous subsolvus levels of any elements exsolved into exsolution lamellae. The resulting XRF data presented in this report are some of the first analyses of TiO_2, V, Mn, Cr, P, and Ni, in Highlands iron ore and magnetite since those published by Bayley (1910).

RESULTS

The resulting data indicates that there are two distinct populations of iron deposits within the New Jersey Highlands:

Group 1- is a population characterized primarily by a low titanium content including < 0.2 weight percent TiO_2 in the whole rock and < 0.25 weight percent TiO_2 in the magnetite concentrate (Fig. 4). Group 1 samples are also characterized by a wide range of MnO and by elevated calcium, sulfur, copper, and zinc whole rock content.

Group 2- is a population characterized primarely by a TiO_2 range of 0.6 to 4.9 weight percent within the whole rock and a range of 0.7 to 5.4 weight percent within the magnetite concentrate. There is a distinct gap separating the TiO_2 content of the two groups (Figure 4).

INTERPRETATIONS

Group 1 Iron Deposits.

Group 1 deposits include most of the deposits contained within the Franklin Marble and any of the carbonate enriched meta-sedimentary rocks of the New Jersey Highlands including some but not all of the rocks described as "skarns" by Sims

New Jersey Magnetite Concentrates
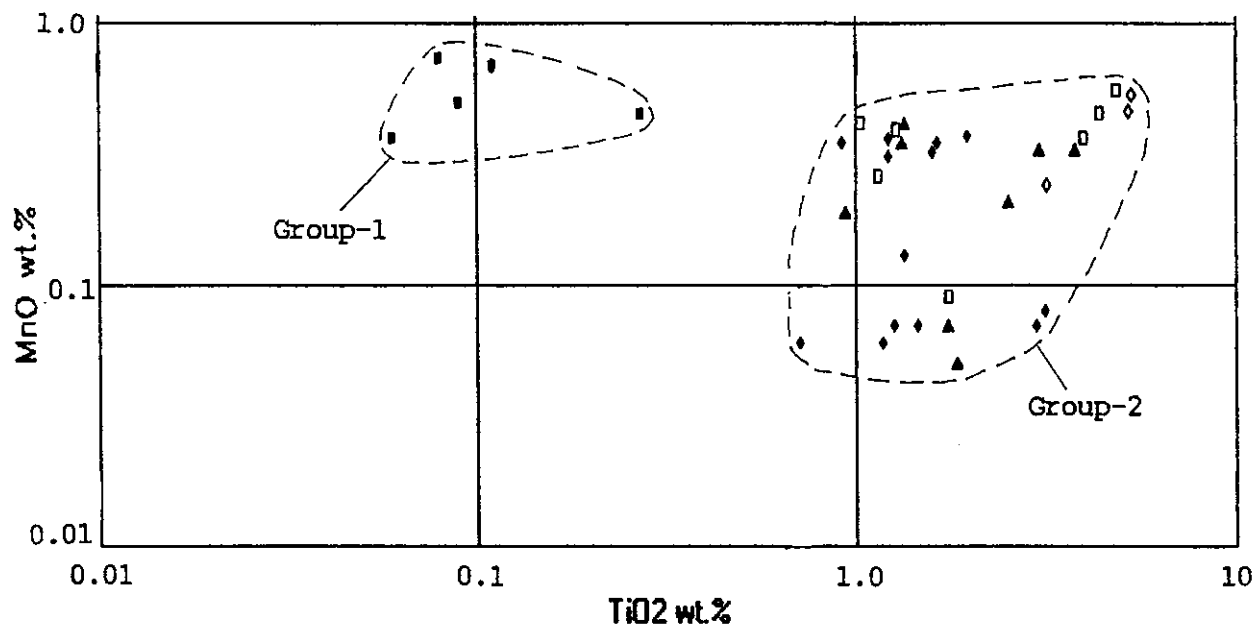
Figure 4: Log-Log plot of TiO_2 and MnO content of New Jersey magnetite ores illustrating the distinction between Group-1 iron ores (low TiO_2, variable MnO) and Group-2 ores (0.7 to 5.3 % TiO_2 and < 0.6 percent MnO).

(1958) and other authors. Such deposits are common in Warren County, near Franklin, New Jersey, and near Andover, New Jersey. The host rocks of Group 1 deposits are typically composed of magnetite, carbonates, garnet, sulfides, plagioclase, amphibole, and pyroxene. The ore mineral is typically magnetite but a few deposits contain abundant hematite. In each case the deposits are devoid of ilmenite phases other than very rare ilmenite exsolution lamellae contained within magnetite.

Group 1 Warren County Deposits.

The magnetite deposits of Warren County are described by Kastelic (1979) as sharply bounded tabular-shaped bodies composed of magnetite and quartz with minor pyrite. Most of the magnetite deposits of Warren County are hosted by Franklin Marble or calc-silicate lenses adjacent to or surrounded by marble.

One of the larger mines in the marble belt is the Ahles mine which was described by Bayley (1910) as a deeply altered soft limonite-pyrolusite rock with minor residual magnetite containing up to 11 percent MnO_2, but very low concentrations of TiO_2, P_2O_5, and S (Table 2).
None of the mines in the marble belt have been preserved and are no longer visible although the Ahles mine dump is a source of ore samples.

The iron ores hosted by calc-silicate rocks include: (1) the Kaiser mine which is hosted by a garnet-biotite-clinopyroxene schist that is bounded by amphibolite and marble; The magnetite of the Kaiser mine contains rare exsolution lamellae of ilmenite; (2) the Barton mine described by Bayley (1910) as interlayered hornblende, biotite, and magnetite; The Barton mine is hosted by quartz-epidote gneiss containing magnetite and garnet and is associated with pyroxenite layers; (3) the Pequest mine which is hosted by a magnetite and calcite bearing diopside pyroxenite surrounded by quartz-epidote gneiss; and (4) the Washington mine which is a pyrite-bearing magnetite-quartz rock associated with diopsidic clinopyroxenite and granitic pegmatites. Kastelic (1979) interprets the protolith of these deposits as siliceous siderite muds intercalated with siliceous dolomite and minor pyrite which was metamorphosed into magnetite-quartz concentrations in various calc-silicate assemblages.

Group 1 Andover Deposits.

A second example of Group 1 iron deposits is represented by the Andover mining district (Figure 5) described by Sims and Leonard (1952). The district consists of two large mines (the Andover and the Sulphur Hill) and two small mines (the Tar Hill and the Longcore). The ore at the Sulphur Hill mine is disseminated magnetite with calcite, dolomite, andradite garnet, pyroxene, and pyrrhotite with minor pyrite, marcasite, sphalerite, chalcopyrite, galena, and molybdenite. The ore at the Andover mine consists primarely of hematite, fine grained earthy iron hydroxides, red amorphous silica (jasper) and variable concentrations of relic magnetite. The Andover ore is interpreted by Sims and Leonard (1952) as the product of supergene alteration of Sulfur Hill type ore.

Group 1 Franklin Deposits.

Other examples of Group 1 deposits are the magnetite deposits associated with the footwall marble of the Franklin zinc ore body near field trip stop 4. The deposits have been described by Spencer and others (1908) and may be genetically related to the zinc deposit that has been recently described as volcanogenic by Metsger (personal communication) and will be visited during next years GANJ field trip. An example of the Franklin deposits is the Pikes Peak mine (Table 2) that is one of several small magnetite disseminations, typically described as skarns, that occur in the marble at Franklin.

Proposed Metamorphosed Volcanogenic Origin.

The chemical composition of the Group 1 iron deposits, particularly the very low titanium content, resembles typical Precambrian banded iron formation (BIF), (Table 2). We are not, however, suggesting that the titanium depleted group are BIFs. The titanium depleted group, unlike typical BIFs are not banded with jasper or chalcedony, and are not primarely hematite deposits. We are instead suggesting that the depositional environment of the titanium depleted group may share some of the characteristics of BIFs. The protolith of BIF deposits is usually interpreted as marine sediment that has been enriched in iron by either distal or proximal volcanic processes (Gilbert and Park, 1986). Support for such interpretations is found by comparing BIFs with iron concentrations currently being precipitated near volcanic vents. Rock composed largely of iron and silica with titanium values

	SulfurHill	Andover	Ahles	PikePeak	MineH.Pa	Goebic	Biwabik	Hamersl	Brazil	Pacific	SulfurHill
SiO2	29.39	5.98	16.96	1.67	30.45	28.53	46.4	42	0.4	52.42	1.02
TiO2	0.04	0.07	0	0	0.1	0.06	0.04	0.06	0.01	0.02	0.06
Al2O3	1.78	3.84	4.06	0.28	0.96	0.92	0.9	0.3	1.23	0.36	0.03
Fe2O3t	32.52	74.83	50.91	45.12	67.35	68.56	40.58	37.3	51.01	30.26	98.21
MgO	1.17	1.25	1.54	7.53	0.17	0.43	2.98	2.88	8.33	3.97	0.02
MnO	0.33	0.45	11.28	2.9	0.1	0.22	0.63	0.14	0.25	0.49	0.36
CaO	19.49	2.38	0.66	17.63	0.07	0.06	1.6	6.7	14.75	0.26	0.17
Na2O	0.19	0.08	0.08	0	0	0.32	0.04	0.13	0.81	2.14	0.02
K2O	0.02	0.02	0.29	0	0	0.35	0.13	0.14	0.07	3.16	0
P2O5	0.04	0.3	0.33	0.08	0.06	0.04	0.08	0.06	0.04	0.03	0.02
LOI	15.18	4.61	12.29	22.49	1.28	0.1	8.62	9.59	22.23	6.75	0.11
Total*	100.15	93.81	98.4	97.7	100.54	99.59	102	99.3	99.13	99.86	100.02
Ba	140		14400			86			27	209	5
Cr	38					190			38	14	49
Ni	4										6
S	4958					82					7
Sc	47					43					5
Sr	10					2					4
V	22					1260			42		64
Zn	740					18				28	6
Zr	28					26					7

Table 2: Chemical composition of iron ore samples and magnetite
concentrates from mines hosted by marbles or calc-silicate lenses
within marble from the New Jersey Highlands compared with analyses of
typical BIF (Banded Iron Formation) from the Gogebic and Biwabik
Ranges of the Lake Superior District (Biwabik, Bayley and James, 1973;
Lepp, 1972), Brockman iron formation from Hamersley Australia
(Hamersl, Davy, 1983), Dolomitic Itabirite from Minas Gerais, Brazil
(Brazil, VanN.Door, 1973), and an average of five samples of
hydrothermal black smoker sediment from the Galapagos hydrothermal
mounds of the east Pacific Rise (Pacific, Barrett and others, 1988).
High totals are primarily due to listing of iron as Fe2O3; low totals
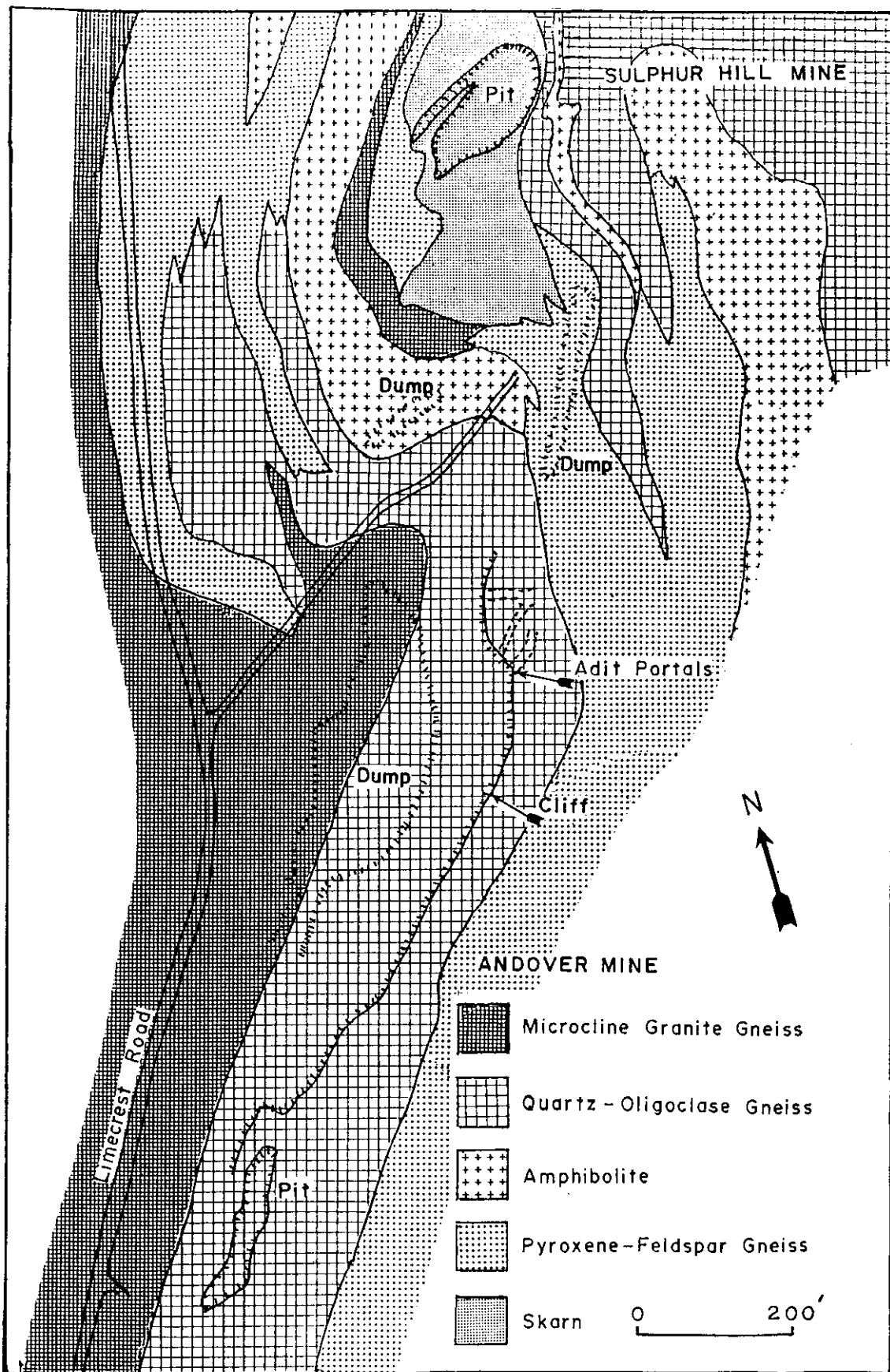are due to unreported CO2.

Figure 5: Geologic map of the Andover mining district after Sims and Leonard (1952). The skarn unit here is a carbonate-magnetite-garnet-sulfide rock and the ore zone of the Andover mine is hosted by calc-silicates rock.

comparable to BIFs and Group-1 deposits have been found near volcanic vents along the East Pacific Rise (Table 2). The chemical composition of some nontronitic sediments from the Galapagos hydrothermal mounds, DSDP Leg 70 (Barrett and others 1988), are particularly similar to Group-1 samples.

Although the banding and the mineralogy of many of the Precambrian iron formations of the Lake Superior province differ from Group-1 deposits, there are several chemical similarities (Table 2). The very low TiO_2, K_2O, Na_2O and Al_2O_3 content and comparable SiO_2, MgO, and CaO contents of both Group-1 and Bewabik Iron Formations, particularly ore from the "Siderite Facies" may be meaningful (Bayley and James, 1973). The solubility of TiO_2 in volcanic exhalatives is apparently particularly low. In the case of Group-1 ore, Ca, Fe, and Mg carbonates probably reacted with silicates during Granulite Facies metamorphism to form the garnet and amphibole and calc-silicate assemblages typical of Group-1 ore deposits.

Kastelic (1979) also interprets the iron ores of Warrern Co. New Jersey as meta-sedimentary and rejects the suggestion made by earlier workers that the magnetite rich calc-silicate rocks are skarns formed by the intrusion of granitic rock. Kastelic (1979) points out an absence of igneous intrusions that could have been the source of iron-bearing fluids.

Group 2 Iron Deposits

Group 2 iron deposits are common throughout the New Jersey Highlands (Fig. 1) but are most likely to be hosted by three lithologies: 1) quartz-oligoclase gneiss (the Losee Gneiss), 2) metasedimentary quartz-potassium feldspar gneisses and associated schists, and 3) amphibolites and related rocks. A few Group 2 deposits are also mapped within quartz diorites and granite but with few exception are found to be hosted within unmapped amphibolite layers when examined closely. The iron deposits in each of these rock types are also associated with magnetite bearing pegmatites.

The principal ore mineral in each of the Group 2 iron deposits is magnetite. The magnetite is typically accompanied by minor concentrations of hema-ilmenite or ilmeno-hematite and in a few cases by hematite. These oxide concentrations may be disseminated within semi-schistose gneissic rock but more commonly occur as networks of veins, one to twenty cm thick, parallel to the foliation of the gneisses. The principal gangue minerals are biotite, K-spar,
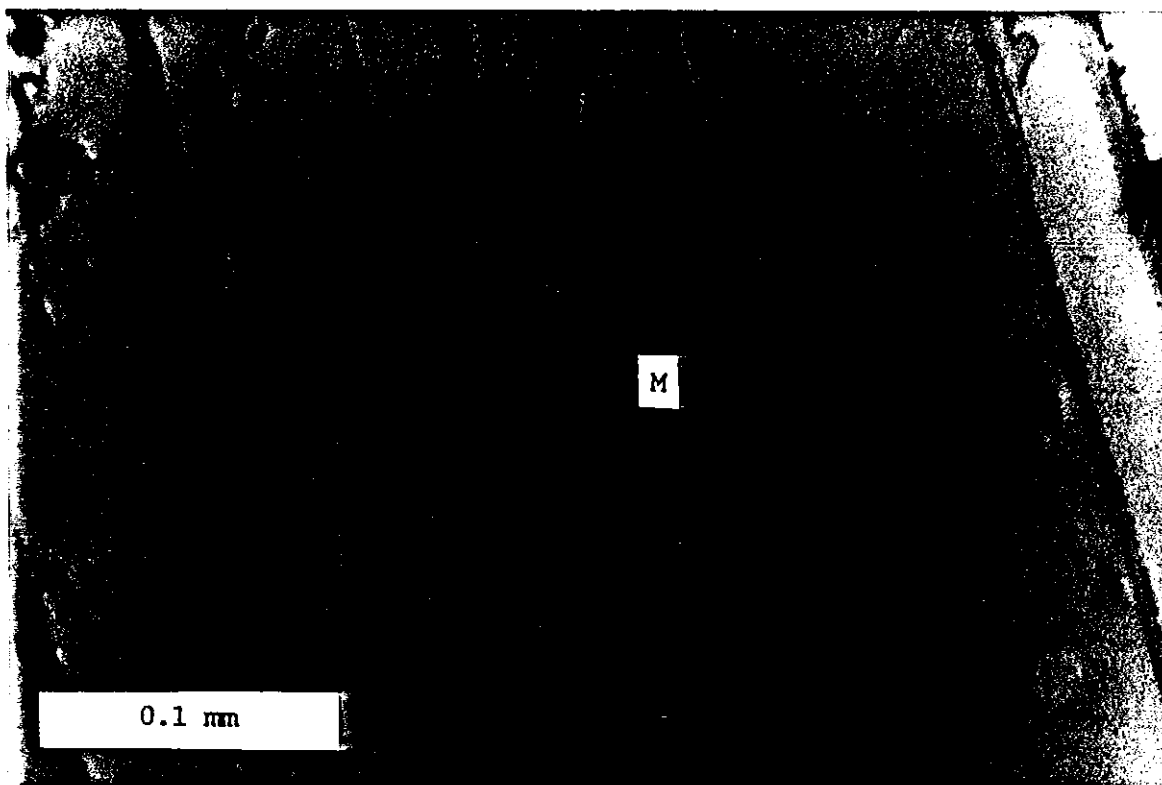
Figure 6: Polished magnetite surface from an Edison iron ore sample
with parallel blades of ilmenite (dark gray) lined with spinel.
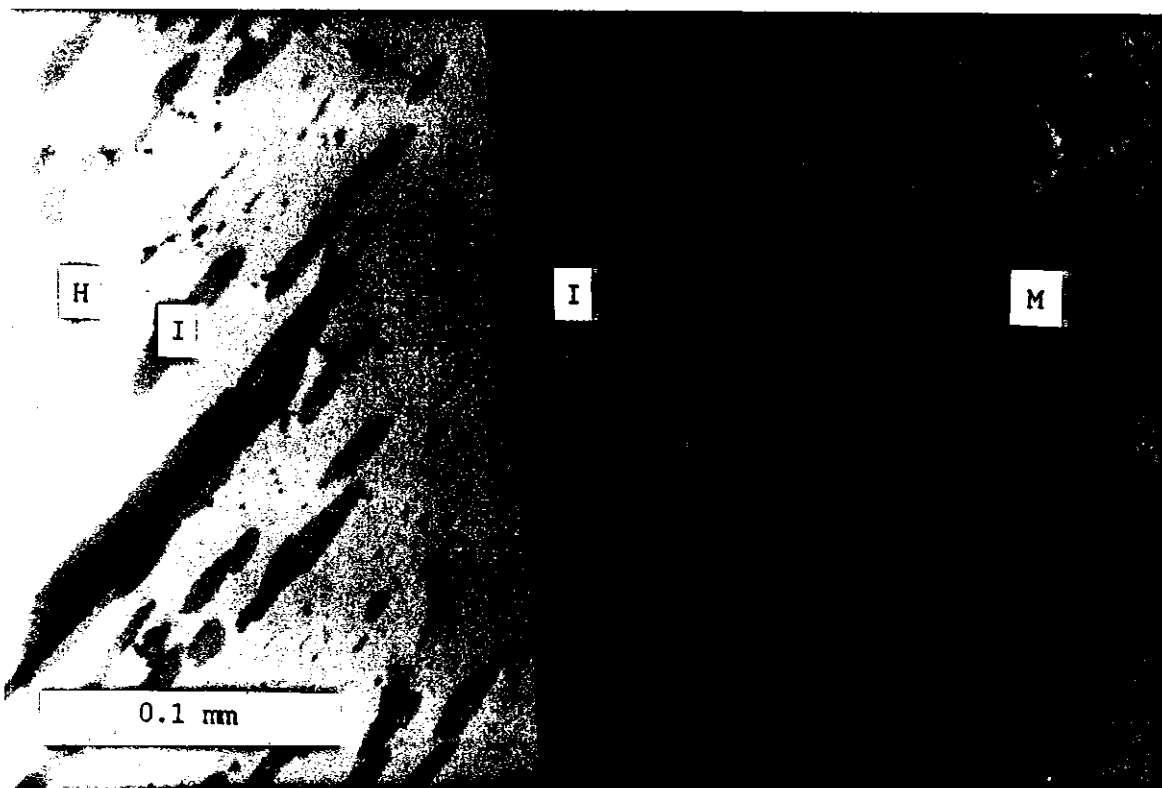
Figure 7: Polished opaque oxides from an Edison iron ore sample
illustrating: hematite (H) with ilmenite exsolution lamellae (I) and
magnetite (M) with thin veins of hematite that are separated by a thick
band of ilmenite.

quartz, amphibole, chlorite, pyroxene, and plagioclase. The biotite is commonly partially altered to chlorite but secondary alteration has not effected most ore deposits other than some local weathering, particularly wherever sulfides are present. The oxide phases seem to have crystallized in equilibrium with biotite and K-spar on the basis of mutual grain boundaries.

The magnetite grains contain thin widely spaced exsolution lamellae of ilmenite (Fig. 6). If weathering or hydrothermal alteration has effected the deposit, varying degrees of hematite replacement occurs along micro-cracks in the magnetite host or along lattice planes forming a grill-like intergrowth (Fig. 6).

The magnetite at most Group 2 deposits is accompanied by co-existing ilmeno-hematite or hemo-ilmenite (Fig.7) intergrowths that are approximately the same grain size at the magnetite. The coexisting iron-titanium oxide grains are less susceptible to secondary alteration than the magnetite although some pseudo-rutile is apparent in several samples.

The chemical characteristics of Group 2 iron deposits are much different than those of any known BIF or marine volcanic vent deposits. The titanium content in particular is beyond the range of iron ore from any of the major banded iron formations of the Lake Superior province, Australia, or South America (Table 2). The TiO_2 content of the magnetite from Group 2 deposits instead falls within a range of values (0.7 to 5.3 weight percent) that overlaps the range of magnetite that has crystallized at low igneous temperatures out of granitic rock or pegmatites (Puffer, 1972, 1975). The similarity in chemistry, mineralogy and geologic setting of Group 2 deposits suggests that they share a common origin although details differ particularly with respect to the origin of their various host rocks.

(1) Group 2 Deposits hosted by Quartz-Oligoclase Gneiss:

Most of the larger iron deposits hosted by Quartz-Oligoclase Gneiss (Losee Gneiss) are located in the Dover mining district. The Dover district included the largest and most productive mines in New Jersey. Sims (1958) has observed that: "The ore deposits of the Dover district are in three main types of host rocks - oligoclase-quartz-biotite gneiss, skarn, and gneissic albite-oligoclase granite. Each type has

	Evers	Baker	Allen	Randel	ScrubOak	Richard[*]	Leonard[*]	Elizabeth[*]	Evers	Baker	Allen	Randel	ScrubOak
% magnet.	39	85	81	86	66	—	—	—	99	99	99	99	99
SiO2	48.75	8.32	10.96	6.74	25.68	3.77	3.56	1.38	0.84	0.93	0.45	0.32	1.05
TiO2	1.32	2.54	1.29	2.78	0.61	1.3	1.15	1.09	2.63	2.92	1.68	3.17	0.95
Al2O3	1.51	1.08	1.01	0.98	2.38	0.79	0.44	0.55	0.1	0.12	0.05	0.1	0.75
Fe2O3t	41.61	89.55	86.26	90.49	71.22	93.97	93.97	93.78	98.78	98.81	99.86	98.74	98.65
MgO	1.42	0.81	2.4	0.61	0.52	0.64	1.68	0.1	0.02	0.05	0.03	0.02	0.2
MnO	0.07	0.06	0.06	0.08	0.05	0.06	0.03	0.03	0.09	0.07	0.07	0.08	0.06
CaO	2.03	0.62	0.91	1.12	0.58	1.23	1.66	0.68	0.08	0.03	0.03	0.03	0.08
Na2O	0.55	0.62	0.41	0.01	0.96	0.12	0.1	0	0.04	0.03	0.03	0.03	0.08
K2O	0.12	0.11	0.27	0.05	0.31	0.14	0.12	0	0.03	0.02	0.02	0	0.06
P2O5	2.01	0.04	0.04	0.11	0.19	0.45	0.54	0.49	0.12	0.02	0.03	0	0.07
LOI	0.62	0.21	0.19	0.25	0.37	0	0	0	0.13	0.14	0.12	0.03	0.08
Total	100.01	103.96	103.8	103.22	102.87	102.47	103.25	98.1	102.86	103.13	102.37	102.58	101.99
Ba	134	65	86	85	—	—	—	—	low	10	5	6	—
Cr	59	171	182	162	230	—	—	—	110	197	198	174	—
Ni	3	2	4	5	48	—	—	—	5	3	7	6	—
S	80	117	75	360	—	110	210	100	9	6	6	6	—
Sc	21	42	45	40	—	—	—	—	4	4	7	5	—
Sr	17	4	4	2	—	—	—	—	0	2	2	0	—
V	318	780	560	650	351	950	800	800	649	824	621	695	—
Zn	14	31	25	33	—	—	—	—		3	2	2	—
Zr	32	22	23	20	—	—	—	—	7	6	5	5	—

[*] Bayley (1910)

Table 3: Chemical composition of iron ore samples and magnetite concentrates from mines hosted by Losee Gneiss and related oligoclase-quartz-biotite gneisses within the New Jersey Highlands.

yielded a substantial proportion of the iron-ore production from the district. Magnetite concentrations (sub-ore) occur locally in amphibole and granite pegmatite." Sims (1970), however, defines the albite-oligoclase granite as "... medium grained rock that is composed almost entirely of plagioclase (An_8-An_{15}) and quartz." with minor muscovite, augite, hornblende, and biotite. Since the Losee Gneiss and the gneissic albite-oligoclase granite have the same texture and mineral composition we have found them to be indistinguishable and group them together (Figure 1).

The ores hosted by the Losee Gneiss consist of black, dense and massive lenses composed principally of magnetite with minor quartz and oligoclase as the principal gangue minerals. Some magnetite lenses also contain minor but highly variable quantities of biotite, amphibole, pyroxene, and apatite. The chemical compositions of high grade iron ores from several magnetite mines hosted by Losee Gneiss are presented in Table 3 and Figure 4. Both the ore and the magnetite from Losee hosted mines typically contains about 1 to 2 percent TiO_2; about 10 times as much as found in Marble hosted ore.

The largest iron mines hosted primarily by the Losee Gneiss are the Mount Hope, Richards, and Scrub Oaks mines, although portions of these mines include other rock types, particularly amphibolite. These three mines were also the three last mines in New Jersey to go out of production.

The main shaft at the Mount Hope mine is 2694 feet deep with levels at 200 foot intervals. The Mount Hope mine includes eleven separate tabular ore deposits that trend about N45E and plunge NE, parallel to the prevailing structures (Sims, 1958). The deposits are confined to a zone about 100 meters wide. Of the eleven Mount Hope deposits the major ones hosted by Losee Gneiss are the Teabo, Elizabeth, Leonard, and Finley deposits. The Teabo deposit is a tabular body up to ten meters thick striking N45E and dips 55°SE. The Elizabeth deposit is in the same plane as the Teabo, also strikes N45E but dips 70°SE and is up to 7 meters thick. The Leonard deposit, up to 8 meters thick, and oriented N45E with a vertical dip, was mined continuously from the surface to its intersection with the Mount Hope fault and then to the 1700' level of the Mount Hope mine north-east of the fault (Sims, 1958). The Finley deposit is up to 3 meters thick and unites with the Leonard deposit in the axial area of the Mount Hope syncline; for structural details see Sims, 1958.

The Richard Mine consists of two deposits: the Mount Pleasant and the Richard. The main shaft is 1,244 feet deep with levels spaced every 200 feet. As of 1958 the Mount Pleasent deposit was being developed on the 1300 and 1500 levels and the Richard deposit was being developed on the 1500 level. The Richard deposit is tabular, strikes N40E and dips 30 to 50°SE, with an average thickess of 5 meters. It locally contains thin layers of biotite schist. The Mount Pleasent deposit consists of three well-defined shoots that dip 40 to 60°SE (Sims, 1958). The largest shoot is about 3 meters thick and is associated with pegmatites.

The Scrub Oaks mine consists of six levels 250 feet vertically apart. The deposit is a tabular body that includes several shoots. The ore body and the country rock strike N33°E and dip 55°SE . Unlike the Mount Hope and Richard ore which is massive magnetite rich rock, the Scrub Oaks ore consists of magnetite veinlets and disseminations with rare massive layers. The Scrub Oaks ore also includes considerable hemati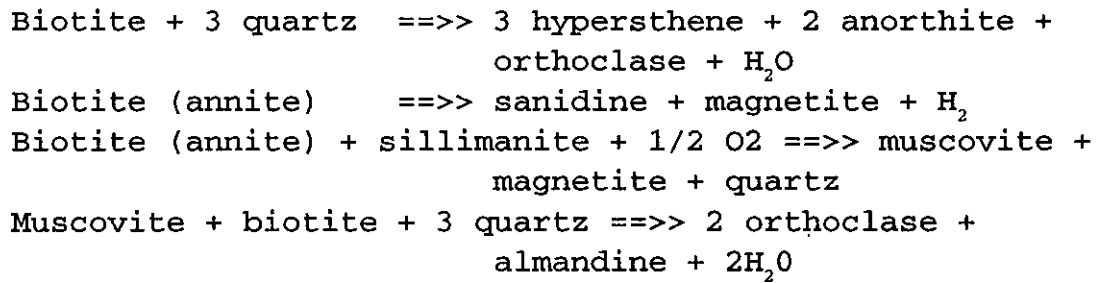te. At the 1586 and 1587 stopes of the no. 5 level hematite forms about 50 percent of the ore but is less than 5 percent of the ore elsewhere in the mine (Sims, 1958). The gangue minerals of the Scrub Oaks ore include the albite and quartz of the host Losee Gneiss but also include common apatite and tourmaline, neither of which are found in Losee Gneiss outside of the ore deposit. In addition, their are several rare-earth minerals concentrated in the ore, particularly in coarse grained magnetite ore zones and associated pegmatites (Klemic and others, 1959). Doverite, xenotime, bastnaesite, chevkinite, apatite, zircon and monazite are the principal radioactive rare-earth bearing phases concentrated at Scrub Oaks that are described by Klemic and others, 1959).

PROPOSED ORIGIN -

The Losee Gneiss is calc-alkaline rock composed principally of oligoclase, quartz and biotite with variable but typically minor quantities of magnetite, hornblende, pyroxene; garnet, and sillimanite. Some of the balanced prograde metamorphic reactions involving these minerals that are transitional to or within the granulite facies as presented by Hyndman (1985) include:

Biotite + gas ==>> biotite + sanidine + magnetite + gas
Biotite + quartz ==>> sanidine + magnetite + hematite + H_2O

```
Biotite + 3 quartz  ==>> 3 hypersthene + 2 anorthite +
                              orthoclase + H₂O
Biotite (annite)     ==>> sanidine + magnetite + H₂
Biotite (annite) + sillimanite + 1/2 O2 ==>> muscovite +
                              magnetite + quartz
Muscovite + biotite + 3 quartz ==>> 2 orthoclase +
                              almandine + 2H₂O
```
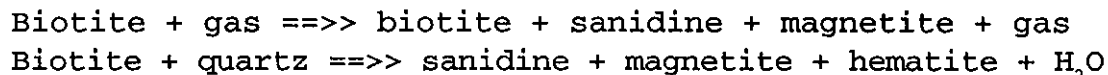
and at lower temperatures and pressures

```
57 Chloritoid + 4 O₂ ==>> 3 Almandine + 12 Staurolite +
                              8 Magnetite + 51 H₂O
```
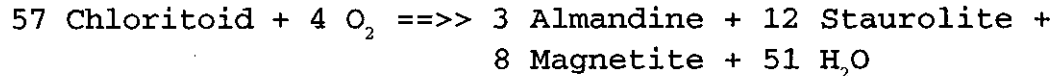
Each of these reactions involve the kind of compressional prograde regional metamorphism that led to the development of the Losee Gneiss and in most cases result in the generation of water and magnetite. The phase boundaries represented by the first of these reactions are illustrated in Figure 8 after Wones and Eugster (1965). The phase boundary between the biotite + gas and the biotite + sanidine + magnetite + gas fields has been experimentally determined (Wones and Eugster (1965). The gas in this case is $H_2O+O_2+H_2$ and would be saturated in both potassium and iron. It is also clear from Figure 8 that as temperatures are increased the Fe/Fe+Mg ratio of the biotite is decreased. Iron saturated water expelled from biotite (or chloritoid) as temperatures are increased would be driven out of high pressure zones into any permeable avenue of escape such as shear zones where magnetite would then precipitate. A similar proposed origin for some of the iron deposits of the New Jersey Highlands was proposed by Puffer (1980).

The release of iron from biotite accompanied by any dehydration and precipitation of anhydrous phases such as garnet would set up a complex iron and potassium saturated hydrothermal system. Released water would also contain any other volatiles present in the initial biotite such as Cl and F.

Martin and Piwinskii (1969) have experimentally shown that iron, under a wide range of pressures, fractionates into a vapor phase out of calc-alkaline rock. They found that the presence of a melt, of a specific rock type, or of chloride, fluoride, sulfide, or carbonate anions is not required for the leaching and transport of iron in a vapor phase. Their subsolidus experiments confirm that iron behaves like silica,
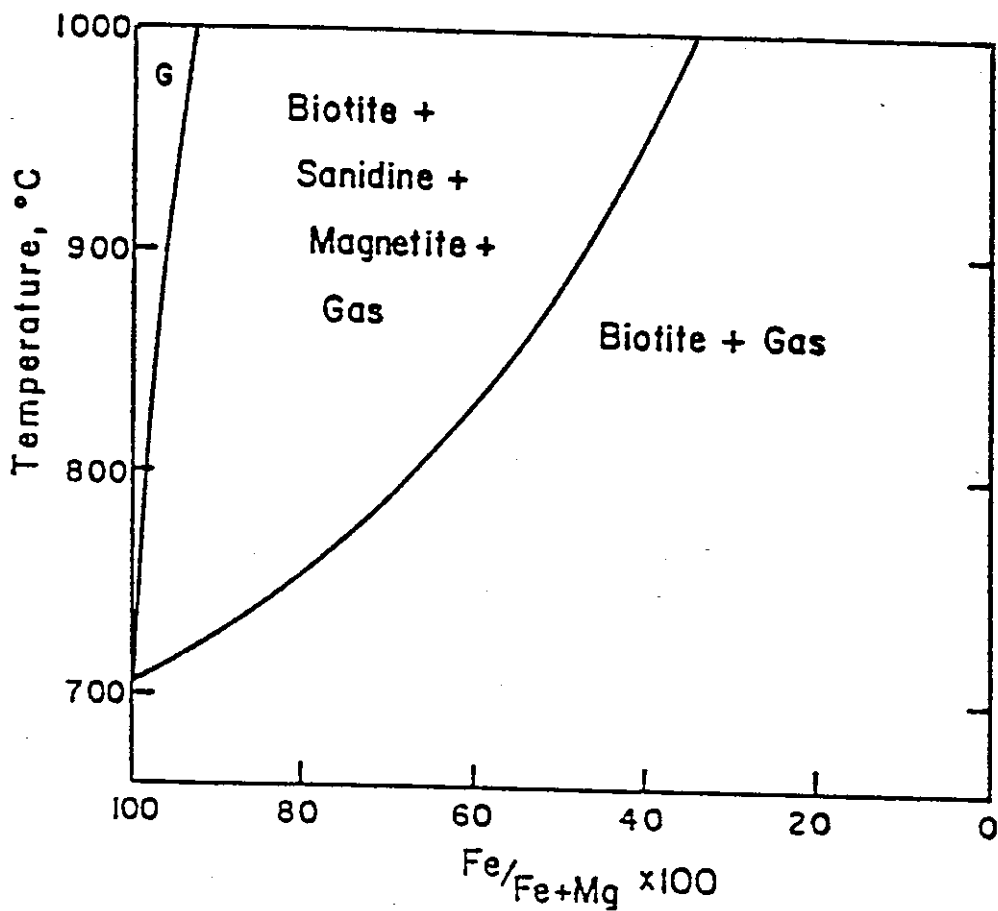
Figure 8: Experimentally determined temperature - composition projection of $K(Fe,Mg)_3AlSi_2O_{10}(OH)_2 + H_2 + H_2O$ bulk composition at 2070 bars after Wones and Eugster (1965). Note decreasing Fe/Fe + Mg of biotite with increasing temperature.

potassium, and sodium which are leached and then migrate readily from high temperatures (700°C at 5 kb) towards low temperature zones (560° to 450°C) unlike calcium and magnesium which do not.

(2) Group 2 Deposits hosted by Metasedimentary Quartz-Potassium Feldspar Gneiss:

Some of the larger and relatively well known deposits hosted by metasedimentary gneisses include the Sherman-Bunker deposits and the Edison deposits of the Franklin quadrangle (Figure 9 and Table 4). The host-rock consists of varying amounts of magnetite, quartz, and potassium feldspar ranging from a quartzite to a potassium feldspar-quartz-magnetite gneiss. Typical ore as described in detail by Baker and Buddington (1970) consists of magnetite, quartz, and potassium feldspar with accessory biotite, sillimanite and garnet. The biotite content is particularly variable and occurs in schistose layers. Portions of the Edison deposit are mineral-ized with sulfides (pyrite, chalcopyrite, and molybdenite) that have locally led to saprolitic weathering through sulfuric acid leaching. Pegmatites composed of magnetite, quartz, potassium feldspar and biotite are common throughout the Edison mine.

The potassium feldspar of the Edison mine is non-perthitic to slightly perthitic orthoclase. Chemical analysis of potassium feldspar from Edison iron ore (Baker and Buddington, 1970) indicates that it is extremely rich in barium (up to 2.28 percent BaO). Garnets separated from quartz potassium feldspar gneisses were also analyzed by Baker and Buddington (1970, Table 5) and found to be rich in manganese ranging from 4.9 to 14.51 percent MnO or 11 to 34.2 mole percent spessartite. The highest MnO contents are in garnet from a magnetite rich layer in the Roberts mine, northeast of Edison while the lowest MnO contents are in barren quartz-microcline gneiss near the Roberts mine. Baker and Buddington (1970) conclude that manganese is enriched in the ore zone as compared with the iron-poor wallrocks. Garnet in the ore zone is also rich in iron (23.5 percent FeO) compared to magnesium (1.11 percent MgO) that converts to 50.7 mole percent almandine compared to only 4.6 mole percent andradite.

<table>
			IRON ORE				MAGNETITE			
	Ed1	Ed5	Ed10	Ed11	Ed12b	Av.12Ed	Av.8Bens.	Ed5	Ed12b	Benson
%magnet.	13	17	25	28	19	22	27	98	98	98
SiO_2	59.41	59.48	56.21	53.35	60.24	56.47	49.45	1.32	1.53	1.17
TiO_2	0.68	1.29	1.28	1.45	0.96	1.18	0.83	1.46	1.29	1.34
Al_2O_3	15.85	13.16	9.14	9.16	12.2	9.64	9.9	0.39	0.68	0.66
Fe_2O_3t	14.36	17.94	26.83	29.81	19.83	23.42	28.44	98.75	98.88	98.76
MgO	0.46	0.45	0.82	0.58	0.49	0.74	1.45	0.22	0.19	0.31
MnO	0.09	0.09	0.33	0.05	0.35	0.19	0	0.6	0.39	0.5
CaO	0.65	0.02	0.35	1.38	1.55	1.29	1.3	0.02	0.04	0.05
BaO	0.27	0.29	0.67	0.24	0.07	0.31	0	0.02	0	0
Na_2O	0.44	0.65	0.25	0.22	0.18	0.35	0	0.01	0.04	0.06
K_2O	7.67	7.28	4.34	4.36	3.95	6.53	7.19	0.06	0.07	0.04
P_2O_5	0.75	0.26	0.32	1.08	0.23	0.31	0.3	0.19	0.06	0.12
Total*	100.63	100.91	100.54	101.68	100.05	100.43	98.86	103.04	103.17	103.01
Cr	145	150	142	144	142	141	–	195	235	240
Ni	46	44	45	46	51	46	–	2	30	56
S	27	27	234	137	23	95	–	–	–	280
Sr	67	142	132	147	106	138	–	16	–	11
V	140	160	180	80	30	169	–	550	420	690
Zn	112	70	216	112	130	118	–	164	–	168
Zr	740	243	330	345	634	486	–	53	–	68
</table>

Table 4: Chemical composition of iron ore samples and magnetite concentrates from mines hosted by metasedimentary K-spar gneisses at the Edison iron mine (for sample locations see Figure 9b), compared with iron ore from the Benson Mine, New York analyzed by Palmer (1970).

77

500   0   500⁻   1000   1500   2000 FEET

100   0   100   200   300   400   500   600 METERS
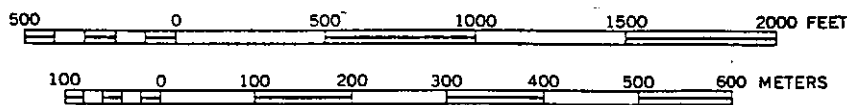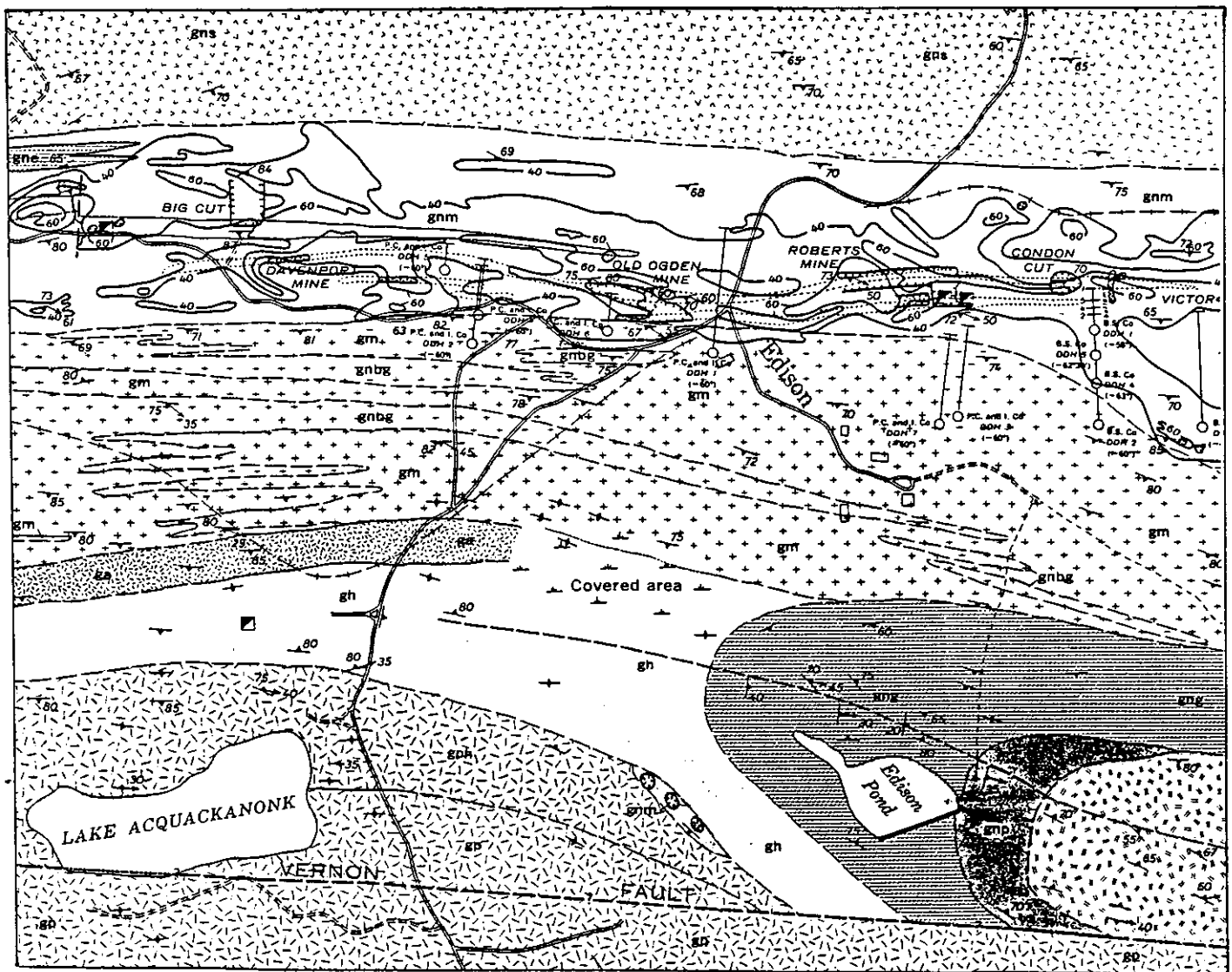
APPROXIMATE MEAN
DECLINATION, 1970

Outline of inferred magnetite ore

Magnetic contour
Dip needle survey

Mine shaft

Opencut or prospect pit

ga Alaskite, composed of perthite, quartz, with oligoclase, biotite, magnetite and hornblende

gh Hornblende granite, composed of quartz and perthite with hornblende, biotite, and magnetite

gng Garnet-biotite-quartz-feldspar gneiss composed of quartz oligoclase, and perthite with garnet, biotite, pyroxene, hornblende, and magnetite

gph Hypersthene granite composed of quartz, perthite, anti-perthite, with hypersthene, biotite, and magnetite

gp Pyroxene granite, composed of quartz, perthite, and antiperthite with ferrohedenbergite, ilmenomagnetite, ilmenite, and hornblende

gno Quartz-oligoclase gneiss (Losee Gneiss), composed of quartz and oligoclase with biotite, chlorite, epidote, garnet, microcline, ilmenomagnetite, and ilmenite

gns Syenite gneiss, composed of oligoclase, perthite and augite with accessory ilmenomagnetite and magnetite

gnm Quartz-potassium-feldspar gneiss, composed of quartz, potassium feldspar, and magnetite with hematite, ilmenite, rutile, biotite, garnet and sillimanite

gm Quartz-microcline gneiss, composed of microcline, and quartz with garnet, ilmenomagnetite, and biotite

gnbg Biotite-quartz-feldspar gneiss composed of oligoclase, perthite, and quartz with biotite, garnet, and magnetite

Figure 9a: A portion of a geologic map by Baker and Buddington (1970) illustrating the geologic setting of the Edison iron mine.
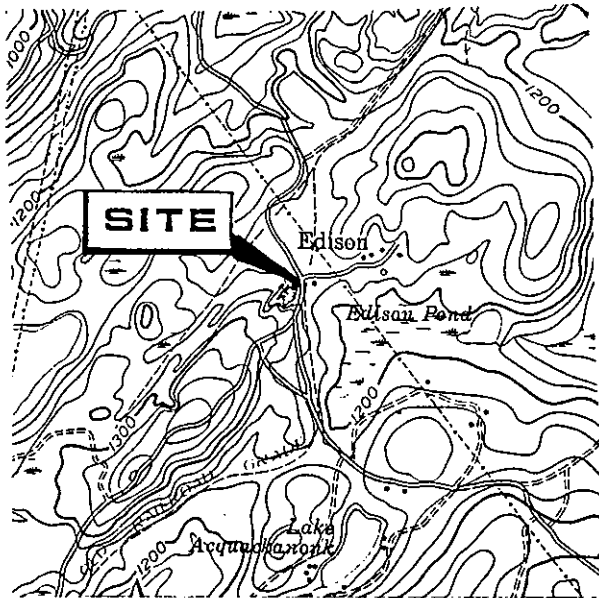
SOURCE: USGS FRANKLIN, N.J. QUADRANGLE
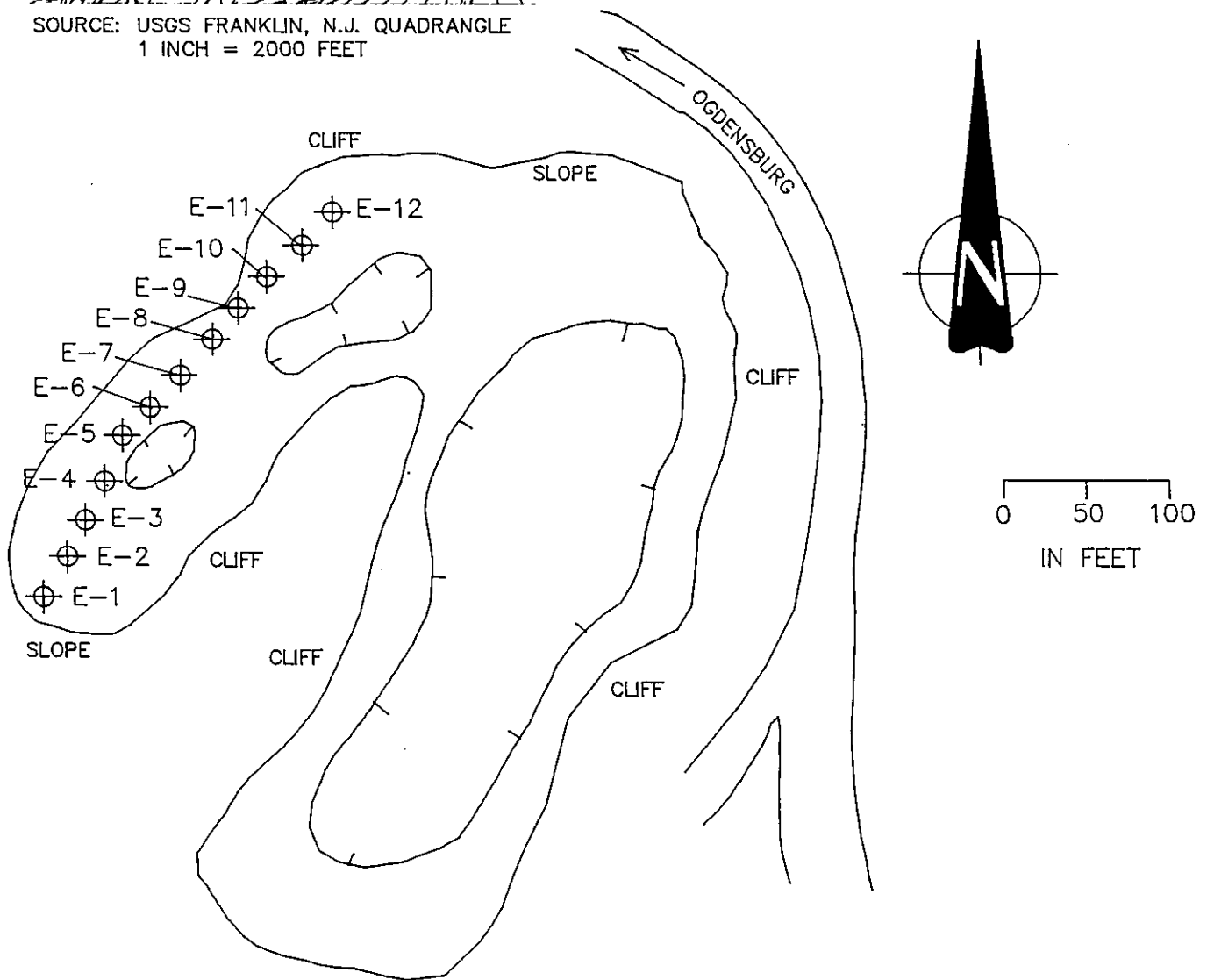1 INCH = 2000 FEET

Figure 9b: Field sketch of the open pit at the Edison iron mine (Figure 9a) with the location of iron-ore samples E-1 through E-12 (Table 4).

The iron-titanium oxides of the ore zones include ilmenomagnetite (magnetite with ilmenite lamellae), hemato-ilmenite (ilmenite with hematite microintergrowths, and ilmenohematite (hematite with ilmenite microintergrowths). Ilmenomagnetite is the most abundant oxide phase making up well over 95 percent of the oxides in most deposits. The intergrown ilmenite occurs as thin blades or lamellae that resemble exsolution lamellae but originate from subsolidus oxidation and contemporaneous exsolution of ulvospinel (Buddington and Lindsley, 1964). The ilmenite lamellae make up much less than one percent of typical polished magnetite surfaces but there presence indicates titanium saturation and initial crystallization temperatures higher than the magnetite-ulvospinel solvus. Wherever any alteration, particularly weathering, has occurred the magnetite surfaces have been partially oxidized to martite. Hemato-ilmenite grains are less likely to be altered than the magnetite but some weathered grains are partially replaced by pseudo-rutile as the result of iron leaching.

PROPOSED ORIGIN -

The Edison Mine is surprisingly similar to the Benson magnetite mine in New York as described by Palmer (1970). Both mines are hosted by similar potassic metasedimentary rocks surrounded by similar hornblende granites and plagioclase gneisses of Grenville age. The iron ores at both mines are mineralogically and chemically indistinguishable (Table 5). Palmer (1970) considered each of three origins that have been proposed for the Benson Mine: 1) Metamorphic Differentiation, 2) Hydrothermal, and 3) Metasedimentary. The reason why Palmer (1970) does not favor a metamorphic differentiation origin is because the thickness of the proposed leucocratic plagioclase gneiss source zone is only about the same at the adjacent ore zone. It, therefore, seemS unreasonable to Palmer (1970) to suggest that the proposed source zone contained enough iron to supply the ore zone. Palmer (1970) suggests that the hydrothermal origin is inadequate because it dose not explain the high degree of stratigraphic control on magnetite deposition and because of the lack of any chemical or structural control that might have forced the precipitation of iron. Palmer (1970) favors a metasedimentary origin because it would explain the conformable relationship of the ore zone to the host rock. Palmer recognizes, however that

	Biotite Losse15	Biotite Hibernia	Biotite Hibern618	Biotite Edison-8	Biotite Scott	Garnet Edison153	Hornblend Hiber.471	Hornblende Hiber.696	CPX Hiber.906
SiO2	39.43	38.31	39	38.25	34	36.38	53.5	42.4	51.5
TiO2	1.31	2.45	1.95	4.13	4.3	0.05	0.35	1.7	0.23
Al2O3	14.36	12.31	13	14.38	14.5	20.82	5.1	13.1	1.6
FeOt	11.92	11.13	11.45	18.1	14.79	23.27	10.67	15.3	13.25
MnO	0.24	0.03	0.4	0.54	0.14	14.51	0.1	0.14	0.11
MgO	16.41	20.41	20.5	8.9	11	1.11	15.8	10.2	11
CaO	1.79	1.32	0.2	0.48	0.65	3.58	9.5	11	18.6
Na2O	1.87	0.97	0.22	0.11	0.22	0	2.35	1.4	1.35
K2O	7.3	8.91	10.8	9.08	8.2	0	1.14	2.1	0.06
P2O5	0.13	0.79	nd	0.87	nd	0	nd	nd	0
LOI	3.92	3.51	nd	3.97	nd	0	nd	nd	0
total	98.68	100.14		98.81		99.72			97.7
Ba	290	310	350	1100	−	−	<10	150	40
Cr	620	170	<10	20	300	−	<10	30	170
Cu	5	5	8	5	15	−	55	13	11
Ni	160	90	110	2	240	−	65	82	45
Rb	126	240	nd	128	−	−	−	−	−
Sc	20	15	11	20	<10	−	130	210	70
Sr	166	60	<30	40	−	−	<30	70	30
V	200	360	55	235	620	−	70	820	280
Zr	78	55	<10	285	100	−	45	70	115

Table 5: Composition of minerals associated with New Jersey Highlands iron ores including garnet from the Edison mine (Edison-153, Baker and Buddington, 1970); biotite, hornblende, and pyroxene associated with the Hibernia mine (Hibernia 618, 471, 906, Collins, 1969a) and new analyses of biotite from the Edison mine (Edison-8), Losee Gneiss (Losee-15), and Hibernia ore (Hibernia).

the proposed sedimentary protolith of the Benson ore must have been higher in Al_2O_2, TiO_2, Zr and especially K_2O than virtually any known sediment type of comparable silica and iron content. Palmer, therefore proposes a sedimentary protolith intermediate between detrital and chemical environments with additions of alumina and potash from detrital clay or sand and minor zircon, rutile and apatite. The high levels of Zr (250 to 740 ppm) and TiO_2 (1 to 3 %) in the Edison ore zone (Table 4), however, would require concentrations of zircon and rutile rarely (if ever) seen mixed with marine chemical precipitates such as the banded iron formations that Palmer compares with Benson iron ore.

We sugest that the exposed thickness of leucocratic plagioclase gneiss adjacent to the Benson deposit may not be typical of thinknesses unexposed at depth, or may have been eroded away or structurally displaced. We also suggest that a major portion of the iron contained within the ore zones at Benson and Edison may have originated from within the metasedimentary units and was simply mobilized and reprecipitated in ductile shear zones in response to a drop in water pressure. Precipitation of iron oxide in these shear zones was not highly stratigraphically controlled and is concentrated in several host rocks including the plagioclase gneiss, metasediments, and amphibolites. Iron precipitation and accompanying shearing must, however, have preceded granite emplacement, because of the virtual absence of iron deposits in the granites.

The upper stability of iron biotite (annite) was experimentally determined by Ernst (1970), Figure 10. The conversion of biotite + quartz into the magnetite + sanadine + quartz + iron saturated fluid field may be forced by an increase in O_2 or decrease in temperature at constant composition. Increases in fO_2 typically occur in shear zones where hydrothermally fluids have migrated and would be accompanied by a temporary drop in temperature as fluids escape into overlying rocks. These temporary reversals in temperature and fO_2 would occur whenever major ruptures or fluid pressure releases occurred during prograde metamorphism and may result in the kind of iron depo-sition that is found in the Edison Iron mine.

The importance of $fO2$ as a control on the phase equilibria of biotite, sanadine, magnetite and ilmenite was studied by Wones and Eugster (1965) culminating in their development of the equation:
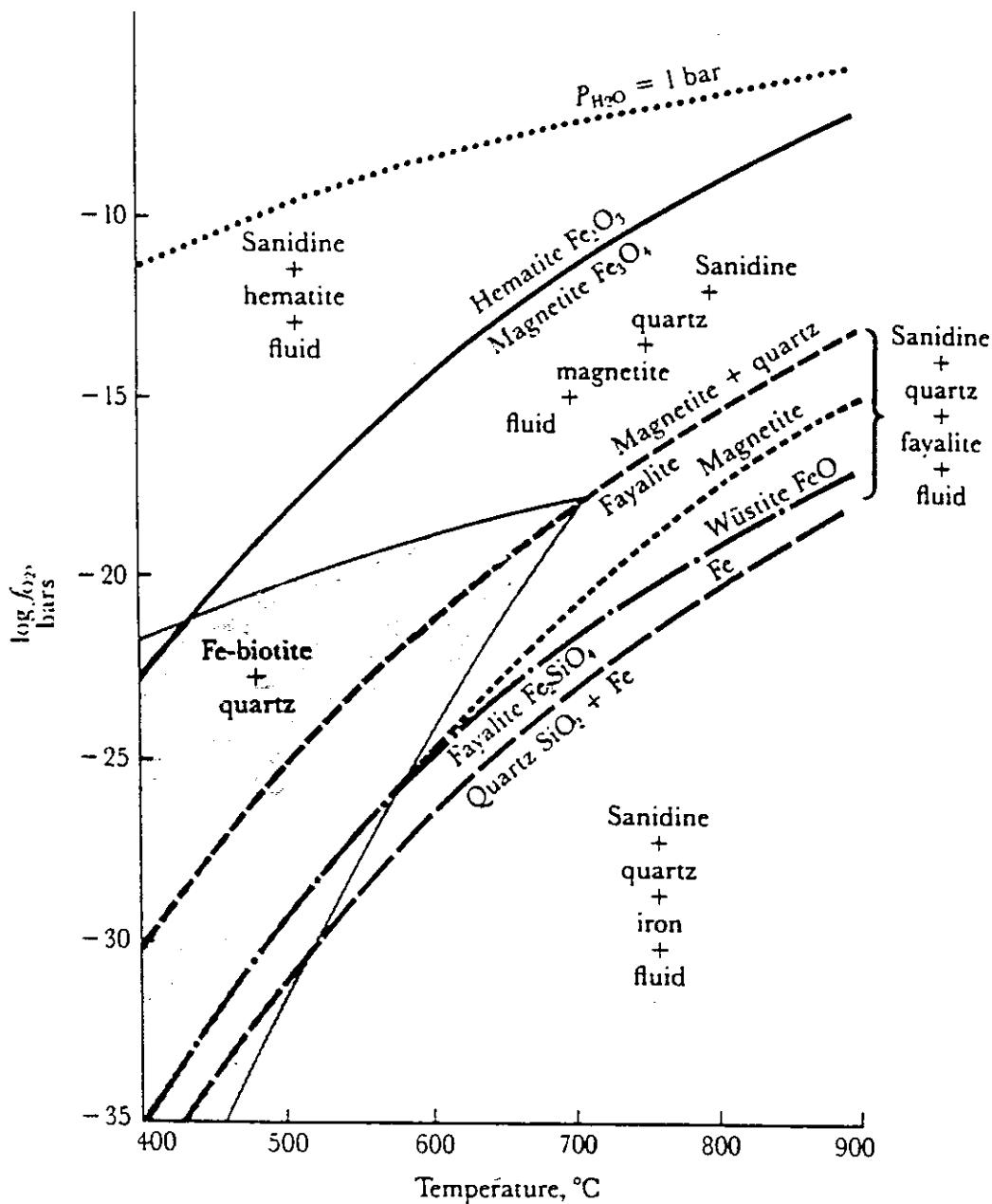
Figure 10: Temperature/fO₂ (oxygen fugacity) diagram illus-
trating the stability field of Fe-biotite (annite) with quartz
after Ernst (1976). The stability field of biotite expands
with increasing Mg.

$$\log f_{H_2O} = \frac{3428 - 4212(1-x_1)2}{T} + \log x_1 + 1/2 \log f_{O_2}$$
$$+ 8.23 - \log a_{KAlSi_3O_8} - \log a_{Fe_3O_4} \quad (\pm 0.20)$$

The fH_2O of a biotite + magnetite + ilmenite + sanadine assemblage in the host rock adjacent to the ore zone of the Edison iron mine (Table 5) was calculated using Wones and Eugster's equation. Our analyses indicate that the Fe_3O_4 in the magnetite = 0.914, the $aKAlSi_3O_8$ in host rock K-spar = 0.95, and the $x1$ (mole fraction of annite) in the co-existing biotite = 0.5328. The temperature and fO_2 are determined using the magnetite/ilmenite geothermometer of Buddington and Lindsley (1970), (Table 6) to yield a T of 1005°K, and log fO_2 of -13.667 which when applied to the Wones and Eugster equation yields a log fH_2O of 3.70281 atm or a fH_2O of 5044.4 atm. A fH_2O of 5044 atms. and a temperature of 732°C is in good agreement with a granulite facies metamorphic environment and supports our interpretation that the biotite + magnetite + ilmenite + sanadine host rock assemblage at Edison is an equilibrium assemblage.

Iron saturated vapors released from the biotite precipitated at slightly lower temperatures and higher oxygen fugacities (Table 6) as predicted by Figure 10 to form magnetite concentrations in shear zones. The chemical compositions of several coexisting magnetite + ilmenite (and ilmeno-hematite) pairs separated from the ore zone at the Edison mine and from a pegmatite analyzed by Puffer (1975) are listed in Table 6. The oxide pairs yield temperatures in a 706 to 748°C range only slightly less than the 732°C of the host rock and the 707°C of a pegmatite located in the Edison ore. The oxygen fugacity range (-log fO_2) of the magnetite ore zone is 11.5 to 13.3, slightly higher than that of the host rock; again in good agreement with reactions illustrated in Figure 10.

(3) Group 2 Deposits hosted by Amphibolite:

Amphibolites occur within each of the rock types of the New Jersey highlands and may include several genetic types (Puffer and others, Chapter 4). The amphibolites occur as layers or lenses from a few cm thick to over 100 m in thick-

84

	Ed.Mt	Ed.Ilmen	Ed.4peg	Ed.4peg	145 mt	145 imen	149 mt	149 imen	154 mt	154 imen
wt %										
Fe_2O_3	53.72	6.44	70.31	60.43	70.23	56.61	68.49	46.59	63.94	29.1
FeO	31.06	41.45	26.57	14.25	21.77	2.83	25.27	16.32	26.45	12.79
TiO_2	2.8	40.44	0.7	20.29	1.01	16.16	0.88	23.67	1.39	30.63
Mole %										
Fe_3O_4	91.4		98.1		97		97.5		95.9	
Fe_2TiO_4	8.6		1.9		3		2.5		4.1	
Fe_2O_3		14.3		60.5		60		49.1		18.7
$FeTiO_3$		85.7		39.5		40		50.9		81.3
Temp.	732		707		748		717		706	
log fo2	-13.665		-12.11		-11.46		-12.133		-13.332	

Table 6: Chemical composition of co-existing magnetite and ilmenite from iron ore samples, a pegmatite sample, and K-spar gneiss taken from the Edison iron mine with temperature and oxygen frgacities based on the Buddington and Lindsley (1964) geothermometer and oxygen geobarometer. Data includes analyses from Puffer (1975) and Baker and Buddington (1970).

ness but are typically unmappable at most map scales. The plagioclase of the amphibolites is typically andesine but the hornblende, pyroxene and biotite contents are highly variable.

The amphibolites that host iron ore deposits are not typical New Jersey amphibolites (Chapter 4). They are mineralologically, texturally, and chemically different than meta-basalts or meta-shales. The hornblende plus pyroxene to plagioclase ratio is much higher than most New Jersey amphibolites and they are typically coarser grained. Unlike most New Jersey amphibolites those associated with Group 2 deposits are characterized by high MgO and low concentrations of TiO_2, Al_2O_3, and P_2O_5. These compositions (Chapter 4) are similar to ultramafic basaltic rock such as picrite except for Ni and Cr contents that are much lower. Shales or metavolcanic rocks including picrites are unlikely to have been the protolith of the host rock amphibolites but two possibilities remain: 1) the refractory residue left from the partial melting of quartz-oligoclase gneisses. The REE enriched amphibolite schlieren within the REE depleted Losee Gneiss (Volkert and Puffer 1992) is an example or; 2) shear zones that have accumulated mafic phases such as actinolite (Gates, Chapter 6). As MgO, CaO, and FeO are mobilized by the pressures that lead to shearing, actinolite, magnetite and other mafic minerals may precipitate along fault planes at low pressure.

Iron deposits hosted by amphibolite include several described by Sims (1958) as "hornblende skarn" deposits. Some of the larger magnetite mines hosted by "hornblende skarn" or amphibolite are the Hibernia Mine and the Taylor deposit of the Mount Hope Mine. Both deposits and their associated amphibolites are contained within Losee Gneiss. Losee Gneiss is also locally the wall rock of the ore throughout portions of many of the larger amphibolite hosted iron mines.

The Hibernia mine, as of 1958, was the third largest producer in the Dover district with production in excess of 5 million tons of ore averaging 50 percent iron. The deposit is tabular and averages about 3 meters thick. The ore is composed of coarse grained massive magnetite with 2 to 20 percent hornblende (or pyroxene) as the principal gangue mineral with minor quartz, plagioclase, biotite and pyrite (or pyrrhotite). The Taylor deposit was the principal source of ore at the Mount Hope mine. The ore is in part massive and in part laminated with layers of hornblende, pyroxene, and biotite.

Most of the magnetite deposits in the Ringwood-Sterling

district and many of the deposits of the Dover district are hosted by amphibolites. Collins (1969) mapped the 24 square mile area around the Dover magnetite district and sampled 773 specimens of amphibolite. Collins compared the amphiboles in unmineralized amphibolites with those containing magnetite deposits and found that hornblende in unmineralized rock is relatively fine grained and aluminous (9.5 to 13.1 percent Al_2O_3) and is typically rich in TiO_2, FeO, MnO, CaO, K_2O, V, Cr, Zn, Pb, Sr, and Ba. In contrast the amphiboles of ore deposits is coarse grained containing only 5.1 to 5.5 percent Al2O3 but high concentration of SiO_2, MgO, Na_2O, Be and Bi. Collins also found that the magnetite in country rock amphibolites is relatively rich in MnO, TiO_2, V, Cr, Co, Ni, Cu, Zn, and Pb compared to magnetite in ore zones. Biotite and clinopyroxene contents also tend to be lower in the amphibolites of country rocks than in ore zones.

PROPOSED ORIGIN -

The magnetite bearing amphibolite/pyroxenite rocks consist primarely of hornblende, plagioclase, clinopyroxene (principally augite with some diopside), and orthopyroxene (principally hypersthene) and magnetite with minor quartz, mica, garnet, sillimanite, epidote, calcite and chlorite. Prograde metamorphic reactions within the Amphibolite facies that involve this assemblage include:

2 Epidote ==>> plagioclase + garnet + hematite +
                     quartz + H_2O

Hornblende + calcite + quartz ==>> Diopside + epidote +
                     CO_2 + H_2O

Ferrotremolite + fluid ==>> Magnetite + quartz +
                     orthopyroxene + fluid
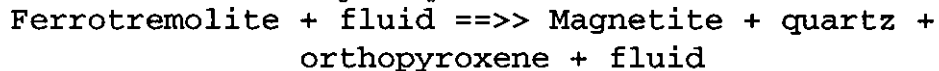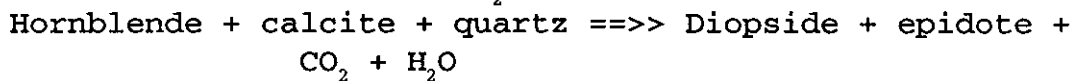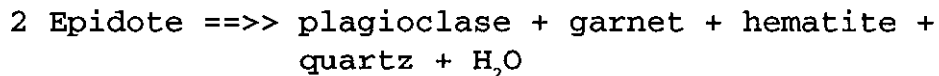
Prograde reactions transitional to or within the granulite facies include:

Hornblende + quartz ==>> hypersthene + anorthite +
                     clinopyroxene + H_2O

Hornblende + 2 biotite + 17 quartz ==>> 15 hypersthene +
                     4 orthoclase + 3 plagioclase + 5 H_2O
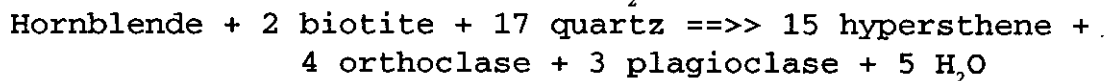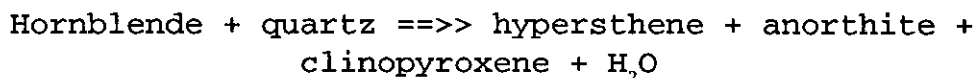
Each of these reactions generate hydrothermal water similar to the water released by the biotite reactions described above. To the extent that the Fe/Mg ratio of each of the amphibole phases decrease during re-equilibration, any

released water would be also be iron saturated. To the extent that chlorine and fluorine are also expelled from hornblende during dehydration, these anions would be available to complex with iron and aid in transmitting it to precipitation sites.

The stability of synthetic iron amphibole("ferrotremolite") was determined experimentally by Ernst (1966), (Figure 11) and just as was the case with annite (Figure 10) the amphibole breaks down to yield magnetite bearing assemblages in relatively low temperature, oxidizing environments. Pyroxenes are also generated by the dehydration of the amphiboles corresponding to those found as gangue in Highlands iron ore.

A series of papers authored by Collins and Hagner (Collins, 1969 a,b, Hagner and Collins, 1963, Hagner and others, 1963, Hagner and Collins, 1955) have developed the idea that the amphibolite and hornblende "skarn" hosted magnetite deposits of the New Jersey Highlands are the product of iron bearing fluids released during regional metamorphism. They provide evidence suggesting that iron rich ferromagnesian silicates in amphibolites and amphibole rich gneisses have recrystallized in shear zones as Mg-rich silicates plus magnetite. The process involves a decrease in modal hornblende a slight increase in modal clinopyroxene and biotite and a disappearance of orthopyroxene as magnetite concentrations are approached. They suggest that this process occurs in an open system but without the introduction of material from a magmatic source. Their calculations measure the chemical changes that would occur if amphibolites composed of various hornblende, clinopyroxene, orthopyroxene, plagioclase, magnetite, and apatite assemblages were recrystallized to form various skarns such as hornblende-albite skarn, clinopyroxene-hornblende-albite skarn, or a clinopyroxene-albite skarn. They also assume that MgO and Na_2O values are not changed. In most cases CaO, TiO_2, MnO, Al_2O_3 is lost, SiO_2 is released to form quartz, K_2O is released to form biotite or potassic feldspar, and iron is released to form magnetite. Resulting volume losses "... would generate stresses and 'openings' to which ore-bearing fluids might migrate and precipitate magnetite." (Collins, 1969). Hagner and others (1963) claim that their calculations correspond to what they observe in the field and in thin section.

Their calculations are similar to conventional mass-balance calculations although they do not balance due to a loss of Ca, Ti, Mn, and Al. But since they assume open system conditions these elements may have been flushed out through
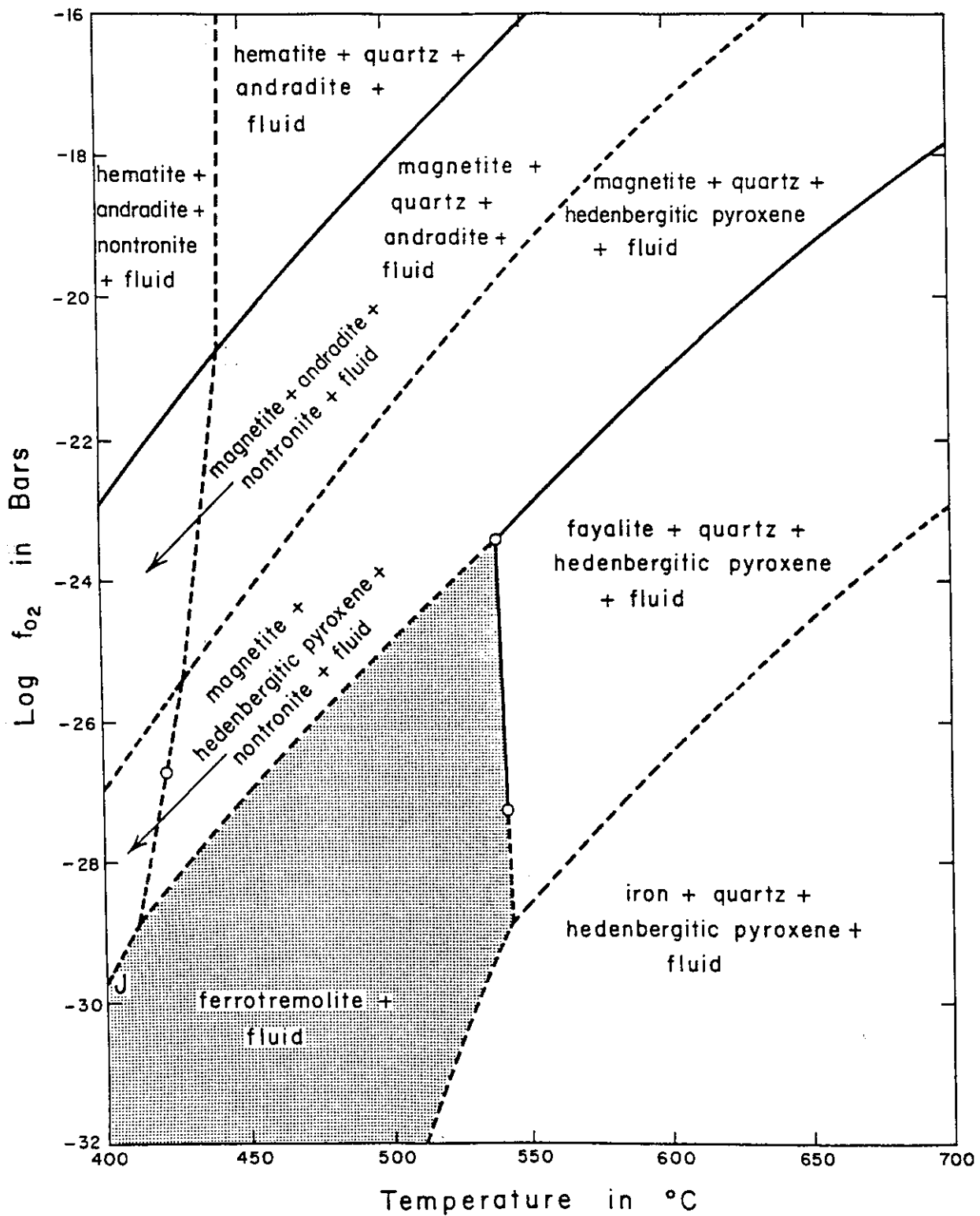
Figure 11: Log fO$_2$ - Temperature diagram illustrating the stability field of ferrotremolite (ferroactinolite) with fluid at 3 kb fluid pressure after Ernst (1966).

	IRON ORE						MAGNETITE						
%magnet	Taylor —	Blue 57	Hib.vein 82	Hib.ore 71	H.Ledge 84	Ford 75	Taylor	Hib.vein	Hib460-617*	Hib471*	H.Ledge	Ford	Fairview*
SiO2	3.87	17.85	8.35	12.48	3.4	6.31	0.93	2.73	0.8	1			1.1
TiO2	0.79	0.83	1.98	1.19	4.39	3.54	0.83	1.03	0.6	1.1	3.78		1.8
Al2O3	0.54	1.62	1.86	1.84	1.02	0.83	0.42		0.5	0.5			0.6
Fe2O3		64.57	87.57	80.88	91.46	86.61							
MgO	0.74	15.03	1.46	1.92	0.78	1.64			<.1	<0.1			<0.1
MnO	0.05	0.15	0.05	0.05	0.29	0.21	0.06	0.07	0.06	0.03	0.33	0.23	0.05
CaO		0.42	1.38	2.35	0.84	4.03			<0.1	<0.1			<0.1
Na2O		0.42	0.07	0.61	0.32	0.11							
K2O		0.04	0.11	0.13	0.03	0.12							
P2O5		0.03	0.54	0.92	0.7	0.54		0.02					
LOI		1.36	0.93	0.56	0.39	0.38							
Total		102.32	104.3	102.93	103.62	104.32							
Ba		129			65	242			<20	<20			<20
Cr	242	231	260	255	303	150	263		<10	<10			390
Ni	27	42	50	40	3	4	30		150	95			130
S		122	140		1070	55		63					
Sc		35				39		47	<3	<3			<3
Sr		4			3	6		1	<30	<30			<30
V	659	600	1600	1500	900	503	690		850	680			850
Zn		47			98	71		26	<20	<20			<20
Zr		28			628	30		22	<10	<10			<10

*Collins (1969a)

Table 7: Chemical compositions of iron ore samples and magnetite concentrates from iron mines or portions of mines hosted by amphibolites within the New Jersey Highlands.

hydrothermal systems.

The most compelling evidence in support of hornblende as a source of iron for amphibolite hosted magnetite deposits is the consistent decrease in the iron content of hornblende as magnetite ore is approached. For example, the FeO content of hornblende from the country rock near the Hebernia magnetite deposit is 15.3 weight percent, considerably higher than the 10.67 percent FeO in hornblende gangue from the ore zone (Table 7). The iron content of biotite from country rock adjacent to Hibernia ore is also much richer in iron than biotite in the ore (Collins (1969) but it is less abundant at Hibernia than hornblende. The biotite in Hibernia ore and other amphibolite hosted ore is extremely depleted in iron and could be characterized as a phlogopite. Some of the iron depleted biotite, particularly the biotite of skarn or "skol" deposits may be the product of reactions such as:

Dolomite + K-spar + H_2O ==>> phlogopite + calcite + CO_2
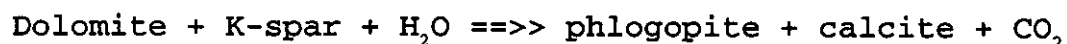
To the extent that CO_2 was involved in the development of Hibernia biotite and magnetite equilibria, the modeling techniques of Wones and Eugster (1965) would not apply. Carbonates, however, are rarely found in more than trace amounts in amphibolite hosted ores.

ACKNOWLEDGEMENTS:

REFERENCES

Appel, P.W.U., and LaBerge, G., 1987, Precambrian Iron-Formations: Theophrastus Publications, Athens, Greece, 674 pp.

Baker, D.R., and Buddington, A.F., 1970, Geology and magnetite deposits of the Franklin Quadrangle and part of the Hamburg Quadrangle, New Jersey: USGS Prof. Paper 638,73 pp.

Barrett T.J., Jarvis Ian, Longstaffe, F.J., and Farquhar, Ron,1988, Geochemical aspects of hydrothermal sediments in the eastern Pacific Ocean: An update: American Mineralogist,v.26,p.841-58

Bayley, W.S., 1910, Iron mines and mining in New Jersey:
    New Jersey Geol. Survey Final Rept, v. 7, 512 pp.

Bayley, W.S., 1941, Precambrian geology and mineral resources
    of the Delaware Water Gap and Easton quadrangles, New
    Jersey and Pennsylvania: U.S. Geol. Survey Bull.930. 98 pp.

Bayley, R.W., and James, H.L., 1973, Precambrian iron-formations of
    the United States: Econ. Geol., v. 68, p.934-59.

Buddington, A.F., 1966, The Precambrian magnetite deposits of
    New York and New Jersey: Econ. Geol., v. 61, p. 484-510.

Buddington, A.F., and Leonard, B.F., 1962, Regional geology of
    the St. Lawrence County magnetite district, Northwest
    Adirondacks, New York: USGS Prof. Paper 376, 145 pp.

Buddington, A.F., and Lindsley, D.H., 1964, Iron-titanium
    oxide minerals and synthetic equivalents: Journal of
    Petrology, v. 5, p. 310-357.

Buddington, A.F., Fahey, J., and Vlisidis, A., 1955, Thermome-
    tric and petrogenetic significance of titaniferous magne-
    tite: American Journal of Science, v. 253, p. 497-532.

Collins, L.G., 1969a, Regional recrystallization and the
    formation of magnetite concentrations, Dover magnetite
    district, New Jersey: Econ. Geol., v. 64, p. 17-33.

Collins, L.G., 1969b, Host rock origin of magnetite in
    pyroxene skarn and gneiss and its relation to alaskite
    and hornblende granite: Econ. Geol. v. 64, p. 191-201.

Davy, R., 1983, A contribution on the chemical composition of
    Precambrian iron-formations: in Trendall, A.F. and
    Morris, R.C. (editors) Iron Formation Fact and Problems:
    Elsevier, Amsterdam p. 325-344.

Drake, A.A., Jr., 1984, The Reading Prong of New Jersey and
    eastern Pennsylvania: An appraisal of rock relations
    and chemistry of a major Proterozoic terrane in the
    Appalachians, in Bartholomew, M.J., ed., The Grenville
    event in the Appalachians and related topics: GSA Special
    Paper 194, p. 75-109.

Drake, A.A., Kastelic R.L. and Lyttle, P.T., 1985, Geologic map of the eastern parts of the Belvidere and Portland Quadrangles, Warren County, New Jersey: Geologic Quadrangle Map, U.S. Geological Survey, Map 1-15

Ernst, W.G., 1966, Synthesis and stability relations of ferrotremolite: American Journal of Science, v.264, p.37-65.

Ernst, W.G., 1976, Petrologic Phase Equilibria: Freeman, San Francisco.

Eugster, H.P., and Wones, D.R., 1962, Stability relations of the ferruginous biotite, annite: Jour. of Petrology, v. 3, p. 81-124.

Garrison, M.J., and Rutstein, M.S., 1982, Reinterpretation and origin of the magnetite mines of Western Putnam County, N.Y.: Geol.Soc.America Abstracts with Program, v.14, p.20.

Gunderson, L.C., 1986, Geology and geochemistry of the Precambrian rocks of the Reading Prong, New York and New Jersey - Implications for the genesis of iron-uranium-rare earth deposits, in Carter, L.M.H. (Editor), USGS Research on Energy Resources - 1986, Programs and Abstracts; USGS Circular 974, p. 19.

Hagner, A.F., and Collins, L.G., 1955, Source and origin of magnetite at the Scot Mine, Sterling Lake, New York: Science, v. 122, p. 1230-1231.

Hagner, A.F., Collins, L.G., and Clemency, C.V., 1963, Host rock as a source of magnetite ore, Scott Mine, Sterling Lake, New York: Econ Geol., v. 58, p. 730-768,

Hotz, P.E., 1953, Magnetite deposits of the Sterling Lake, NY - Ringwood, NJ area: USGS Bull. 982-F.

Hyndman, D.W., 1985, Petrology of igneous and metamorphic rocks: McGraw-Hill, New York, 786 pp.

Kastelic, R.L., Jr., 1980, Origin of the Washington magnetite deposit, Warren County, New Jersey: Geol, Soc. Amer, Abstracts with Program, v. 12, p. 44.

Kastelic, R.L., Jr., 1979, Precambrian geology and magnetite deposits of the New Jersey Highlands in Warren County, New Jersey: MS Thesis, Lehigh University, 155 pp.

Klemic, H, Heyl, A.V. Taylor, A.R., and Stone, J., 1959,
    Radioactive rare-earth deposit at Scrub Oaks Mine, Morris
    County New Jersey: US Geological Survey Bulletin
    1082-B, 59 pp.

Martin, R.F., and Piwinskii, A.J. 1969, Experimental data
    bearing on   the movement of iron in an aqueous vapor:
    Economic Geology, v. 64, p. 798-803.

Neumann, G.L. and Mosier, M., 1948, Certain magnetite deposits
    in New Jersey:U.S.Bureau of mines Rept. of Inv.42225,35 pp.

Palmer, D.F., 1970, Geology and ore deposits near Benson
    Mines, New   York: Econ. Geology, v. 65, p. 31-39.

Postel, A.W., 1952, Geology of Clinton County magnetite
    district, New York: U.S. Geol. Survey Prof.Paper 237,88 pp.

Puffer, J.H., and Volkert, R.A., 1991, Generation of
    trondjhomite from partial melting of dacite under
    granulite facies conditions: an example from the New
    Jersey Highlands, USA:Precamb Research v. 51, p. 115-125.

Puffer, J.H., 1980, Iron ore deposits of the New Jersey
    Highlands: in Manspeizer, W. (Editor), Field studies of
    New Jersey Geology and Guide to Field trips. 52nd Annual
    Meeting of the New York State Geological Association,
    Newark, New Jersey, pp.202-208.

Puffer, J.H., 1972, Iron bearing minerals as indicators of
    intensive variables pertaining to granitic rocks from the
    Pegmatite Points area,Colorado:Amer.Journal of Science,
    v.272,p.273-289.

Puffer, J.H., 1975, Some North American iron-titanium oxide
    bearing pegmatites: Amer. Journal of Science, v. 275,
    p. 698-730.

Puffer, J. H., 1980, Precambrian rocks of the New Jersev
    Highlands: in Manspeizer, W. (Editor), Field studies of
    New Jersey Geology and Guide to Field trips. 52nd Annual
    Meeting of the New York State Geological Association,
    Newark, New Jersey, p. 42-53.

Spencer, A.C., Kummel, H.B., Wolff, J.E., Salisbury, R.D., and
    Palache, C., 1908, Description of the Franklin Furnace
    Quadrangle (New Jersey): U.S. Geol. Surv., Geologic Atlas,
    Folio 161,27 pp.

Sims P.K., 1953, Geology of the Dover magnetite district, Morris County, New Jersey: US Geol. Survey Bull. 982-G, p. 245-305.

Sims P. K., 1958, Geology and magnetite deposits of Dover District, Morris County, New Jersey: US Geol. Survey Prof. Paper 287, 162 pp.

Sims P.K. and Leonard, B.F., 1952, Geology of the Andover mining district, Sussex County, New Jersey: State of New Jersey Dept of Conservation and Econ. Development Bull. 62, 46 pp.

Smith, L.L. 1933, Magnetite ore of Northern New Jersey: Econ. Geol., v. 28, p. 658-677.

Troxell, J. R., 1948, The Ahles iron mine, Warren County New Jersey, US   Bur Mines RRept. Inv., 4240, 8 pp.

VanN.Dorr, John, 1973, Iron formation in South America: Econ. Geol., v. 68, p. 1005-1022.

Volkert, R.A., Monteverde, D.H., and Drake, A. A., Bedrock Geologic Map   of the Stanhope Quadrangle, Sussex and Morris Coundies, New Jersey, 1989, New Jersey Geological Survey, Geologic Quadrangle Map GQ-1671.

Wones, P.R., and Eugster, H.P., 1965, Stability of biotite: experiment, theory, and application: Amer. Mineralogist, v. 50, p. 1228-1272.

CHAPTER 4

AMPHIBOLITES AND PYROXENITES OF THE NEW JERSEY HIGHLANDS

John H. Puffer, Edmund Osian, Sivajini Gilchrist,
Michelle Connolly, Camille Forrest, Douglas Mullarkey,
and John Ratti, Geology Department, Rutgers University,
Newark, New Jersey 07102

INTRODUCTION

The objective of this study is to characterize the chemical composition of the amphibolites and pyroxenites of the New Jersey highlands in order to develop a better understanding of their most probable protolith or protoliths.

The amphibolites of the New Jersey Highlands are composed of sodic plagioclase and hornblende in subequal amounts (Figure 1) with commonly substantial amounts of both ortho- and clino-pyroxene and biotite and minor quartz, apatite, pyrite or pyrhotite and highly variable concentrations of magnetite. They were referred to as the Pochunk Gneiss on the Lewis and Kummel (1906) map of New Jersey but have since been referred to simply as amphibolite. The amphibolites are typically black to dark green or if pyroxene is a major component they are typically greenish gray. Pegmatite veins are commonly intruded into the amphibolites.

Maxey (1971), on the basis of chemical analyses of 56 amphibolite samples from throughout the New Jersey Highlands, concludes that they"... are ortho- rather than para-amphibolites. Variation trends established for major and trace elements are those expected for metamorphosed basalts rather than meta-morphosed shale-carbonate mixtures." Kastelic (1979) on the other hand concludes that the amphibolites of Warren County, New Jersey are metasediments on the basis of 5 analyses that display high Ba contents (230 to 990 ppm) and a negative correlation between Mg content and Cr and Ni.

Drake (1984) agrees with Kastelic (1979) and concludes that "... evidence is abundant that a great deal of the amphibolites in the Reading Prong results from the metamorphism of sedimentary rocks and that at least some probably results from the metamorphism of mafic intrusive rocks. The amphibolites within the Losee Metamorphic Suite are thought to be metamorphosed volcanic rocks. Other amphibolites may be metavolcanic, but the evidence is equivocal."

Figure 1: Photomicrograph of typical amphibolite interpreted
as a meta-basalt sampled along Rt 15. Note the coarse grain
size and the unaltered plagioclase (white) and hornblende
(gray).
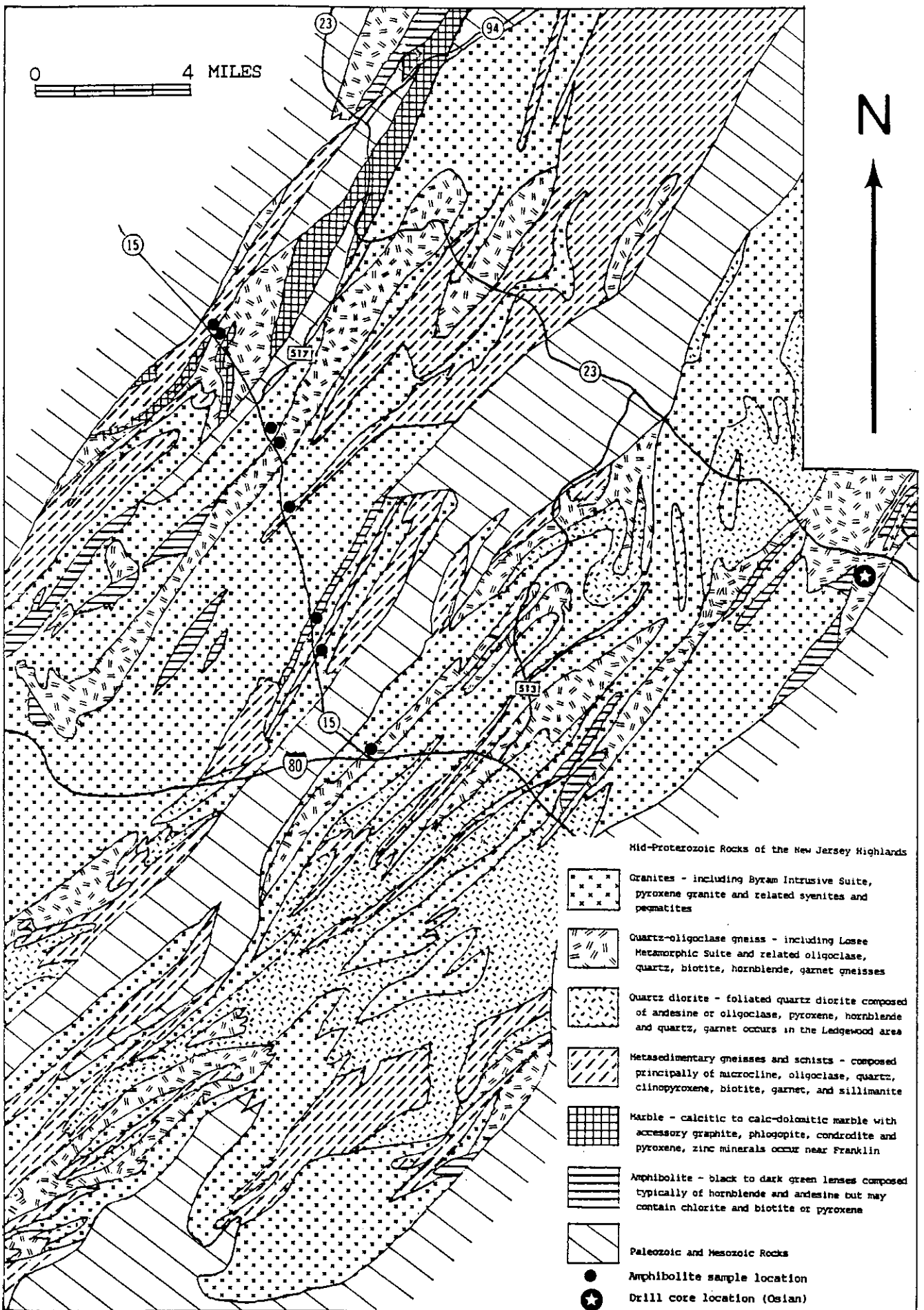
Figure 2: Geologic map of the central New Jersey Highlands with
locations of amphibolite samples collected along Rt. 15 and drill
cores from near the intersection of Rt. 23 and the Ramapo fault.

The legend (right side of map) reads:

Mid-Proterozoic Rocks of the New Jersey Highlands

Granites - including Byram Intrusive Suite,
pyroxene granite and related syenites and
pegmatites

Quartz-oligoclase gneiss - including Losee
Metamorphic Suite and related oligoclase,
quartz, biotite, hornblende, garnet gneisses

Quartz diorite - foliated quartz diorite composed
of andesine or oligoclase, pyroxene, hornblende
and quartz, garnet occurs in the Ledgewood area

Metasedimentary gneisses and schists - composed
principally of microcline, oligoclase, quartz,
clinopyroxene, biotite, garnet, and sillimanite

Marble - calcitic to calc-dolomitic marble with
accessory graphite, phlogopite, condrodite and
pyroxene, zinc minerals occur near Franklin

Amphibolite - black to dark green lenses composed
typically of hornblende and andesine but may
contain chlorite and biotite or pyroxene

Paleozoic and Mesozoic Rocks

● Amphibolite sample location

✪ Drill core location (Oslan)

METHODS

Samples of amphibolite and pyroxenites from several
locations throughout the New Jersey Highlands (Figure 2) were
collected and chemically analyzed. Most of the samples were
collected from outcrop locations, particularly road-cuts and
quarry-cuts, with care taken to avoid rock with obvious
weathering effects. In addition, several drill core samples
were collected.

Amphibolites and pyroxenites were identified in the field
on the basis of their (black, dark gray to dark green) and
typically coarse-grained, granoblastic appearance although
some samples were semischistose. Most of the samples are
amphibolites but no attempt was made to distinguish
amphibolites from pyroxenites in the field; they share
overlapping physical appearances, particularly samples that
contain both amphibole and pyroxene. All the sampled
collected are composed largely of a hornblende, pyroxene,
plagioclase, and biotite mineral assemblage but with a wide
modal range. None of the samples collected are fine grained,
but our collection includes several very coarse grained
samples that are commonly referred to as "skarns".

The samples were chemically analyzed with Rigaku XRF
equipment at the geochemistry lab of Rutgers University in
Newark. Analytical standards include NBS Basalt, USGS
standards AGV1, G2, BCR1, BHVO1, GSP1, JB1, and a Rutgers New
Brunswick basalt standard IZ.

RESULTS

The analyzed samples of amphibolite and pyroxenite may be
separated into three chemical groups. Group 1 includes about
two-thirds of the samples and is chemically characterized by a
TiO_2 range of 1 to 3.5 percent Figure 3, and an Al_2O_3 range
of 13 to 17 percent (Table 1, Figure 4). Group 2 includes
about one-sixth of the samples and is characterized by a TiO_2
range of 0.1 to 1 percent and an Al_2O_3 range of 16 to 23
percent (Table 2, Figures 3 and 4). Group 3 includes the
remaining one-sixth of the samples and is characterized by a
TiO_2 range of 0.1 to 1 percent and an Al_2O_3 range of 5 to 15
percent (Table 3, Figures 3 and 4).

Table 1.
Meta-basalts

wt.%	998Qtz-Th	2300I-Th	745 Al b+d	Osian1A	Osian3B	Osian4A	Osian6	Osian7A	Osian8
SiO2	51.6	48.8	47.2	52.1	52	49	44.6	48.9	48.75
TiO2	1.6	1.6	2.4	0.82	1.75	1.03	1.42	2.22	2.25
Al2O3	16	15.5	15.8	13.6	13.8	12.85	11.92	12.48	12.84
FeO	10.5	11.05	10.88	10.14	11.21	9.37	12.33	12.83	12.8
MgO	5.8	8.3	7	6.14	5.7	9.85	9.67	7.5	7.6
MnO	0.18	0.17	0.16	0.15	0.11	0.07	0.07	0.17	0.2
CaO	9.8	10.2	10.1	8	6	8.5	9.55	9.25	10.1
Na2O	2.4	2.3	3.2	3.7	3.98	4.2	2.6	3.06	3.4
K2O	0.8	0.7	1.4	0.94	2	1.25	1.09	1	1.06
P2O5	0.21	0.23	0.48	1.31	0.59	0.17	0.13	0.4	0.38
LOI*	0.8	0.9	1	3	3	3	3	3	3
Total	99.69	99.75	99.62	99.9	100.14	99.29	96.38	100.81	102.38
ppm									
Ba	250	215	444	292	553	297	248	68	72
Cr	153	218	187	160	80	175	405	159	170
Ni	77	130	101	51	0	78	66	36	18
Sr	471	350	774	491	300	170	180	228	160
V	266	183	236	150	180	191	254	324	345
Zr	111	91	138	280	210	115	78	115	120
Ba	20 to 1200	10 to 1000	20 to 1000						
Cr	2 to 500	15 to 500	5 to 550						
Ni	5 to 350	5 to 350	3 to 350						
Sc	10 to 60	10 to 55	10 to 50						
Sr	7 to 2000	57 to 1000	18 to 2000						
V	10 to 600	60 to 450	37 to 500						
Zr	20 to 335	27 to 230	15 to 320						

wt.%	Osian9B	Osian11	Osian16	Osian17	Osian19	Rt15-2a	Rt15-3a	Rt15-4a	Rt15-5a
SiO2	46.5	45.9	50.5	52.4	53	52.03	49.2	48	48.6
TiO2	1.31	1.59	1.5	1.09	3.72	1.44	1.42	1.8	0.64
Al2O3	8.88	12.72	13.28	14.32	11.6	14.1	12	12.2	15.4
FeO	11.9	12.35	10.45	8.85	12.4	11.23	12.5	13.73	9.7
MgO	11.21	10.63	5	6.4	5.57	5.63	9.6	6.6	7.4
MnO	0.07	0.2	0.12	0.11	0.22	0.16	0.16	0.47	0.15
CaO	10.67	8.57	8.05	6.57	8.77	8.55	7.5	8.75	9.9
Na2O	2.5	2.95	3.6	3.7	3.12	4.26	3.7	3.41	3.6
K2O	1.96	1.74	2.3	2.4	0.96	1.13	2.4	1.7	1.25
P2O5	2.03	0.14	0.76	0.22	0.88	0.33	0.16	0.32	0.25
LOI*	3	3	3	3	3	1.64	1.43	2.86	2.24
Total	100.03	99.78	98.55	99.06	103.24	100.5	100.07	99.84	99.13
ppm									
Ba	616	204	280	532	72				428
Cr	540	136	68	47	48	140	340		114
Ni	127	67	30				27	6	40
Sr	96	248	260	314	148	69	72	200	410
V	204	236	155	100	340	153	245	231	200
Zr	166	82	84	170	217	125	71	62	67

wt%	Rt15-6a	Rt15-8a	Rt.15Path	Maxey 49Amphi.	range high	low
SiO2	51.11	49.5	49.78	50	55.05	44.06
TiO2	1.7	2.7	2.81	1.72	3.43	0.59
Al2O3	13.72	12.51	11.49	15.43	17.65	12.99
FeO	10.59	12.99	11.55	11.53	14.89	8.07
MgO	6.51	5.43	7.01	6.35	9.34	3.87
MnO	0.13	0.23	0.16	0.2	0.37	0.11
CaO	7.01	10.19	9.35	9.35	11.99	6.06
Na2O	3.81	3.26	4.38	2.14	4.84	0.44
K2O	2.59	0.58	0.72	1.27	2.6	0.39
P2O5	0.34	0.49	0.2	0	n.d.	n.d.
LOI*	2.35	2.09	2.48	1.98	2.77	1.23
Total	99.86	99.87	99.93	99.97		
ppm						
Ba			110			
Cr	130	110	90	111	304	8
Ni	19	6	26	46	226	1
Sr	273	82	175			
V	193	372	550			
Zr	173	133	66			

Table 1: Chemical composition of Amphibolites from New Jersey interpreted as meta-basalts compared with major element averages (Manson, 1967) of 998 quartz-normative-tholeiitic-basalts (998Qtz-Th), 230 olivine-normative-tholeiitic-basalts (230Ol-Th), and 745 alkali-olivine-normative-basalts and diabase samples (745 Al b+d) with trace element averages and ranges (Prinz, 1967). Samples from drill core collected near the intersection of Rt-23 and I-287 are labeled Osian-; those from Rt-15 are labeled Rt15-; the average and range of 49 New Jersey Amphibolites analyzed by Maxey (1971) that we interpret as meta-basalt is also listed.
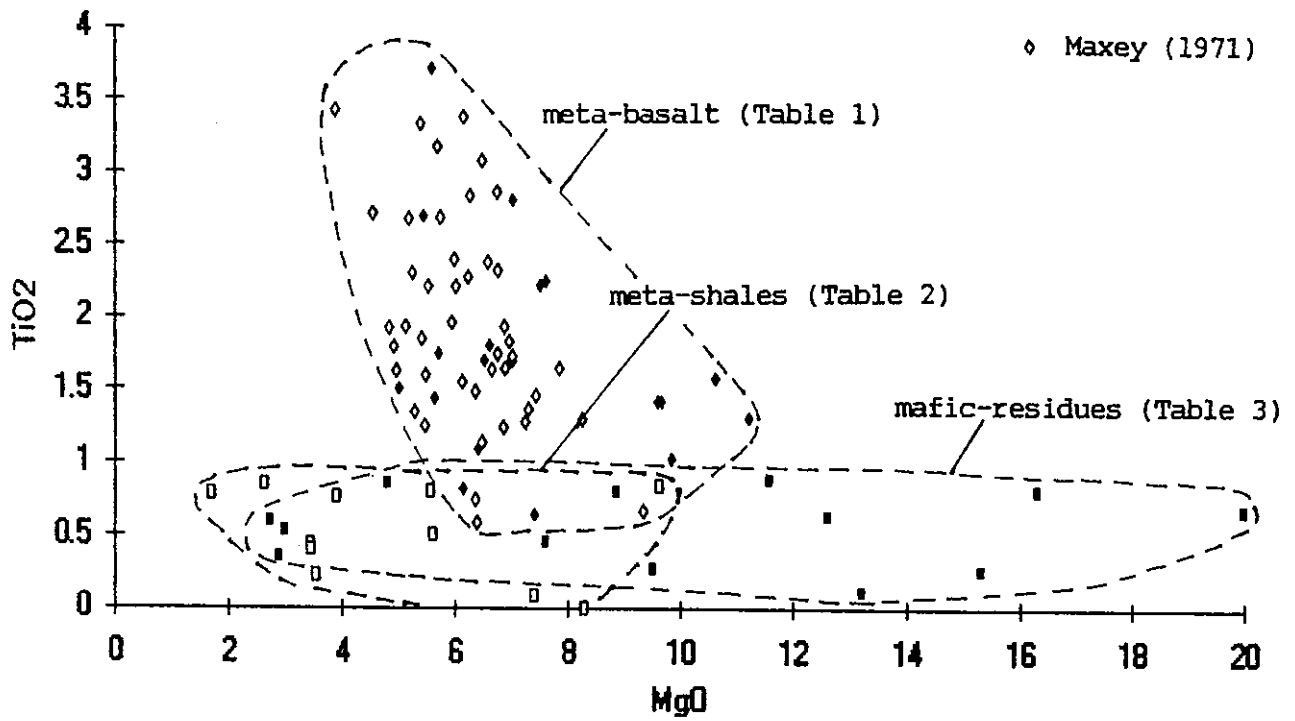
Figure 3: TiO$_2$/MgO plot of amphibolites from the New Jersey Highlands (Tables 1,2,3).

	Shale	Osian10	Osian18	Osian21	Osian22	MaxB-11	MaxB-18
SiO2	59.93	61.75	57	59	63.4	46.64	48.65
TiO2	0.85	0.44	0.78	0.76	0.4	0	0.08
Al2O3	16.63	16	16.4	16	15.76	22.63	17.42
FeOt	6.03	4.25	5.85	6	4.23	5.15	11.26
MgO	2.63	3.44	1.7	3.9	3.45	8.29	7.39
MnO	0	0.05	0.08	0.9	0.06	0.92	0.17
CaO	2.18	4.82	1.85	4.6	4.15	12.46	9.67
Na2O	1.73	4.36	4.4	4.16	4.1	2.17	1.34
K2O	3.54	1.4	6.16	1.85	1.36	0.08	1.24
LOI*	6.65	3	3	3	3	1.64	2.78
total	100.17	99.51	97.22	100.17	99.91	99.98	100
Ba	580	706	1826	640	708		
Cr	90	30	0	40	49	27	45
Ni	68	27	0	42	24	7	39
Sr	300	808	280	640	732		
V	130	60	46	94	50		
Zr	160	195	762	181	165		

	MaxG-2	MaxI-48	MaxI-22	MaxI-55
SiO2	48.89	49.92	52.31	56.43
TiO2	0.84	0.5	0.8	0.22
Al2O3	16.04	17.34	18.29	19.51
FeOt	9.85	10.33	8.87	7.75
MgO	9.63	5.61	5.56	3.54
MnO	0.13	0.24	0.31	0.13
CaO	7.89	10.56	8.97	8.06
Na2O	1.19	2.49	2.84	1.87
K2O	2.81	1.07	0.75	1.16
LOI*	2.72	1.95	1.31	1.32
total	99.99	100.01	100.01	99.99
Cr	180	125	84	27
Ni	51	28	15	15

Table 2: Chemical composition of Amphibolites from New Jersey interpreted as meta-shales compared with a major element average of 85 shales (Shaw, 1956) with trace element averages by Turekian and Wedepohl (1961). Samples labeled Osian- are drill-core from near the intersection of Rt-23 and I-287; samples labeled Max- were analyzed by Maxey (1971).
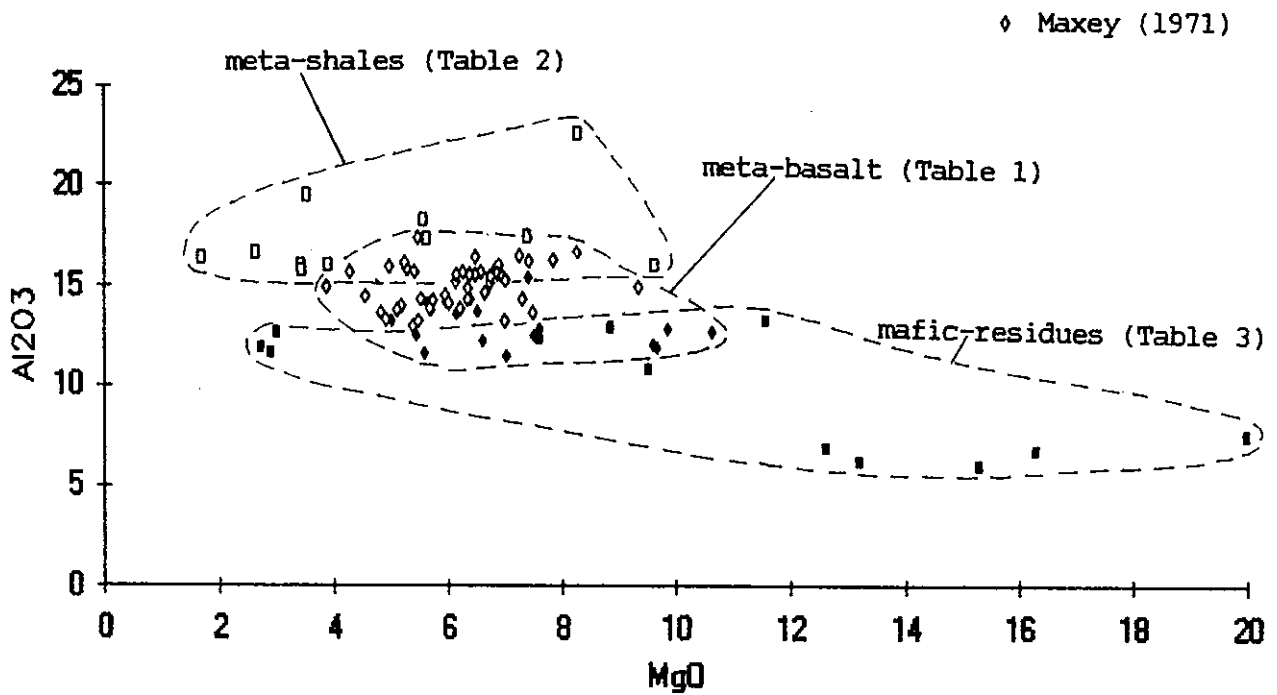
Figure 4: Al_2O_3/MgO plot of amphibolites from the New Jersey Highlands (Tables 1,2,3).

%	Osian5	Osian9A	Osian14	Osian20	Green P.	Hi Ledge	Hibernia	Blue
SiO2	45.5	51.75	65.4	49.6	45.37	50.53	48.2	41.95
TiO2	0.68	0.63	0.53	0.6	0.11	0.81	0.27	0.26
Al2O3	7.52	6.88	12.64	11.88	6.22	6.72	10.81	5.97
FeO	12.67	13.11	5.82	9.95	17.5	12.4	15.52	20.26
MgO	19.98	12.62	3	2.74	13.21	16.31	9.52	15.31
MnO	0.17	0.1	0.03	0.14	0.17	0.32	0.05	0.14
CaO	6.7	6.7	1.75	18.67	12.31	6.42	2.78	10.41
Na2O	0.7	1.8	5.56	1.74	0.95	1.85	5.21	1.38
K2O	2	1.89	0.94	0.34	0.26	0.51	1.81	0.48
P2O5	0.2	0.01	0.28	0.27	0.81	0.03	0.03	0.04
LOI*	3	3	3	3	3.85	4.31	5.63	4.33
Total	99.12	98.49	98.95	98.93	100.76	100.21	99.83	100.53
PPM								
Ba	496	140	214	68	90	450	280	41
Cr	625	88	70	63	10	170	60	115
Ni	307	57	30	0	2	100	46	44
Sc	18	19	24	29	22	33	13	29
Sr	180	46	140	148	30	42	90	28
V	90	260	226	100	20	117	161	217
Zr	85	125	260	90	52	163	109	48

%	Kastelic 3	Kastelic 4	Kastelic 5	Mac-H-18	R-15-Bi
SiO2	51.3	56.8	68.3	48.66	45.72
TiO2	0.46	0.86	0.35	0.8	0.89
Al2O3	12.3	15.3	11.6	12.92	13.28
FeO	9.4	6.6	4.8	13.43	12.86
MgO	7.6	4.8	2.9	8.86	11.57
MnO	0.25	0.16	0.1	0.21	0.31
CaO	13	4.8	4.6	11.3	9.99
Na2O	1.7	3.3	2.3	0.57	2.94
K2O	2.6	5.03	2.8	1.02	1.76
P2O5	0.25	0.18	0.09	0	0.19
LOI*	2.01	1.77	2.49	2.22	1.06
Total	100.87	99.6	100.33	99.99	100.57
PPM					
Ba	690	990	500		
Cr	10	21	40	229	
Ni	12	26	12	32	
Sc					
Sr	360	250	280		
V	260	150	68		
Zr	57	140	52		

Table 3: Chemical composition of Amphibolites from New Jersey interpreted as refractory mafic residues. Samples labeled Osian- are drill-core from near the intersection of Rt-23 and I-287; samples from magnetite iron mines include the Davenport mine near Green Pond (GreenP.), the High Ledge mine (Hi.Ledge), the Hibernia mine and the Blue mine; samples R-15-Bi is from Rt-15 near field trip stop 2; samples Kastelic- are from Warren County as analyzed by Kastelic (1979); Sample Max-H-18 was analyzed by Maxey (1971).

GEOLOGIC SETTING

Group 1

Most of the Group 1 samples are amphibolites and pyroxene bearing amphibolites. Group 1 amphibolites are typically exposed as concordant or partially discordant lenses of highly variable thickness (1 to 500 m) and represent each of the amphibole exposures that are over 20 m thick. Group 1 amphibolites commonly occur as boudons within the metasedimentary schists, gneisses, and marble units. They also commonly occur as thick concordant lenses or sheets within the Losee Gneiss (a quartz-oligoclase gneiss). They less commonly occur as irregular shaped semi-concordant bodies or xenoliths within the hornblende granites of the Highlands but are less commonly found as xenoliths within the pyroxene granites.

Group 2

Group 2 samples typically occur as concordant lenses or boudons within the metasedimentary units of the Highlands or less commonly as lenses within the Losee Gneiss or xenoliths within granites. They are commonly rich in plagioclase and contain highly variable amounts of pyroxene.

Group 3

Group 3 samples typically occur as thin selvage zones within or at the margins of the Losee Gneiss. They are typically associated with pegmatites and with magnetite ore deposits (see Chapter 3). Several samples are very coarse grained and have been described as "skarns" by Sims (1958). Their mineralogy is highly variable but commonly includes considerable pyroxene.

INTERPRETATION

Group 1

The chemical range of Group 1 samples with few exceptions is within the chemical range of common basaltic rock types (Table 1). The few exceptions (for example samples J-3 and J-8, Maxey, 1971) are consistent with chemically altered basalt, particularly basalt that has undergone weathering. A range of basalt types are represented by Group 1 but most samples are

chemically equivalent to quartz tholeiites and plot on variation diagrams (Figures 3 through 6) along scattered but readily apparent tholeiitic fractionation trends. Titanium enrichment (Figure 3) and nickel and chrome depletion trends (Figures 5 and 6) are particularly apparent. Each of these trends are typical of tholeiitic fractionation processes.

The establishment of an igneous fractionation trend is probably the strongest argument in support of a meta-igneous origin for the Group 1 Highlands amphibolites. One of the clearest and most straight forward discussions of the chemical distinction between ortho- and para-amphibolites was made be Leake (1964). Leake (1964) argues that although the Cr, Ni and Ti values of ortho-amphibolites are commonly higher than para-amphibolites, overlapping ranges commonly make clear distinctions difficult. Leake (1964) instead suggests that if enough analyses are available to establish the kind of igneous fractionation trends that invariably characterize suites of igneous rock, the trend itself is evidence that the protolith was igneous. Similar fractionation trends were found by to be absent from populations of analyzed shales. The data that we present confirms the observations of Leake (1964); compare Figure 6 with Figure 7.

We are not suggesting that all of the basaltic protoliths of Group 1 amphibolites were co-magmatic or were developed during a single fractionation event. There may have been several magmatic events involving basaltic rock, both intrusive and ex-trusive. But the dominant magmatic event (or events) involved quartz tholeiitic magma. The CIPW normative content of the average of 49 Group 1 samples analyzed by Maxey (1971) includes 0.42 percent quartz and 23 percent hypersthene and a calculated plagioclase composition of An61.

Quartz tholeiitic basaltic rock chemically similar to Group 1 rock is typically interpreted as "within plate" basalt (Pierce and others, 1981; Figure 8) and includes most flood basalt occu-rrences associated with tectonic extension. Although Group 1 samples overlap the mid-ocean-ridge-basalt (MORB) field of Figure 8 it is unlikely that MORB basalts are represented in Group 1, with one possible exception, on the basis of their low MgO, Ni, and Cr content (Table 1).

If most of the amphibolites of the New Jersey Highlands were emplaced as "within plate" basaltic rock during rifting or any kind of tectonic extension they would be tectonically in-compatible with the compressional continental margin model proposed for the development of the Losee Gneiss by Puffer and Volkert (1991). The Group 1 amphibolites found within the
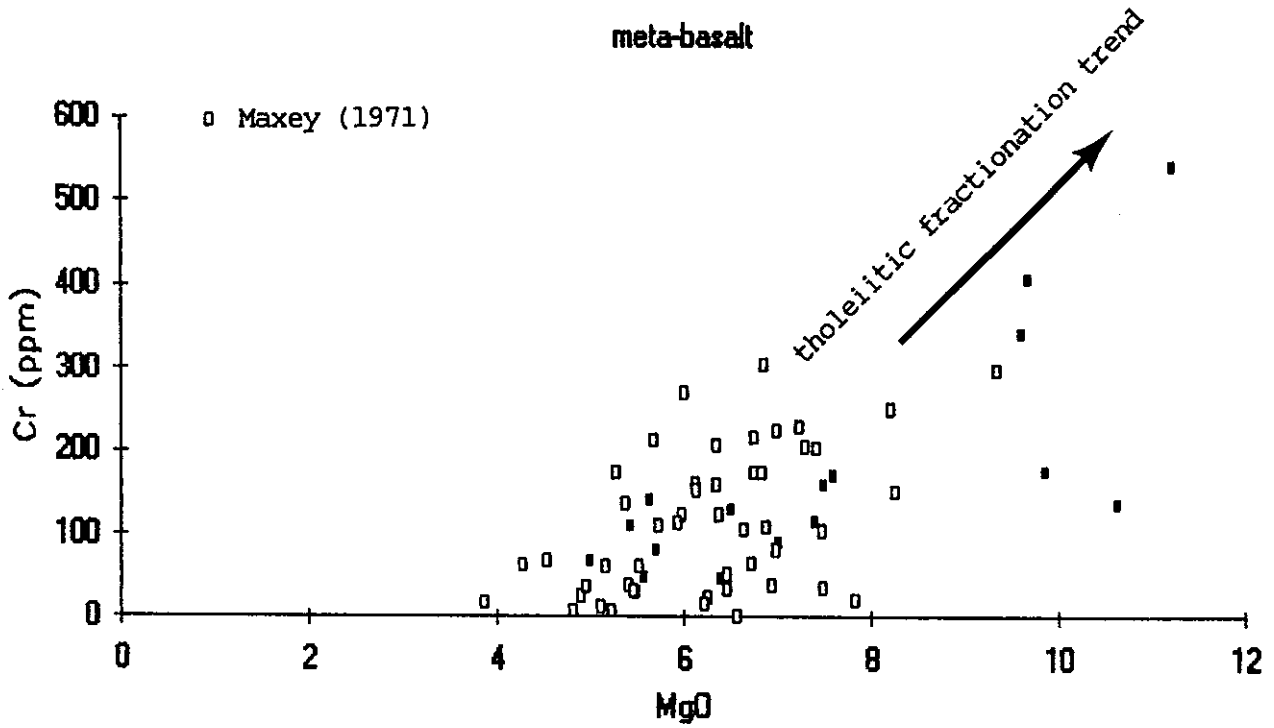
Figure 5: Cr/MgO plot of New Jersey Highlands amphibolite samples interpreted as meta-basalts. Note the scattered but clear fractionation trend typical of basaltic rock suites.
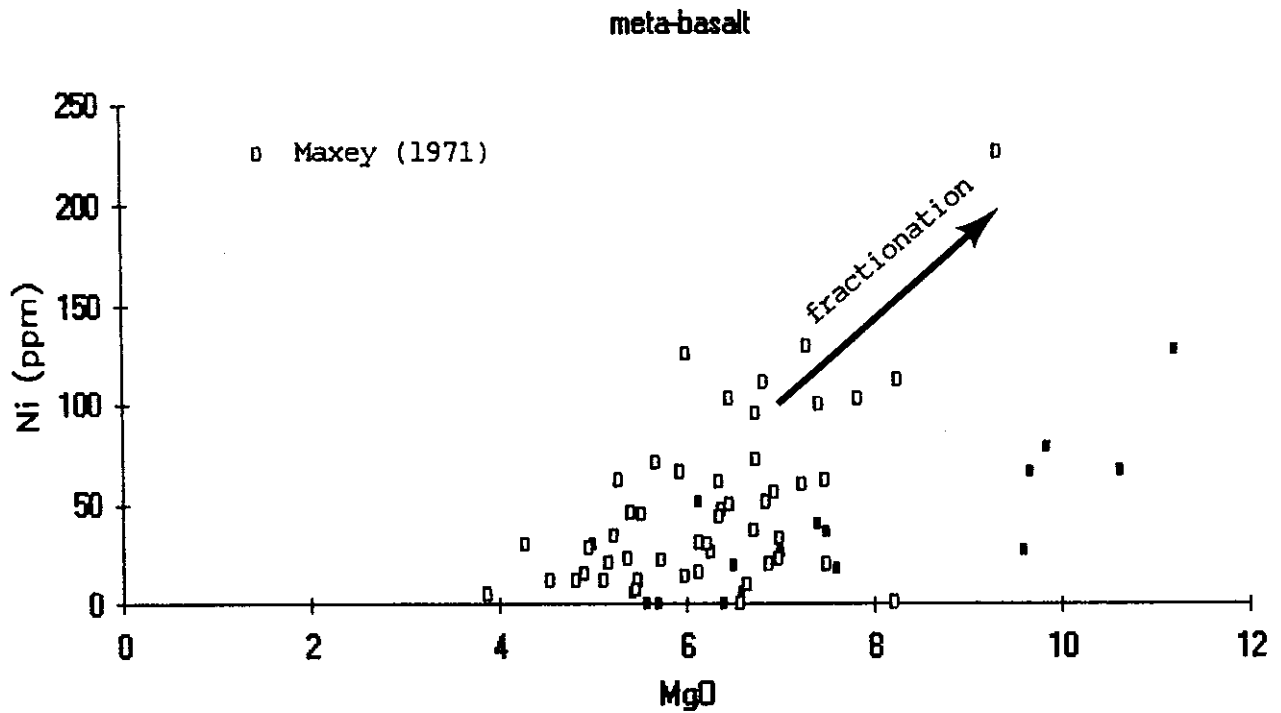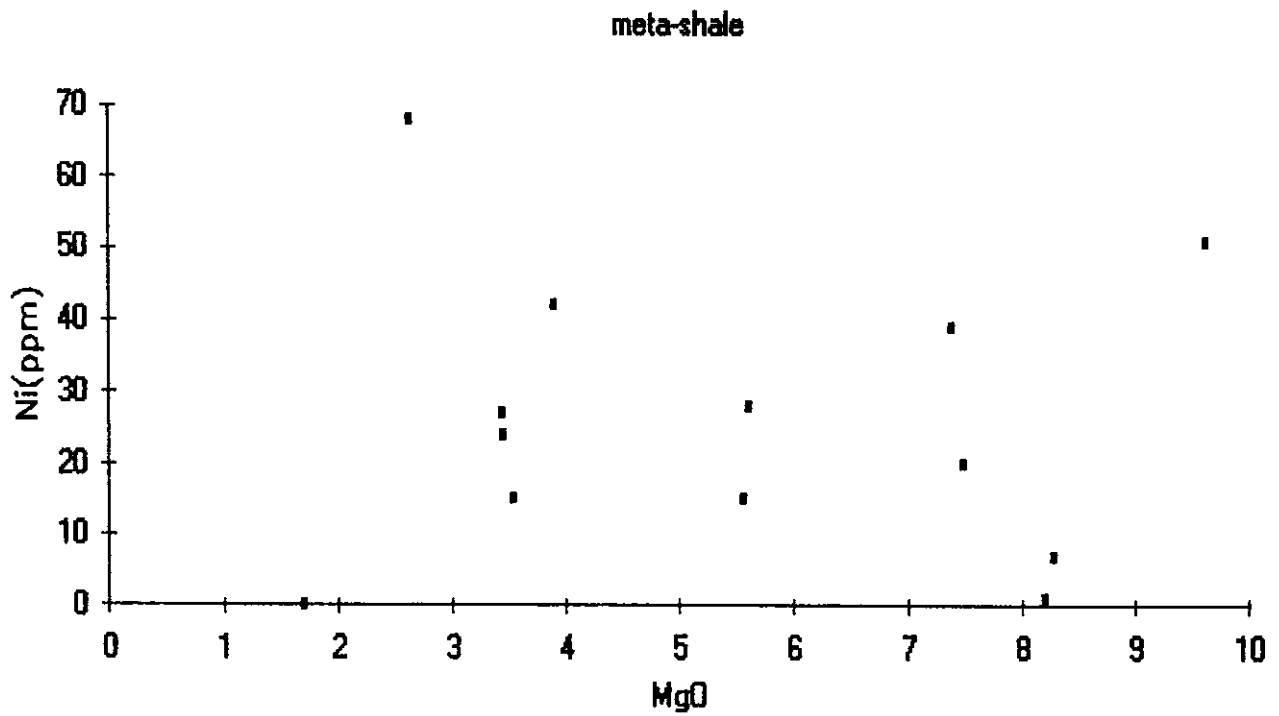
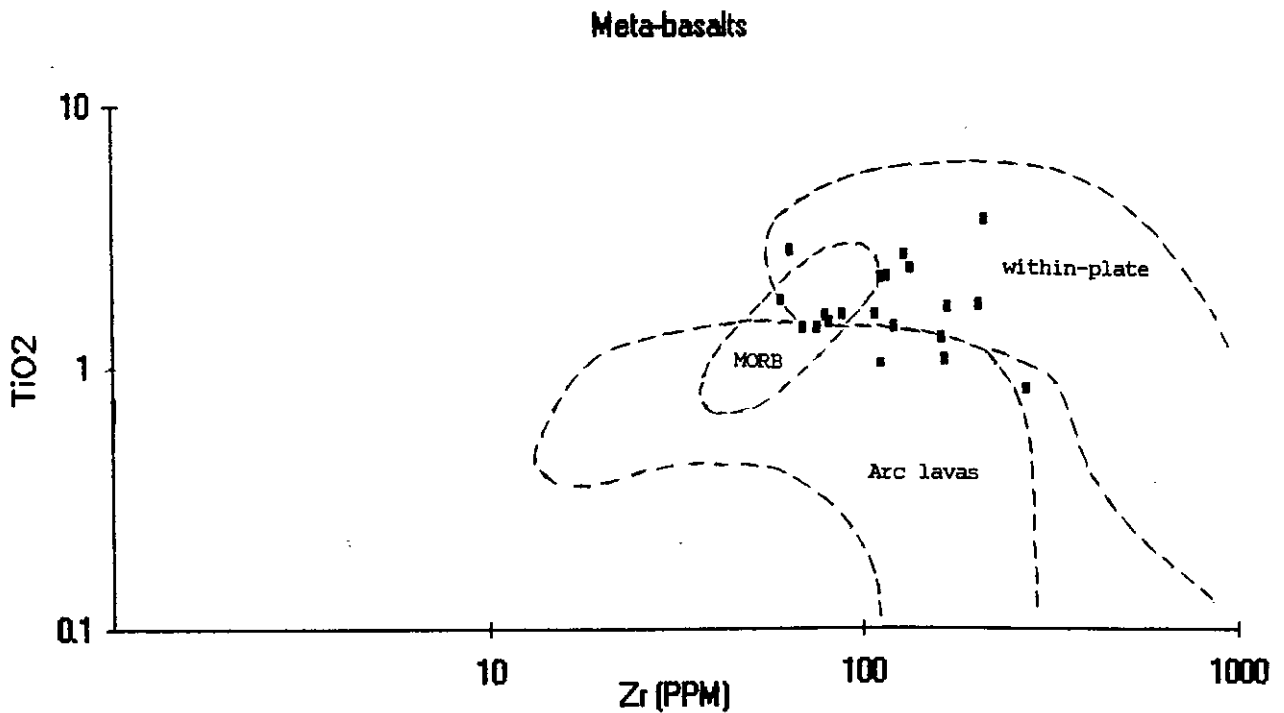Figure 6: Ni/MgO plot of New Jersey Highlands amphibolite samples interpreted as meta-basalts. Note the scattered but clear fractionation trend typical of basaltic rock suites.

Figure 7: Ni/MgO plot of 12 New Jersey Highlands amphibolites
samples interpreted as meta-shales (Table 2). Note the
absence of any fractionation trend.

Meta-basalts

Figure 8: Log-Log plot of TiO$_2$ and Zr content of New Jersey Highlands amphibolites interpreted as meta-basalts (Table 1). Note the overlap of amphibolite compositions onto fields that Pierce and others (1981) interpret as within-plate basalt (including continental flood basalts and rift-basin basalts) and MORB (mid-ocean-ridge basalts).

Losee Gneiss were, therefore, probably emplaced after the
compressional development of Losee calc-alkaline magmatism.
But since the Group 1 amphibolites are clearly granoblastic to
semischistose metamorphic rocks, the extensional or within
plate tholeiitic magmatism must have preceded the last
pervasive metamorphic development of the Highlands and must
have preceded the emplacement of the relatively
unmetamorphosed late protero-zoic diabase dike swarm described
by Volkert and Puffer (in press). It may also be significant
that the chemical range of the Group 1 amphibolites overlaps
the chemical range of the late proterozoic quartz tholeiitic
dike swarm although Group 1 amphi-bolites are more chemically
diverse.

Group 1 also includes a few samples that are not
chemically equivalent to quartz tholeiitic basaltic rock. For
example, two samples from Maxey's (1971) data base (I-61 and
I-98) have the chemistry of a typical basaltic andesite; a
magma type that would be tectonically consistent with Losss
calc-alkaline magmatism. Sample I-52 (Maxey, 1971) is
chemically equivalent to oceanic olivine normative basalt and
sample J-57 (Maxey, 1971) is chemically equivalent to typical
alkaline olivine basalt. These deviations from the dominant
quartz tholeiitic magma type indicate that perhaps several
diverse basaltic events occurred during the development of the
New Jersey Highlands as might be expected considering its long
and probably complex geologic history.

Group 2

The outstanding chemical characteristic of Group 2
amphibolites (16 to 23 percent Al2O3, averaging 18 percent and
0.1 to 1.5 percent TiO2, averaging 0.5 percent) are
inconsistent with basaltic or any known igneous magma types
but fall within the range of pelitic sedimentary rocks (Shaw,
1956; Table 2). Although Group 2 compositions are not
particularly common among shales they fall well within the
shale range (Table 2) and there is nothing chemically
inconsistent with the possibility of a marine pelitic
sedimentary protolith.

Group 3

Group 3 amphibolites and pyroxenites are interpreted as
the refractory residues left from the partial melting (or
anatexis) of metamorphic rocks to form felsic igneous melts.

The chemistry of Group 3 amphibolites is characterized by depletion in elements generally recognized as mobile and enrichment in elements generally regarded as refractory (Shaw. 1977). The MgO content of Group 3 amphibolites is particularly high (Table 3) and would qualify them as ultramafic if they were igneous. Group 3 amphibolites are found as schlerin or wispy irregular lenses near the contacts of igneous units that probably crystallized in-situ. The chemical diversity of the group seems to be related to their geologic setting. Samples GreenP, Hi.Ledge, Hibernia, and Blue, (Table 3) were collected at the margins of magnetite ore deposits mixed with pegmatites. They are depleted in iron and titanium relative to the magnetite concentrations and are depleted in silica, aluminum, potassium and zirconium relative to adjacent pegmatites but are greatly enriched in magnesium (10 to 16 percent). A similar trend is indicated by amphibolite samples Kastelic 3, 4, and 5 (Table 3). Samples 3, 4, and 5 (Kastelic, 1979) were taken 4, 1, and 0 meters from a pegmatite near Belvidere, New Jersey.

Sample R-15-Bi (Table 3) was collected near the margin of some fused Losee Gneiss trondhjemite (sample M, Figure 9) that Puffer and Volkert (1991) describe as the product of in-situ partial fusion of a banded meta-dacite protolith (R-15-Ba, Figure 9). Evidence that sample R-15-Bi represents a mafic refractory residue from such fusion includes the chondrite normalized rare earth element (REE) distribution pattern (Figure 9) with a negative Eu anomaly that balances the positive Eu anomaly of adjacent Losee Gneiss trondhjemite sample M.

Alternatively, a few of the amphibolites that we have interpreted as mafic-residues (Table 3) instead may have developed in shear zones. As MgO, CaO, and FeO are mobilized by hydrothermal solutions during either prograde or retrograde metamorphism, actinolite, epidote, chlorite, and other mafic minerals may precipitate in ductile shear zones. For a discussion of this possibility see Chapter 6.

500

100

50

Chondrite/ Sample

R-15-Bi

10

R-15-Ba

M

1

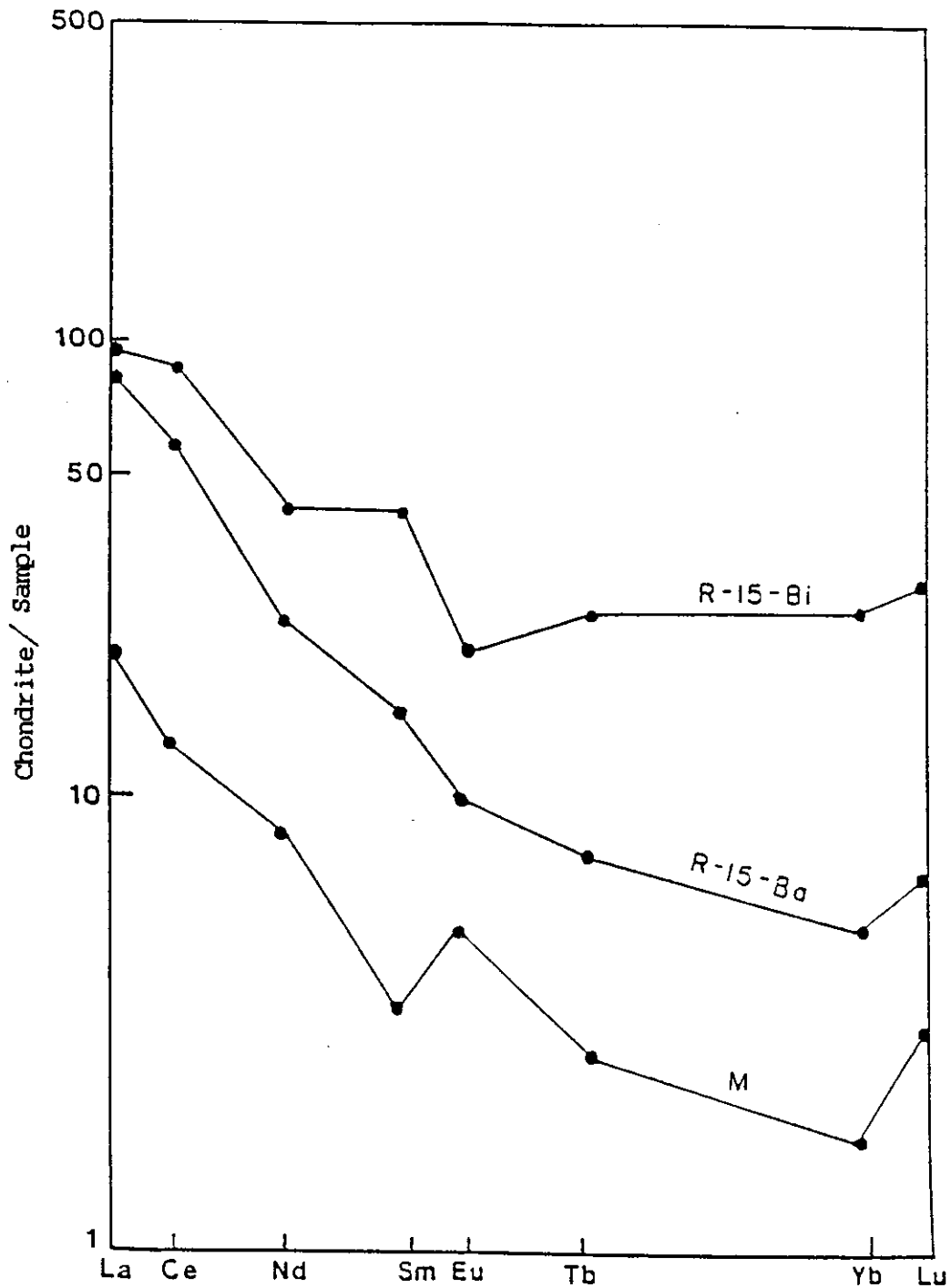La Ce   Nd   Sm Eu   Tb   Yb Lu

Figure 9: Chondrite normalized REE diagram depicting highly fractionated trondhjemite (sample M) interpreted by Puffer and Volkert (1991) as the fusion product of banded Losee Gneiss (sample R-15-Ba) leaving a refractory mafic residue (sample: R-15-Bi). Samples are from Rt-15 near field trip Stop 2.

REFERENCES:

Drake, A.A., Jr., 1984, The Reading Prong of New Jersey and
eastern Pennsylvania: An appraisal of rock relations and
chemistry of a major Proterozoic terrane in the Appala-
chians, in Bartholomew, M.J., ed., The Grenville event in
the Appalachians and related topics:GSA Special Paper
194, p. 75-109.

Kastelic R.L., Jr, 1979, Precambrian geology and magnetite
deposits of the New Jersey Highlands in Warren County,
New Jersey: Masters thesis, Lehigh University, Bethlehem,
Pennsylvania, 155 pp.

Leake, B.E., 1964, The chemical distinction between ortho- and
para-amphibolites: Journal of Petrology, v.5, p. 238-254.

Lewis J.V., and Kummel, H.B.,1910, Geologic Map of New Jersey:
State of New Jersey Dept. of Conservation and Econ. Dev.
Atlas Sheet 40, revised in 1950 by Johnson, M.E.,

Manson, V. 1967, Geochemistry of basaltic rocks: in Hess, H.H.
(editor) Basalts, v. 1, Wiley Interscience, New York,
p. 220-250.

Maxey, J.H., 1971, Metamorphism and origin of Precambrian
amphibolites of the New Jersey Highlands: Ph D thesis,
Rutgers University, New Brunswick, New Jersey, 155 pp.

Pierce, J.A., Alabaster, T., Shelton, A.W., and Searle, M.P.,
1981, The Oman ophiolite as a Cretaceous arc-basin
complex: Evidence and implications: Royal Society of
London Philosophical Transactions, ser. A, v. 300,
p. 299-317.

Prinz, M., 1967, Geochemistry of basaltic rocks: Trace
Elements:in   Hess, H.H. (editor) Basalts, v. 1, Wiley
Interscience,New York,   p. 271-323.

Puffer, J.H., and Volkert, R.A.,1991, Generation of
trondhjemite from partial melting of dacite under
granulite facies conditions: an example from the New
Jersey Highlands, USA: Precambrian Research, v. 51,
p. 115-125.

Shaw, D.M., 1956, Geochemistry of pelitic rocks 111, Major
    elements and general geochemistry: Geol. Soc. America
    Bull. v. 67, p. 919-934.

Shaw, D.M., 1977, Trace element behavior during anatexis: in
    Dick, H.J.B. (editor) Magma Genesis, Oregon Dept. Geol.
    Mineral Ind. Bull., v. 96, p. 189-215.

Sims, P.K., 1958, Geology and magnetite deposits of Dover
    District, Morris County, New Jersey: US Geol. Survey
    Prof. Paper 287, 162   pp.

Turekian and Wedepohl, K.H., 1961, Distribution of the
    elements in some major units of the earth's crust: Geol.
    Soc. America Bull., v. 72, p. 175-192.

Volkert, R.A., and Puffer, J.H., in press, Late Proterozoic
    diabase dikes of the New Jersey Highlands: A remnant
    of Iapetan rifting in the north-central Appalachians:
    United States Geological Survey, Professional Paper.

CHAPTER 5

A BRECCIA DIKE COMPLEX IN THE FRANKLIN MARBLE
AT MCAFEE, NEW JERSEY

Thomas D. Gillespie, C.P.G., Trenton State College
Langan Engineering and Environmewntal Services

A network of breccia dikes occurs at an isolated outcrop within the Franklin Band of Marbles, adjacent to the fault-contact with a Paleozoic carbonate outlier, on Route 94 in McAfee, New Jersey (Fig. 1). Specifically, the outcrop forms a fault scarp on the western block of the East Fault, which generally separates the Franklin Band and rocks of the Byram Metamorphic Suite (as defined by Drake, 1984) and overlying Paleozoic carbomate outliers. Regional geology has been defined in numerous previous works, particularly related to the iron and zinc ore deposits in the region (Hague, et.al., 1956, Buddington and Baker, 1970).

The outcrop is a conspicuous feature in an otherwise flat, sediment-filled valley, floored by the two carbonate formations on either side of the East Fault. The dike complex occurs in one of the numerous strike-parallel, en-echelon, lens-shaped gneisses which form inclusions within the Franklin Band, as described by Hague, et.al., 1956. In McAfee, the gneiss is of variable composition, mainly a quartz-rich microcline gneiss, which is likely of sedimentary origin. The breccia dikes occur exclusively within this gneiss inclusion.

The breccia dike complex consists of a network of connected dikes with an overall northeast to southwest trend which branch toward the southwest. The dike rocks are a breccia composed of angular clasts of microcline gneiss and Franklin Marble, set in a carbonate matrix. The dikes range in size from 2cm to 2 meters wide and up to 50 meters long. There is a general decrease in dike width toward the southwest; i.e., in the direction of intrusion, as implied by the bifurcation direction. Dike injection was rapid and well within the brittle regime, although later recrystallization has destroyed some of the original textures and fabric.

McAfee is located in the New York Recess of the Reading Prong, at the intersection of two major Paleozoic structural trends: The East Fault, and the Beemerville-Cortlandt cross-trend of intracontinental alkalic dikes (Ratcliffe, 1981). Both of the structural trends are depicted in Figure 2. Of even more direct significance, the outcrop is adjacent to the East Fault, and contains an isolated lamprophyre dike (Beemerville Nepheline Syenite), identified both in the current study, and by Ratcliffe.

The East Fault is one of an extensive system of northeast-trending faults which segment the Highlands Province into a series of fault blocks (Smith, 1969). These faults are interpreted as mostly normal faults related to Mesozoic extension, but are also believed to have been reactivated Paleozoic reverse and/or transverse faults. The Beemerville-Cortlandt Igneous Crosstrend consists of a series of Taconic age (Late Ordovician), intracontinental alkalic intrusives, with compositions ranging from camptonite and carbonatite to nepheline syenite (Ratcliffe 1981, Maxey 1976).

The occurrence of the McAfee Breccia Dike Complex at the convergence of these two structural features raises the question of whether there is a causal relationship with either. The presence of the carbonate-dominated breccia dikes could be consistent with alkali igneous intrusions. However, the
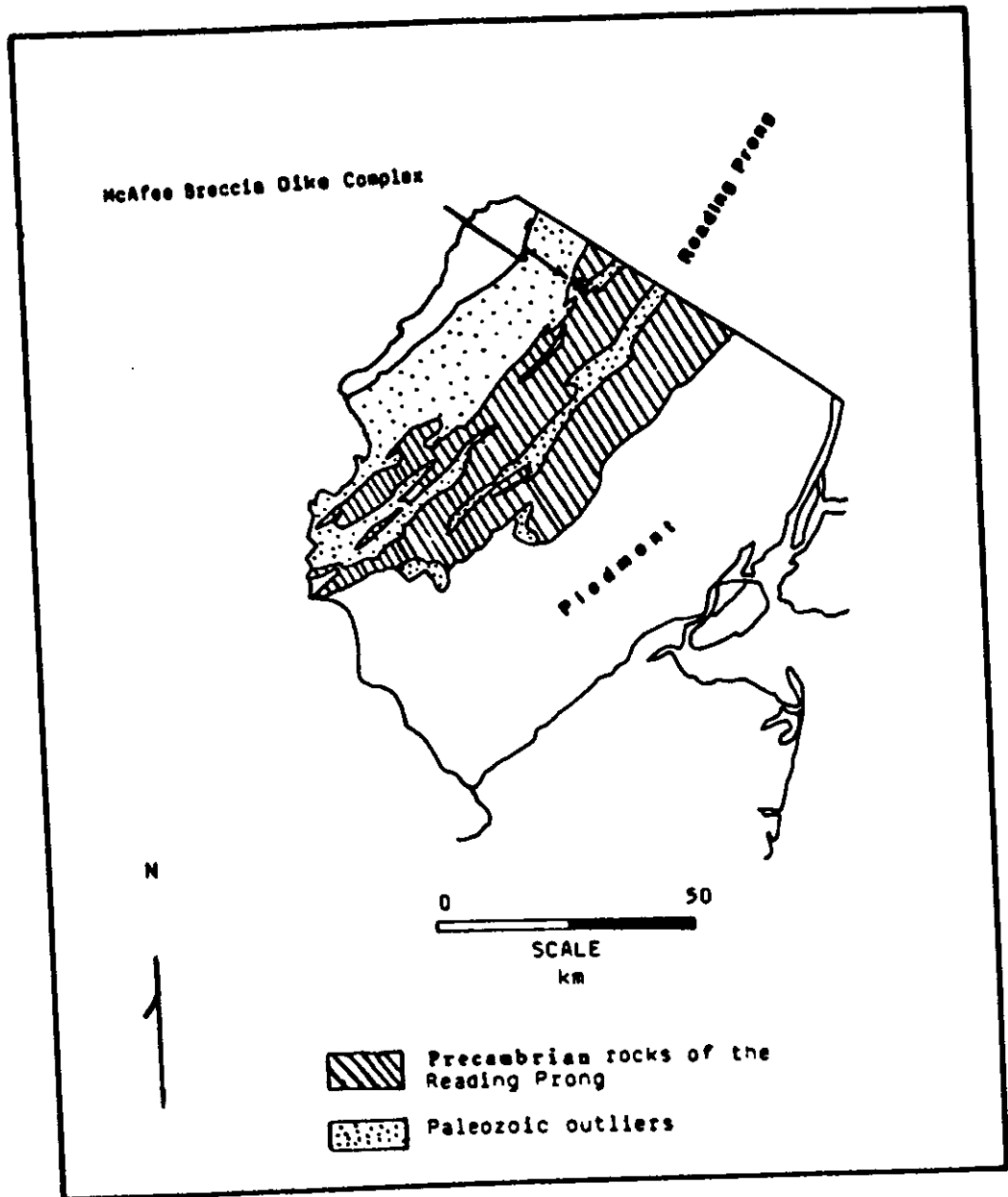
Figure 1: The New Jersey Highlands physiographic province. Shown are the Precambrian metamorphic bedrock and Paleozoic sedimentary outliers in the Reading Prong. The location of the McAfee Breccia Dike Complex is also shown.
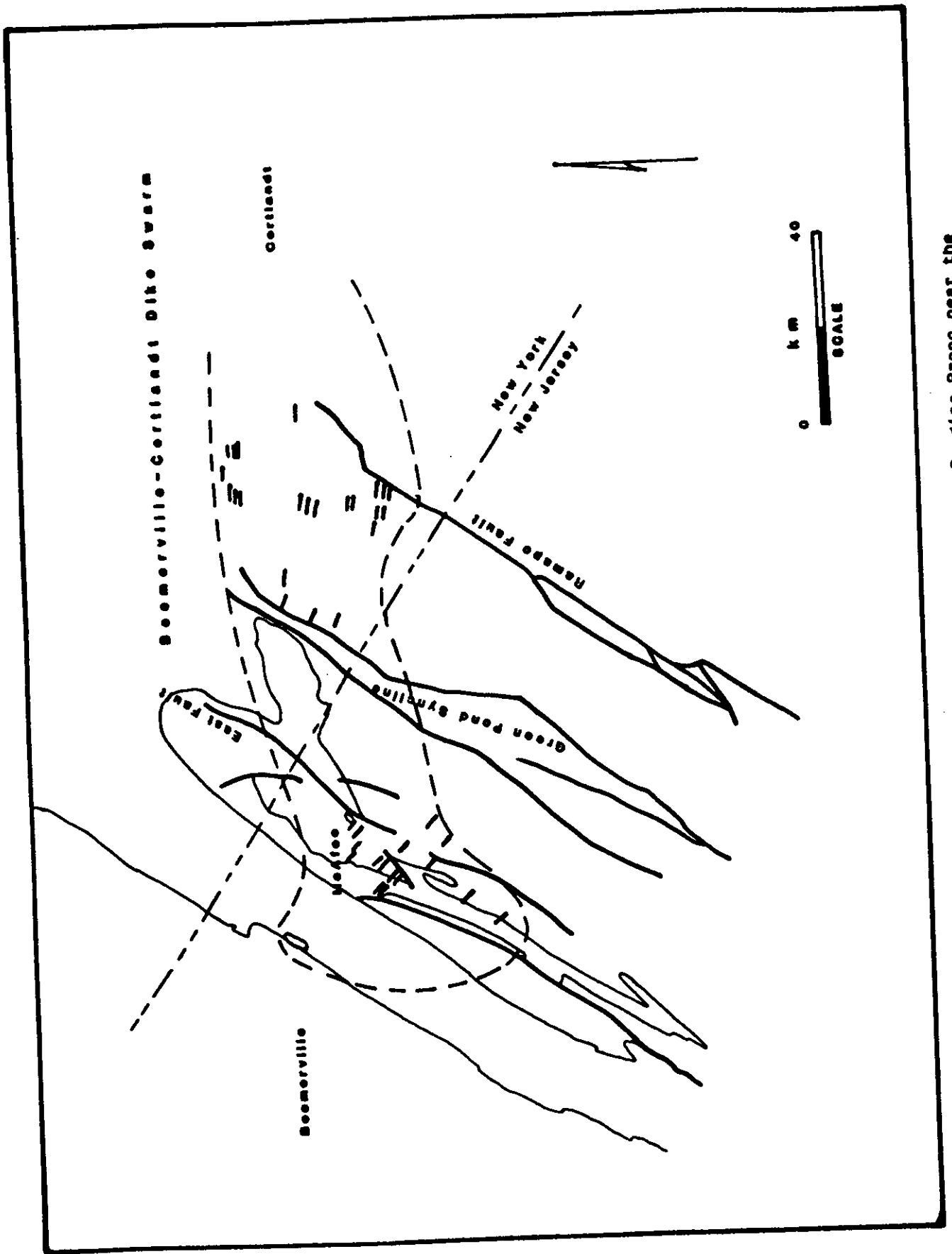
Figure 2: Major structural features in the Reading Prong near the New Jersey - New York border. Data from Ratcliffe, 1981.

119

presence of a zone of brecciation in association with a fault is an equally plausible alternative.

The complex is composed of three principal rock types: The Franklin Marble, a quartz, microcline gneiss, and the carbonate-rich breccias. Descriptions of the various rock types are provided in the ensuing paragraphs. A geologic map of the complex is shown in Figure 3.

Franklin Marble

The Franklin Marble is a light grey to white, coarsely crystalline marble with euhedral crystals, and an abundance of graphite, biotite, haematite and magnetite. The rock was metamorphosed to upper amphibolite facies, presumably during the Grenville Orogeny.

Twinning occurs in nearly 100% of the crystals which exhibit interlocking, mosaic texture and a lack of sub- grain boundaries. Examination of twin planes and data from chemical and X-Ray diffraction data reveals that it is primarily dolomitic, with approximately 30% CaO and 21% MgO by weight, and very minor amounts of other major oxides. This is consistent with compositions from other nearby outcrops which range from almost pure calcite to dolomite with MgO concentrations of approximately 23%.

Gneissic Rocks

Gneisses at the complex are light tan to white to grey, medium- to-coarse grained quartz and potassium feldspar rocks, which collectively form an inclusion within the Franklin Marble. The gneiss body is actually a heterogeneous mix of several gneissic sub-types, predominantly quartz-microcline, quartz-microcline-hornblende and quartz gneisses, which meet in randomly oriented gradational contacts, presumably reflecting original sedimentary facies changes.

Microcline gneiss is the most common variety. It is a light tan to nearly white, medium-to-coarse grained rock composed primarily of quartz and microcline. Toward the east it grades into a quartz-orthoclase-hornblende gneiss, which is identical in appearance to the microcline gneiss except that it also contains augen of hornblende which range from about 2 mm up to 2 cm and define a local lineation. At the west of the outcrop the microcline gneiss grades locally into a quartz gneiss, which is a coarse-grained, white to light grey rock composed almost entirely of quartzite, but contains approximately 40% pink potassium feldspar locally. The feldspar-rich domains occur in distinct linear zones, which are present in right lateral ptygmatic folds with amplitudes of approximately 10 to 15 cm.

Bulk chemical analyses show the rocks are rich in silica and aluminum and poor in mafic minerals. The rock is similar to regional sedimentary gneisses (Drake1984) and differs from regional igneous gneisses primarily in the amount of iron.

Lamprophyre Dike

The igneous dike on the outcrop is a dark grey to black, very fine grained rock which cross-cuts microcline gneiss and one of the breccia dikes at an attitude of approximately N70W. Work in this study, by Ratcliffe (1982, personal communication), and by Maxey (1976) has identified this dike as a lamprophyre related to the Beemerville-Cortlandt crosstrend.

In thin section it is a micro-porphyry composed of medium-grained, sub-hedral to anhedral phenocrysts of diopside, biotite, orthoclase and nepheline, set in a fine-grained matrix composed of nepheline, orthoclase, sphene, magnetite and apatite. The rock has been altered, as evidenced by a fine-grained matrix replacing original coarse grained phenocrysts still seen as ghost crystals.
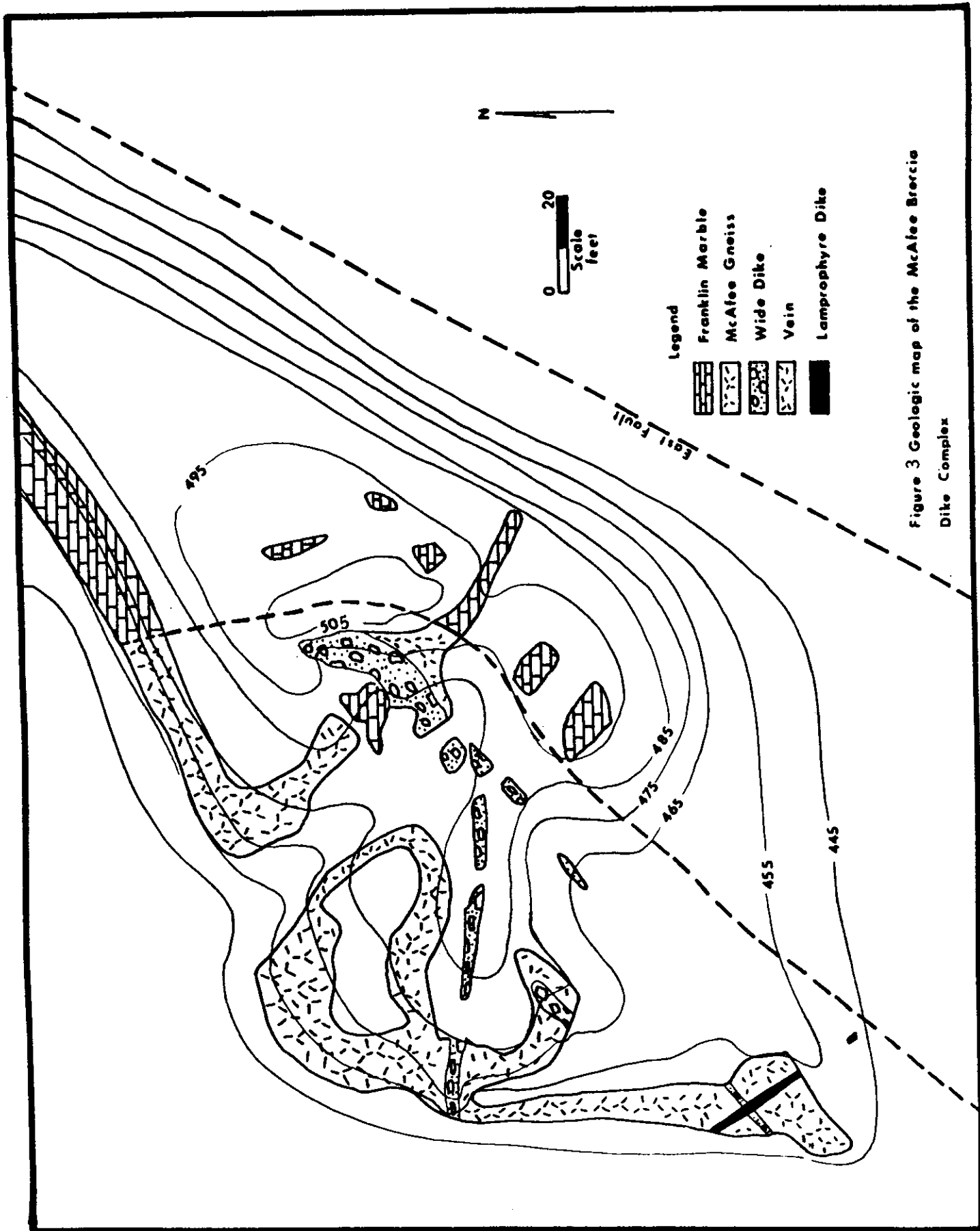
Figure 3 Geologic map of the McAfee Breccia Dike Complex

Carbonate Breccia Dikes

The breccia dikes are composed of a matrix of carbonate, typically dolomite, with clasts of either gneiss or marble. There are several types of dikes present at the complex, characterized by differences in matrix texture and composition, by clast type, shape and frequency, and by the relationship between the clasts and the matrix. Discussions of the different components of the dikes follows.

Matrix Composition

The matrix of the dikes is principally dolomitic. It is light buff to medium brown in color with a surface texture which ranges from a rough granular to a smooth, glacially polished surface. In fresh surfaces it is a dark grey, dense, crystalline dolomite.

There are three matrix varieties, distinguished by crystal size. A coarse-grained domain is composed of equigranular, elongate, euhedral crystals, generally greater than 1 cm in length. The crystals within this domain are aligned preferentially so that their long axes are parallel, and nearly always normal to the long axis of the linear domainal boundaries and contacts, even where the orientations change. Crystals are nearly all twinned, and typically display coxcombe structure at the domainal boundaries. This domain tends to occur in narrow, linear zones adjacent to wall rock or clast margins.

A fine-grained domain, which comprises the bulk of the matrix, is composed of subhedral, equigranular, interlocking crystals of dolomite, approximately 0.2 to 0.4 mm in diameter, which display no signs of internal strain. Twinning occurs in isolated crystals but it is believed that these represent microclasts of Franklin Marble, rather than the matrix.

A cryptocrystalline domain contains no resolvable features on any optical scale. It is a light tan to brown rock which occurs in random locations, but rarely in contact with a clast or wall rock.

Contacts between the domains are sharp with no gradation, but also with no discontinuity. At contact boundaries between the coarse variety and either of the two finer-grained types, coxcombe structure is common.

Clast Compositions

Clasts occur throughout the complex in a variety of shapes, sizes and compositions. In general the composition of the clasts at any location is a function of the adjacent or nearby wall rock composition. Gneissic clasts tend to be angular with clean sharp edges with nearly orthogonal sections, are generally medium to large in size (5 cm to over 1 m in length), and do not contain internal fractures. Marble clasts tend to be more irregular in shape with rounded corners and irregular edges. None of the clasts examined show evidence of ductile deformation apart from that already present in the suspected parent, host rock, but all display extensive brittle deformational features.

Texturally there are two types of clasts present; polycrystalline rock fragments; and microclasts, composed of individual crystal fragments. The polycrystalline clasts are similar in mineralogy, texture and geochemistry to their respective parent (wall) rocks. They occur in contact with all matrix types, and resemble xenoliths in their relative size, and in their apparent disconnection with the matrix material.

The microclast sub-domain is composed primarily of individual sub-hedral to anhedral crystals of silicate minerals of approximately equal size with the crystals of the surrounding matrix. Microclasts are present only in the fine grained matrix domain and generally occur in narrow linear zones which are parallel to wall rock/clast contacts, although they are also present throughout the matrix domain. These zones are formed of approximately equal parts of silicate and carbonate materials and are generally separated from wall rocks by a narrow zone of pure matrix.

Clast/Matrix Interface

There are two types of clast/matrix interface present. The first type generally forms between the coarse grained, coxcombe-textured domain and the clasts/wall rocks, the domains are separated by a narrow dark zone which is optically irresolvable. This zone resembles glass, but it is not known if it represents the chemical disequilibrium of a true glass phase. The glass typically contains microclasts which have been cataclastically fragmented in situ and collectively define flow patterns.

The second type, is a clear sharp boundary and is generally formed by the contact of the wall rock/clasts with the finer grained matrix variety. Here the mobile carbonate has fragmented the clast into microclasts and incorporated them into the matrix.

Breccia Dike Types

The breccias dikes occur primarily in gneissic host rocks and form a network of dikes which begin on the east side of the outcrop as a single trunk dike, and branch outward toward the southwest. The dikes are primarily vertical and occur in nearly all horizontal orientations, with two prominent orientations at about N90E-80S and N40E-80 SE (Figures 4 and 5).

Contacts between the breccia and the host gneiss are moderately well exposed. In many places talus covers contacts where adjacent rocks are heavily iron stained. Elsewhere, exposed contacts are sharp, linear or curvilinear boundaries with no apparent sign of chemical transfer of material across the interface, although there is some physical interfingering of the breccia into cracks in the gneiss.

There are three specific dike types which are depicted in Figures 7 through 11, and are discussed in the following paragraphs. All of the dikes discussed are found at a single location on the outcrop, shown in Figure 6.

The first type are small-scale, narrow vein-like dikes which are typically less than 5 cm wide, have parallel sides, and usually terminate in a crack tip. They generally form as offshoots of the larger dikes and usually occur within isolated joint planes. The matrix is typically free of clasts, and is composed of the coarse-grained, euhedral variety. Matrix crystals tend to be parallel, with long axes normal to dike walls. There are typically two rows of crystals which meet along the center axis of the dike. These small scale dikes are referred to as veins, or as incipient dikes (Figure 7).

Similar to the incipient dikes are in-situ brecciation zones (Figures 8, 9 and 10) in which the host rock has been brecciated by a closely-spaced network of veins. In many of these zones separated blocks of the host rock can still be reconstructed across the zone. The matrix is generally the coarse grained euhedral variety, although in areas of increased dilation the fine-grained matrix is also present adjacent to wall rocks or clast margins.

Wide dikes are those which are greater than 0.5 m thick, and are characterized by the presence of polycrystalline clasts. The matrix is primarily the fine-grained variety, with the coarse variety generally forming only a narrow zone around the perimeter of some large clasts or along wall rock contacts. A representation of the fully developed, wide dikes is shown in Figure 11. The shape and orientation of the clasts within these dikes suggest flow patterns parallel to dike margins. This is most pronounced in wide dikes which have experienced the greatest dilatation, and presumably a higher flow rate than dikes of low dilation near the downgradient fringe of the complex.

Origin of Matrix

There are three possible sources for the matrix: 1) The Franklin Marble; 2) The Kittatinny Assemblage of Cambrian-Ordovician limestones, (both of which are local carbonate rocks); or 3) magmatic or hydrothermal material related to the Beemerville-Cortlandt crosstrend.
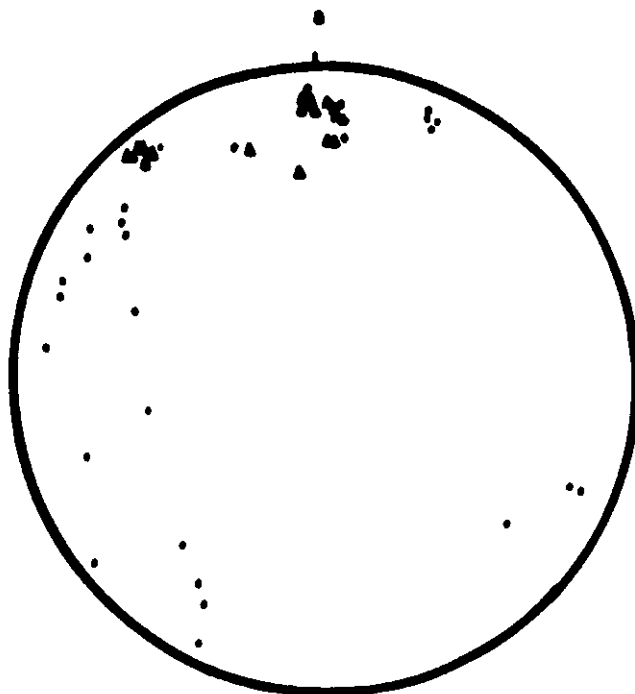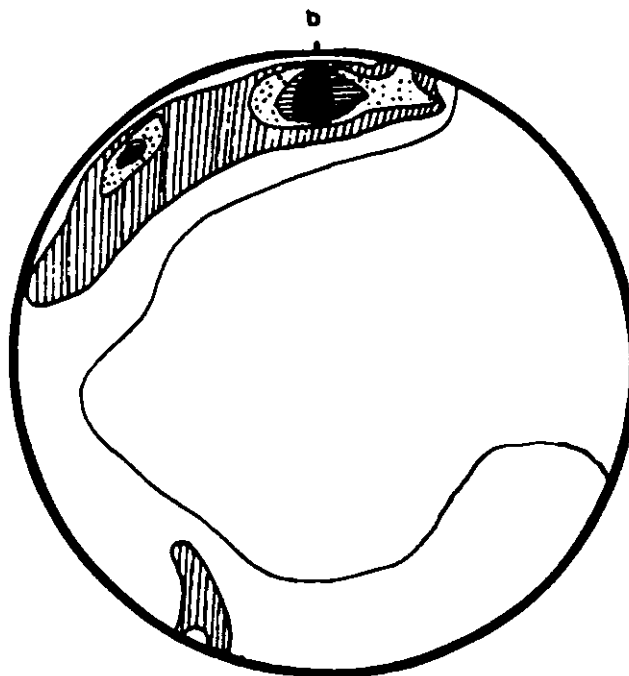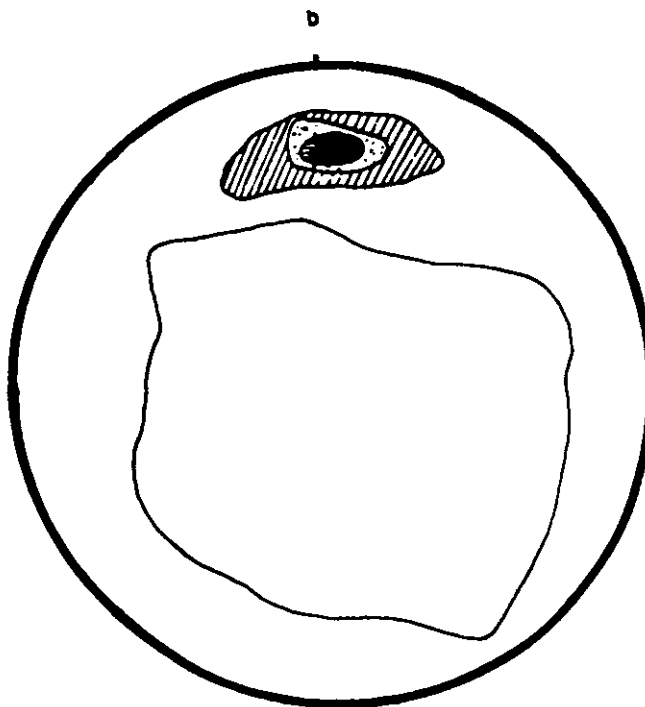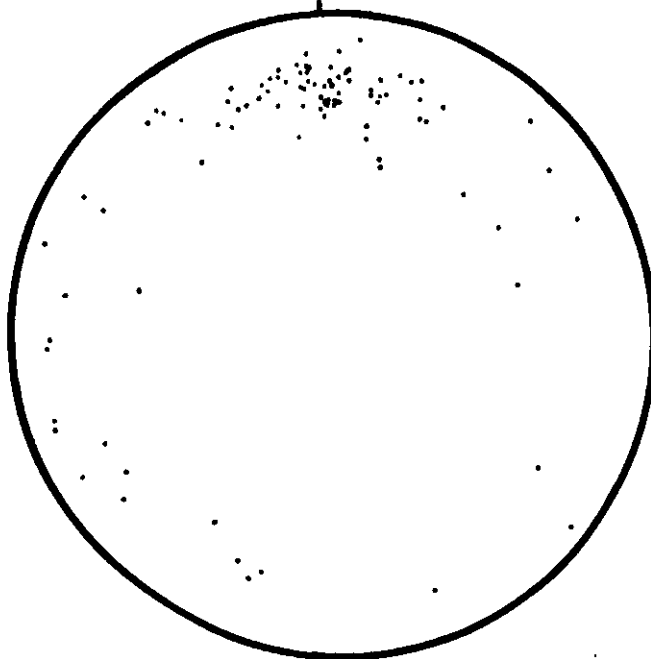
Figure 4 : Equal area projections of poles to dike contacts. a) Poles to dike orientations, b) Contours of dike distribution calculated per 1% area of net.

Figure 5 : Equal area projection of poles to dike related joints.
a) Poles to joint orientations, b) Contours of joint orientation
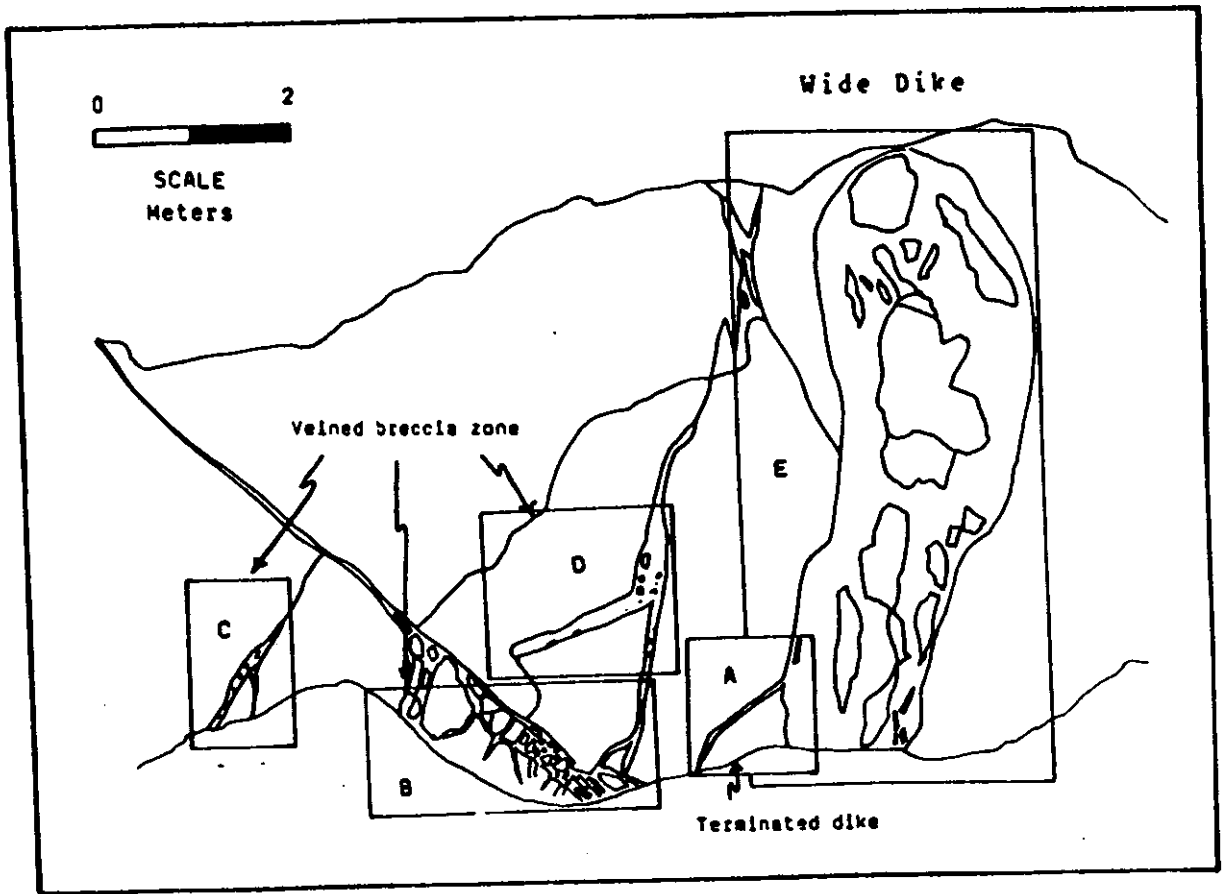distribution calculated per 1% of net area.

Figure 6. Various types of breccia dikes. Area A through E are depicted in detail in Figures 7 through 11.
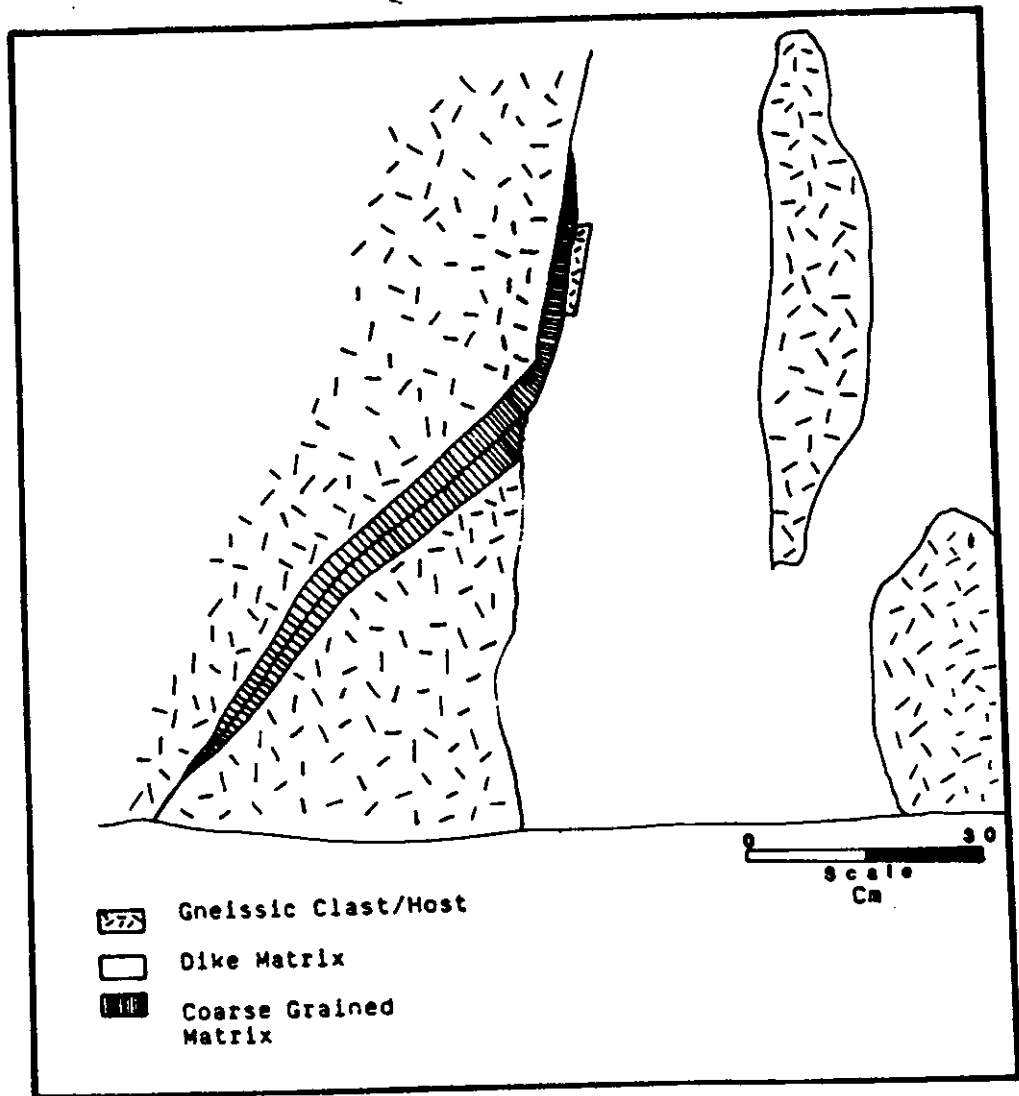
Figure 7. Incipient dike which formed as offshoot of main dike trunk. Matrix is composed of parallel, euhedral crystals which meet in center of dike.
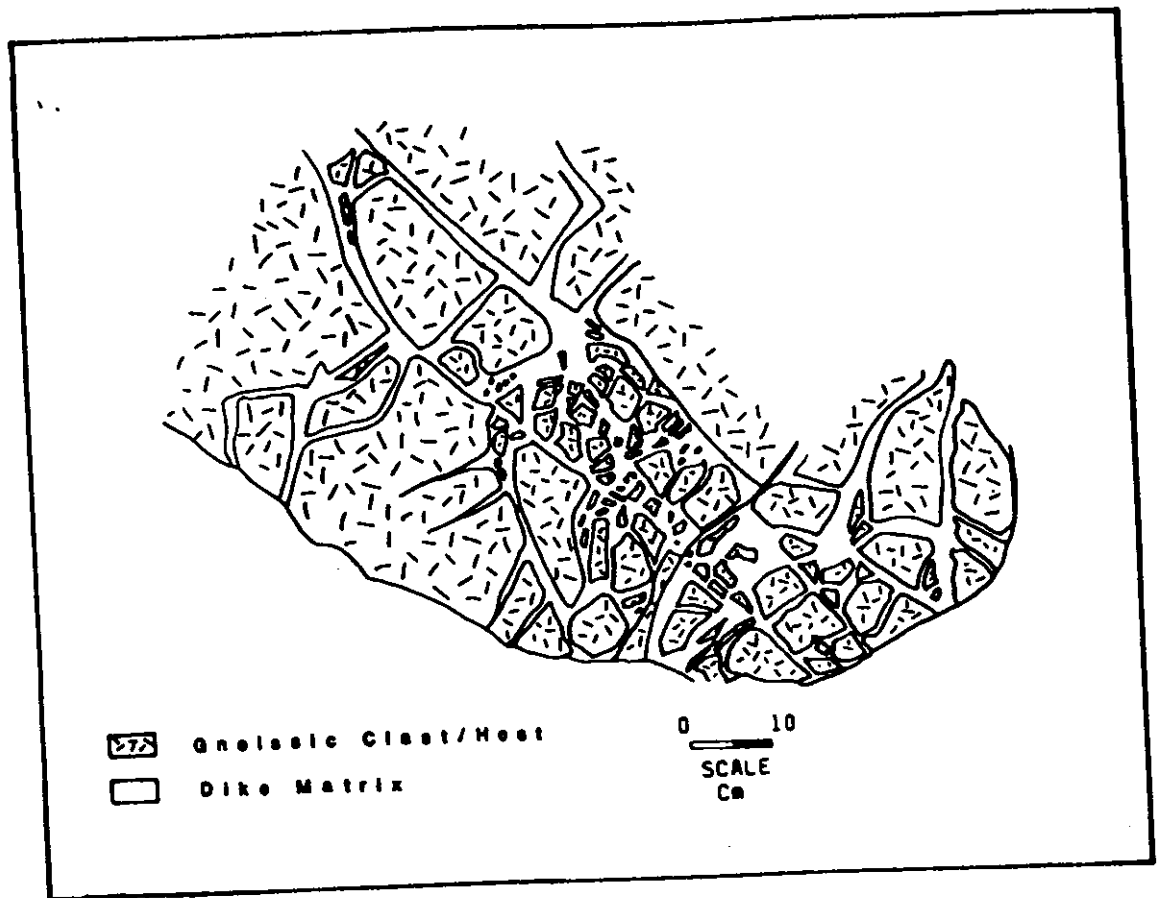
Figure 8.   In-situ brecciation zone, in which clasts can be reconstucted across zone. Matrix is coarse variety.
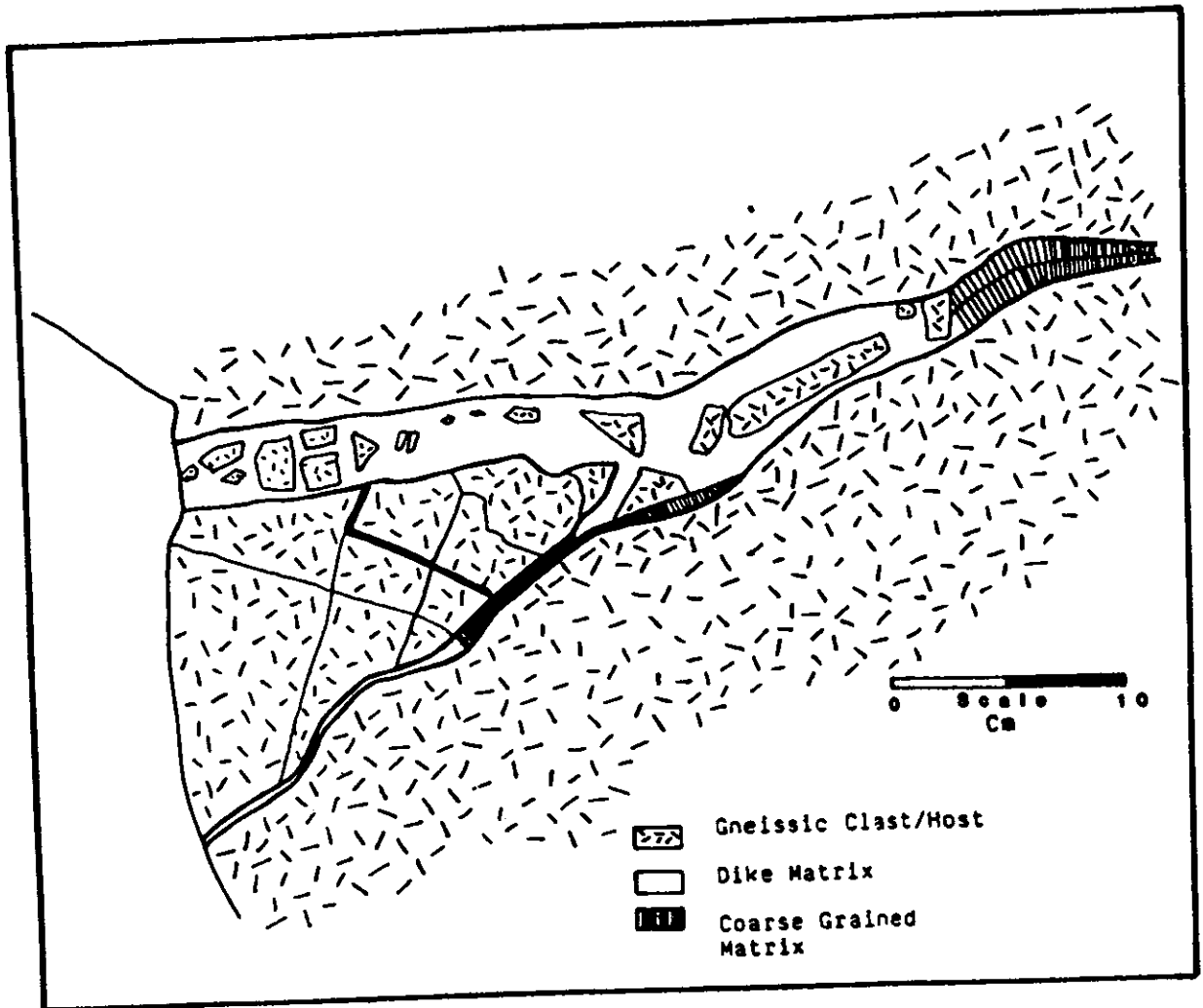
Figure 9. In-situ brecciation zone with increased matrix volume. Clasts can still be correlated with wall rock to some degree. Matrix is mostly fine-grained variety with coarse-grained type along wall rock/clast margins.

Figure 10.   Insitu brecciation zone in which few clasts can be related directly to wall rock.   Matrix/clast ratio has increase from that in Figures 8 and 9, as has degree of clast fragmentation. Matrix variety is completely fine-grained.

Figure 11. Full wide dike development with mega-clast inclusions.
Gneissic clasts are set is a dense, finely crystalline matrix.
Small incipient dike at lower left is depicted on Figure 7.

Two emplacement mechanisms are envisioned: 1) intrusion of carbonatite-type volcanism, as in gas diatremes; and 2) injection of a fault breccia into a joint network.

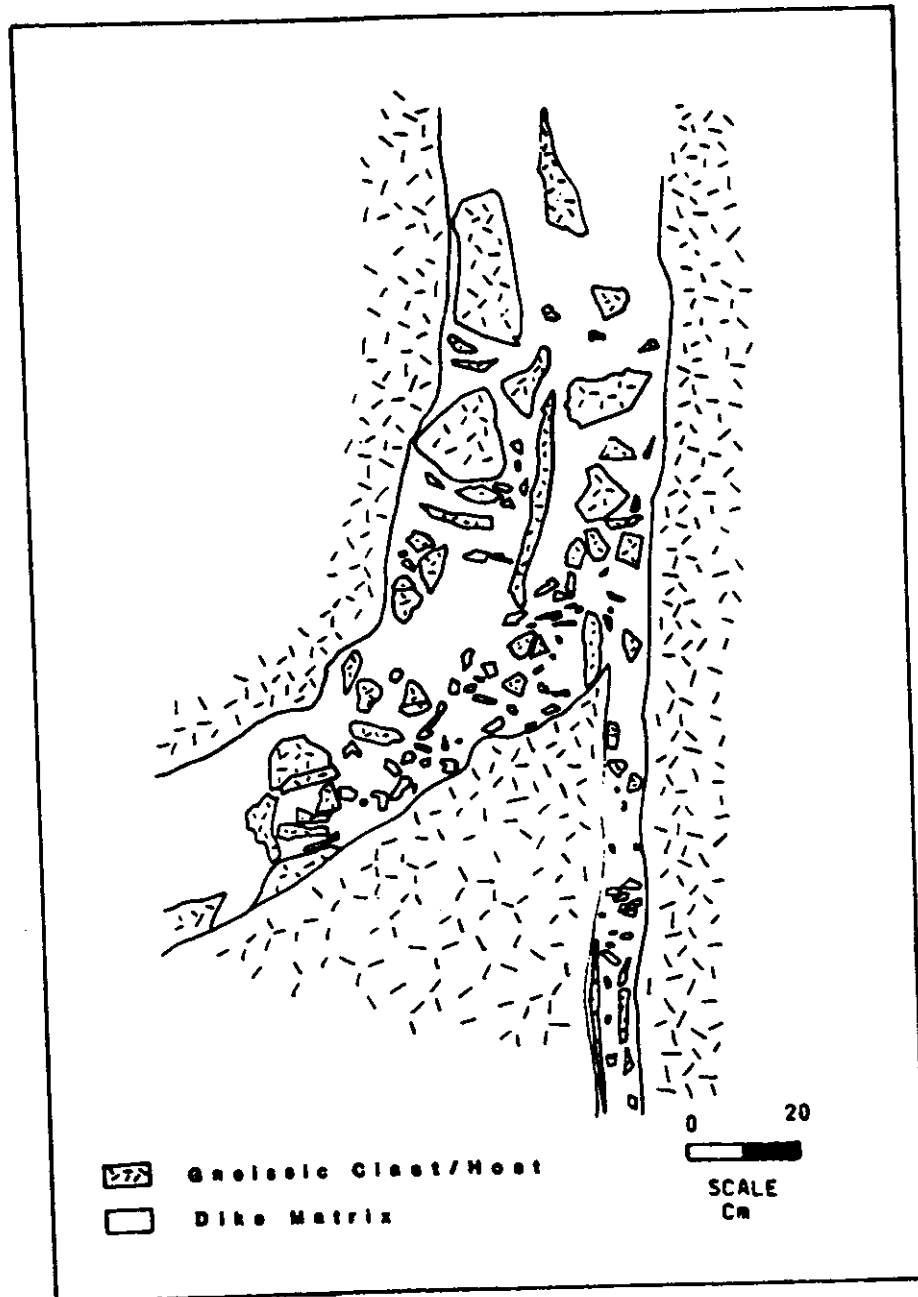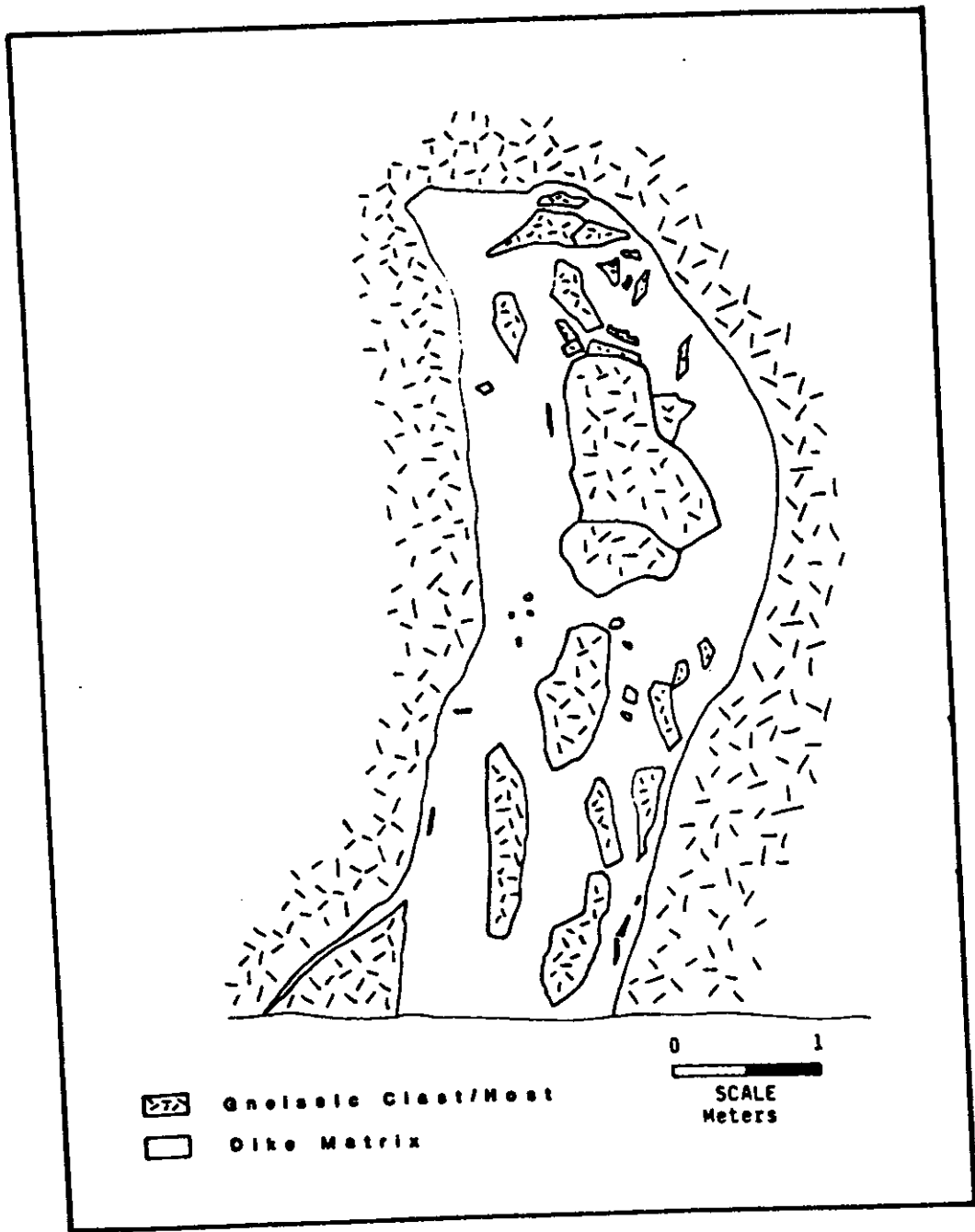To determine the origin of the matrix material, bulk chemical data (Table 1) were plotted on Harker chemical variation diagrams (Figure 12). Using these data, the formation of the matrix can be interpreted as mixing between the Franklin Marble and the quartz-microcline gneiss.

The possible mixing between gneiss and marble was tested by constructing a mixing line using Ca/SiO_2 vs. SiO_2/Mg, shown as Figure 13. These parameters were selected because they constitute the highest percent, by volume, of the major oxides in the two rock types, and can also be found in significant concentration in the matrix samples, as well as in the Kittatinny Assemblage. The mixing line supports the gneiss and Franklin Marble combination. These relations should not be construed as chemical mixing. Rather, mixing is believed to have been purely mechanical, as explained in the ensuing sections.

Emplacement Mechanics and Tectonic Constraints

The determination of the origin of the matrix precludes a volcanic origin, so the intrusion mechanism must be related to movement on the nearby East Fault, in a process similar to fault zone brecciation. That mechanism, by itself, however, can not explain the occurrence of discrete dikes at such distances from the actual fault plane. Neither can it explain localized in-situ brecciation in a rock separated from the fault plane by approximately 50 meters of unfractured rock, nor the restriction of intrusion into discrete flow channels along two predominant orientations.

The crystals in the coarse-grained matrix domain are well formed and strain free, possessing prism and pyramidal zones. They are elongate normal to the crack/vein walls and meet in the center of the zone in medial sutures, which indicates crystallization from the wall rock inward. The crystals contain no clasts and there is no evidence of strain, precluding ductile intrusion/deformation. The presence of an optically unresolvable (glass) between the wall rocks/clasts and matrix, as well as flow fabric expressed in the micro-clasts entrained in that zone, are indicative of brittle deformation. All of these textures indicate crystallization in an environment free of shear stress; crystallization from a fluid.

The brecciation observed in the in-situ breccia zones and the dilatent crack tips shows that emplacement was rapid and in pressure and temperature conditions well below those of solid state flow. However, it is difficult to visualize post-injection crystallization of a fluid matrix which clearly supported large clasts.

The fine-grained sub-domain is believed to represent the intrusion of a cataclasite which followed the primary fluid. Within the domain there is evidence of granular flow parallel to the wall rocks, abrasion along clast margins, support of large clasts and extensive dilation.

On the outcrop, dike types are transitional. The fine matrix can be found in the center of breccias with coxcomb rims, and typically the veins, composed primarily of the coarse-grained matrix, open into the larger dikes, composed of the fine matrix variety.

Considering these observations, and considering that there is a continuity between the matrix domains, two successive mechanisms of a single intrusion event are envisioned. The primary intrusion was by a fluid phase which intruded the host along extant planes and brecciated the rock by hydrofracturing. This was followed by a fluid-rich cataclasite which dilated the dikes and entrained the brecciated blocks and transported them down a pressure gradient.

This is consistent with the outcrop pattern of the dikes which decrease in width toward the southwest. Likewise, there is an increase in the frequency of incipient dikes and in-situ brecciation zones toward the southwest. The various dike types, therefore, likely represent the different stages in dike development frozen on the outcrop. The incipient dikes and in-situ brecciation zones represent the opening stages of

Table 1
Major Element Chemical Analysis

Sample No.	SiO	TiO	Al2O3	FeO	MnO	MgO	CaO	Na2Oc	K2O	Total
M1-A1	72.79	0.26	13.68	0.58	ND	0.85	0.57	3.49	6.08	98.32
M1-A2	8.981	0.04	1.43	1.8	0.1	18.31	27.72	0.38	0.61	59.37
M1-A3	75.69	0.02	0.15	0.57	0.03	4.68	7.06	0.07	0.08	88.35
M1-A4	15.71	0.1	3.27	2.46	0.15	14.53	25.01	0.91	1.25	63.45
M1-A5	5.61	0.04	1.3	1.9	0.13	18.14	27.39	0.32	0.54	55.37
M1-A6	73.68	0.2	12.96	1.07	0.01	1.62	0.82	5.45	2.06	97.87
M1-B1	4.44	0.03	1.12	1.46	0.14	18.98	28.12	0.28	0.54	55.81
M1-B2	0.45	0.03	0.12	1.2	0.13	21.05	31.13	0.08	0.04	54.23
M1-B3	3.92	0.03	0.59	1.58	0.14	19.39	29.03	0.23	0.19	55.1
M1-B4	1.65	0.09	0.21	0.96	0.1	20.43	30.14	0.11	0.06	53.81
M1-B5a	5.5	0.03	0.96	1.32	0.11	18.16	28.1	0.28	0.33	54.79
M1-B5b	3.19	0.03	0.55	1.41	0.12	19.93	29.84	0.18	0.22	55.47
M1-B6	6.7	0.03	1.09	1.63	0.12	13.75	28.79	0.33	0.44	58.00
M1-B7	0.68	0.04	0.15	0.27	0.03	1.69	1.13	0.04	0.1	4.13
M1-B8	17.13	0.12	3.67	1.9	0.03	17.46	23.98	0.32	2.19	66.86
M1-B9	25.91	0.15	3.04	2.06	0.07	12.85	23.63	0.57	1.4	69.68
M1-C1a	0.33	0.02	0.05	1.13	0.22	17.01	34.1	0.04	0.03	52.93
M1-C3	35.82	0.03	0.98	0.87	0.08	13.1	19.19	0.35	0.32	70.74
M1-C4	3.75	0.03	0.41	1.56	0.19	17.62	38.2	0.09	0.23	56.08
M1E1a	31.45	0.04	0.75	1.77	0.1	14.79	22.22	0.26	0.28	71.66
M1-E2	77.82	0.05	0.44	0.72	0.04	3.16	8.13	0.1	0.14	90.61
M1-E3	43.61	0.03	0.5	1.3	0.07	11.02	16.51	0.17	0.18	73.39
DM-01	12.06	0.03	0.45	1.52	0.11	20.02	29.64	0.06	0.14	64.03
R1-01	0.31	0.02	0.07	0.66	0.09	24.17	35.98	ND	6.0	67.31
M3-02	0.05	0.01	0.03	1.49	0.19	21.87	34.69	ND	ND	58.33
M4-01	0.89	0.03	0.1	0.08	0.01	2.87	60.25	ND	ND	64.23
M3-04	ND	0.01	0.03	0.18	0.01	1.41	62.82	ND	ND	64.46
M3-05	1.39	0.01	0.04	0.94	0.13	22.64	34.96	ND	ND	60.11
M2-A1	3.46	0.04	0.17	1.34	0.11	22.00	32.49	ND	ND	59.61
M2-B1	ND	0.03	0.1	0.33	0.04	23.25	33.8	0.32	2.39	57.55
COX	22.8	0.14	3.61	1.56	0.11	16.26	24.78	0.04	0.07	71.97
MF101	0.21	0.03	0.15	0.89	0.07	21.74	30.94	0.04		54.14
MF102	0.4	0.03	0.23	0.5	0.05	21.56	30.64	0.11	ND	53.52
MF103	0.24	0.01	ND	ND	ND	0.01	1.2	0.03	ND	1.49
MF104	ND	0.02	0.07	0.53	0.1	21.42	30.84	ND	0.04	53.02
M1D1	72.48	0.22	13.51	0.62	ND	0.68	0.74	2.63	4.53	95.81
M1D4	52.51	0.55	18.47	6.01	0.04	5.53	1.84	5.64	3.77	94.36
M1MD1	40.45	4.21	12.36	13.2	0.18	4.5	9.26	1.36	5.36	86.68
M1MD2	40.7	4.21	12.62	13.55	0.26	4.62	9.26	1.42	5.08	87.72
M1MD3	41.02	4.21	13.06	12.22	0.26	4.54	9.04	1.91	4.61	87.47

Sample lithologies listed by number in Table 2.

Table 1 (cont.)

Trace Element Chemical Analyses

Sample No.	P	Rb	Ba	Sr	V	Cr	Ni	Zr	Sc	Cu
M1-A1	6.3	220.8	526.7	55.3	14.8	7.7	6.7	287.9	3.0	10.8
M1-A2	1.8	ND	39.1	2866	39.1	14.1	10.3	56.8	4.6	7.5
M1-A3	1.8	ND	13.2	34.6	17.8	9.9	9.1	1.1	2.0	12.8
M1-A4	2.4	41.4	102.5	150.3	27.1	11	8.5	78.5	5.9	6.0
M1-A5	1.5	4.2	31	105.7	20.9	10.2	7.8	50.4	2.9	7.0
M1-A6	7.9	103.6	162.8	89.9	8.7	6.8	4.5	391.1	1.6	7.0
M1-B1	2.3	13.6	37.2	89.3	6.8	8.1	5.4	33.00	1.6	3.2
M1-B2	2.3	6.9	10.5	103	12.1	12.1	5.2	47.1	1.7	3.1
M1-B3	1.1	4.2	4.1	139.8	28.6	12.3	9.4	20.8	3	4.8
M1-B4	1.1	5.8	21.4	225.1	47.5	18.2	17.3	28.2	4.1	8.3
M1-B5a	2.1	19.1	35.4	145.3	77.9	23.4	17.9	60.8	6.3	10.9
M1-B5b	1.8	9.7	20.7	117.9	41.8	15.1	10.00	86.9	3.4	6.5
M1-B6	2.6	25.7	60.4	1075.5	26.7	13.7	11.5	126.8	2.7	8.6
M1-B7	3.7	12.6	91.7	1269.8	27.7	15.1	16.8	140.0	2.7	7.0
M1-B8	3.2	211.3	567.4	173.7	22.9	9.6	7.4	585.3	3.6	6.1
M1-B9	1.5	94.4	50.1	154.8	46.9	13.7	9.2	102.4	6.1	7.2
M1-C1a	2.5	5.3	17.3	122.3	28.8	11.9	11.1	11.8	2.2	4.0
M1-C3	3.5	3.8	13.8	56.8	28.0	11.1	9.9	84.9	2.0	13.6
M1-C4	2.0	16.8	26.8	103.1	41.8	12.7	9.2	25.9	3.6	14.8
M1E1a	1.8	7.4	14.8	70.6	13.4	8.9	12.9	68.4	2.1	10.3
M1-E2	2.4	ND	7.7	47.4	14.6	6.3	4.8	28.2	2.4	5.3
M1-E3	1.5	9.1	11.9	57.2	6.8	7.1	6.1	63.3	1.9	6.5
DM-01	2.4	3.1	18	70.4	109.0	32.5	17.9	ND	7.7	ND
R1-01	2.1	9.0	15.5	260.6	90.3	32.8	17.0	ND	8.0	ND
M3-02	2.5	10.6	5.7	52.6	89.6	26.6	14.4	ND	7.0	ND
M4-01	2.5	16.7	20.9	687.9	113.4	37.4	19.1	ND	8.0	ND
M3-04	1.9	16.00	10.1	512.8	108.1	38.7	21.4	ND	8.0	ND
M3-05	2.3	4.6	5.5	97.5	86	26.1	15	ND	6.6	ND
M2-A1	3.7	6.6	22.8	80.1	94.1	33.3	13.6	ND	7.4	ND
M2-B1	2.0	ND	24.3	64.4	83.7	27.5	15.4	ND	6.1	ND
COX	4.7	35.6	212.7	48.6	87.5	32.6	12.2	105.7	7.9	3.5
MF101	0.9	5.6	65.4	62.3	23.3	12.7	8.7	18.4	2.3	ND
MF102	0.8	7.5	0.3	76.2	24.8	14.4	9.2	29.9	2.2	4.7
MF103	0.7	6.1	3.3	358.5	35.6	15.1	11.1	23	2.6	4.7
MF104	0.6	8.3	1.3	377.3	43	15.4	11.8	21.8	2.8	4.8
M1D1	ND	ND	ND	ND	ND	ND	ND	ND	ND	ND
M1DA	2.0	521	290	307	20	6	7	ND	2	0
M1MD1	5.0	239	1449	1268	365	14	19	ND	15	16
M1MD2	0	166	1270	1071	320	11	15	ND	15	11
M1MD3	0	166	1189	1471	321	12	16	390	14	10

Table 2
Sample Lithologies by Designated Number

Sample No.	Lithology
M1-A1	Gneiss
M1-A2	Matrix
M1-A3	Matrix
M1-A4	Matrix
M1-A5	Matrix
M1-A6	Gneiss
M1-B1	Matrix
M1-B2	Matrix
M1-B3	Matrix
M1-B4	Matrix
M1-B5a	Matrix
M1-B5b	Matrix
M1-B6	Matrix
M1-B8	Matrix
M1-B9	Matrix
M1-C1a	Matrix
M1-C3	Matrix
M1-C4	Matrix
M1-E1a	Matrix
M1-E2	Matrix
M1-E3	Matrix
Dm-01	Matrix
R1-01	Matrix

Table 2 Cont.

Sample No.	Lithology
M2-A1	Marble
M2-B1	Marble
M3-02	Marble
M3-04	Marble
M3-05	Marble
M4-01	Marble
MF-101	Marble
MF-102	Marble
MF-103	Marble
MF-104	Marble
COK	Dolomite *
M1-D1	Gneiss
M1-D4	Gneiss
M1-MD1	Lamprophyre
M1-MD2	Lamprophyre
M1-MD3	Lamprophyre

* Siliceous dolomite from the Kittatinny Assemblage.
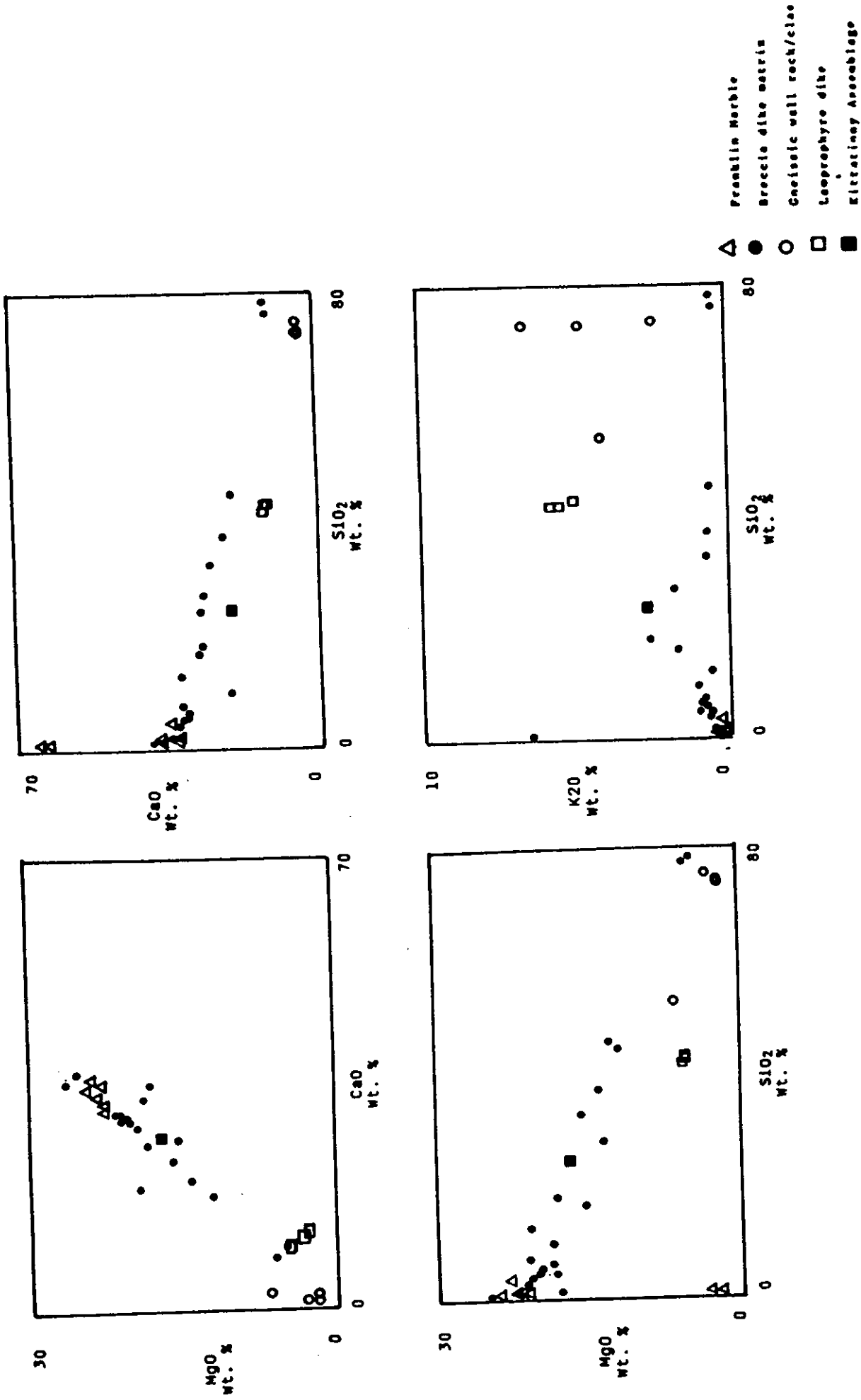
Figure 12. Harker chemical variation diagrams. Dike matrix tends to plot between end members consisting of Franklin Marble and quartz-microcline gneiss. Lamprophyre data plot outside the trend. Rocks of the Kittatinny Assemblage diverge from the trend mostly in trace element compositions.
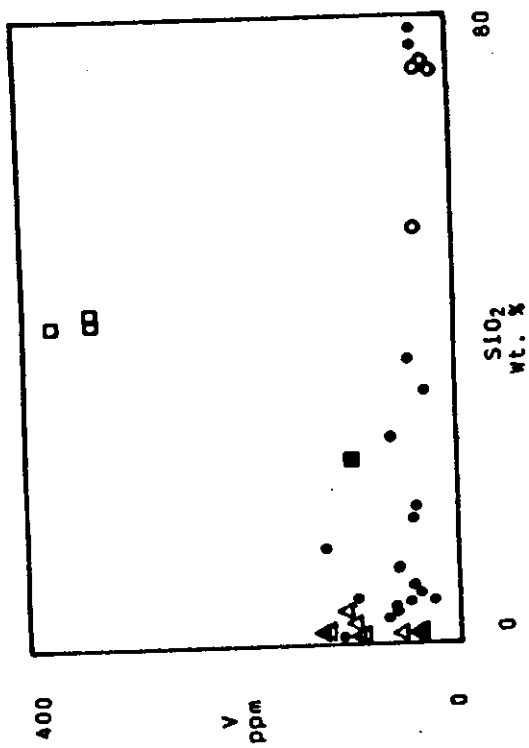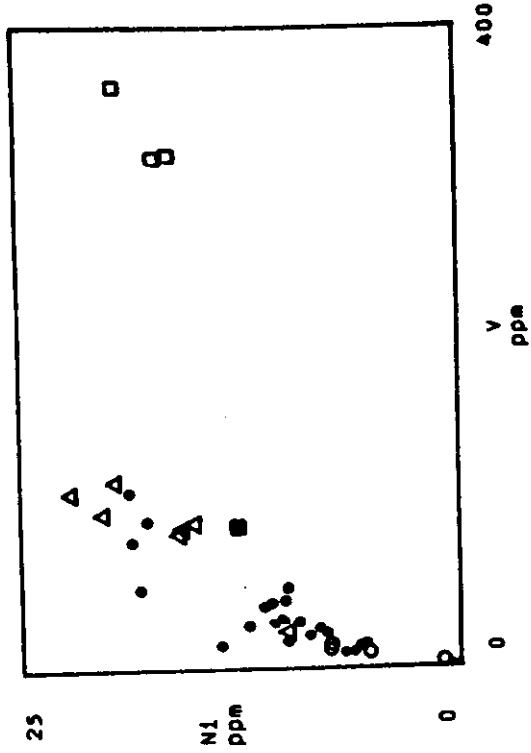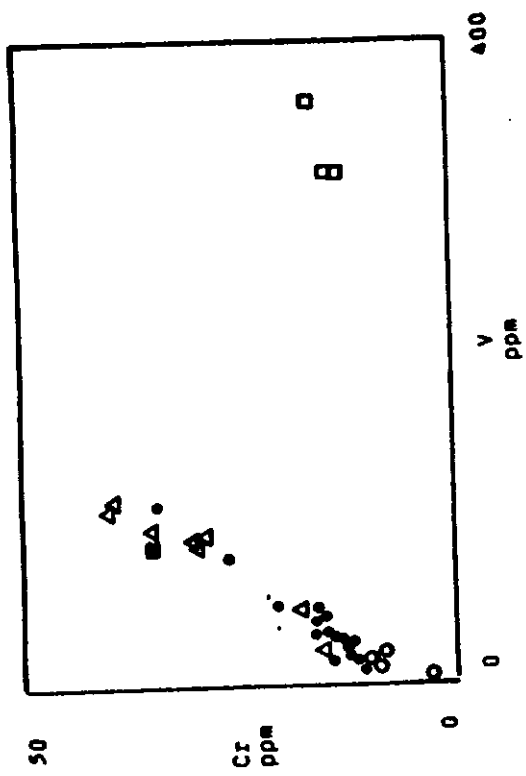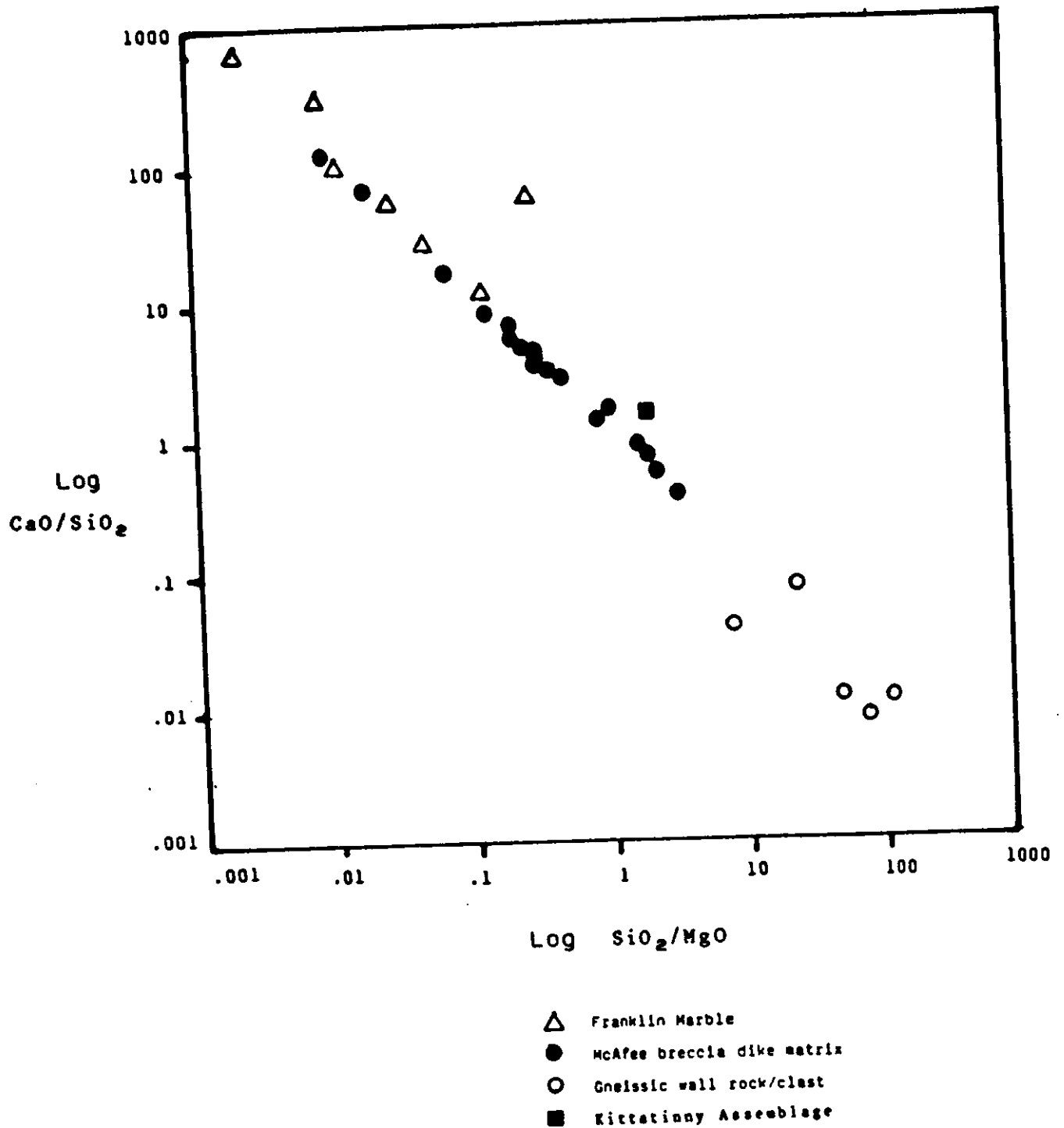
Figure 12 Cont.

138
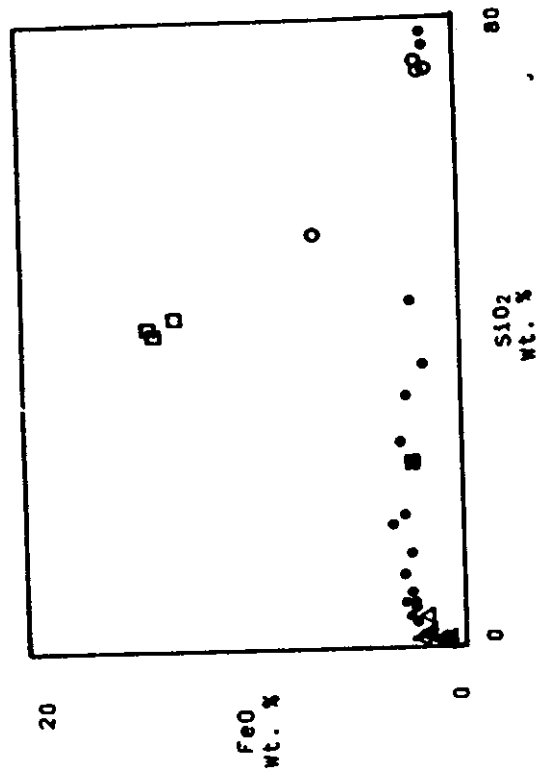
Figure 13. Full logarithmic plot of Cao/SiO$_2$ vs SiO$_2$/MgO. Line demonstrates that the matrix formed as a mix of Franklin Marble and Quartz-Microcline Gneiss.

dike development and the wide dikes later developmental stages. The increased frequency of incipient dikes in a halo around the wide dikes, with the highest concentration toward the southwest supports an emplacement direction from northeast to southwest, beginning at the East Fault. Figure 14 is a reconstruction of the breccia dikes, based on present contacts, which shows these relationships.

The age of emplacement of the dikes can be approximated by examination of the cross cutting contact of the lamprophyre dike with the breccia dike (Figure 15). The lamprophyre crosscuts the breccia dike and thus postdates it, but the breccia dike matrix was still mobile to some extent indicating that the two events occurred at roughly the same time. Radiometric ages of rocks in the Beemerville - Cortlandt Cross-trend in this area, cited by Ratcliffe, 1981, are approximately 444 +/- 22 m.a., Ordovician. This places the breccia dike intrusion in the late Taconic Orogeny.

If the breccia dikes formed during the Taconic Orogeny, their formation should conform to the regional kinematic and dynamic constraints operating at that time. Ratcliffe (1981) compiled tectonic data from the early Paleozoic for the region and concluded that the primary tectonic transport direction was approximately S 70 W. Therefore, any model to describe the formation and emplacement of the McAfee Breccia Dike Complex must accommodate the following aspects:

a) Dike emplacement occurred in a northeast to southwest direction;

b) The emplacement occurred in at least two stages: an initial fluid facies followed by a facies composed of a cataclasite of matrix and microclasts;

c) The source of the carbonate matrix material was the local Franklin Marble;

d) Microclasts were formed by cataclasis of both the Franklin Marble and gneiss, along the East Fault;

e) Polycrystalline clasts were formed by in situ brecciation caused by hydrofracturing;

f) Dilation of the McAfee Gneiss to accommodate the emplacement of matrix material must be along a conformable orientation with the coeval stress regimes defined by other regional structural features, and must be consistent with local stress regimes near the fault zone;

g) The mechanism of matrix generation and transport must conform to the regional kinematic orientation and dynamic constraints.

An explanation of the introduction of the matrix into gneissic rocks must accommodate both hydrofracturing and dilatency mechanisms. The coeval operation of both of these mechanisms can be explained by the hydrofracturing law which states that

$$P_{(H2O)} + T_0 > S_3$$
where:

$P_{(H2O)}$ = pore pressure,

T_0 = tensional strength of the rock and,

S_3 = the magnitude of minimum principal stress.
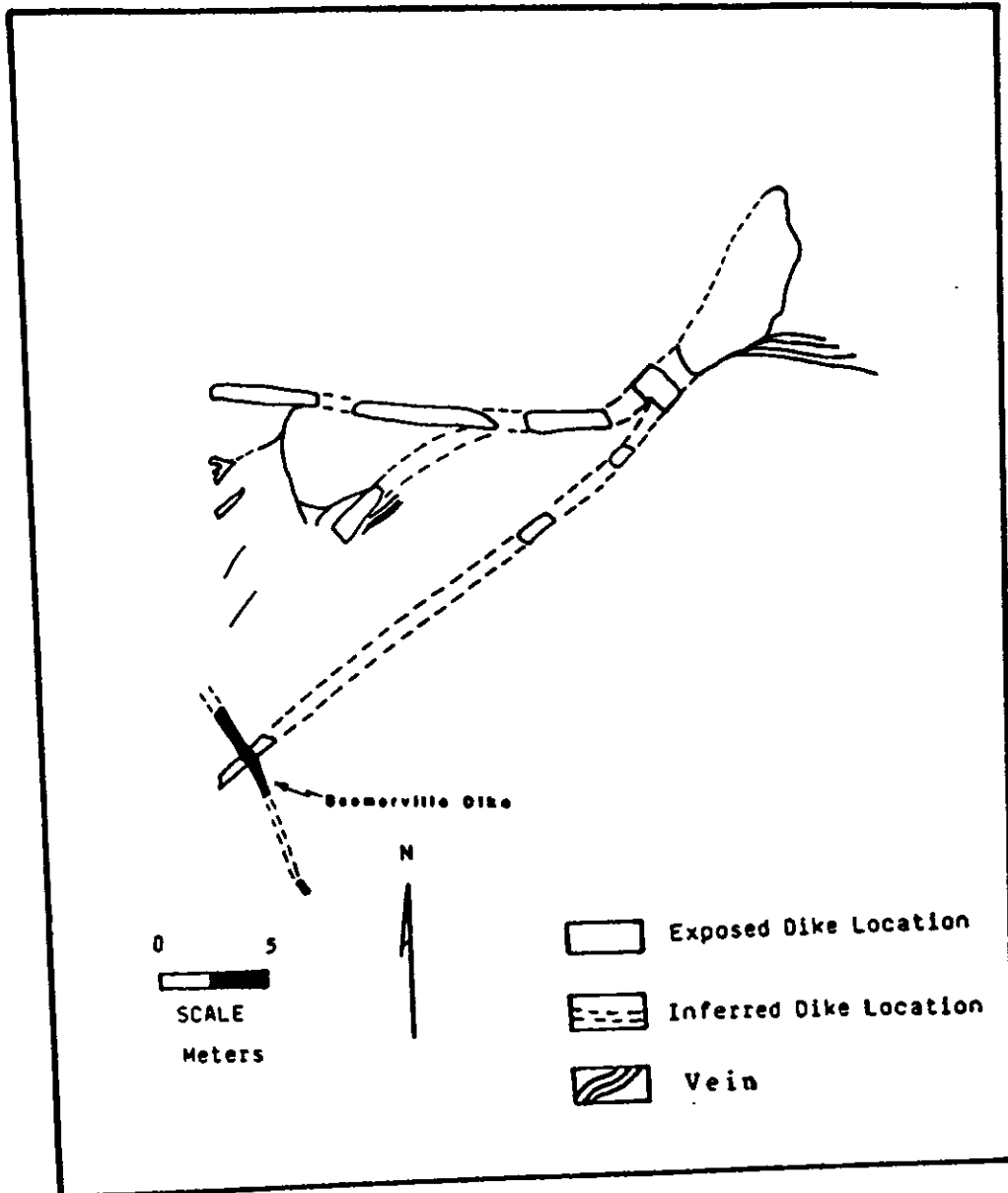
Figure 14;   Reconstruction   of   Breccia   Dikes;   inferred   dike
locations,   represented   by   the   broken   line,   are   based   on
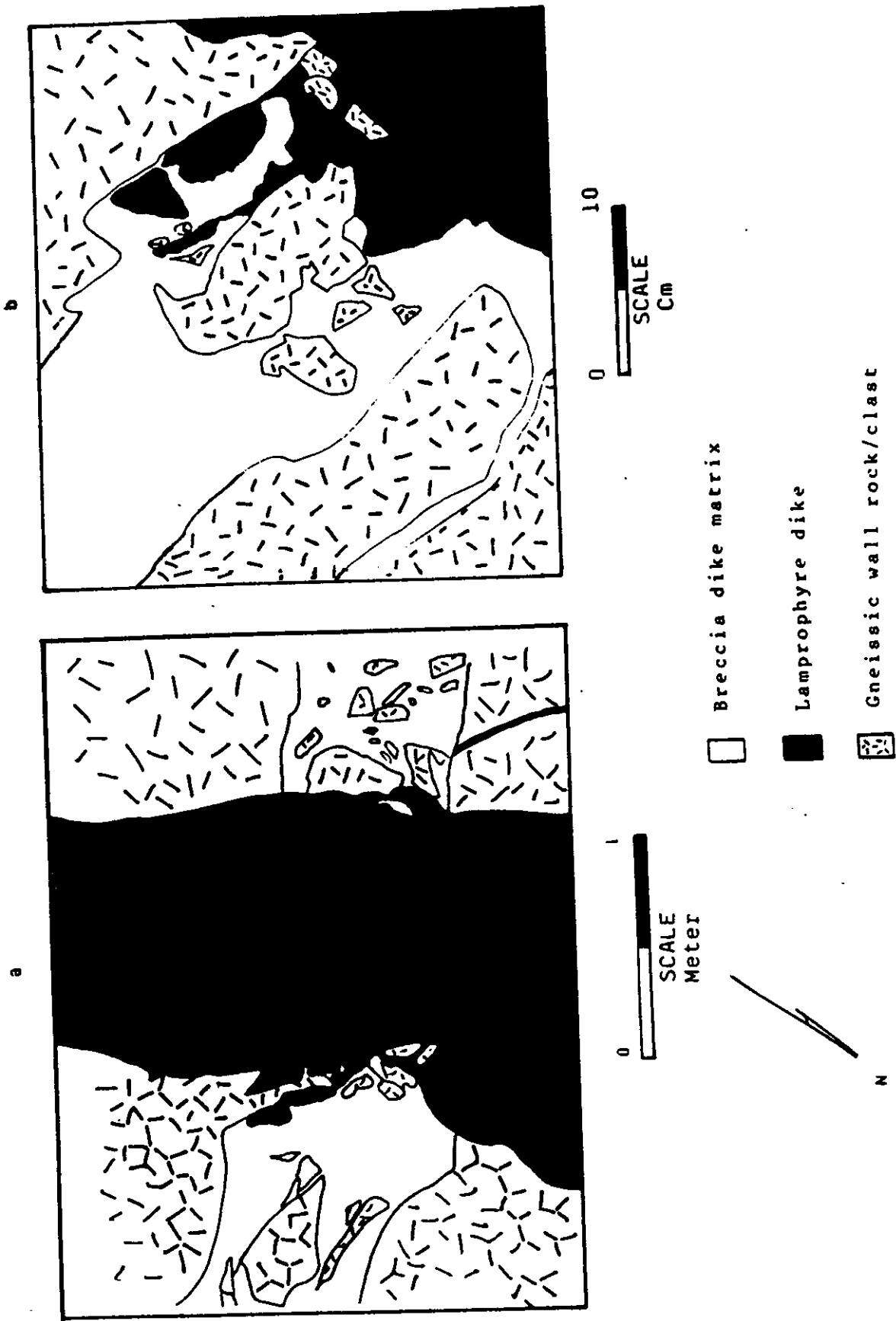assumption of original dike continuity.

Figure 15. Contact of lamprophyre and breccia dike. a) Cross-sutting contact. b) Detail of left contact from (a) which shows mobile behavior of both dike types.

Breccia dike matrix

Lamprophyre dike

Gneissic wall rock/clast

The state of stress in this situation is $S_1 > S_2 > S_3$, and dilatency under a tectonic stress regime occurs along planes containing the S_1-S_2 axes of principal stress, (Secor, 1965; Hubbert, 1951; Hubbert and Rubey, 1959; Hubbert and Willis, 1957; Sibson 1977). At the McAfee complex, however, there is a fracture network which branches into two principal orientations. This deviation from the hydrofracturing law can be explained by considering that the law is only applicable to homogeneous materials. In materials which contain planar anisotropies, the behavior departs from the ideal and the planes of fracture may deviate from those predicted. This situation is possible if the presence of the McAfee gneiss created an asperity in the fault plane and locally locked motion. Eventual failure and separation of the gneiss from the east block, and reconnection of the fault plane across the asperity, through right lateral oblique motion could account for the generation and injection of a fluid and cataclastic mush into a set of joints in the gneiss in a northeast to southwest direction. It would also account for the dilatency in the gneiss to accommodate the cataclasite. The gneiss, which was held stationary along an active fault, and which was enclosed within a carbonate rock with significantly different ductility, would be compressed, elastically, in a direction roughly parallel to the fault plane. Rupture on the fault plane would relieve that local stress concentration within the gneiss, which would be expressed by dilation in the brittle regime.

It is envisioned that a cataclasite was generated at shallow depth in the crust as a result of seismicity on the East Fault. Excess pore fluid was pumped under high fluid pressure (by a mechanism possibly related to filter pressing) into extant planes in the adjacent McAfee Gneiss where hydrofracturing of the host rock occurred. This was followed by injection of the cataclasite, composed of fragments of carbonate and silicate rock and carbonate rich fluid. Clasts fragmented during the hydrofracturing were incorporated and transported with the cataclasite as dike dilation and propagation continued.

Assuming that Ratcliffe's tectonic transport data (1981) represents S_1, and recognizing that all of the dikes are sub-vertical (S_3 horizontal), S_2 would be vertical. Movement along the East Fault, therefore, would be reverse with a right lateral oblique component (Anderson 1951). This is consistent with the injection of dikes from the fault plane toward the southwest along tensile cracks associated with the fault. The structures associated with intrusion of the complex are depicted in Figure 16.

Figure 17 depicts the relationship between the McAfee Breccia Dike Complex and the East Fault. The figure demonstrates that extensional, normal during the Mesozoic and Cenozoic occurred along a reactivated Paleozoic compressional or transpressional fault.

The hydrofracturing, cataclastic brecciation and mobilization of large scale clasts seen at the McAfee Breccia Dike Complex are most closely related to the concept of seismic pumping as described and defined by Sibson (1975). In the case of seismic pumping, high pressure fluids or pseudotachylyte, generated by intermittent activity along a fault plane, is pumped through fault-related cracks and joints where it hydrofractures the wall rocks in a branching pattern, parallel to the maximum compressive principal stress, that he refers to as a ladder network of in-situ brecciation.

The similarities seen between features resulting from this mechanism and those observed in the McAfee dikes suggests that a mechanism similar to seismic pumping could account for the initial penetration and hydrofracturing at McAfee. In the McAfee case, however, the fluid phase is not related strictly to pseudotachylyte, although such is likely present, as observed along clast/wall rock margins, but is a hypothetical fluid along the fault plane which was under high fluid pressures.

The second stage in the formation of the breccia dikes at McAfee differs from seismic pumping in that the matrix was a cataclasite capable of sustaining shearing stresses, and which caused extensive dilation and clast transport.
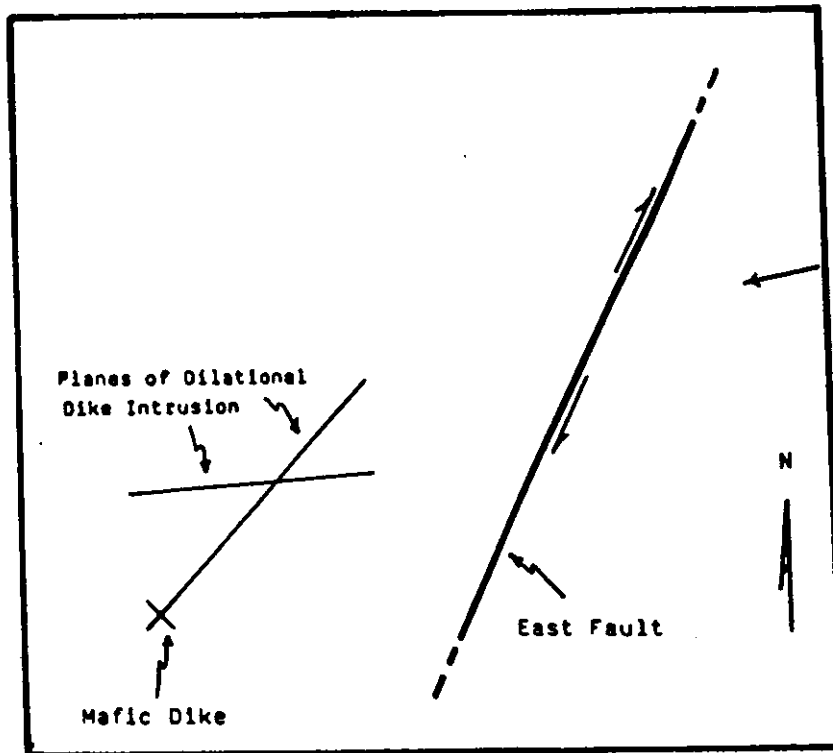
Figure 16. Schematic representation of the major brittle deformational features near the McAfee Complex. The two planar orientations of dike intrusion define a conjugate joint set, the acute bisectorix of which intersects the East Fault at approximately N60E. This coincides with the principal direction of tectonic transport during the Taconic Orogeny, N70E, as defined by Ratcliffe, 1981, and depicted by the arrow at right.
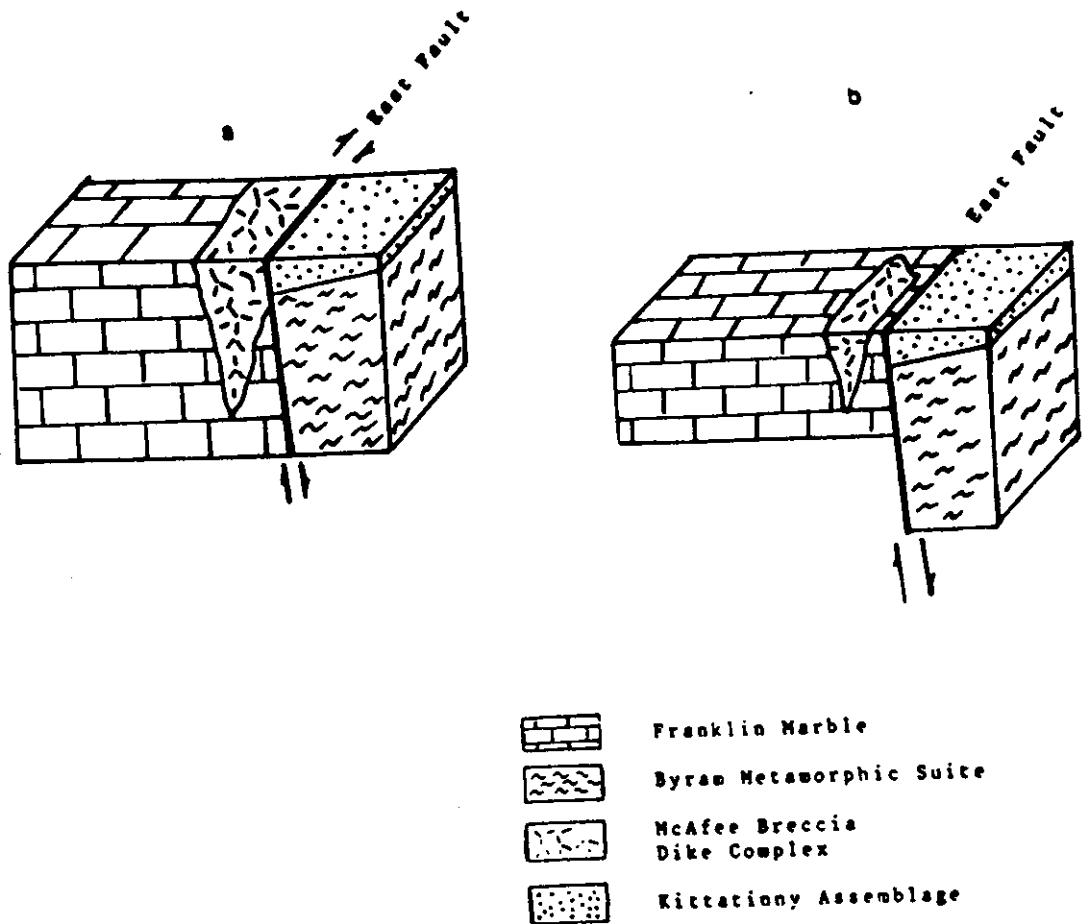
Figure 17.   Schematic block diagrams of the McAfee Complex. a) at
the time of intrusion, during compressional-transpressional
faulting. b) after normal faulting in Mesozoic-Cenozoic.

REFERENCES

Anderson, E.M., 1951, The Dynamics of Faulting: 2nd ed., Oliver and Boyd
    Ltd., Edinburgh.

Baker, D.R., and Buddington, A.F., 1970, Geology and magnetite deposits
    of the Franklin Quadrangle and part of the Hamberg Quadrangle, New
    Jersey: U.S.G.S. Prof. Paper 638, 73 pp.

Drake, A.A., 1984, The Reading Prong of New Jersey and eastern
    Pennsylvania: an appraisal of rock relations and chemistry of a
    major Proterozoic terrane in the Appalachians: Geological Society
    of America Special Paper 194, p. 75-109.

Hague, J.M., Baum, J.L., Hermann, L.A., and Pickering, R.J., 1956,
    Geology and structure of the Franklin-Sterling area, New Jersey:
    Geological Society of America Bulletin, v. 67, p. 435-474.

Hubbert, M.K., 1951, Mechanical basis for certain familiar geologic
    structures: Geological Society of America Bulletin, v. 62, p. 355-
    372.

Hubbert, M.K., and Willis, D.G., 1957, Mechanics of hydraulic
    fracturing: American Institute of Mining and Metall. Petroleum
    Engineers Trans., v. 210, T.P. 4597, p. 153-168.

Hubbert, M.K., and Rubey, W.W., 1959, Role of fluid pressure in
    mechanics of overthrust faulting: Geological Society of America
    Bulletin, v. 70, p. 115-206.

Maxey, L.R., 1976, Petrology and geochemistry of the Beemerville
    carbonatite-alkalic rock complex, New Jersey: Geological Society
    of America Bulletin, v. 87, p. 1551-1559.

Ratcliffe, N.M., 1981, Cortland-Beemerville magmatic belt: a probable
    late Taconian alkalic cross trend in the central Appalachians:
    Geology, v. 9, p. 329-335.

Secor, D.T., Jr., 1965, Role of fluid pressure in jointing: American
    Journal of Science, v. 263, p. 633-646.

Sibson, R.H., 1977, Fault rocks and fault mechanisms: Journal Geol. Soc.
    London, v. 123, p. 191-213.

Smith, B.L., 1969, The Precambrian geology of the central and
    nertheastern parts of the New Jersey Highlands: in Subitzky, S.
    (editor) Geology of selected areas in New Jersey and eastern
    Pennsylvania and guidebook of excursions: New Brunswick, N.J.,
    Rutgers Univ. Press, p. 51-131.

CHAPTER 6

CHEMICAL CHANGES IN MYLONITES AND CATACLASITES

OF THE RESERVOIR FAULT ZONE, NEW JERSEY

Alexander E. Gates, Department of Geology, Rutgers,
The State University of New Jersey, Newark, NJ 07102

ABSTRACT

The history and distribution of deformation in cataclasites
and mylonites within the Reservoir fault can be correlated
with contemporaneous metamorphic mineral reactions and
chemical changes resulting from evolution of throughgoing
halogen-rich fluids. The segment of the fault studied lies in
Grenville gneiss of the New Jersey Highlands. The protolith of
the fault rock is augite and edenite-hornblende quartz
dioritic gneiss with antiperthite and minor ilmenite, apatite,
and zircon. Minor amphibolite layers are also present. Fault
rocks were first retrograded to magnesio-hastingsite-rich
rocks by amphibole, pyroxene and plagioclase consuming
reactions that radically changed the bulk composition from
felsic to mafic. These rocks and remaining protolith were
further retrograded to ferro-actinolite dominated assemblages
with minor albite, epidote, apatite, biotite and titanite.
Final products in the retrogression are actinolite, chlorite,
biotite, albite, and epidote. Halogen components of the fluid
are recorded by the OH site in hydrous minerals. Edenite-
hornblende is F-rich as is early magnesio-hastingsite. There
is a gradual transition to Cl-rich compositions midway through
the magnesio-hastingsite stability zone with F loss in
amphiboles adjacent to fractures that opened at this time.
There is a transition to halogen-poor ferro-actinolite and
finally F- and Cl-free actinolite and chlorite. Biotite shows
the same F-rich to F = Cl transition as amphibole.

Deformation of protolith is purely brittle throughout the
retrograde sequence. The Reservoir fault rocks are dominated
by well foliated cataclasite-mylonite. F-rich hastingsite is
ubiquitous in the central part of the zone where it
extensively replaces plagioclase and fills fractures. The
amphibole is aligned and commonly granulated and indurated
with variably Cl-rich hastingsite. In areas of less intense
deformation, cracks are filled with ferro-actinolite-,
actinolite-, or chlorite-rich assemblages depending upon
timing and location of activation. The F- and Cl-rich
hastingsite is also fractured and filled with the later
assemblages. Late cataclasite in restricted zones along the
western margin of the fault is filled with randomly oriented

assemblages of actinolite, chlorite, biotite, apatite, epidote, and pyrite.

INTRODUCTION

Chemical changes in fault zones have been documented to cause a variety of chemical and mineralogical changes in the deformed rocks. Mineral reactions in mylonites have been used to chart the progress of deformation and fluid infiltration (Beach and Fyfe, 1972; Losh, 1989; Gilotti, 1989; Gates and Speer, 1991). Significant changes in bulk chemistry have also been reported (Beach, 1976; 1980; Kerrich et al., 1978; Sinha et al., 1988) with accompanying volume changes. O'Hara (1988), and Gates and Gundersen (1989), found increases in trace element abundances and ratios and Selverstone (1990) found changes in major elements that indicate volume loss of up to 75% in high strain parts of mylonite zones. All cases are involve granitic protoliths and although there are modal mineral changes, especially in terms of abundances, because the systems are simple, mineral changes are generally not profound. In most mylonite zones studied, bulk chemical changes were found to be relatively small and largely reflect the addition or removal of silica, H_2O, and/or alkalis (Beach, 1976; Kerrich et al., 1978; Sinha et al., 1988; Gates and Speer, 1991).

In rocks that were sheared under brittle conditions or at the brittle-ductile transition, bulk changes can be more profound. Because fractures open in the deforming rock, fluids can travel distances and in much higher abundance. Where veining and induration of cataclastic rocks is evident, the chemical changes are typically more profound (Kerrich et al., 1984; Yardley, 1986; McCaig, 1987; Losh, 1989, Gates and Kambin, 1990). Dilatant fractures, both on the grain and rock scale, fill with the mineral most chemically favored for precipitation from the throughgoing fluid. In most cases, the precipitant is quartz and bulk chemistry changes only by the addition of silica (Kerrich et al., 1984; Losh, 1989; Yardley et al., 1992). In cases where the fluid contains significant amounts of volatiles other than H_2O, chemical changes can be profound (Kerrich et al., 1984; Gates and Kambin, 1990). The Reservoir fault, New Jersey Highlands, provides an example of likely the most extreme chemical changes possible in a shear zone that results from metamorphic reactions (ie: not from vein filling). This paper will demonstrate, 1) the deformational and associated metamorphic evolution of the fault zone, 2) how fluid composition can be used as a constraint on the timing of deformation, and 3) how fluids can change a felsic rock into a mafic rock by mass transfer.
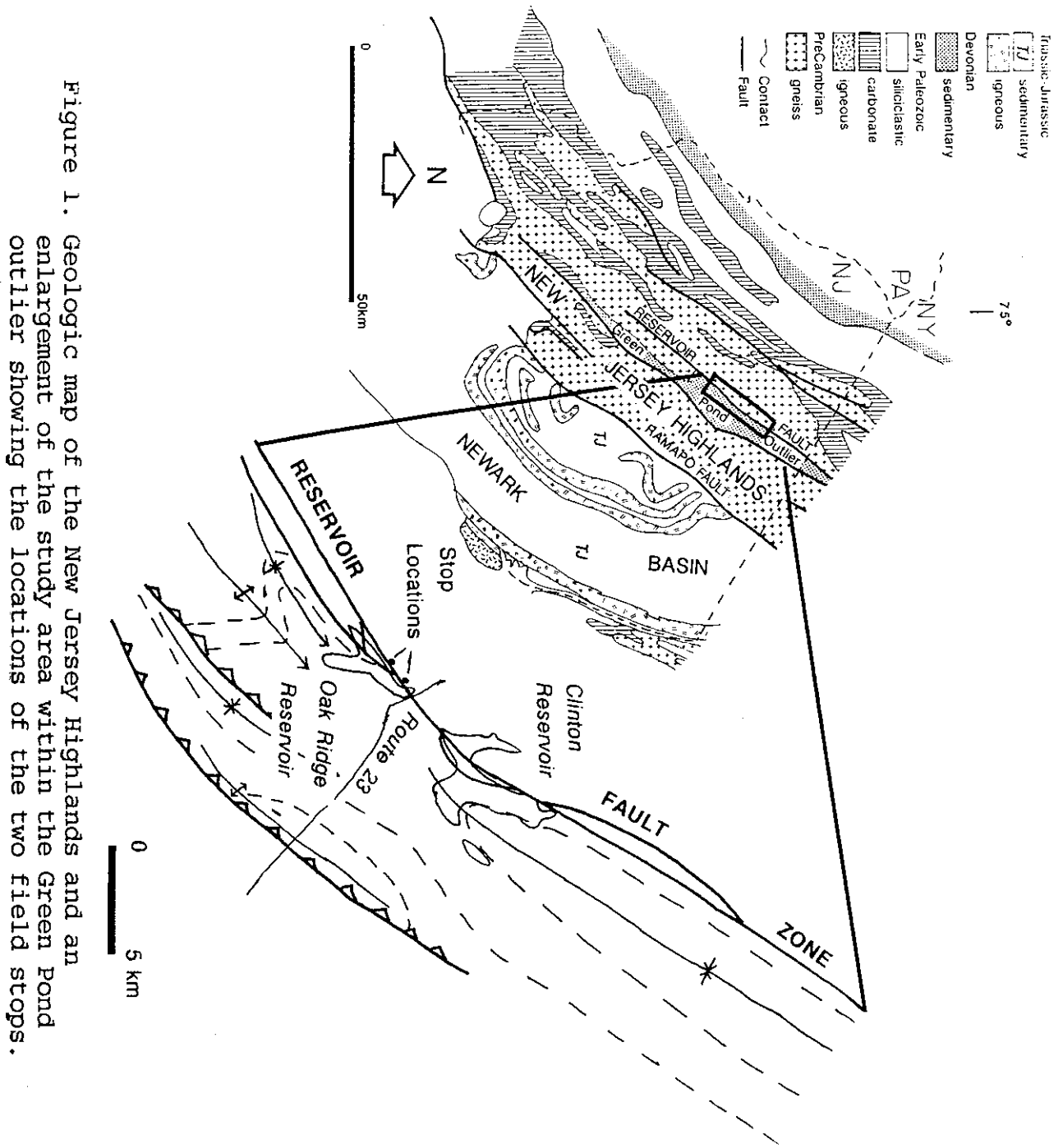
Figure 1. Geologic map of the New Jersey Highlands and an enlargement of the study area within the Green Pond outlier showing the locations of the two field stops.

Table 1. Stratigraphy of the study area and surroundings.

DEVONIAN
Skunnemunk Conglomerate: Thick bedded, quartz pebble conglomerate with red-purple medium-grained sandstone matrix. Locally cross bedded and with medium-grained sandstone interbeds. 900 m thick.
Bellvale Sandstone: Thin to thick bedded gray, medium-grained sandstone and black shale. Locally fossiliferous and cross bedded. 600 m thick.
Cornwall shale: Thin to thick bedded, fissile black shale interlayered with laminated gray siltstone. 300 m thick.
Esopus Formation: Thin interlayers of gray mudstone and medium-grained sandstone. Fossiliferous. 60-100 m thick.

SILURIAN
Poxono Island Formation: Medium-bedded gray dolomite interlayered with thin bedded medium-grained calcareous sandstone. 80-130 m thick.
Longwood Shale: Purple shale with interlayers of red cross-bedded, medium-grained sandstone. 100 m thick.
Green Pond Conglomerate: Tan to red quartz pebble conglomerate with a medium-grained sandstone matrix and silica cement. Interlayers of cross-bedded sandstone. 300 m thick.

ORDOVICIAN
Martinsburg Formation: Black, slaty shale with thin interbeds of siltstone and medium-grained sandstone. Moderately fossiliferous and crossbedded.

PRECAMBRIAN
Granite Pegmatites: Very coarse-grained, uraniferous with quartz, plagioclase, microcline, muscovite, biotite and accessory zircon, apatite and secondary epidote, hematite, and monazite. 1 to 10 m thick.
Quartzofeldspathic Gneiss: Gneiss of granitic and quartz dioritic composition with antiperthitic plagioclase, quartz, varietal amphibole, pyroxene and biotite and accessory ilmenite, apatite, and zircon and secondary epidote, titanite, hematite, chlorite, monazite, and amphibole.Granitic composition also contains K-spar, magnetite and local scapolite and graphite but plagioclase is typically not antiperthitic.
Amphibolite Gneiss: Thin layers of amphibolite within granitic gneiss. Composed of hornblende, pyroxene, plagioclase, minor titanite, and magnetite with secondary epidote, chlorite, and calcite.

REGIONAL GEOLOGY

The Reservoir Fault is a multiply activated shear zone that bounds the western side of the Silurian-Devonian Green Pond outlier in the New Jersey Highlands (Figure 1). The shear zone is best developed in the Grenville gneisses of the Losee Metamorphic Suite (Lewis and Kummel, 1912; Hague et al., 1956; Drake, 1984). These rocks are dominantly layered quartzo-feldspathic gneiss with lesser amphibolite-granulite gneiss. The quartzo-feldspathic gneiss is apparently derived from layered volcaniclastics and calcsilicates (Drake, 1984; Gundersen, 1986) with scapolite, pyroxene, garnet, and retrograde tremolite assemblages or plagioclase-pyroxene-amphibole-garnet assemblages (Malizzi and Gates, 1989). These rocks were intruded by uraniferous pegmatite dikes (up to 100 ppm) along the Reservoir Fault subsequent to granulite facies metamorphism (Malizzi and Gates, 1989).

To the east of the Reservoir Fault, the Green Pond outlier contains a near complete section from Late Ordovician Martinsburg Formation to early Middle Devonian Skunnemunk Conglomerate (Catskill facies) (Darton, 1894; Kummel and Weller, 1902; Herman and Mitchell, 1991) (Table 1). Martinsburg Formation shale is exposed against the Reservoir Fault only in one area. The dominant basal unit is the conglomeratic Green Pond Formation which is Silurian and rests unconformably on basement in most of the area. The overlying Silurian Longwood Shale and Poxono Island Formation (limestone) are thin and sparse. Devonian units are dominated by the lower Cornwall Shale, Bellvale Sandstone and Skunnemunk Conglomerate which caps the sequence. Underlying Devonian Kanouse Sandstone, Esopus Formation and Connelly Conglomerate are thin and poorly exposed.

The timing of movement on the Reservoir Fault is poorly constrained by geochronolgy or the stratigraphy of the area and as a result, there is no consensus (Figure 2). Hull et al. (1986) and Malizzi and Gates (1989) speculated on Grenville movement on the fault, possibly recorded by the uraniferous pegmatites. Based on correlation with Canada Hill granite, the age of metamorphism for the gneisses is greater than 913 Ma (Helenek and Mose, 1984) but movement could have been synchronous. Helenek (1987) proposed Late Proterozoic wrench faulting and normal faulting during Late Proterozoic rifting as proposed for the nearby Ramapo fault (Costa and Gates, 1992) cannot be precluded. The age of movement examined herein must post-date this period but whether is was simply a late phase of deformation or the result of Late Proterozoic or Paleozoic activity is not clear. The Reservoir fault was certainly active several times during the Paleozoic-Mesozoic(?). Ratcliffe (1980), Mitchell and Forsythe (1988) and Malizzi and Gates (1989) documented two post-depositional phases of movement, one of which preserved the Green Pond outlier through west-side-up movement. Lewis and Kummel (1912) and Ratcliffe (1980) considered the entire Green Pond outlier to be preserved in a Mesozoic graben. Malizzi and Gates (1989)

Proposed Ages and and Senses of Movement for The Reservoir Fault

AGE	?	Normal	Reverse	Dextral Strike-Slip	Sinistral Strike-Slip
Neotectonism	R				
Mesozoic		R, L+K			M+G
Alleghanian II					M+F
Alleghanian			H, M+F, M+G	M+G	
Acadian		F		F	
Taconic			R, H		
Late Proterozoic		I		He	He
Grenville	R,M+G				

L+K = Lewis and Kummel (1912), R = Ratcliffe (1980), H = Hull et al.
(1986), M+F Mitchell and Forsythe (1988), He = Helenek (1989), M+G =
Malizzi and Gates (1989), F = Finks (1990), I = inference from Costa and
Gates (this volume)

Figure 2. Chart showing proposed senses and times of movement on
the Reservoir fault and the source of the proposals. Two
senses proposed for a single event in a study indicates
a composite movement (ie: normal + dextral strike-slip =
dextral transtensional movement).

however, considered all Mesozoic movement to be sinistral transcurrent. Finks (1990) proposed that the thick, high energy Devonian sedimentary rocks were deposited in a restricted dextral transtensional pull apart basin, accounting for it's separation from the Catskill depocenter. Ratcliffe (1980) proposed Taconic movement on the zone as well as neotectonism. Clearly, however, the dominant deformation in the Green Pond outlier is Alleghanian and compressional in nature (Hull et al., 1987, Mitchell and Forsythe, 1988, Herman and Mitchell, 1991) and the Reservoir fault was certainly active during this event. Malizzi and Gates (1989) proposed that this movement may have been dextral transpressional based on study of kinematic indicators in the fault zone.

This paper investigates a phenomenal process that is illustrated in the rocks of the Reservoir fault. During brittle dextral transcurrent movement of unknown age, fluids infiltrated the fault zone to such a degree that cataclasites underwent extreme geochemical changes. Because such retrograde processes have not been studied in the New Jersey Highlands, it is not possible to place the age of movement within this context without detailed geochronologic analysis. The event was post-Grenville because the rocks record a lower metamorphic grade and pre-Triassic (likely Alleghanian also) because they are of too high a grade.

CATACLASITES AND MYLONITES

The part of the Reservoir fault considered in this study is completely contained within the granitic and amphibolite gneisses of the New Jersey Highlands (Malizzi and Gates, 1989) (Figure 1). The fault zone grades from purely brittle rocks along its western edge to quasi-plastic mylonites and ultramylonites towards the east side of the zone. It is possible that the zone graded back into purely brittle rocks on the eastern side as well but later movement may have removed part of the fault zone, leaving a lithologically asymmetric zone. The eastern mylonitic edge of the zone is now in contact with sedimentary rocks of the Green Pond outlier.

Brittle deformation of the granitic gneiss is locally intense as indicated by extensive fault breccia and cataclasite. Within these rocks, feldspars are fractured or granulated and offset along microfaults that primarily exploit cleavage planes. Where systematic, these microfaults are both synthetic and antithetic depending upon orientation of the extended grains. Commonly, however, fracturing is intense and seemingly random and no offset directions can be determined. The fractures are filled with amphibole, epidote, calcite, chlorite, and hematite. Quartz shows extreme lattice misorientation including undulose extinction, deformation lamellae, and deformation bands, much of which likely reflects submicroscopic cataclasis (see Tullis and Yund, 1987) and not plastic deformation. Quartz also exhibits extensive fractures that are filled with essentially the same minerals as feldspar. Other minerals including hornblende, pyroxene, .

oxides and rare scapolite are simply offset along fractures and like the feldspar show extensive reaction textures.

In the fractured rocks, feldspars show metamorphic reaction textures to epidote but primarily to amphibole intergrowths where they are open to fractures (Plate 1A). Typically, the most complete replacement occurs closest to the fracture but in many cases, the new minerals permeate the entire grain. Eastward into the shear zone, the granitic and amphibolite gneiss has undergone extensive brecciation and cataclasis. The matrix of these rocks is virtually all amphibole. In the well developed cataclasite parts of the shear zone, rounded xenoclasts can range to 0.5 m but the much more common relict component is 0.5 - 1.0 mm xenocrysts of quartz and feldspar (Plate 1B). The relict material floats in a matrix of randomly oriented 0.1 - 0.5 mm clear amphibole with chlorite, biotite, plagioclase, epidote and rare pyrite.

In the mylonitic (semi-brittle) part of the shear zone, deformation appears to have continued past the brittle stage. Although xenoclasts, xenocrysts and coarse grained amphibole cores continued to undergo brittle deformation within the central part of the shear zone, fine grained amphibole and chlorite display marginal plastic deformation. A well developed S-C mylonitic fabric formed in the amphibole-rich matrix including late C' planes (terminology of Simpson and Schmid, 1983) (Plate 1C). S planes are composed exclusively of fine-grained amphibole and the cores of amphibole porphyroclasts whereas C and C' planes are fine-grained amphibole with variable amounts of chlorite. Larger grains of amphibole including porphyroclast cores commonly exhibit varying amounts of brittle fracturing primarily as microfaulting along cleavage planes and subsequent bending of the microfault blocks with amphibole and chlorite filling the fractures. These large grains also commonly exhibit rims and asymmetric tails of finely recrystallized amphibole and form rotated S-type porphyroclasts (terminology of Passchier and Simpson, 1986). SEM images of the seemingly solid cores of these amphibole porphyroclasts show that most are granulated and indurated with epitaxial amphibole of a different composition (Plate 1D). Where strain is highest, the rock is fine-grained and ubiquitously layered forming an ultramylonite. The S-C fabric, rotated porphyroclasts and offset of brittle grains consistently show a dextral transcurrent sense of shear (Plate 1C).

Locally, small xenoclasts of granitic gneiss also appear mylonitic. Quartz and feldspar exhibit S-C fabric and rotated porphyroclasts with a dextral transcurrent sense of shear consistent with that in the matrix. The grains, however, show severe alteration and some cataclasis, indicating that they were not stable with the final shearing. They may record an early higher temperature phase of the shearing that produced the amphibole mylonite or an earlier completely separate event.

Table 2. Representative analyses and mineral formulae for mineral
phases from the Reservoir fault zone (see text).

	F-Hastingsite	Actinolite	Edenite	Cl-Hastingsite	Ferro-Actinolite
SIO2	43.35	52.31	46.73	40.24	50.89
TIO2	.75	.00	1.39	.14	.12
A2O3	8.74	1.67	6.00	15.77	.36
FEO	18.14	19.19	14.97	11.05	28.34
MNO	.15	.33	.17	.14	.60
MGO	11.44	11.88	13.61	13.72	4.96
CAO	10.59	11.97	10.21	11.74	11.70
BAO	.00	.00	.00	.00	.00
NA2O	2.43	.63	2.37	2.46	.19
K2O	1.66	.32	1.14	1.57	.09
F	1.92	.10	.94	.47	.00
CL	1.01	.00	.22	2.18	.00
H2O	.82	1.97	1.50	1.25	1.91
SUM	101.00	100.37	99.25	100.73	99.16
-O= F+CL	1.04	.04	.45	.69	.00
SUM	99.96	100.33	98.80	100.04	99.16

	Biotite	Chlorite	Epidote
SIO2	37.46	32.00	37.73
TIO2	2.21	.00	.07
A2O3	14.54	16.70	23.35
FEO	19.80	25.34	12.95
MNO	.23	.00	.25
MGO	13.29	13.36	.02
CAO	.07	.36	22.81
BAO	.00	.00	.00
NA2O	.14	.02	.02
K2O	6.32	.18	.05
F	1.01	.20	.00
CL	1.04	.00	.03
H2O	3.21	11.47	1.86
SUM	99.32	99.63	99.14
-O= F+CL	.66	.08	.01
SUM	98.66	99.55	99.14

	Pyroxene	Titanite		K-Spar Lams	Plagioclase
SIO2	51.25	30.90	SIO2	66.32	66.62
TIO2	.00	27.79	TIO2	.00	.00
A2O3	2.32	5.96	A2O3	19.91	19.90
FEO	11.21	2.65	FEO	.11	.15
MNO	.34	.00	MNO	.03	.00
MGO	12.23	.22	MGO	.00	.00
CAO	21.92	28.33	CAO	.06	.00
BAO	.00	.00	BAO	.00	.00
NA2O	.71	.05	NA2O	1.00	.16
K2O	.02	.36	K2O	12.82	13.88
F	.15	1.85	F	.16	.09
CL	.00	.02	CL	.02	.00
SUM	100.00	98.13	SUM	100.25	100.71
-O= F+CL	.00	.78	-O= F+CL	.00	.00
SUM	100.00	97.35	SUM	100.25	100.71

Table 3. Representative whole-rock analyses for rocks from the Reservoir fault zone.

Oxide	Quartzofeldspathic Gneiss (protolith)	Metamorphosed Fault Rock
SiO_2	75.42	43.96
TiO_2	0.07	0.39
Al_2O_3	13.62	14.99
Fe_2O_3	1.13	12.77
MnO	0.01	0.14
MgO	0.26	15.49
CaO	0.83	1.73
Na_2O	5.83	1.91
K_2O	3.10	0.80
P_2O_5	0.10	0.15
Cr_2O_5	0.04	0.04
L.O.I.	0.57	6.73
TOTAL	101.00	99.10

PETROLOGY AND GEOCHEMISTRY OF THE FAULT ZONE

Mineral chemistry was analyzed using the JEOL JXA-8600 Superprobe at Rutgers University, New Brunswick. Compositions were measured in weight percent and converted to mineral formulae using the Fortran program SUPERRECAL. Representative analyses of minerals from within each zone and described in the text are presented in Table 2. Amphiboles were named using the Fortran program AMPHTAB on the basis of calculated formulae. The two bulk chemical analyses presented were performed on representative samples by Chemex Inc., Sparks, NV, using ICP-AES techniques. These analyses are presented in Table 3.

The rocks of the Reservoir fault zone began as Grenville gneiss prior to deformation. Synchronous with deformation and restricted to rocks within the fault zone, there was a hydrothermal retrograde metamorphic event. Evolution of physical conditions and fluid compositions is profound and recorded by metamorphic reactions, changes mineral chemistry and, in part, by changes in bulk composition. The protolith of the fault rocks are preserved along the western margin of the fault and as xenoclasts and xenocrysts throughout the fault rocks. The protolith is primarily a quartz dioritic gneiss with antiperthite, varietal edenite to hornblende, and augite and minor ilmenite, apatite, zircon and reported scapolite (Malizzi and Gates, 1989) with a granoblastic texture. The amphiboles in this rock are F-rich (1.5 - 2.0 wt. %) and Cl-bearing (to 0.5 wt. %) (Table 2). Feldspar is albite with exsolution lamellae of K-spar. The bulk composition (Table 3) is typical for similar Grenville rocks of the New Jersey Highlands and is characterized generally as felsic.

The first evidence of retrogression is the reaction of edenite-hornblende and locally augite to magnesio-hastingsite along fractures and cleavage planes (Plate 1A). In more deformed rock, plagioclase is lamellae-free along fractures and grain boundaries and shows reaction textures to magnesio-hastingsite. Ilmenite has overgrowths of titanite. Within the central part of the fault zone, reactions progressed much further. Only small pods of highly deformed and lamellae-free albite remain in the otherwise magnesio-hastingsite rock. Minor phases include titanite, apatite and pyrite (possibly from later retrogression). This first retrograde amphibole records an evolution of fluid composition within its stability field. Cores of early magnesio-hastingsite are F-rich with contents similar to the edenite but with higher Cl contents (0.6 to 1.0 wt. %). The optically continuous overgrowths, fracture fillings and material that indurates pulled-apart and granulated grains, in contrast, are zoned to Cl-rich compositions with 1.0 to as much as 2.4 wt. % in the latest rims but with little to no F (Plate 1D). There is zoning of F adjacent to fractures in early formed magnesio-hastingsite as well. Profiles show a progressive drop in F content from 1.5 - 2.0 wt. % to 0.5 - 0.75 wt. % with no change in any other element including Cl (Figure 3). Such a unimodal change in a
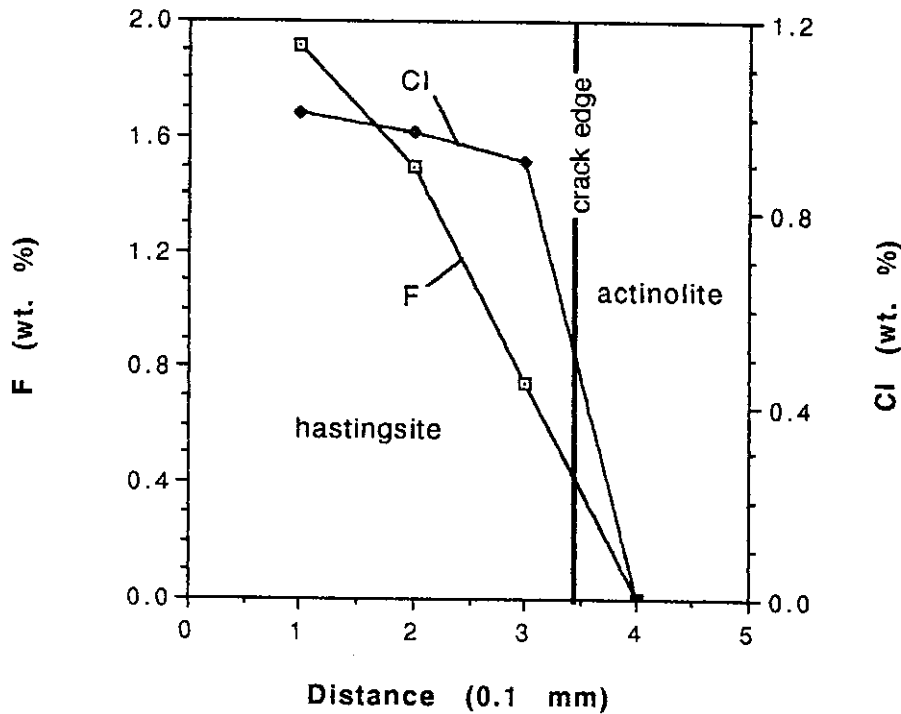
Figure 3. Composite graphs showing concentrations of F and Cl
within a single grain of hastingsite across its boundary
with actinolite. The loss of F with no concommitant loss
of Cl is interpreted to reflect diffusion of volatiles
at the grain boundary into a Cl rich fluid.

volatile is likely the result of diffusion but because Cl did not change, the fluid was likely Cl-rich.

Overgrowths and fracture fillings on the chloro-hastingsite are of optically continuous ferro-actinolite and subsequently amphibole (Plate 1D). The transition between the two can only be observed in SEM or microprobe traverses. Unlike the magnesio-hastingsite assemblages, the ferro-actinolite is more commonly intergrown with other minerals, especially in areas with minimal amounts of magnesio-hastingsite. The assemblages include fine-grained epidote, albite, titanite, apatite, pyrite and locally muscovite and biotite but are still dominated by amphibole. These minerals can be found in shear bands and in veins that parallel foliation in all rocks (Plate 1C). Biotite also shows the transition from F-rich to Cl-rich compositions but within ferro-actinolite and actinolite-bearing assemblages. Explanations for this apparent incongruity are that there was a thermal gradient within the shear zone and actinolite was produced in some parts while magnesio-hastingsite was produced in others, the F to Cl transition in fluid was not everywhere synchronous, or the biotite could be in disequilibrium with the present assemblage.

GEOCHEMICAL CHANGES DURING DEFORMATION

The two analyses in Table 3 appear to be from completely different rocks but actually one is the protolith of the other. The gneisses within and adjacent to the Reservoir fault zone are dominantly granitic in composition with an order of magnitude lesser amounts of amphibolite. The average composition of the quartz dioritic gneiss (Table 3) is that of a monzogranite with few varietal mafic minerals. The chemistry reflects a typical felsic rock with very high SiO_2 and Al_2O_3 and very low FeO and MgO. The bulk chemistry of heavily replaced, amphibole-rich fault zone rocks, on the other hand, yields the typical composition of mafic rocks but with a high volatile content. Changes in silica and iron are especially profound. The process of chemical change within this shear zone shows how a felsic rock can be changed into a mafic rock, a direction not usually considered by petrologists.

These chemical changes are end-products of a profound allochemical retrograde metamorphic evolution within a shear zone and are reflected in the corresponding mineralogical changes. The observed protolith assemblages in granitic gneiss are augite + low-Ca feldspar + ilmenite, or edenite-hornblende + low-Ca feldspar + ilmenite ± scapolite ± garnet. These assemblages were produced during granulite facies metamorphism of the Grenville orogeny. The first retrograde assemblage is magnesio-hastingsite which is locally potassian and consistently a fluoro amphibole + titanite ± albite + pyrite(?) (Table 2). The proportion of amphibole in this assemblage is about 90 to 95%. The first step in this retrogression requires large amounts of Fe and Mg to be added

to the rock and large amounts of Si, Na, K and Al to be
flushed out. It is clearly responsible for the major
proportion of the bulk chemical change in the rock.

The early hastingsite is F-rich but subsequent hastingsite
became progressively more Cl-rich and amphibole analyses with
equal parts of F and Cl (~1%) are common (Table 2). The
transition continued, however, and the latest hastingsite
observed is Cl-rich and contains no F. Because the chloro-
hastingsite is predominantly restricted to zones containing
fluoro-hastingsite, it is inferred that most of the changes in
bulk chemistry occurred during initial retrogression.
Therefore, F-rich fluids are likely better vehicles of
chemical change than Cl-rich fluids. The same transition of F-
rich to Cl-rich was observed in biotite within lower grade
assemblages. If this F-Cl transition is everywhere
synchronous, then the biotite is in disequilibrium with the
present assemblage and formed during magnesio-hastingsite
production but in a rock with different bulk chemistry.
Alternatively, the fault zone may have had a steep temperature
gradient during retrogression as the result of shear heating
or because the fluid controlled the thermal architecture. In
this case, assemblages reflecting different physical
conditions could have been formed at the same time but in
different places. The biotite could then be in equilibrium
with the current assemblage but the other hydrous phases must
have not accepted the halogens into the OH site.

Ferro-actinolite rich assemblages succeeded the hastingsite
assemblages and include albite, epidote, titanite, apatite,
biotite(?) and chlorite(?). Some of the ferro-actinolite
contains 0.5 to 1.0% F but most is F-free and virtually all is
Cl-free (Table 2). The final retrograde amphibole is
actinolite and it is virtually always associated with chlorite
in varying proportions. Other common associations include
epidote, apatite, albite, titanite and biotite(?). These later
assemblages do not involve any major changes in bulk chemistry
of the zone.

DISCUSSION

With the evolution of mineral compositions within the fault
zone both in terms of reactions and the evolution of volatiles
and their proportions in the fluid, a well constrained
sequence of chemical-mineralogical events can be established.
This sequence can be used as a measure of relative timing for
structural evolution within the fault zone. The minerals and
their compositions within and around fractures constrains the
relative timing of the activation of individual fractures
within the metamorphic evolution of the fault zone. The most
significant implications of these spatial and temporal
distributions are that they record the shifting of activity
within the fault zone.

The central part of the fault zone records the most
complete geochemical evolution. In this area, few relict
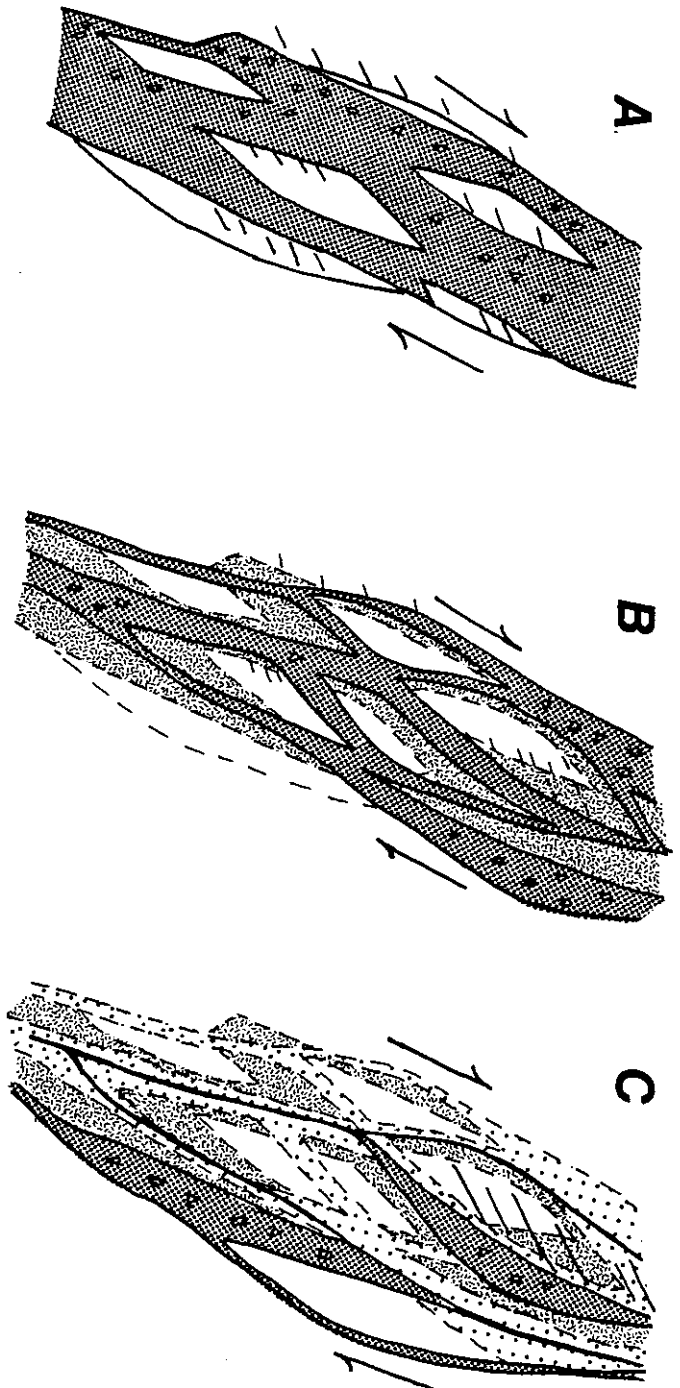patches of plagioclase and even fewer pyroxene grains remain

Figure 4. Model for the evolution of an idealized shear zone using the temporal and spatial relations observed in the Reservoir fault zone. A) Dextral faulting along the fault, cataclasis, and reaction of protolith to fluoro-hastingsite-dominated assemblages. B) Narrowing of established zones and establishment of new areas of movement and cataclasis and reaction to chloro-hastingsite-dominated assemblages. Dark shade = active areas, light shade = inactive or dormant parts of previously active zone. C) Further narrowing of old zones, establishment of new zones, and general shifting of the active zone to the west (right) concommitant with metamorphic reactions that produced actinolite- and ferro-actinolite-bearing assemblages. Dark shade = active areas, light shade = inactive parts of the previously active zone.

162

enclosed within hastingsite and actinolite but no edenite-hornblende remains (Plate 1C). The early hastingsite is F-rich and granulated. Epitaxial overgrowths of variably F-rich to Cl-rich hastingsite indurated the old grains and held them together (Plate 1D). The evolution from F-rich to Cl-rich hastingsite shows that the early hastingsite deformed in a series of anastomosing shear zones that grew narrower with time. The highly deformed areas adjacent to the shear planes record the entire F- to Cl-transition whereas fractures within the lensoid interareas commonly contain F-rich or less commonly Cl-rich hastingsite fillings, and the rest of transition is absent. In many cases, ferro-actinolite or actinolite fills the fractures in F-rich hastingsite within the far interior of the lenses with no Cl-rich actinolite at all. Similar extensive deformation along anastomosing planes of weakness with much slower progressive deformation into the lensoid interareas was observed in serpentinite (Gates, 1992) and may be an important process in shear zones at the brittle-ductile transition.

Missing segments of the record of the metamorphic evolution are even more profound away from the central part of the fault zone. Chloro-hastingsite on fluoro-hastingsite was observed in only a few locations. More commonly, fluoro- or chloro-hastingsite is directly overgrown by ferro-actinolite or actinolite but spatial relations are not regular. Some areas at the western margin of the fault zone contain cataclasite with randomly oriented actinolite, chlorite, and biotite and no record of earlier amphibole phases (Plate 1B). These zones likely formed in the latter stages of shearing within areas with little early fault activity or retrogression. Because the biotite appears to record the F- to Cl-transition, these areas may have had minor early activity but had a different bulk composition than the central fault because the massive influx of Fe and Mg and removal of Si and Al did not take place until much later and to a lesser degree.

Deformation within the Grenville gneiss surrounding the Reservoir fault is exclusively brittle.These rocks show the largest gaps in their record of metamorphic evolution. In these rocks, F-rich hastingsite, Cl-rich hastingsite, ferro-actinolite, actinolite, biotite or chlorite or any combination of these can be observed reacting from the primary pyroxene or edenite-hornblende. It just depends upon the timing of fracture activation as to which reaction will have occurred. No spatial pattern of retrogression was identified during this study; much more detailed analysis is required to determine where and when the fault margin was deformed.

Besides the regular thinning of the central part of the shear zone the spatial and temporal distribution of activity appears irregular to almost chaotic. However, it shows that shear zones do not move continuously and smoothly nor do they completely open during seismic activity. Instead, large parts of the shear zone can be active early and then remain dormant for long periods of time (fluid evolution is a slow process) before reactivating (Figure 4). Fluids can cause reactions

within the fault zone that cement the zone shut and force the next increment of movement to be taken up on another segment of the fault or to establish a new zone of movement in previously undeformed rock or dormant fault. Each gap in the sequence of reactions represents a period of dormancy. Where only one retrograde assemblage fills the fault, only one period of movement took place and the fault plane was cemented achieving a strength greater than the force exerted by the fault. In general, fluids were effective in causing reactions to cement the central part of the zone early in the history, allowing minor movement on thin faults and forcing the reactivation of dormant zones and the activation of new zones along the western edge of the Reservoir fault zone.

CONCLUSIONS

The history and timing of fracture activation can be recorded within a shear zone with a concurrent well-constrained physical-chemical evolution that is unidirectional (ie: no cycling of fluids within the same set of physical conditions). These throughgoing fluids are capable of causing profound chemical changes in the fault rocks. In the case of the Reservoir fault, a felsic rock was changed into a mafic rock by such processes.By considering mechanical deformation in conjunction with metamorphic reactions, a better understanding of both is gained. Fault rocks that otherwise appear chaotic can be shown to actually have some degree of organization using this type of analysis.

ACKNOWLEDGMENTS

REFERENCES

Beach, A.E., 1976, The interrelations of fluid transport, deformation, geochemistry and heat flow in early Proterozoic shear zones in the Lewisian complex; Philosophical Transactions of the Royal Society of London, v. A280, p. 569-604.

Beach, A.E., 1980. Retrogressive metamorphic processes in shear zones with special reference to the Lewisian Complex. Journal of Structural Geology, vol. 2, p. 257-263.

Beach, A.E. & Fyfe, W.S., 1972. Fluid transport and shear zones at Scourie, Sutherlands: Evidence of overthrusting? Contributions to Mineralogy and Petrology, vol. 36, p. 175-180.

Costa, R.E., and Gates, A.E., 1992, Mylonitization of mylonites: Evidence for the opening and closing of the Iapetus Ocean from the Ramapo Fault; Geological Society of

America Abstracts with Programs, vol. 24, p. 14.

Darton, N.H., 1894, Geologic relations from Green Pond, New Jersey to Schunemunk Mountain, New York; Geological Society of America Bulletin, vol. 5, p. 367-394.

Drake, A.A., Jr., 1984, The Reading Prong of New Jersey and eastern Pennsylvania; An appraisal of rock relations and chemistry of a major Proterozoic terrane in the Appalachians, in Bartholemew, M.J., (ed.), The Grenville Event in the Appalachians and Related Topics; Geological Society of America Special Paper 194, p. 75-109.

Finks, R.M., 1990, The Green Pond outlier as a Silurian right-lateral transpressional basin; Geological Society of America Abstracts with Programs, vol. 22, p. 15.

Gates, A.E., 1992, Domainal failure of serpentinite in shear zones, State-Line mafic complex, Pennsylvania, USA; Journal of Structural Geology, vol. 14, p. 19-28.

Gates, A.E. & Gundersen, L.C.S., 1989; Role of ductile shearing in the concentration of radon in the Brookneal zone Virginia. Geology, vol. 17, p. 391-394.

Gates, A. E. and Kambin, R.C., 1990, Comparison of the natural deformation of the State-Line serpentinite, USA with experimental studies; Tectonophysics, vol. 182, p. 249-258.

Gates, A.E. and Speer, J.A., 1991, Allochemical retrograde metamorphism in shear zones: and example in metapelites, Virginia, USA; Journal of Metamorphic Geology, v. 9, p. 581-604.

Gilotti, J.A., 1989, Reaction progress during mylonitization of basaltic dikes along the Sarv thrust, Swedish Caledonides; Contributions to Mineralogy and Petrology, vol. 101, p. 30-45.

Gundersen, L.C., 1986, Geology and geochemistry of the Precambrian rocks of the Reading Prong, New York and New Jersey - Implications for the genesis of iron-uranium-rare earth deposits, in Carter, L.M.H. (ed.), USGS Research on Energy Resources - 1986 Programs and Abstracts; U.S. Geological Survey Circular 974, p.19.

Hague, J.M., Baum, J.L., Hermann, L.A., and Pickering, R.J., 1956, Geology and structure of the Franklin-Sterling area, New Jersey; Geological Society of America Bulletin, v. 68, p. 435-473.

Helenek, H.L., 1987, Possible Late Proterozoic wrench tectonics in the Reading Prong, New York-New Jersey-Pennsylvania; Northeastern Geology, vol. 9, p. 211-223.

Helenek, H.L., and Mose, D.G., 1984, Geology and geochronology of Canada Hill Granite and its bearing on the timing of Grenvillian events in the Hudson Highlands, New York, in Bartholemew, M.J., ed., Grenville Events and Related Topics in the Appalachians: Geological Society of America Special Paper, v. 194, p. 57.

Herman, G.C., and Mitchell, J.P., 1991, Bedrock geologic map of the Green Pond Mountain region from Dover to Greenwood Lake, New Jersey; New Jersey Geological Survey Geologic Map Series 91-2.

Hull, J., Koto, R., and Bizub, R., 1986, Deformation zones in

the Highlands of New Jersey, in Husch, J.M., and Goldstein, F.R. (eds.), Geology of the New Jersey Highlands and Radon in New Jersey; Geological Association of New Jersey Field Guide, vol. 3, p. 19-67.

Kerrich, R., Fyfe, W.S., Gorman, B.E., & Allison, I., 1978. Local modification of rock chemistry by deformation. Contributions to Mineralogy and Petrology, vol. 65, p. 183-190.

Kerrich, R., La Tour, T.E. & Wilmore, L., 1984. Fluid participation in deep fault zones: evidence from geological, geochemical and $^{18}O/^{16}O$ relations. Journal of Geophysical Research, vol. 89, p. 4331-4343.

Kummel, H.B., and Weller, S., 1902, The rocks of the Green Pond mountain region: Annual Report of the State Geologist 1901, N.J. Geological Survey, p. 1-51.

Lewis, J.V., and Kummel, H.B., 1912, Geologic map of New Jersey (1910-1912): N.J. Department of Conservation and Economic Development, Atlas Sheet 20.

Losh, S., 1989, Fluid-rock interaction in an evolving ductile shear zone and across the brittle-ductile transition, central Pyrenees, France; American Journal of Science, v. 289, p. 600-648.

Malizzi, L. D. and Gates, A. E., 1989, Late Paleozoic deformation in the Reservoir Fault zone and Green Pond Outlier; N. Y. State Geological Association Field Trip Guidebook, vol. 61, p. 75-93.

McCaig, A.M., 1987, Deformation and fluid-rock interaction in metasomatic dilatant shear bands; Tectonophysics, vol. 135, p. 121-132.

Mitchell, J.P., and Forsythe, R., 1988, Late Paleozoic non-coaxial deformation in the Green Pond Outlier, New Jersey Highlands; Geological Society of America Bulletin, vol. 100, p. 45-59.

O'Hara, K., 1988. Fluid flow and volume loss during mylonitization: an origin for phyllonite in an overthrust setting, North Carolina, U.S.A. Tectonophysics, vol. 156, p. 21-36.

Passchier, C.W., and Simpson, C., 1986, Porphyroclast systems as kinematic indicators: Journal of Structural Geology, v. 8, p. 831-843.

Ratcliffe, N.M., 1980, Brittle faults (Ramapo, fault) and phyllonitic ductile basement rocks of the Ramapo seismic zones, New York and New Jersey, and their relationship to current seismicity, in Manspeizer, W. (ed.), Field Studies of New Jersey Geology; New York State Geological Association Guidebook, vol. 52, p. 278-311.

Selverstone, J., Morteani, G., and Staude, J.M., 1991, Fluid channeling during ductile shearing: Transformation of granodiorite into aluminous schist in the Tauern Window, Eastern Alps; Journal of Metamorphic Geology, vol. 9, p. 419-431.

Simpson, C. and Schmid, S.M., 1983, An evaluation of criteria to deduce the sense of movement in sheared rocks; Geological

Society of America Bulletin, vol. 94, p. 1281-1293.

Sinha, A.K., Hewitt, D.A., and Rimstidt, J.D., 1988, Metamorphic petrology and strontium isotope geochemistry associated with the development of mylonites: An example from the Brevard fault zone, North Carolina; American Journal of Science, vol. 288-A, p. 115-147.

Tullis, J., and Yund, R.A.,1987, Transition from cataclastic flow to dislocation creep of feldspar: Mechanisms and microstructures; Geology, vol. 15, p. 591-595.

Yardley, B.W.D., 1986, Fluid migration and veining in the Connemara schists, Ireland, In: Walther, J.V., and Wood, B. J., eds., Fluid-rock interactions during metamorphism, Advances in Physical Geochemistry, 5, Springer-Verlag, New York, p. 109-131.

Yardley, B.W.D., and Bottrell, S.H., 1992, Silica mobility and fluid movement during metamorphism of the Connemara schists, Ireland; Journal of Metamorphic Geology, vol. 10, p. 453-464.

CHAPTER 7

MULTIPLE EPISODES OF MOVEMENT ON THE RAMAPO FAULT SYSTEM, NORTHERN NEW JERSEY

Ralph E. Costa, Woodward-Clyde Consultants, Wayne, NJ 07470
and Alexander E. Gates, Department of Geology, Rutgers,
The State University of New Jersey, Newark, NJ 07102

ABSTRACT
     The Ramapo fault system in New Jersey has a long and
complex kinematic history indicating at least four and possibly
five periods of movement. Proterozoic Z southeast-dipping
normal faulting, associated with continental rifting developed
under greenschist facies conditions. Compressional tectonics
during the Taconic orogeny reactivated the zone as a series of
ductile southeast-dipping reverse faults under mid- to upper
greenschist facies conditions. Reactivation of the Ramapo fault
system as southeast-dipping reverse faults at the brittle-
ductile transition and east-southeast- and west-northwest-
dipping reverse faults, northeast- and southwest-dipping normal
faults, and conjugate north-northwest- and south-southeast-
dipping right-lateral strike-slip and east- and west-dipping
left-lateral stike-slip faults within the brittle regime is
consistent with an Alleghanian paleostress maximum that trended
east-southeast.
     Reactivation of the Ramapo fault system as a complex
brittle fault set under chlorite-zeolite metamorphic conditions
is consistent with a Triassic paleostress maximum that trended
approximately north-south. This fault set included south-
southwest- and north-northwest-dipping reverse, southeast- and
northwest-dipping normal, and a conjugate set of northeast- and
southwest-dipping right-lateral strike-slip and southeast-
dipping left-lateral strike-slip faults. Retrograded Late
Ordovician (?) basaltic dikes were sheared in the ductile regime
during Triassic reactivation of the Ramapo fault system.
Possible Jurassic reactivation of the Ramapo fault zone as
southeast- and northwest-dipping right-lateral strike-slip
faults is consistent with a paleostress tensor that trended
east-northeast.
     Neotectonic investigation of the Ramapo fault system
revealed deformed glacial sediments which are better explained
by ice-contact glacial processes and gravitational slumping
rather than tectonic reactivation.

INTRODUCTION
     Multiple reactivations of preexisting zones of weakness are
common in the Appalachians (Wilson,1965; Hatcher,1972;
Bobyarchick and Glover,1979; Swanson, 1986). These ductile
Taconic reverse faults, like the Brookneal zone (Gates, 1991),

were reactivated as Alleghanian strike-slip and Mesozoic brittle normal faults. One of the best examples of multiply reactivated zones of weakness is the Ramapo fault system. Ratcliffe (1971; 1980) has convincingly documented a history of multiple reactivation for the Ramapo fault which spans from the Precambrian to possibly Recent.

The oldest documented movement on the Ramapo fault zone is manifested in semiductile shear zones and is dated at approximately 1 Ga (Ratcliffe, 1980). This late Grenvillian reverse right-lateral strike-slip faulting is recorded as mylonitization of Proterozoic Y rocks developed under regional greenschist facies metamorphic conditions (Ratcliffe, 1980). In southeastern New York, the syntectonic Canopus pluton provides an absolute age for this activity. An Rb/Sr whole rock analysis dates this movement at 1070 Ma (Ratcliffe, 1980).

In northern New Jersey and southeastern New York, late Taconic ductile to semibrittle reactivation of this zone has been recorded as thrust, reverse and right-lateral oblique slip motion (Ratcliffe, 1980). Within the Ramapo fault zone of southeast New York, plutonic and dike rocks of the Rosetown pluton and Cortlandt Complex were shown to postdate or be partly synchronous with faulting. Rb/Sr, K-Ar, and $^{40}Ar/^{39}Ar$ dating of the igneous rocks constrains this Taconic faulting to approximately 450-460 Ma (Ratcliffe, 1980; Ratcliffe, 1981; Ratcliffe et al., 1982). Acadian(?) reactivation is proposed based on K-Ar dates of approximately 379 Ma recorded in muscovite within these faults (Ratcliffe et al., 1982).

Mesozoic extensional reactivation of the Ramapo fault occurred along the previously developed mylonite zones. This deformation was brittle and resulted in the development of cataclasite and gouge (Ratcliffe,1980). Analysis of zeolite-chlorite slickensides and drag of cataclastic fabrics indicate Triassic right-lateral normal and Jurassic left-lateral strike-slip motion (Ratcliffe, 1980). Syntectonic folding within the Newark basin is directly related to this movement and the development of antithetic normal faults and near vertical east-northeast-striking extension fractures indicate a stress field in which extension was oriented north-northwest (Ratcliffe and Burton, 1985).

There is evidence for current seismicity along the Ramapo fault zone. Historical records and fault plane solutions for recent seismic activity indicate that the Ramapo fault zone is active along the previously established Mesozoic brittle zones (Page et al., 1968). This upper crustal seismicity is restricted to depths between 1 and 10 km (Aggarwal and Sykes, 1978).

Additional studies suggest that recent seismic activity in southeastern New York and northeastern New Jersey should be, to a large degree, attributed to activity along the Ramapo fault zone (Isacks and Oliver, 1964; Yang and Aggarwal, 1981). Kafka et al. (1985) found that about half of the microearthquakes within the greater New York area occurred within 10 km of the Ramapo fault.

Despite the comprehensive studies of the Ramapo fault zone in the past (Ratcliffe, 1971; 1980), except for limited exposure and several drill cores, most of the work along the Ramapo fault system (Ratcliffe, 1971; 1980) has been conducted in southeast New York State and extrapolated into New Jersey. However, important new exposures of the Ramapo fault have been exhumed as a result of construction of the final leg of I-287 in northern New Jersey. Many of the exposures were only available for short periods of time during the construction of drainage culverts that have since been completed and backfilled.

The orientation of extensive brittle fault plane and slickensides are analyzed by a tensor analysis (Reches; 1987) computer program developed by Hardcastle (1989). Single fault planes with two sets of overprinting slickenlines are used to assign relative ages to two different paleostress directions responsible for brittle reactivation along the Ramapo fault. Complex brittle fault geometries will be proposed for these two phases of fault reactivation.

A neotectonic investigation of the Ramapo fault was carried out in the field. Extensive exposures of stratified glacial drift along the Ramapo fault were examined for evidence of Recent tectonic deformation.

REGIONAL GEOLOGY

The northeast-trending Ramapo fault system (Fig. 1) in northern New Jersey and southeastern New York juxtaposes Proterozoic Y crystalline rocks of the Reading Prong with Triassic and Jurassic sedimentary and igneous rocks of the Newark Basin. In southeastern New York, north of the Newark Basin, the many splays of the Ramapo fault include the Thiells, Mott Farm Road, Timp Pass and Canopus faults, known collectively as the Canopus fault zone (Ratcliffe, 1980). The Canopus fault zone separates the rocks of the central portion of the Hudson Highlands from the eastern Hudson Highlands. To the south, Ratcliffe (1980) suggested that there is a probable connection of the Hopewell and Flemington-Furlong faults (Fig. 1) with the Ramapo fault. The Hopewell and Flemington-Furlong faults are moderately southeast-dipping intrabasinal normal faults developed late in the history of the Newark basin (Schlische and Olsen, 1988). The Chalfont fault is a north-dipping intrabasinal left-lateral transfer fault which is connected to the southwestern terminus of the Flemington-Furlong fault (Schlische, 1992).

The Proterozoic Y rocks of the New Jersey Highlands consist of predominantly light colored sodic-rich gneisses, granites, and lesser amphibolite (Drake, 1984). These rocks have been metamorphosed to upper amphibolite through hornblende granulite facies (Dallmeyer, 1974). The rocks are roughly grouped as the Losee Metamorphic Suite and the Byram Intrusive Suite (Drake, 1984). The Lossee gneiss consists of oligoclase-quartz gneiss, albite-oligoclase granite and albite pegmatite. The Byram Intrusive Suite, consists of microperthite- or microcline-bearing hornblende granite, alaskite, biotite granite, pegmatite and hornblende-quartz syenite and marble, pyroxene gneiss,
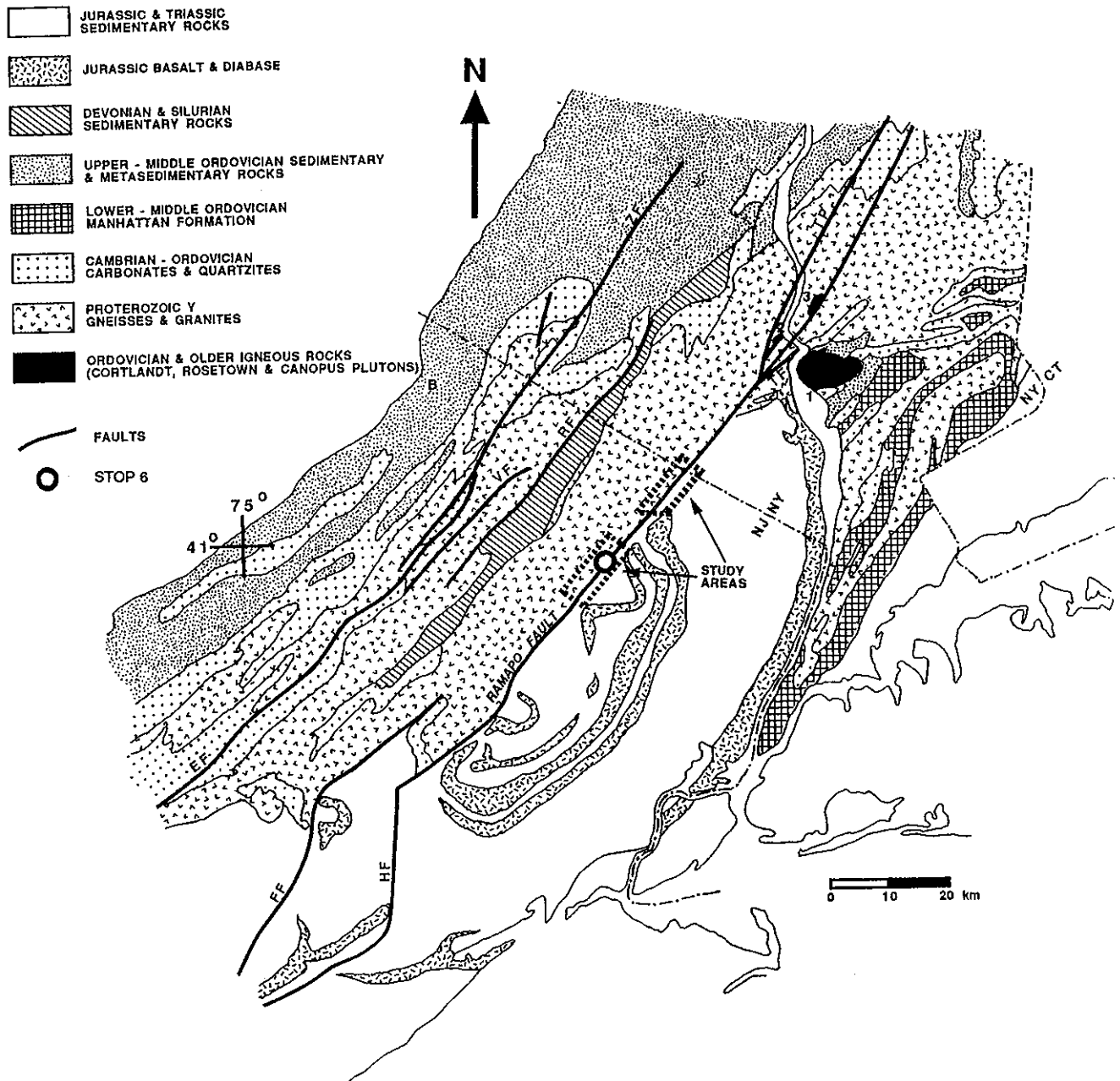
Figure 1: Regional geologic map of northern New Jersey and southeastern New York showing areas of study and location of field trip stop 6 at Riverdale, NJ. Thiells fault=TF; Flemington fault=FF; Hopewell fault=HF; Reservoir fault=RF; East fault=EF; Vernon fault=VF; Zero fault=ZF; Cortlandt Complex=1; Rosetown Pluton=2; Canopus Pluton=3; Beemerville, NJ=B.

epidote-scapolite-quartz gneiss, quartz-epidote gneiss, pyroxene and hornblende skarns, pyroxenite, biotite-quartz-feldspar gneiss and potassic feldspar gneiss.

A 60-km long belt of east-west- to northwest-striking alkalic dikes and lamprophyres extend southwest from the Cortlandt Complex into the Reading Prong at Beemerville, New Jersey. These dikes are considered to be equivalents of the Cortlandt Complex (Ratcliffe, 1981; Maxey, 1976). An earlier unrelated suite of northeast-southwest-trending mafic dikes intrude the Reading Prong and Hudson Highlands and may be related to Proterozoic Z rifting at approximately 650-600Ma (Puffer *et al.*, 1991; Ratcliffe, 1983; 1987).

The approximate 10,000 meter thick Triassic-Jurassic sedimentary and igneous rocks (Olsen, 1980) of the Newark basin (Fig. 1) rest unconformably on Paleozoic and Precambrian basement rocks and dip 5° - 25° northwest, into the Ramapo fault.

Faults

The Ramapo-Canpous fault zone has a long and complex history of multiple reactivation (Ratcliffe, 1971; 1980). This history began as ductile reverse faulting during the Grenville Orogeny (about 1.1-1.2 Ga) and included reactivation as a ductile reverse fault during the Taconic Orogeny (approximately 450 Ma). The zone was also reactivated as semi-brittle reverse and strike-slip faults during the Alleghanian Orogeny (approximately 300 Ma) and brittle normal fault during Mesozoic rifting (about 200 Ma).

Many other parallel-subparallel faults in the New Jersey and Hudson Highlands had similar histories of polyphase deformation. In the New Jersey Highlands, Hull, *et al.* (1986) recognized Grenville mylonites crosscut by Alleghanian chlorite-rich breccias and ultracataclasites and Mesozoic epidote-rich slickensides and narrow gouge zones. Stephens, *et al.* (1988) proposed middle to late Paleozoic dip-slip fault movements for the Zero fault (Fig. 1). Malizzi and Gates (1989) documented Alleghanian dextral strike-slip followed by Mesozoic sinistral stike-slip along the Reservoir fault (Fig. 1 and this trip, stop 5).

Within the Newark basin, Sanders (1962) presented evidence for dextral strike-slip displacement of Mesozoic rocks along the Hopewell and Flemington faults. Burton and Ratcliffe (1985, 1985a) recognized a polyphase movement history for the Flemington fault. Immediately adjacent to a Taconic mylonite of the Flemington fault they found brittle dextral and sinistral oblique normal faulting preserved in cataclastic fabrics and slickensides of Mesozoic rocks. In Pennsylvania, Lucas *et al.* (1988) indicated sinistral strike-slip reactivation along the Ramapo fault between 195 Ma and 165 Ma. This reactivation was due to northeast directed shortening. At the neck between the Newark and Gettysburg basins, they discovered the Jacksonwald syncline folds late Triassic and early Jurassic synrift sedimentary and igneous rocks.

Mafic Dikes

Several highly discordant retrograde basaltic dikes within the Ramapo fault system crosscut the foliation of the Losee and Byram gneisses at Riverdale and Mahwah, New Jersey, respectively (Costa, 1991). Because the dikes from Riverdale and Mahwah have similar igneous and shear textures, degree of retrograde metamorphism and weathering, orientations and chemistries they are thought to be equivalents (Costa, 1991).

Despite similatities to Jurassic Quarryville diabase (Smith et al., 1975) and Late Ordovician Cortlandt Complex (Bender et al., 1984) the chemistry of the dikes remains enigmatic (Costa, 1991). The degree, grade and directions of shearing and the orientations of the dikes suggest that they may be Late Ordovician Cortlandt-Beemerville equivalents.

The dikes in Riverdale, seen at stop 6A of this trip, strike between 110 and 140 and dip steeply (52° - 76°) to the southwest. The dikes are less than two meters in thickness. The dikes tend to thin near the surface and are not visibly traceable parallel to strike. The dikes show various amounts of brittle normal faulting (top to the north-northeast), reverse ductile shearing (top to the north-northeast)(Plate 1, Fig. 2), and late normal (top to the south-southwest) folding of the sheared fabric. Some of the dikes, or parts thereof, remain relatively unsheared, whereas others are intensely sheared and have well developed S-C fabric (Lister and Snoke, 1984).

FAULT DESCRIPTIONS

Mylonites

Along strike, the entire Ramapo fault system varies in thickness from approximately 5 km to 10 km (Ratcliffe, 1980). It consists of many parallel to subparallel zones of fine-grained well foliated and poorly to moderately lineated type II S-C mylonites (Lister and Snoke, 1984) and ultramylonites developed in the Precambrian gneisses. Moderate to steeply southeast-dipping retrograde shear zones, up to 25 m thick, developed in granitic and calc-silicate gneisses and exhibit a mesoscopic S-C fabric. Within the dominant foliation, C planes typically dip 40° - 50° towards the southeast. The average angle between S and C planes is 20°, but varies from 6° to 40°. C' planes, where present, are spaced from 1.0 mm to 1.0 cm and oriented approximately 20° - 30° shallower than the C plane (Costa, 1991). Kinematic indicators from the mylonites along the Ramapo fault system in northern New Jersey consistently indicate reverse top to the northwest shearing.

Both σ-type and δ-type quartz porphyroclasts (Passchier and Simpson, 1986) are present within the mylonites. Cores of the σ-type and δ-type quartz porphyroclasts define the southeast-dipping S plane and have tails of dynamically recrystallized quartz. Type B2a and type B2b quartz ribbons (Boullier and

Bouchez, 1978) and dynamically recrystallized tails on porphyroclasts (Passchier and Simpson, 1986) define the C plane. The C' plane, where present, is defined by assymetric boudinage quartz ribbons. Dynamically recrystallized quartz subgrains (0.01 mm to 0.1 mm) are present within the ribbons. Unrecrystallized larger quartz grains (1.0 mm to 3.0 mm) show undulose extinction and contain deformation bands.

Potassium feldspar and plagioclase also form σ-type and δ-type (Plate 1, Fig. 3) (Passchier and Simpson, 1986) porphyroclasts with tails of recrystallized feldspar, quartz, muscovite and chlorite. Cores of these porphyroclasts define the southeast-dipping S plane. The C plane is defined by the porphyroclast tails. Edges of feldspar porphyroclasts are commonly dynamically recrystallized. Plagioclase porphyroclasts have deformed twin lamellae. Feldspar porphyroclasts, less commonly, show pull-apart textures and are antithetically sheared (Stauffer, 1970).

Hornblende commonly underwent a brittle response. Pull-apart (Stauffer, 1970) hornblende porphyroclasts underwent reaction-enhanced ductility (White, *et al.*, 1980) in which crude σ-type porphyroclasts subsequently evolve from antithetically sheared fragments (Plate 1, Fig. 4). In these retrograded grains, metamorphic reactions generated chlorite, tremolite-actinolite, biotite and muscovite as fillings within conjugate shear planes and tails on porphyroclasts.

Chlorite and muscovite "fish" (Eisbacher, 1970; Lister and Snoke; 1984) and aligned muscovite, tremolite and biotite define the southeast-dipping S-C fabric. Biotite commonly undergoes reaction enhanced ductility (White, *et al.*, 1980). A C' plane commonly develops within the chlorite-rich zones.

The ductile behavior exhibited by the feldspar porphyroclasts (Plate 1, Fig. 3), indicates that temperatures of deformation of the Precambrian rocks were in excess of 450 $\pm$ 50° C (Sibson, 1977; Sibson, 1983; Tullis and Yund, 1977). This mineral response, similar to Simpson (1985), is indicative of deformation at mid- to upper greenschist metamorphic facies conditions.

The steeply south-dipping mafic dikes are severly retrograded to greenstone and sheared. Chlorite "fish" (Eisbacher, 1970) define the S and C planes which dip approximately 80° and 60° toward the south, respectively. The C' plane (Simpson, 1984) dips approximately 40° towards the south. Late calcite veins within these dikes are concordant to the C' and less commonly are discordant to the phyllonite foliation and dip approximately 60° toward the north-northeast. The foliation of these sheared dikes is consistently reverse, top to the north-northeast (Plate 1, Fig. 2). This foliation is subsequently overprinted by late folding with a normal sense of shear (Costa, 1991).

Brittle-Ductile Transition

Deformation at the brittle-ductile transition occurs in mylonites of the Proterozoic Y gneisses along the Ramapo fault system. The semi-ductile fabric overprints the previously developed ductile mylonites. Reactivation of the southeast-dipping mylonite zones indicates reverse faulting towards the northwest.

Moderate to steep southeast dipping type II S-C mylonites (Lister and Snoke, 1984) contain ductile quartz as sigmoidal type B2b ribbons (Boullier and Bouchez, 1978) and σ-type (average 0.2 mm) porhyroclasts (Passchier and Simpson, 1986). Characteristics of the core of the quartz porphyroclast include undulose extinction, deformation bands and dynamic recrystallization or plucked (Stauffer, 1970) grain boundaries. Quartz porphyroclast tails are composed of chlorite and dynamically recrystallized quartz. Brittle feldspars (0.1 mm to 5.0 mm) show slight to intense undulose extinction, fragmentation, plucked grain boundaries, kinked twinning and pull-apart textures including antithetic conjugate shears (Stauffer, 1970; Gates and Glover, 1989). Ductile behavior of smaller feldspar grains (<0.08 mm) results in σ-type porphyroclasts with tails of chlorite, muscovite and quartz. Plagioclase is commonly slightly sericitized and sausseritized and there is minor recrystallization to quartz and muscovite along antithetic shear planes. Brittle feldspars developed tails of chlorite, quartz, epidote and muscovite.

Fine grained chlorite, muscovite and biotite "fish" (Eisbacher, 1970; Lister and Snoke, 1984) are common and hornblende displays brittle antithetic pull-apart structures (Stauffer,1970). Magnetite (0.02 mm to 0.135 mm) porphyroclasts are brittle and have antithetic conjugate shears.

Hornblende is commonly brittle, with some reaction-enhanced ductility to chlorite, tremolite-actinolite and sericite. Biotite partly reacted to chlorite and muscovite. Brittle magnetite porphyroclasts are antithetically sheared. These brittle shear planes are commonly filled with chlorite and epidote. Epidote porphyroclasts are commonly antithetically sheared.

Quartz deformed in the ductile regime, whereas feldspars underwent brittle deformation. These mechanical responses indicate that temperatures of deformation for this phase of reactivation were between the ductile-brittle transitions for quartz (300 $\pm$ 50°C) and feldspar (450 $\pm$ 50°C) (Sibson, 1977; 1983; Tullis and Yund, 1977). Mineral response and metamorphic reactions are indicative of deformation at lower greenschist metamorphic facies conditions (Simpson, 1985).

Brittle Faults

Cataclastic textures (Sibson, 1977) that overprint the early ductile and brittle-ductile fabrics indicate brittle strike-slip (Plate 1, Fig. 5) and normal reactivation of the southeast-dipping faults. Cataclastic seams (0.5 mm to 1.5 cm

thick) offset grains and early fabrics and are themselves offset by later faults. Southeast-dipping foliated greenish-gray to black gouge zones approximately 4.0 cm to 5.0 cm thick are commonly enriched in calcite and sheared antithetically (Passchier and Simpson, 1986). In addition, there are two generations of type I (Beach, 1975) quartz, calcite and chlorite filled tension gashes (Costa, 1991) and two generations of primary and secondary (Harding, 1974) (Fig. 6) planar, curvi-planar and listric brittle fault arrays with slickenlines.

Slickenside coated fault surfaces are most commonly coated with fibrous or stepped slickenlines of fine grained chlorite, tremolite-actinolite, limonite and calcite with lesser amounts of quartz and epidote. Two generations are evident by overprinting relations on a single fault surface. Each generation of brittle faults includes four sets of moderate to steeply-dipping faults. The early generation of steeply-dipping brittle faults includes east-southeast- and west-northwest-dipping reverse faults, northeast- and southwest-dipping normal faults and a conjugate set of north-northwest- and south-southeast-dipping right-lateral strike-slip and east- and west-dipping left-lateral strike-slip faults (Fig. 7a-d). The later set of brittle faults includes south-southwest- and north-northwest-dipping reverse faults, southeast- and northwest-dipping normal faults and a conjugate pair of northeast- and southwest-dipping right-lateral strike-slip and southeast-dipping left-lateral strike-slip faults (Fig. 8a-d). An additional set of northwest- and southeast-dipping right-lateral strike-slip faults is present (Fig. 9a). Fault planes also developed chatter marks and tension gashes filled with random combinations of calcite, tremolite-actinolite, chlorite and quartz.

Mineral response of this group is exclusively brittle. Microscopic and mesoscopic cataclastic textures, gouge development, brittle conjugate shears and extension fractures overprint previously developed ductile and semi-ductile fabrics. Extension fractures and conjugate shears contain calcite, quartz, fluorite, pyrite and recrystallized chlorite. Quartz and feldspars are typically undulose, broken, crushed and have plucked grain boundaries. Hornblende, magnetite and secondary pyrite are brittle. Chlorite and hematite fill some of the shear fractures. Recrystallized sheared and unsheared veins of chlorite are present. Biotite is pulled apart with very minor reaction to chlorite.

TIMING FOR MOVEMENTS ALONG THE RAMAPO FAULT

In addition to its development as a Grenvillian reverse fault (Ratcliffe, 1980), the Ramapo fault system has a long and complex reactivation history which includes up to five periods of fault movement. These movements are summarized in Table 1.

The dominant reverse ductile deformation which resulted in the development of the southeast dipping type II S-C mylonite (Lister and Snoke, 1984) and ultramylonite zones is post-Grenvillian in age. The mineralogy and texture which are
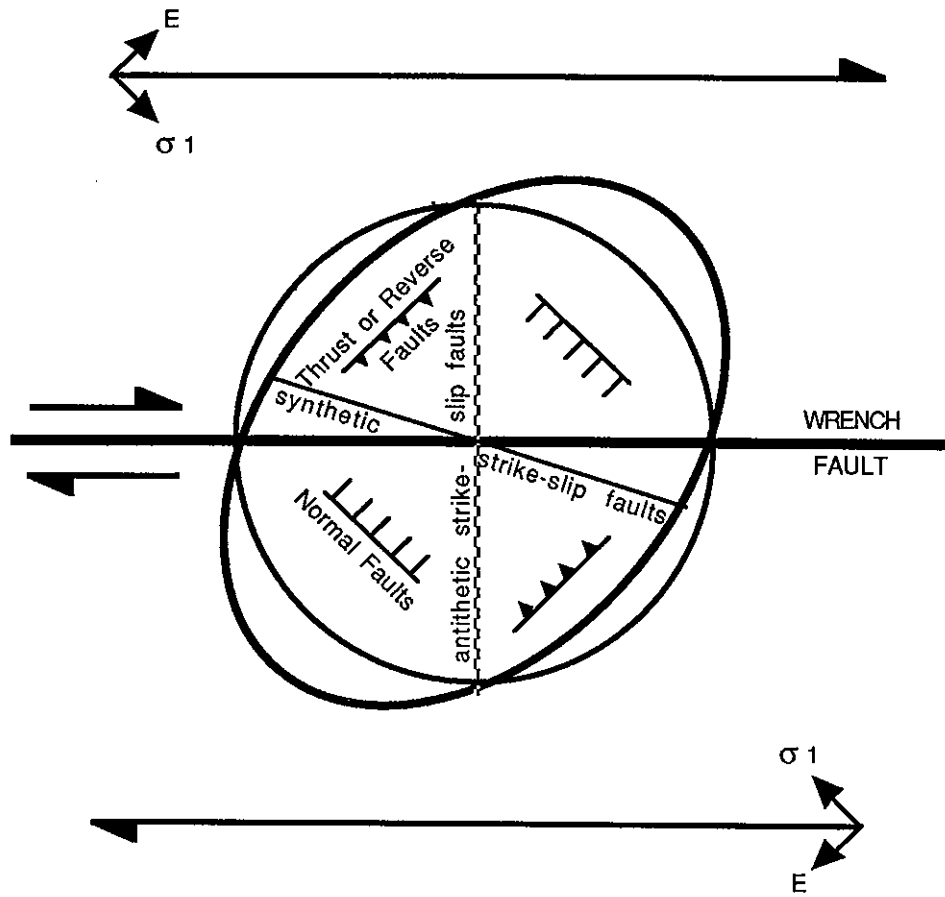
Figure 6: Strain ellipse and idealized fault geometry based
on a northwest-southeast-trending maximum
compression direction ($\sigma 1$). A complex set of
brittle faults develops which includes: northwest-
and southeast-dipping reverse or thrust faults,
northeast- and southwest-dipping normal faults,
and conjugate pairs of strike-slip faults. The
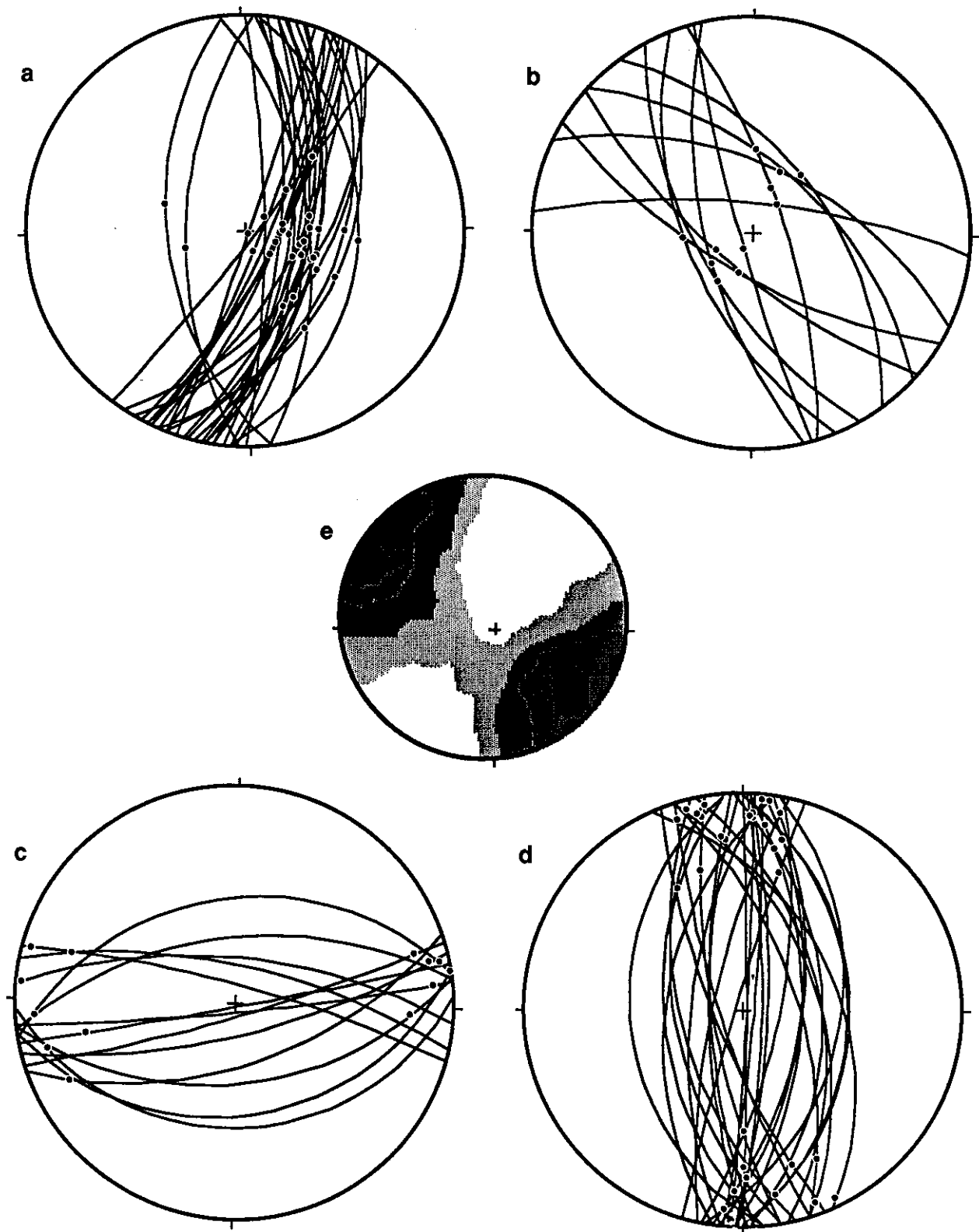left-lateral solution is the mirror image. (After
Harding, 1975).

Figure 7:   Equal angle plots (a-d) for early brittle faults
and slickenlines.   (a) Reverse faults, n=30; (b)
Normal faults, n=11; (c) Right-lateral strike-slip
faults, n=13; (d) Left-lateral strike-slip faults,
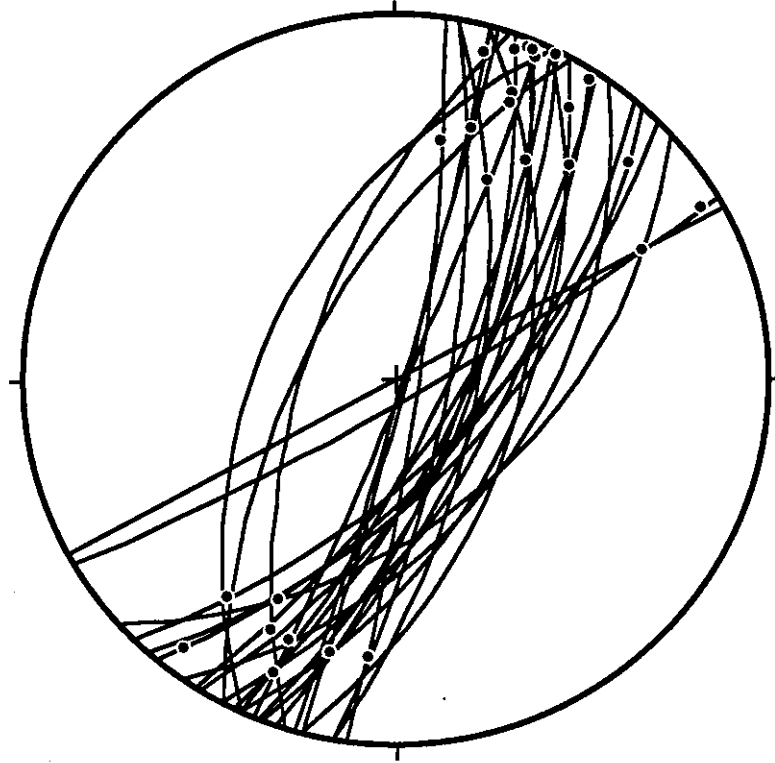n=30.   (e) Kamb contour of early compressional P-
axis, n=27. CI=2.0 sigma.
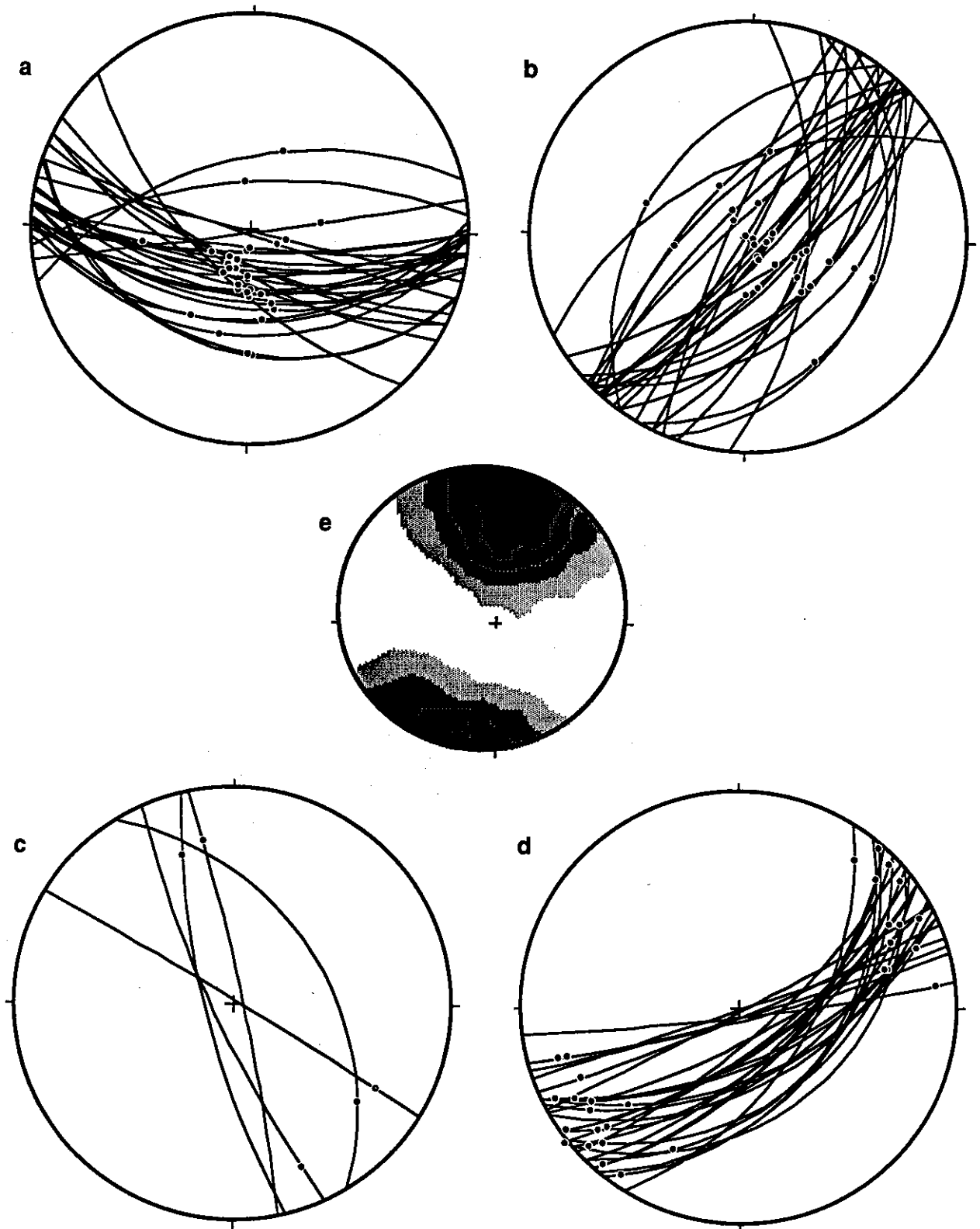
Figure 8: Equal angle plots (a-d) for late brittle faults and slickenlines. (a) Reverse faults, n=30; (b) Normal faults, n=27; (c) Right-lateral strike-slip faults, n=5; (d) Left-lateral strike-slip faults, n=30. (e) Kamb contour of late compressional P-axis, n=27. CI=2.0 sigma.
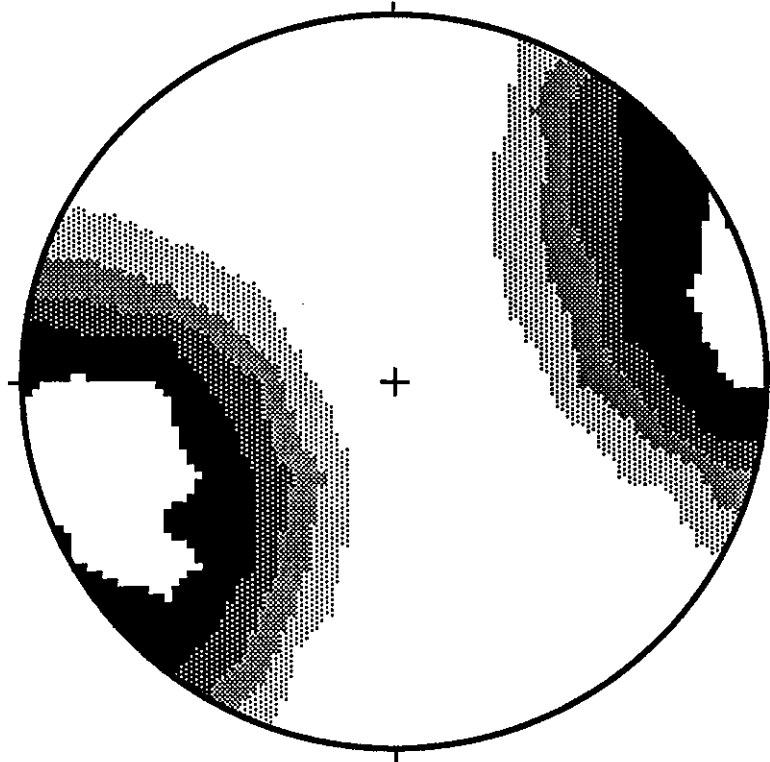
Figure 9: Equal angle plot (a) and corresponding Kamb
contour (b) for additional right-lateral faults,
n=26.   CI=2.0 sigma.

Table 1: Summary Table of Deformation within Highland Rocks of the Ramapo Fault Zone, Northern New Jersey

Approximate Time (BP)	Fault Episode for RFZ	Features and Textures Developed Within Highland Rocks	Approximate Temperature (C) and Facies	Description of Brittle Faults Developed Within Highland Rocks	Description of Mafic Dikes Within Highland Rocks	Approximate Trend of Inferred Maximum Paleostress
<18.5 Ka	Neotectonic	None	None	None	None	ENE-WSW (Zoback et al., 1985)
150 Ma	Jurassic	Brittle strike-slip reactivation: Overprinted and crosscut by gouge, cataclasite and brittle faults	<300 Chlorite-Zeolite facies	None	None	ENE-WSW
200 Ma	Triassic Crustal extension associated with opening of the Atlantic Ocean	Complex brittle reactivation: Overprinted and crosscut by gouge, cataclasite and brittle faults, development of extension fractures, development of type I tension gashes	<300 Chlorite-Zeolite facies	Complex system includes: SSE- and NNW-dipping reverse faults, SE- and NW-dipping normal faults, NE- and SW-dipping right-lateral strike-slip faults, SE-dipping left-lateral strike-slip faults.	Sheared by E-W-striking ductile reverse faults	NNE-SSW
300 Ma	Alleghanian North America/Africa continent-continent collision	Complex semi-brittle reactivation: Crosscut by cataclasite, Semi-brittle feldspars, development of type I tension gashes	350 - 400 Lower greenschist facies	Complex system includes: ESE- and WNW-dipping reverse faults, NE- and SW-dipping normal faults, NNW- and SSE-dipping right-lateral strike-slip faults, E- and W-dipping left-lateral strike-slip faults.	Offset by E-W-striking brittle normal faults	NW-SE
450-460 Ma	Taconic Continent/Island arc collision	SW-dipping semi-brittle reverse reactivation: pervasive S-C fabric, recrystallized quartz ribbons, porphyroclasts of quartz and feldspar, brittle hornblende	400 - 500 Mid to Upper greenschist facies	None	Intruded Highland rocks	NW-SE
800-900 Ma	Proterozoic Z Crustal extension associated with opening of the Iapetus Ocean	SW-dipping semi-brittle normal reactivation: pervasive S-C fabric, recrystallized quartz ribbons, porphyroclasts of quartz and feldspar, brittle hornblende	350 - 400 Lower greenschist facies	None	None	NE-SW
1.1-1.2 Ga	Proterozoic Y Grenvillian Continent/Continent collision	Development of RFZ as SW-dipping semi-ductile right-lateral strike-slip fault: Regional greenschist facies, intrusion of syntectonic granites (Ratcliffe, 1980)	400 - 500 Mid to Upper greenschist facies	None	None	NW-SE

present are indicative of a lower grade deformation than those reached during the Grenville orogeny. In New Jersey, the Grenville orogeny reached hornblende granulite (Drake, 1969) to granulite (Smith, 1969) facies. Granulite facies is indicative of temperatures between 700°C and 800°C (Turner and Verhoogen, 1960). Based on the deformation features and metamorphic grade of deformation (Simpson, 1985), the reverse mylonites and ultramylonites within the study area formed at mid- to upper greenschist metamorphic facies. In addition, the fine grained nature of the mylonites along the Ramapo fault are indicative of mylonites which formed at lower temperatures (White *et al.*, 1980). Because the feldspar is ductile, the temperature of deformation must be in excess of 450 $\pm$ 50°C (Sibson, 1977; 1983; Tullis and Yund, 1977). Assuming an average geothermal gradient of 20° - 30°C (Sibson, 1977) mylonite development occurred at depths between 15 km and 22 km.

Ratcliffe (1980; 1981) and Ratcliffe *et al.* (1982) assigned a late Taconic age reverse ductile movement to the Ramapo fault zone of southeastern New York based on radiometric dates of plutonic and dike rocks of the Rosetown pluton and Cortlandt Complex which are shown to postdate or be partly synchronous with faulting. The late Taconic event occurred approximately 450 - 460 Ma based on Rb/Sr analysis of biotite and whole rock samples, K-Ar analysis of biotite, hornblende and whole rock samples and $^{40}Ar/^{39}Ar$ analysis of hornblende and biotite.

Along the Ramapo fault in New Jersey, the mafic dikes can be used to constrain Taconic fault movement. Although the dikes have not been radiometrically dated they are most likely Late Ordovician in age. The chemistry of the highly altered basaltic dikes (Costa, 1991) does not match the chemistry of Proterozoic Z metabasalts (Ratcliffe,1983; 1987; Puffer *et al.*, 1991), however it may be an addition to the already highly diverse chemistry of the Cortlandt-Beemerville dike swarms (Bender *et al.*, 1984; Ratcliffe, 1981). The orientation of the basaltic dikes is consistent with the approximate east-west trend of Cortlandt-Beemerville dikes. This orientation requires an approximate north-south extension which can be explained by a Taconic or Alleghanian paleostress rather than a Proterozoic Z or Mesozoic paleostress. The dikes do not record any Taconic reverse shearing, however, they were subjected to Alleghanian brittle normal offset. They were apparently emplaced during the Late Ordovician, and subsequently retrograded and offset during the Alleghanian orogeny. During the approximate north-south-trending maximum compression of the Triassic, ductile reverse shearing was recorded in the severely retrograded basaltic dikes (Plate 1, Fig. 2).

The dominant Taconic ductile reverse mylonite fabric overprints a previously developed normal mylonite fabric. Microstructural evidence of shearing that predates the Taconic reverse shearing includes folded mylonites. The vergence of these folds indicates reverse reactivation during the Taconic

182

orogeny. Porphyroclasts of hornblende (Plate 1, Fig. 4),
magnetite and feldspars indicate two clearly opposite phases of
movement. During the early phase of normal movement, the
porphyroclasts developed thin planar antithetic shears
(Passchier and Simpson, 1986; Stauffer, 1970). Hornblende and
feldspar porphyroclasts develop tails by reaction to chlorite
and quartz, respectively (Dixon and Williams, 1983; White, et
al., 1980; White and Knipe, 1978). Reverse reactivation
developed a younger set of antithetic shears, in both hornblende
and magnetite which are opposite to, crosscut and displaced the
earlier set. The early set of antithetic shears are opened on
one side to form a "V" as the porphyroclasts are rotated in the
opposite sense during the later movement (Plate 1, Fig. 4).

The early set of antithetic shears can be devoid of mineral
filling or contain one or two generations of reaction softened
chlorite or recrystallized quartz as filling. The second
generation of antithetic shears which crosscuts the early
generation are typically not as opened and rotated and are
devoid or contain one generation of mineral filling.
Porphyroclast tails which developed during the early phase of
shearing were folded and pulled back underneath the
porphyroclast core as it rotated in the opposite sense during
the second phase of movement. Alternately, porphyroclast cores
developed during the early phase may be subsequently rotated
into a position which is at an inconsistent and peculiarly high
angle to the dominant pervasive fabric of the oppositely
directed second movement. Mineral responses which include
ductile quartz and brittle feldspars, hornblende and magnetite
indicate the pre-reverse mylonitization occurred at lower
greenschist metamorphic facies (Simpson, 1985). The lower
greenschist facies normal faulting is older than the Taconic
ductile reverse by virtue of overprinting relationships.

Subsequent to Taconic reverse faulting , steeply
southeast-dipping Late Ordovician basaltic dikes intruded the
Ramapo fault system. These dikes are offset by Alleghanian
brittle faults which overprint Taconic ductile reverse faults.
Alleghanian deformation within the Proterozoic rocks is
characterized by quartz, the smallest feldspars, muscovite and
biotite which exhibit plastic deformation, whereas larger
feldspars and other minerals exhibit brittle deformation.

Deformation is therefore constrained between 300 $\pm$ 50°C, the
brittle-ductile temperature of transition for quartz, and 450 $\pm$
50°C, the brittle-ductile temperature of transition of feldspar
(Sibson, 1977; 1983; Tullis and Yund, 1977). Therefore the
depth of deformation is estimated at approximately 10 km
(Sibson, 1977).

During the Alleghanian orogeny mesoscopic synchronous
primary and secondary brittle faults (Harding, 1974) and
associated tension gashes (Costa, 1991) developed within the
Ramapo fault system (Fig. 7).

Overprinting slickenlines on a single fault plane allow the
determination of a younger generation of brittle faults

superimposed over the earlier Alleghanian generation. This brittle phase of deformation is responsible for the southeast dipping normal faults which created the Newark basin. The Triassic sediments (Olsen, 1980) within the basin constrain the time of faulting. During Triassic rifting primary and secondary brittle faults (Harding, 1974) and associated tension gashes (Costa, 1991) also develop Fig. 8). The generation of overprinting cataclasitic textures and fault gouge (Sibson, 1977) indicate faulting was under low temperature (i.e. < 250°C) and shallow conditions (i.e. < 10 km). Severly retrograded south-southeast-dipping Late Ordovician basaltic dikes are sheared in the ductile regime and developed S-C fabric. The fabric is folded with a normal vergence which may be due to post-Triassic relaxation. An approximate north-northeast- and south-southwest-trending maximum compression direction (Fig. 8e) is indicated by the complex fault array and tension gashes.

An additional east-northeast- and west-southwest-trending maximum compression direction is indicated by a population of northwest- and southeast-dipping right-lateral strike-slip faults (Fig. 9). The normal folding of the fabric of the sheared Late Ordovician basaltic dikes and this right-lateral strike-slip faulting may both be Jurassic in age.

POST-MESOZOIC AND NEOTECTONICS

Previous Studies of Neotectonism

Although the eastern United States is generally perceived as being a low seismic risk area, there is evidence for neotectonism (Tillman, 1982; Behrendt et al.,1981; Bramlet et al., 1982; Jacobeen,1974; Hutchinson and Grow; 1985). In northern New Jersey and southeastern New York recent seismic activity is concentrated on older faults which have been reactivated (Aggarwal and Sykes, 1978; Ratcliffe, 1971; Sbar and Sykes, 1977; Thompson, 1981). Depths of reactivation are restricted to the upper and middle crust and concentrated at depths less than 15 km (Aggarwal and Yang, 1978; Mitronovas, 1982; Pomeroy et al., 1976; Sbar et al., 1970).

Despite the long history of reactivation of the Ramapo fault system (Ratcliffe, 1980) there is no strong evidence of post-Mesozoic or neotectonic movement within the zone. Previous studies have suggested a possible correlation between historic seismicity and slip on the Ramapo fault at depths extending to approximately 10 km (Isacks and Oliver, 1964; Page et al. , 1968). Although it is proposed that a narrow zone 15-20 km wide parallel to and including the Ramapo fault is the most seismically active area in northern New Jersey and southeastern New York and considered responsible for historic and recent seismicity, the Ramapo fault system is not the only active fault zone in the vicinity of New York City (Aggarwal and Sykes, 1978; Yang and Aggarwal, 1981). Of 61 seismic events in southeastern New York and northern New Jersey, 48% -53% were located within 10 km of the Ramapo fault (Kafka et al., 1985).

Previous Evidence For Tectonics In Quaternary Deposits

The portion of southeastern New York and northern New Jersey that includes the study area was subjected to Wisconsinan glaciation. Deglaciation of the area lasted until approximately 18.5 Ka (Cotter *et al.*, 1986). During this time, extensive amounts of drift, till and glaciofluvial sediments were deposited. Microfaults, cataclastic brecciation and soft sediment slump folding in varved clays (Forsythe and Chisolm, 1989), apparent dextral shear of southeast-flowing tributaries of the Ramapo River (Kafka, *et al.*, 1989) and sag pond development in the Ramapo River valley (Nelson, 1980) may have been initiated by seismic events associated with the Ramapo fault.

Examination Of Quaternary Deposits

Large glacial deposits, exposed within the study areas (Fig. 1), were examined. These stratified exposures were up to 15 m high and 0.5 km in length and contained clasts of Proterozoic gneisses and Paleozoic sedimentary rocks. In addition, they contained phyllonite and mylonite clasts possibly derived from the Ramapo fault.

These unconsolidated deposits were studied for evidence of neotectonics within the Ramapo fault zone since approximately 18.5 Ka. The stratified unconsolidated material was examined for deformation by folding or faulting which might be indicative of recent movement of the Ramapo fault. This study revealed no evidence of offset glacial strata by fault movement. In many places deformed glacial deposits were located, however, they are more suitably explained by glacial processes or gravitational slumping (Costa, 1991).

DISCUSSION

Ratcliffe (1971; 1980) proposed the development of the Ramapo fault system during high grade metamorphic conditions and compressional tectonics of the Grenville Orogeny. In this study, the earliest period of movement along the New Jersey portion of the Ramapo fault represents continental crustal extension at lower metamorphic conditions. Although this period of activity has not previously been documented, there is strong supportive microstructural evidence. In the past, microtextures related to reactivation of mylonites have not been considered for this fault.

Allison and La Tour (1977) described hornblende porphyroclasts within a mylonite which were sheared during one period of activation (Fig. 10). Their model explained the opening of early antithetic and later sympathetic shears. Both sets of shears exploit mineral cleavage directions. However, the microstructural textures of this study cannot be explained according to the Allison and La Tour (1977) model. It is proposed that the textures found in the mylonite zones along the Ramapo fault are the result of two distinct periods of oppositely directed shearing . Each period is responsible for the opening of its own set of antithetic shears. Late shears crosscut early shears as mineral grains were fragmented,

ONE PHASE OF PROGRESSIVE SHEARING
(ALLISON AND LaTOUR, 1977)

TWO PHASES OF PARALLEL AND
OPPOSITELY DIRECTED SHEARING
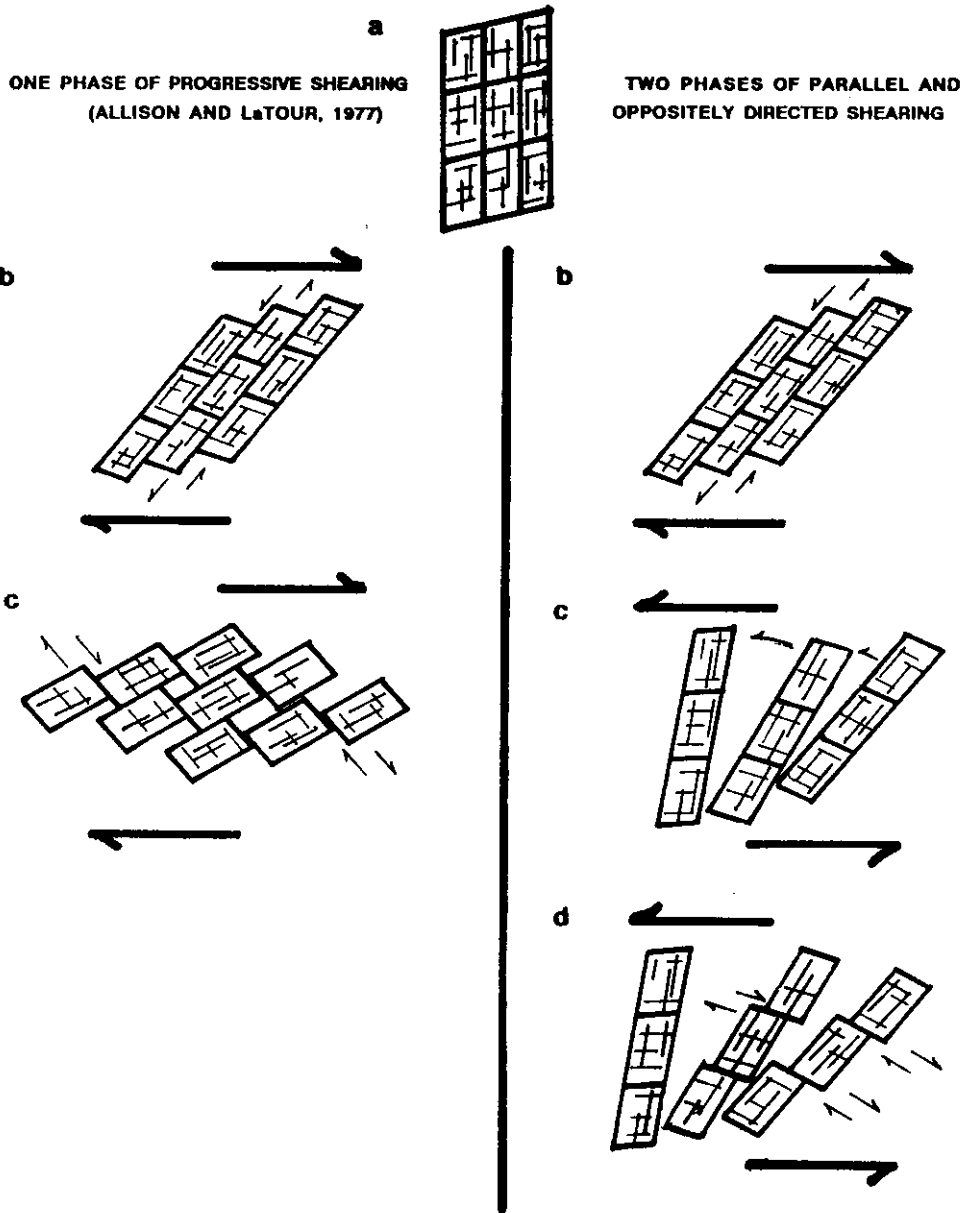
b

b

c

c

d

Figure 10:   On left, idealized hornblende porphyroclast (a) is sheared
          by one phase of right-lateral progressive shear according to
          Allison and LaTour (1977) model.   (b) Porphyroclast rotates
          clockwise and develops antithetic shear planes (indicated by
          small arrows).   (c) Continued right-lateral shear opens
          sympathetic shear planes (indicated by small arrows) and
          extends previously developed antithetic shear planes.
             On right, idealized hornblende porphyroclast (a) is sheared
          by two phases of parallel and oppositely directed shearing.
          (b) Phase I: Right-lateral shear rotates porphyroclast
          clockwise.   Porphyroclast develops antithetic shear planes
          (indicated by small arrows).   (c) Phase II: Left-lateral
          shear rotates porphyroclast counterclockwise (indicated by
          small arrows).   Antithetic shear planes, developed during
          Phase I, are opened on one side to form a "V" shape.   (d)
          Continued left-lateral shear opens a Phase II generation of
          antithetic shear planes (indicated by small arrows) which
          crosscut the Phase I antithetic shear planes.

186

extended and rotated and resulted in "V" shaped early shears (Figs. 4 and 10). The first set of antithetic shears developed during Proterozoic Z extension. During Taconic reverse shearing the second set of antithetic shears formed (Costa, 1991; Costa and Gates, 1992).

The Iapetus Ocean was the result of lateral extension normal to the Appalachians beginnig in the late Proterozoic and lasting until approximately 570 Ma (Rankin, 1975; Wehr and Glover, 1985). This extension was accompanied by hydration of basement rocks and intrusion of Late Precambrian plutons (Evans, 1991). Southeast-dipping mylonites and cataclasites developed between greenschist and amphibolite facies deformation conditions during Late Proterozoic continental crustal extension (Bailey and Simpson, 1993; Simpson and Kalaghan,1989). Brock (1989) correlated late Precambrian to early Cambrian rift-to-drift metasedimentary and metavolcanic rocks of southeast New York and eastern Connecticut to the break-up of the Proterozoic supercontinent. Evidence of Proterozoic Z rifting along the Ramapo fault system, although not previously suggested, is consistant with reports of continental extension elsewhere along the east coast of North America. As the origin of the Ramapo fault zone is proposed as a southeast-dipping Grenville reverse fault (Ratcliffe, 1971; 1980), it is not consistent that a major zone of weakness which has had such a long history of reactivation could have escaped displacement during a major continental rifting episode responsible for the opening of the Iapetus Ocean.

Proterozoic Z rifting in the vicinity of the Ramapo fault is supported by the presence of northeast-striking mafic alkalic dikes in the New Jersey Highlands (Puffer et al. , 1991) and probable rift generated Proterozoic Z northeast-striking metadiabase dikes in the New York and New Jersey Highlands (Ratcliffe, 1987) which intrude Proterozoic Y rocks.

Reactivation of the Ramapo fault during the Taconic orogeny resulted in the development of southeast dipping mylonites with a reverse sense of shear (Ratcliffe, 1971; Ratcliffe, 1980). The Taconic mylonite fabric is the dominant southeast-dipping ductile foliation found within the Ramapo fault system of northern New Jersey. It has obliterated most of the previous kinematic history. Basaltic dikes of Ordovician age constrain the Taconic shearing.

Two distinct complex systems of semi-ductile to brittle faults overprint the Taconic ductile deformation. Relative dating of the two different ages is demonstrated by overprinting relations. The earlier of the two episodes is the result of an east-southeast- and west-northwest-trending maximum compression direction (Fig. 7e). This deformation at the brittle-ductile transition is assigned an Alleghanian age because it overprinted Taconic faults and offset Ordovician basaltic dikes. Mineral response within the mylonites and the proposed maximum compression direction for this episode are similar as those proposed for Alleghanian deformation along the nearby Reservoir fault (Malizzi and Gates, 1989). The maximum compression direction proposed in this study is also in agreement with those

proposed for the early phase of a non-coaxial Alleghanian deformation (Geiser and Engelder, 1983; Mitchell and Forsythe, 1988).

The second episode of brittle faulting is the result of a maximum compression direction which trends approximately north-south (Fig. 8e). Malizzi and Gates (1989) attributed a late brittle overprint on the Reservoir fault to a Triassic maximum compression based on correlation with structures in the Newark basin which indicate a maximum compression direction trending between 020 and 035 (Lucas *et al.*, 1989). Geiser and Engelder (1983) reported a similar trend for maximum compression which deformed middle Carboniferous strata in the Appalachian Plateau of eastern Pennsylvania. Mitchell and Forsythe (1988) analyzed structures which developed in Silurian and Devonian rocks of the Green Pond outlier of New Jersey and attributed them to an approximate north-south trending maximum compression direction. Geiser and Engelder (1983) and Mitchell and Forsythe (1988) both consider the late phase brittle deformation to be the second phase of a non-coaxial Alleghanian deformation. None of the studies, including this one, contain direct evidence which demonstrates this late stage brittle deformation to be Alleghanian or Triassic in age. The brittle mineral responses of the latest movement are consistent with those proposed by Ratcliffe (1980) for Triassic reactivation of the Ramapo fault. In addition, this study provides evidence for Triassic ductile reverse shearing of retrograded east-west-trending Ordovician basaltic dikes.

The presence of two distinct populations of compressional axes indicates the zone did have two phases of brittle activity. The relative timing was extrapolated by examining fault planes with more than one set of slickenlines. The trends of the compression axis for the earlier set of faults do indicate more scatter. The scatter is probably due to rigid body rotation during reactivation which generated the younger population of faults. Inhomogenous strain due to rock compositional anisotropies and the presence of predeveloped fabrics also effects the calculation of the trends of the compression axis. The maximum compression direction for this late stage brittle episode explains a consistent complex brittle fault geometry (Harding, 1975; Bruhn and Pavlis, 1981) (Fig. 6) which includes southeast-dipping normal faults, required for the development of the Newark basin. These southeast-dipping faults were developed by inhomogenous strain due to predeveloped fabric.

A population of southeast- and northwest-dipping right-lateral strike-slip faults have corresponding maximum compression directions uncommon to Alleghanian and Triassic deformation (Fig. 9). These brittle faults are difficult to constrain. The east-north-east- and west-south-west-trending maximum compression directions may represent continued post-Triassic clockwise rotation of compression. This third maximum

compression trend is similar to proposed Jurassic maximum compression (Ratcliffe and Burton, 1985). The normal reactivation of Ordovician basaltic dikes (stop 6B) and the northeast trend of Jurassic Watchung basalt flows are also explained by this Jurassic paleostress.

ACKNOWLEDGEMENTS

REFERENCES

Aggarwal, Y. P. and Sykes, L. R., 1978, Earthquakes, faults, and nuclear power plants in southern New York and northern New Jersey: Science: v. 200, 425-429.

Aggarwal, Y. P. and Yang, J., 1978, Seismic activity and lithospheric stresses in northeastern North America: Geol. Soc. Amer. Abst. Prog.: v. 10, p. 29.

Allison, I. and La Tour, T. E., 1977, Brittle deformation of hornblende in a mylonite: A direct geometrical analogue of ductile deformation by translation gliding: Can. Jour. Earth Sci.: v.14, p. 1953-1958.

Bailey, C.M. and Simpson, C., 1993, Extensional and contractional deformation in the Blue Ridge Province, Virginia: Geol. Soc. Amer. Bull.: v. 105, p. 411-422.

Beach, A., 1975, The geometry of en-echelon vein arrays: Tectonophysics: v. 28, p. 245-263.

Behrendt, J. C., Hamilton, R. M., Ackermann, H. D. and Henry, V. J., 1981, Cenozoic faulting in the vicinity of the Charleston, South Carolina, 1886 earthquake: Geology: v. 9, p. 117-122.

Bender, J. F., Hanson, G. N. and Bence, A. E., 1984, Cortlandt complex: differentiation and contamination in plutons of alkali basalt affinity: Amer. Jour. Science: v. 284, p. 1-57.

Bobyarchick, A. R. and Glover, L., III, 1979, Deformation and metamorphism in the Hylas zone and adjacent parts of the eastern Piedmont in Virginia: Geol. Soc. Amer. Bull.: v. 90, p. 739-752.

Boullier, A. M. and Bouchez, J. -L., 1978, Le quartz en rubans dans les mylonites: Bull. Soc. Geol. Fr.: v. 20, p. 253-262.

Bramlet, K. W., Secor, D. T. and Prowell, D. C., 1982, The Belair fault: A Cenozoic reactivation structure in the eastern Piedmont: Geol. Soc. Amer. Bull.: v. 93, p. 1109-1117.

Brock, P. C., 1989, Stratigraphy of the northeastern Manhattan Prong, Peach Lake quadrangle, New York-Connecticut: in Field Trip Guidebook, Middletown, New York, Dennis Weiss ed., 61st annual meeting of the NYSGA, p. 1-28.

Bruhn, R. L. and Pavlis, T. L., 1981, Late Cenozoic deformation in the Matanuska Valley, Alaska: Three-dimensional strain in a forearc region: Geol. Soc. Amer. Bull.: v. 92, p. 282-293.

Burton, W. C. and Ratcliffe, N. M., 1985, Compressional structures associated with right-oblique normal faulting of Triassic-Jurassic strata of the Newark Basin near Flemington, New Jersey: Geol. Soc. Amer. Abst. Prog.: v. 17, p. 9.

Burton, W. C. and Ratcliffe, N. M., 1985a, Attitude, movement history and structure of cataclastic rocks of the Flemington fault - Results of core drilling near Oldwick, New Jersey. United States Geological Survey Miscellaneous Field Studies Map: MF-1781.

Costa, R.E., 1991, Structural Evolution and neotectonics of the Ramapo fault system, northern New Jersey: Department of Geological Sciences, Rutgers University, Newark, unpublished Master's thesis, 83 p.

Costa, R.E. and Gates, A.E., 1992, Mylonitization of mylonites: Evidence for the opening and closing of the Iapetus ocean from the Ramapo fault zone: Geol. Soc. Amer. Abst. Prog.: v. 24, no. 3, p. 14.

Cotter, J. F. P., Ridge, J. C., Evenson, E. B., Sevon, W. D., Sirkin, L. and Stuckenrath, R., 1986, The Wisconsinan history of the Great Valley, Pennsylvania and New Jersey, and the age of the terminal moraine: in Donald H. Cadwell, ed., Wisconsin Stage of the First Geologic District, Eastern New York, New York State Museum Bulletin No. 455, p. 22-49.

Dallmeyer, R. D., 1974, Metamorphic history of the northeastern Reading Prong, New York and Northern New Jersey: Jour. of Petrology: v. 15, p. 325-359.

Dixon, J. and Williams, G., 1983, Reaction softening in mylonites from the Arnaboll thrust, Sutherland: Scott. Jour. Geol.: 19, p. 157-168.

Drake, A. A., 1984, The Reading Prong of New Jersey and eastern Pennsylvania: an appraisal of rock relations and chemistry of a major Proterozoic terrane in the Appalachians: Geol. Soc. Amer. Spec. Paper no. 194: p. 75-109.

Drake, A. A., 1969, Precambrian and lower Paleozoic geology of the Delaware valley, New Jersey-Pennsylvania: in Seymour Subitsky ed., Geology of selected areas in New Jersey and eastern Pennsylvania and guidebook of excursions: New Brunswick, New Jersey, Rutgers University Press, p. 51-131.

Eisbacher, G. H., 1970, Deformation mechanisms of mylonite rocks and fractured granulites in Cobequid Mountains, Nova Scotia, Canada: Geol. Soc. Amer. Bull.: 81, p. 2009-2020.

Evans, N. H., 1991, Latest Precambrian to Ordovician
    metamorphism in the Virginia Blue Ridge: Origin of the
    contrasting Lovingston and Pedlar basement terranes: Amer.
    Jour. Sci.: v. 291, p. 425-452.
Fisher, D. W., Isachsen, Y. W. and Rickard, L. V., 1970,
    Geologic Map of New York; Lower Hudson sheet, New York
    State Museum and Science Service, Map and Chart series,
    no. 15.
Forsythe, R. D. and Chisholm, L., 1989, Are there earthquake-
    induced deformation structures in the Highlands/Lowlands
    border region of New Jersey?: Geol. Soc. Amer. Abst.
    Prog.: v. 21, p. 15.
Gates, A. E., 1991, The Carolina terrane boundary at Brookneal
    Virginia: A fundamental zone of crustal weakness: Geol.
    Soc. Amer. Abst.: v. 23, p. 33.
Gates, A. E. and Glover, L. III, 1989, Alleghanian tectono-
    thermal evolution of the dextral transcurrent Hylas zone,
    VA piedmont, U.S.A.: Jour. Struct. Geol.: v. 11, p. 407-
    419.
Geiser, P. and Engelder, T., 1983, The distribution of layer
    parallel shortening fabrics in the Appalachian foreland of
    New York and Pennsylvania: Evidence for two non-coaxial
    phases og the Alleghanian orogeny, in Robert Hatcher, H.
    Williams and I. Zietz, eds., Geological Society of America
    Memoir 158, p. 161-176.
Hall, L. M., Helenek, H. C., Jackson, R. A., Caldwell, K. G.,
    Mose, D., and Murry, D. P., 1975, Some basement rocks from
    Bear Mountain to the Housatonic Highlands, in NEIGC 67th
    Annual Meeting, p. 1-29
Hardcastle, K. C., 1989, Possible paleostress tensor
    configurations derived from fault-slip data in eastern
    Vermont and western New Hampshire: Tectonics: v. 8, p.
    265-284.
Harding, T. P., 1974, Petroleum traps associated with wrench
    faults: Amer. Assoc. Petrol. Geol. Bull.: v. 58, p. 1290-
    1304.
Hatcher, R. D., 1972, Developmental model for the southern
    Appalahians: Geol. Soc. Amer. Bull.: v. 83, p. 2735-2760.
Hull, J., Koto, R. and Bizub, R., 1986, Deformation zones in the
    Highlands of New Jersey: in Geological Association of New
    Jersey Guidebook, J.M. Husch and F.R. Goldstein, eds., p.
    19-66.
Huchinson, D. R. and Grow, J. A., 1985, New York Bight Fault:
    Geol. Soc. Amer. Bull.: v. 96, p. 975-989.
Isacks, B. and Oliver, J., 1964, Seismic waves with frequencies
    from 1 to 100 cycles per second recorded in a deep mine in
    northern New Jersey: Bull. Seism. Soc. Am.: v. 54, p.
    1941-1979.
Jacobeen, F. H. Jr., 1974, High angle reverse faulting in the
    Coastal Plain of Prince Georges Count, Maryland: Geol.
    Soc. Amer. Abst. Prog.: v. 5, p. 40.

Kafka, A. L., Schlesinger-Miller, E. A., and Barstow, N. L., 1985, Earthquake activity in the greater New York City area: magnitudes, seismicity, and geologic structures: Bull. Seism. Soc. Am.: v. 75, p. 1285-1300.

Kafka, A. L., Winslow, M. A. and Barstow, N. L., 1989, Earthquake activity in the greater New York area: A fault finder's guide: in Field Trip Guidebook, Middletown, New York, Dennis Weiss ed., 61st annual meeting of the NYSGA, p. 177-204.

Lister, G. S. and Snoke, A. W., 1984, S-C mylonites: Jour. Struct. Geol.: v. 6, p. 617-638.

Lucas, M., Hull, J. and Manspeizer, W., 1988, A foreland-type fold and related structures in the Newark rift basin, in Triassic-Jurassic rifting: Continental breakup and the origin of the Atlantic ocean and passive margins, Warren Manspeizer, ed., Elsevier, N.Y., p. 307-332.

Malizzi, L. D. and Gates, A. E., 1989, Late Paleozoic deformation in the Reservoir Fault zone and the Green Pond outlier, New Jersey highlands: in Field Trip Guidebook, Middletown, New York, Dennis Weiss ed., 61st annual meeting of the NYSGA, p. 75-92.

Maxey, L. R., 1976, Petrology and geochemistry of the Beemerville carbonatite-alkalic rock complex, New Jersey: Geol. Soc. Amer. Bull.: v. 87, p. 1551-1559.

Mitchell, J. P. and Forsythe, R. D., 1988, Late Paleozoic noncoaxial deformation in the Green Pond outlier, New Jersey Highlands, Geol. Soc. Amer. Bull.: v. 100, p. 45-59.

Mitronovas, W., 1982, Earthquake statistics in New York State: Earthquake Notes: v. 53, p. 5-22.

Nelson, S., 1980, Determination of Holocene fault movement along the Ramapo fault in southeastern New York using pollen stratigraphy: Geol. Soc. Amer. Abst. Prog.: v. 12, p. 75.

Olsen, P. E., 1980, Triassic and Jurassic formations of the Newark basin: in Field studies of New Jersey Geology and Guide to Field Trips, Warren Manspeizer, ed., 52nd annual meeting of NYSGA, p. 1-39.

Page, R. A., Molnar, P. H., and Oliver, J., 1968, Seismicity in the vicinity of the Ramapo fault, New Jersey-New York: Seismol. Soc. Amer., Bull.: v. 58, p. 681-687.

Passchier, C. W. and Simpson C., 1986, Porphyroclast systems as kinematic indicators: Jour. Struct. Geol.: v. 8, p. 831-843.

Pomeroy, P. W., Simson, D. W., and Sbar, M. L., 1976, Eathquakes triggered by surface quarrying- the Wappingers Falls, New York sequence of June, 1974: Bull. Seism. Soc. Am.: v. 66, p. 685-700.

Puffer, J. H., Volkert, R. A. and Hoszik, M. J., 1991, Probable late Proterozoic mafic dikes in the New Jersey highlands: Geol. Soc. Amer. Abst. Prog.: v. 23, p. 118.

Rankin, D. W., 1975, The continental margin of eastern North America in the southern Appalachians: The opening and closing of the Proto-Atlantic ocean: Amer. Jour. Sci.: v. 275-A, p. 298-336.

Ratcliffe, N. M., 1971, The Ramapo fault system in New York and adjacent northern New Jersey: A case of tectonic heredity: Geol. Soc. Amer.: v. 82, p. 125-142.

Ratcliffe, N. M., 1980, Brittle faults (Ramapo fault) and phyllonitic ductile shear zones in the Ramapo seismic zones New York and New Jersey, and their relationship to current seismicity: in Field studies of New Jersey Geology and Guide to Field Trips, Warren Manspeizer ed., 52nd Annual Meeting of NYSGA, p. 278-311.

Ratcliffe, N. M., 1981, Cortlandt-Beemerville magmatic belt: a probable late Taconian alkalic cross trend in the central Appalachians: Geology, v. 9, p. 329-335.

Ratcliffe, N. M., 1983, Possible Catoctin age diabase dikes in the Hudson highlands of New York and New Jersey: Geochemistry and tectonic significance: Geol. Soc. Amer. Abst. Prog.: v. 15, p. 172.

Ratcliffe, N. M., 1987, High TiO2 metadiabase dikes of the Hudson Highlands, New York and New Jersey: possible late Proterozoic rift rocks in the New York recess: Amer. Jour. Sci.: v. 287, p. 817-850.

Ratcliffe, N.M., Armstrong, R.L., Mose, D.G., Seneschel, R., Williams, N., and Baiamonte, M.J., 1982, Emplacement history and tectonic significance of the Cortlandt Complex, related plutons, and dike swarms in the Taconide zone of southeastern New York based on K-Ar and Rb-Sr investigations: Am. J. Sci. v. 282, p. 358-390.

Ratcliffe, N. M. and Burton, W. M., 1985, Fault reactivation models for the origin of the Newark basin and studies related to eastern U.S. seismicity: in G.R. Robinson Jr. and A. J. Froelich eds., Proceedings of the Second U.S. Geological Survey Workshop on the Early Mesozoic Basins of the Eastern United States, U.S. Geological Survey Circular 0946, p. 36-45.

Reches, Z., 1987, Determination of the tectonic stress tensor from slip along faults that obey the Coloumb yield condition: Tectonics: v. 6, p. 849-861.

Sanders, J. E., 1962, Strike-slip displacement on faults in Triassic rocks in New Jersey: Science v. 136, p. 40-42.

Sbar, M. L., Rynn, J. M. W., Gumper, F. J., and Lahr, J. C., 1970, An earthquake sequence and focal mechanism solution, Lake Hopatcong, northern New Jersey: Bull. Seism. Soc. Am.: v. 60, p. 1231-1243.

Sbar, M. L. and Sykes, L. R., 1977, Seismicity and lithospheric stress in New York and adjacent areas: Jour. Geo. Res.: v. 82, p. 5771-5786.

Schlische, R.W., 1992, Structural and stratigraphic development of the Newark extensional basin, eastern North America: Evidence for the growth of the basin and its bounding structures: Geol. Soc. Amer. Bull.: v. 104, p. 1246-1263.

Schlische, R. W. and Olsen, P. E., 1988, Structural evolution of the Newark basin: in J. Husch and M. Hozick eds., Geology of the Central Newark Basin, 5th annual meeting of GANJ, p. 43-65.

Sibson, R. H., 1977, Fault rocks and fault mechanisms: J. Geol. Soc. Lon.. v. 123, p. 191-213.

Sibson, R. H., 1983, Continental fault structure and the shallow earthquake source: Jour. Geol. Soc. London: v. 140, p. 741-767.

Simpson, C., 1984, Borrego Springs-Santa Rosa mylonite zone: A late Cretaceous west directed thrust in southern California: Geology: v. 12, p. 8-11.

Simpson, C., 1985, Deformation of granitic rocks across the brittle-ductile transition: Jour. Struct. Geol.: v. 7, p. 503-511.

Simpson, C. and Kalaghan, T., 1989, Late Precambrian crustal extension preserved in Fries fault zone mylonites, southern Appalachians: Geology: v. 17, p. 148-151.

Simpson, C. and Schmid, S. M., 1983, An evaluation of criteria to deduce the sense of movement in sheared rock: Geol. Soc. America Bull., 94, p. 1281-1288.

Smith, B. L., 1969, The Precambrian geology of the central and northeastern parts of the New Jersey Highlands: in Seymour Subitsky ed., Geology of selected areas in New Jersey and eastern Pennsylvania and guidebook of excursions: New Brunswick, New Jersey, Rutgers University Press, p. 35-47.

Smith, R.C.II, Rose, A.W. and Lanning, R.M., 1975, Geology and geochemistry of Triassic diabase in Pennsylvania: Geol. Soc. Amer. Bull.: v. 86, p. 943-955.

Stauffer, M. R.,1970, Deformation textures in tectonites: Can. Jour. Earth Sci.: v. 7: p. 498-511.

Stephens, G. C., Metsger, R. W. and Yang Q., 1988, Shear zone development in marble: Observations on the Zero fault at the Sterling Hill mine, Sussex County, New Jersey: Geol. Soc. Amer. Abst. Prog.: v. 20, p. 180.

Swanson, M. T., 1986, Preexisting fault control of Mesozoic basin formation in eastern North America: Geology: v. 14, p. 419-422.

Thompson, A. M., 1981, Tectonic significance of fracture distribution near the Fall Zone, central and northern New Jersey: Geol. Soc. Amer. Abst. Prog.: v. 13, p. 180.

Tillman, J. E., 1982, Major fault zones and related seismicity in western Connecticut and southeastern New York, Geol. Soc. Amer. Abst. Prog.: 14, p. 91.

Tullis, J. A. and Yund, R. A., 1977, Experimental deformation of dry Westerly granite: Jour. Geophy. Res.: v. 82, p. 5705-5718.

Turner, F. J. and Verhoogen, J., 1960, Igneous and Metamorphic Petrology; 2nd edition, New York, McGraw-Hill Book Co., 694 p.

Wehr, F. and Glover, L. III, 1985, Stratigraphy and tectonics of the Virginia-North Carolina Blue Ridge: Evolution of a late Proterozoic-early Paleozoic hinge zone: Geol. Soc. Amer. Bull.: v. 96, p. 285-295.

White, S. H., Burrows, S. E., Carreras, J., Shaw, N. D. and Humphreys, F. J., 1980, On mylonites in ductile shear zones: Jour. Struct. Geol.: v. 2, p. 175-187.

White, S. H. and Knipe, R. J., 1978, Transformation- and reaction-enhanced ductility in rocks, Jour. Geol. Soc. London: v. 135, p. 513-516.

Wilson, J. T., 1966, Did the Atlantic close and then re-open?: Nature: v. 211, p. 676-681.

Yang, J. P. and Aggarwal, Y. P., 1981, Seismotectonics of northeastern United States and adjacent Canada: Jour. Geophys. Res.: v. 86, p. 4981-4998.

Zoback, M. D., Anderson, R. N., and Moos, D., 1985, In-situ stress measurements in a 1 Km-deep well near the Ramapo Fault Zone: EOS: v. 66, p. 363.

THE MORRIS CANAL: A SERVICE TO THE IRON MINING INDUSTRY
OF NEW JERSEY

Ralph E. Costa, Woodward-Clyde Consultants, Wayne, NJ 07470

INTRODUCTION

Throughout history, canals and the iron industry have existed independently of each other. In New Jersey, the colonial iron industry preceeded the construction of the Morris Canal. The function of the canal was to service the Pennyslvania anthracite and New Jersey iron mining industries. The complimentary relationship of canals and mining in New Jersey was a necessary and integral part of the economic development and success of the State. The two co-existed for about 100 years, although their relationship was suprisingly antagonistic at times. Finally, the development of more economic transportation led to the abandonment of the Morris Canal. The iron industry of New Jersey would continue, without the canal, until it too was gradually replaced by more cost effective out-of-state deposits such as the Lake Superior ore bodies.

In Colonial America, William Penn and others gave thought to constructing a canal across northern New Jersey. George Washington and Thomas Jefferson both supported the development of inland waterways in order to draw the newly formed nation together. By the 1800's, the immediate financial success of New York's Erie Canal, conceived by Governor DeWitt Clinton and completed in 1825, created interests by many states to develop canal systems. Even before the visions and implementations of successful canals, the domestic iron industry had begun.

The colonial iron industry of the United States can be traced to Virginia, where bog iron was being refined as early as 1620 (Neu, 1979). With the arrival of the eighteenth century, significant iron concentrations had begun to be exploited in Virginia, Maryland, eastern Pennsylvania, southeastern New York and adjacent northeastern New Jersey.

Iron ore was known in the Hudson and New Jersey Highlands as early as the 1640's and by 1674 the Andover forge at present day Waterloo, New Jersey was producing iron. However, it was not until approximately 1720 that iron mining and manufacturing had begun to respond to a growing domestic and foreign demand and became an important part of the economy of these areas.

The delay in the beginning of northern New Jersey's iron boom is not certain. It may have been due to the self-serving interests of the politically powerful New York iron importers as they failed to provide government encouragement to develop the iron industry. It is also possible that there was no entrepreneur who possessed sufficient knowledge of the iron industry and capable management skills necessary for the successfull operation of an iron works (Neu, 1979).

Nonetheless, by the beginning of the Revolutionary War, New Jersey iron operations were very active. The War stimulated the iron industry with a demand for iron products and simultaneously burdened the industry with its demand for manpower. Iron workers were sometimes pardoned from military service in order to make iron contributions to the Continental Army. However, the post-Revolutionary War period brought a drop in the demand for iron and a slow time in the New Jersey iron industry.

New Jersey possessed, in abundance, the necessary resources for a successful iron industry: water, wood, limestone flux and iron ore. The water was needed to power the bellows of the furnaces and forges, and the trees were required for the manufacture of charcoal which fueled the blast furnaces. Up to a thousand acres of forest per year was necessary for the operation of each forge. Due to this great demand for fuel, the forests surrounding these established forges were depleted faster than they were naturally replenished. The Union Furnace in the Musconetcong Valley was abandoned after fifteen years of operation and the depletion of 30,000 acres of forest (Neu, 1979). In 1823, 39 of Morris County's 93 iron forges were shut down for lack of fuel (Kalata, 1983).

In 1791, anthracite coal had been discovered in the hills near Mauch Chunk, Pennsylvania. Josiah White, who organized the Lehigh Coal and Navigation Company in 1819, had proven anthracite useful as a fuel (Kalata, 1983). With the depletion of wood for making charcoal, the New Jersey iron industry began to look towards the anthracite coal fields of Pennsylvania in order to fill its needs for fuel. By mid-June 1820, anthracite derived from the Lehigh coal basin at Mauch Chunk was being shipped 110 miles to Philadelphia via the Lehigh and Delaware Rivers. The Lehigh Canal, completed in 1829 under the direction of Josiah White, made the shipment of coal from northeast Pennsylvania to industry in Philadelphia and Trenton more practical.

Transportation of the coal or iron ore was not so easy in New Jersey. Shipment down the Delaware, around Cape May and up the shore of New Jersey was too expensive. The natural inland waters of New Jersey were not navigable. Shipment by horseback, mule, oxcart and wagons all suffered from the inability to transport practical quantities. The system of roads in New Jersey was less than adequate. An additional burden to New Jersey's trade market was that until 1834, import and export through New York Harbor was subject to exorbitant tariffs imposed by New York. Therefore, the convenient use of Newark as a port was replaced by ports at Perth Amboy and Elizabeth.

THE BEGINNING OF THE MORRIS CANAL

Geographically handicapped, New Jersey stood in the economic shadows of Philadelphia and New York. A general economic slump followed the War of 1812. The domestic iron industry had been shut down due to foreign competition.

Domestically, fuel was scarce and expensive, and transportation costly and difficult. The construction of a canal across northern New Jersey was driven by necessity. With the construction of such a canal, Pennsylvania coal could easily be transported eastward and New Jersey iron ore westward. Raw materials, farm products such as produce, hay and manure, and manufactured goods such as beer, lumber and bricks could be floated in both directions.

By 1822, the Morris Canal project had been conceived by a Morristown businessman George Perot Macculloch. Macculloch had been president of the Morris County Agricultural Society and recognized that efficient distribution of farm products was impeded by New Jersey's lack of suitable transportation. In Morristown, he arranged a meeting on August 8, 1822. Interested citizens and distinguished men were invited. Then Governor of New Jersey, Issac Williamson, and Mahlon Dickerson, who served two terms as governor of New Jersey and owned profitable iron workings at Succasunna, were in attendance. As a result of this meeting the New Jersey Legislature passed an act on November 15, 1822 which appointed three men, including George Macculloch, as commissioners to conduct a feasibility study of the proposed canal. They were to employ the technical aid necessary in order to prepare plans for a selected route and cost estimates for its construction. The State had approved $2,000 for the preliminary study.

James Renwick, consulting engineer from Columbia University, conducted the initial surveys. Topographic information was gathered during the spring and summer of 1823. Renwick worked without the aid of a geologic map of New Jersey. The first geologic map of New Jersey was published by Henry D. Rogers in January, 1839 (Widmer, 1969). In addition to the Renwick surveys, Macculloch also depended on "plain good sense and local information of our farmers" to assist in the selection of viable canal routes. Macculloch originally estimated the summit level at Lake Hopatcong was 185 feet above tidewater at Newark and 115 feet above the Delaware River. Renwick's early and final surveys indicated Macculloch had grossly underestimated. The actual summit elevation was 914 feet above tidewater at Jersey City and 760 feet above low water at the Delaware River (Lee, 1979) (Fig. 1). The location of the chosen route of the Morris Canal with respect to generalized bedrock geology is shown in Figure 2.

As part of the plan to sell the canal project on its ability to service the iron industry of New Jersey, Renwick's Morris Canal route map of 1823 highlighted the locations of iron mines, forges and furnaces with respect to the proposed canal route. It had already been established that the magnetite and hematite Highland iron ores were superior in quality to southern New Jersey's limonitic bog iron ore (Bayley, 1910; Puffer, 1980). Until the 1820's, northern New Jersey had been dependent on imported English, Swedish and Russian ores received at New York. It was felt that the development of mines along the route of the proposed canal
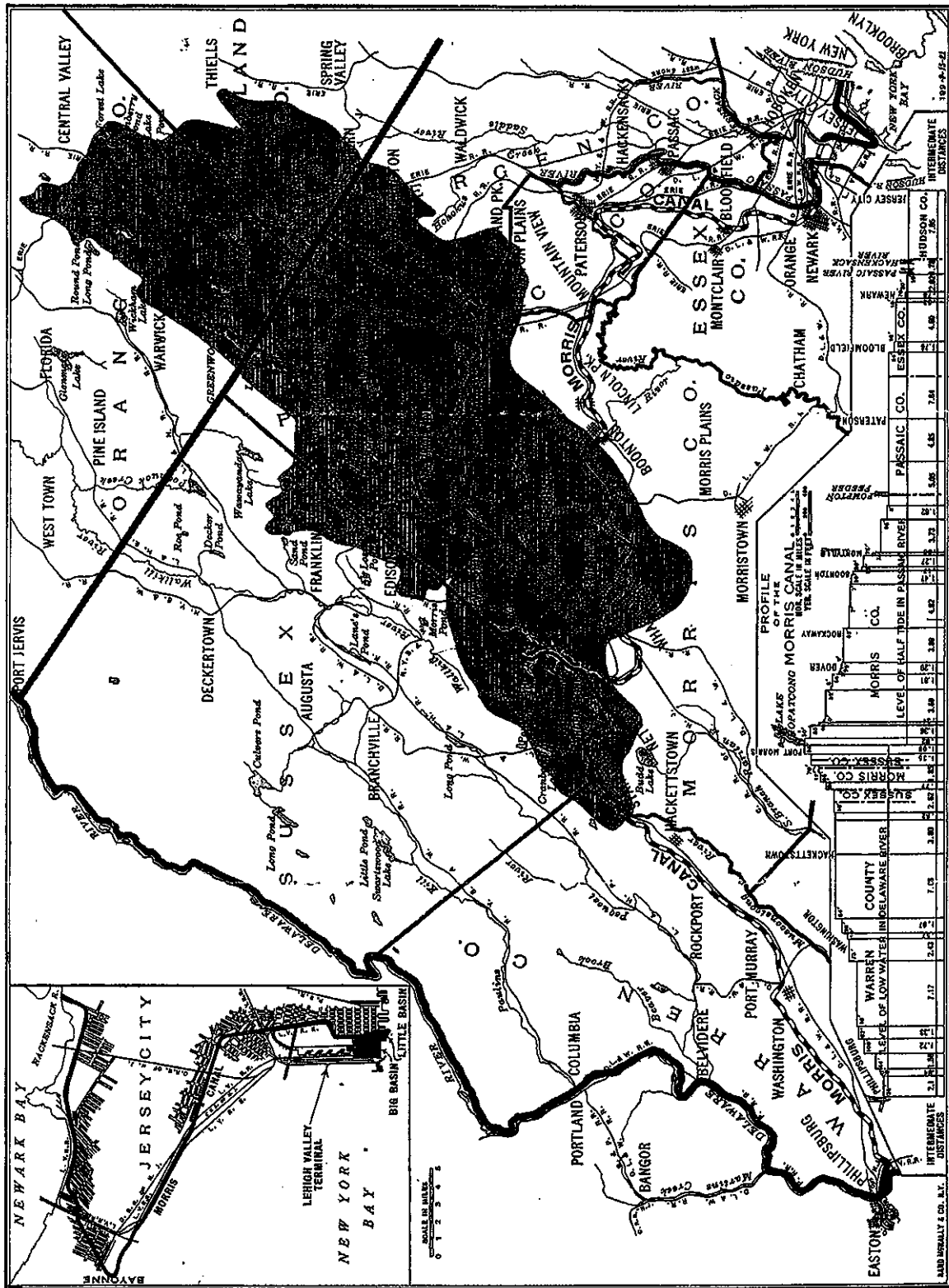
Figure 1: Route and profile of the Morris Canal by the Lehigh Valley Company, 1921. (From Lee, 1979).

PA

NY

DELAWARE RIVER

HUDSON RIVER

$74°$

$41°$

N

③

⑤

⑥

④

②

①

⑧

⑦

① Phillipsburg

② Hackettstown

③ Lake Hopatcong

④ Dover

⑤ Boonton

⑥ Paterson

⑦ Newark

⑧ Jersey City

MESOZOIC

PALEOZOIC

PROTEROZOIC

Morris Canal (approximate)

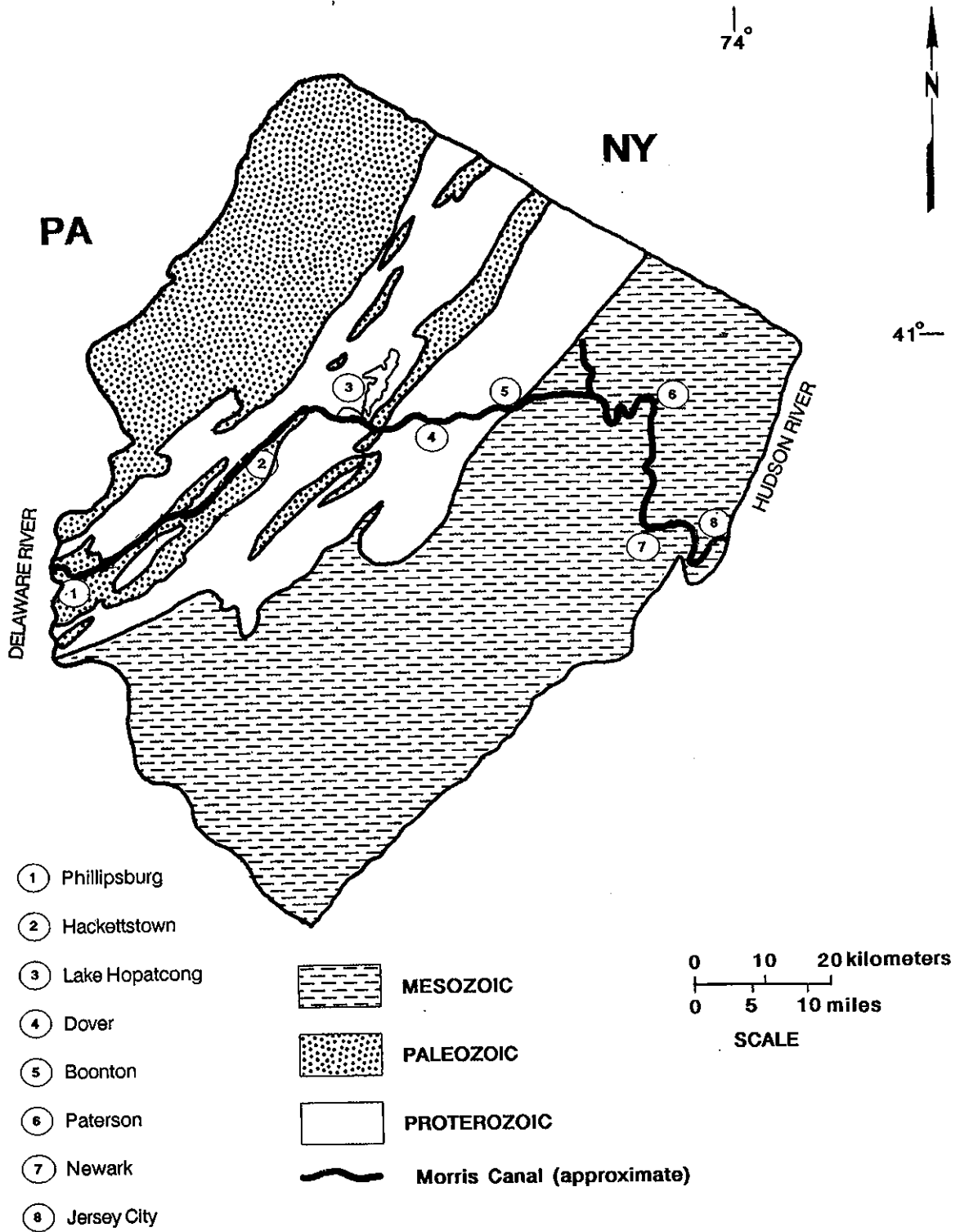0   10   20 kilometers

0   5   10 miles

SCALE

Figure 2:   Approximate location of the Morris Canal
(including Pompton Feeder) with respect to the
Proterozoic Highlands, the Mesozoic Lowlands
(Newark Basin) and the Paleozoic Valley and Ridge
Provinces.

200

could drop the price of iron ore from $90/ton to $55/ton. In addition, a list of minerals was prepared that same year as an Addendum to the Commissioners report in order to boast of the extensive mineral wealth awaiting prospecting.

On December 31, 1824, the New Jersey legislature chartered the Morris Canal and Banking Company "to form an artificial navigation between the Passaic and Delaware Rivers." The Morris Canal project was without the State support that New York's Erie Canal enjoyed. New Jersey had voted against public funding. As a result twenty thousand shares of stock were made available to private investors at $100/share. This provided $2,000,000 start up capital for the Morris Canal and Banking Company. The final cost of the canal and improvements was over $5,000,000.

The right to condemn lands and waters required for the Morris Canal was conferred. The State of New Jersey retained the right to take over the Morris Canal at the end of 99 years at fair valuation. If the State chose not to exercise the option, the charter would remain for 50 additional years. At the end of this time the State would take possession of the canal at no cost.

After a serious corporate financial scandal under Morris Canal and Banking Company President William Bayard Sr., Cadwallader D. Colden was named as the second president of the Morris Canal and Banking Company. Colden, who served as Mayor of New York City from 1818 to 1820, was a supporter of the Erie Canal and the ideas of Robert Fulton. For seven years, until his death in 1834, Colden served as president and successfully oversaw the construction of the early years of the Morris Canal.

George Macculloch maintained regular correspondence with Dewitt Clinton between 1823 and 1826 as the Morris Canal project was getting started. Macculloch sought the technical assistance and public relations expertise that Clinton employed to turn "Dewitt's Ditch" (i.e. the Erie Canal) into an economic success. Ephraim Beach was appointed the chief engineer for the Morris Canal. Having demonstrated his capabilities on the Erie and Schuykill canals, Beach had come to Macculloch's attention through the recommendations of Dewitt Clinton. Beach would work in concert with consulting engineer, James Renwick. Together, with the use of ingenious engineering, they were able to design and build a 90.4 mile canal between the Delaware River at Phillipsburg and the Passaic River at Newark.

Construction of the canal prism began on July 12, 1825 near the town of Ledgewood. With the use of picks, shovels, wheelbarrows and horse and wagons, the original canal was hand-dug by predominantly Irish labor. By 1826, approximately 1,100 men worked on the canal. By 1828, only 14 miles of canal between Phillipsburg and Newark remained to be excavated. The construction of the locks and inclined planes would follow. In 1827 construction of the new dam at Lake Hopatcong began above an old forge dam originally constructed in 1750. This new dam would raise the lake level 5 feet.

Beginning in 1829, small sections were open for local use. On November 4, 1831 the first trip from Newark to Phillipsburg was completed. The spring of 1832 marked the beginning of the first full season the Morris Canal was opened for navigation between Phillipsburg and Newark. By 1836, the eastern terminus of the Morris Canal had been extended 11.75 miles to Jersey City, bringing the total length of navigable waters to 102.15 miles. The 4.26 mile long Pompton Feeder which joins the main canal in Mountain View was completed in 1837. By 1845, with the additional service to the Pompton Iron Works (1.76 miles), and the completion of the Lake Hopatcong Feeder (0.67 miles), and the Big and Little Basins (Fig. 1) at Jersey City (0.42 miles), the Morris Canal system consisted of 109.26 miles of navigable water.

The Morris Canal required the use of a unique combination of 23 traditional lift locks, 11 guard locks (where the canal crossed a lake or river) and 23 inclined planes used to overcome the total change in vertical elevation of 1,674 feet (Lee, 1979). In addition, the Morris Canal also employed aqueducts in order to carry canal boats over natural rivers. At Little Falls, a 45 foot high stone arch aqueduct with an 80 foot span carried the Morris Canal over the Passaic River. Between Mountain View and Lincoln Park, the Pompton River crossing required a 236 foot long aqueduct. These accomplishments rendered Macculloch's Morris Canal project an engineering milestone.

INCLINED PLANES OF THE MORRIS CANAL

The most important engineering application used on the Morris Canal was the inclined plane. Because traditional locks are only useful for small changes in elevations (i.e. <12 ft), it was impractical to rely exclusively on them to overcome the steep gradient proposed by the Morris Canal. The use of one inclined plane could replace many traditional lift locks. In addition, it could raise and lower canal boats in a more timely fashion. In 1828, it was estimated an 80-foot ascent by inclined plane would require 14 minutes. The same ascent by use of traditional locks would require approximately 150 minutes (Vermeule, 1929). James Renwick adapted Robert Fulton's 1794 design of inclined planes used on canals in England to accommodate the Morris Canal. In November 1830, the inclined planes at Dover were successfully tested with five canal boats loaded with iron ore.

The inclined plane was actually a 500 to 1500 ft inclined railway. A wooden cradle (or plane car) open at both ends rode on iron rails. At the bottom of the inclined plane, the cradle was partially submerged in the lower canal prism. The canal boat was then floated onto the cradle and secured to it. Water from the upper canal prism, working under a head of approximately 50 ft, was used to power a turbine. The turbine drove a large drum around which a cable was wound. The cable was attached to the cradle. When the drum was engaged, the cable was reeled; and the canal boat and cradle were hauled up and over the summit of the plane and dropped into the upper

level of the canal. The canal boat was then unfastened and floated out the open end of the plane car into the next level section of canal. The summit of the plane was the brow of the embankment which prevented the water of the upper level from draining down the plane.

The original inclined planes were powered by overshot waterwheels. Between 1847 and 1860, these were ultimately replaced with a more powerful Scotch turbine design. The use of the inclined planes proved so successful that in the late 1800's only slight modifications were made by the Japanese for use on the Biwa Canal. In 1928, the planes were again studied for use in a Brazilian canal.

ENLARGEMENT OF THE MORRIS CANAL

Even before the completion of the Morris Canal, the Canal Company was often mismanaged and as a result plagued with financial difficulties. However, real estate values along the canal boomed. Forges and manufacturers began to enjoy a wider market. There were plenty of indicators that the Morris Canal would be a successful business venture. However, engineering problems, unforeseen before or during the construction of the original canal, began to handicap the Morris Canal service to the iron and coal industries.

The original dimensions of the Morris Canal prism were 32 ft wide at the surface, 20 ft wide at the bottom and 4 ft deep. Original locks were 9 ft wide and 75 ft long. This was sufficient to accomadate the original "flicker" boats with a typical 18 ton cargo. However, the Lehigh Canal boats which carried anthracite from the Pennsylvania coal fields were too large to pass through the locks of the Morris Canal. Cost and competition for the shipment of coal with the Delaware and Raritan Canal (completed in 1833) and the inability of the Morris Canal to accept the larger boats of the Lehigh Canal forced the enlargement of the Morris Canal, its locks and inclined planes. During the enlargement construction, emphasis was on the Western Division in order to accommodate coal interests.

Between 1840 and 1841 locks were enlarged to approximately 11 feet wide and 95 feet long. In 1844, widening of the canal prism commenced. Ultimately, the canal prism would be enlarged to 40 ft wide at the surface, 25 ft wide at the bottom and 5 ft deep. Throughout the 1830s and 1840s the Morris Canal boats were typically 60 to 65 ft in length, 8 1/2 ft in width and hauled an average of 25 to 30 tons. Improved hinged section boats, which were approximately 87.5 ft in length, and 10 ft 5 inches in width and hauled a cargo with an average weight of 65 to 75 tons were purchased by the Morris Canal and Banking Company.

The lift of the original water wheel powered inclined planes was limited to under a 50 ton cargo. A new section boat loaded to capacity could not be hauled by the inclined

planes and improvements were required. By the winter of 1847-1848 the first inclined plane improvement (i.e. upgrade to Scotch turbines) at Port Colden was completed. By 1860 all inclined planes were completed and the gross cargo capacity increased.

WATER SUPPLY FOR THE MORRIS CANAL

Requirements for water were large. The location of the Morris Canal with respect to important bodies of water is shown in Figure 3. In addition to Lake Hopatcong, supply reservoirs for the canal included Greenwood Lake, Bear Pond and Cranberry Lake. The Pompton feeder drew its water from a pond above the feeder dam which received water of the Ramapo, Wanaque and Pequannock Rivers. In addition, water was available from the Musconetcong River above Saxton Falls, the headwaters of the Raritan River at Ledgewood, and the headwaters of the Rockaway River above Boonton. A pumping station at Jersey City on the Hackensack River supplied an 8-mile portion of the canal which passed through Jersey City. The Morris Canal between the Passaic and Hackensack Rivers was subject to tidal influence. Most of the water required used on the canal was to replace that lost to leakage and lockage. An average water leakage rate per mile of the Morris Canal was calculated to be 1.74 cu ft/sec (Vermeule, 1894). Between the Delaware River and Saxton Falls (30.6 miles), 18.44 cu ft/sec water was lost due to leakage and an additional 7.96 cu ft/sec lost to lockage. From Lake Hopatcong to the Pompton Feeder (approximately 28.5 miles) combined water loss to leakage and lockage was 57.2 cu ft/sec. A water leakage rate of 48.3 cu ft/sec was calculated from the head of the Pompton Feeder to Newark (27.2 miles).

THE IRON INDUSTRY

Just as the early promoters of the Morris Canal and Banking Company had intended, the Morris Canal successfully serviced and revitalized the iron mining industry of New Jersey, the anthracite industry of the Lehigh Valley and also the local trade along the route. Upon its completion, ore could be shipped to furnaces at Phillipsburg and Waterloo (Old Andover Furnace) where it could be smelted with Pennsylvanian anthracite. Canal ports such as Dickerson's basin and the Dell and Swede Mine landings were constructed to service the mines of the Wharton and Dover area. In this area, approximately 15 magnetite mines were located within one mile of the Morris Canal. The trace of the Orchard Mine was bounded by the Morris Canal on the south, and the Rockaway River on the north. Nearby, the compass trace of the Erb mine deposit passed through the paths of the Morris Canal and the Rockaway River (Figure 4).

Between Dover and Rockaway an ore landing was constructed to service Swede's Mine. On the north side of the Morris Canal, Swede's magnetite mine lied in the gneisses of Rockaway Township approximately 1 mile east of the Dover. This mine
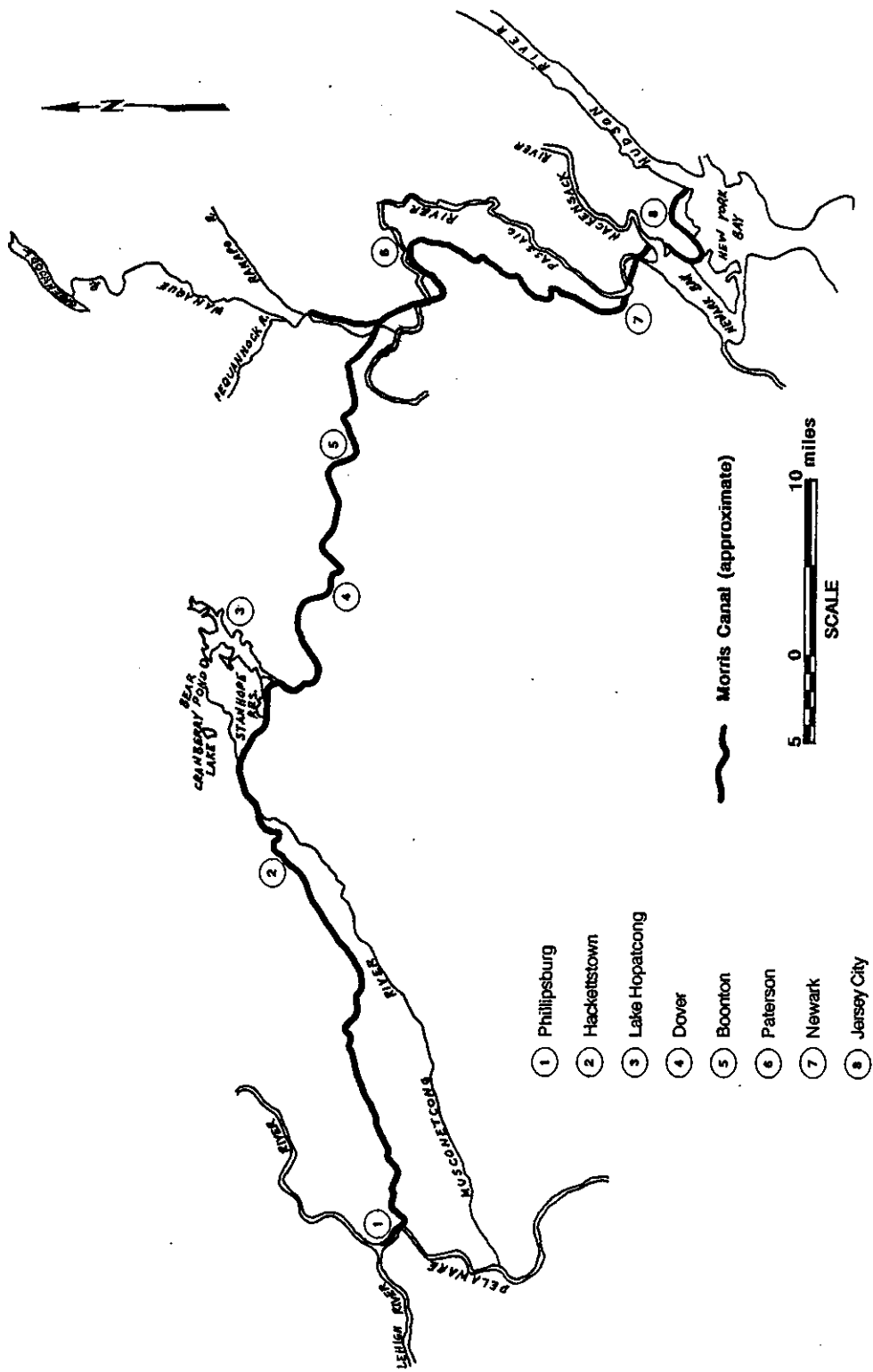
Figure 3: The Morris Canal and its location relative to major bodies of water. (After Vermuele, 1929).

205

Figure 4:   The Morris Canal and magnetite mines in the
            Wharton/Dover area, 1868.   (After, Bayley, 1910).

was worked continuously between 1855 and 1875, straddling the most prosperous years of the Morris Canal.

Within approximately 1 1/2 miles of each other, in present day Roxbury township, ore landings serviced the Dell (or Scrub Oak) Mine and the Dickerson Mine. Both of these mines were very productive and for the 1879-1880 year produced 1,680 tons and 28,900 tons of ore, respectively. The Dell Mine was worked on and off between the 1860s and 1905. Ore still remains at the Dell mine, however, its extraction is cost-prohibitive at today's standards (Baum, 1973).

An ore landing was erected at Waterloo, approximately 34 miles from the Delaware River. Ore from nearby workings could be floated by Morris Canal to service Cooper's Furnace, approximately 1.4 miles from the port on the Delaware.

Unlike the thoughts of a perfectly mutual benefiting relationship of the iron industry and the shipping industry of the Morris Canal, the relationship was at times antagonistic and negotiations were often very lengthy. It was not uncommon to have key players in the iron industry serve on the board of directors for the Morris Canal. Decisions of which sections of canal would be constructed, modified or enlarged were commonly influenced by the potential of personal benefits gained by the ability to service the anthracite smelters of Pennsylvania with iron ore. Their self-serving interests often took precedence over what would be best for the Morris Canal and Banking Company's interests.

Although four potential routes had been proposed during the early Morris Canal surveys (Kalata, 1983) the route which was ultimately chosen seems largely based on the ability of the canal to service the iron industry. During the original construction of the canal emphasis was placed on the Eastern Division in order to accommodate the Highland iron interests. Iron towns along the canal, like Boonton, were able to boom. The New Jersey Iron Company wisely purchased 200 acres of land along the Morris Canal and Rockaway Rivers. By 1831, an iron works was erected on some of this land. Two years later blast furnace was added and by 1848 a prosperous nail factory was opened.

The first inclined plane which was constructed and tested at Rockaway. The choice of this location was undoubtedly a result of the large voice of the iron industry present in the Morris Canal and Banking Company. A 4-mile long level of the canal was constructed between Dover and Rockaway. At the Dover end of the level was Blackwell and McFarlan, importers and manufacturers of iron. The chains being used on the plane were manufactured by McFarlan and floated down the level to Rockaway. At the Rockaway end of the level was a rolling mill and forge. Henry McFarlan also served as the director of the Morris Canal and Banking Company.

Peter M. Ryerson, son of ironmaster Martin Ryerson who had successfully owned and operated the Ringwood, Pompton and Long Pond Iron Works, was instrumental in the construction of the Morris Canal's Pompton feeder which would allow canal boats to dock at the iron works. Peter Ryerson, upon the

death of his father in 1839, took over the Ryerson Iron Works. The works would steadily decline and eventually be lost in the 1840's. Peter, apparently without the ironmaster ability of his father, did ironically become a large stockholder and a director of the Morris Canal Company, acting for several years as the superintendent.

Peter Cooper and Abram S. Hewitt owned or leased iron mines in Passaic, Morris, Sussex and Warren Counties and were important canal customers. Cooper and Hewitt recognized the increased efficiency of shipping the Morris Canal afforded the iron industry. In 1847, they reopened the Andover Mine, extracting primarily hematite, and to a lesser extent, magnetite. They were dependent on this ore being shipped via the Sussex Mine Railroad, built in 1848 by Cooper and Hewitt, to the ore landing on the Morris Canal at Waterloo. Ultimately, this ore was used to supply their Trenton Iron Works, established in 1845. By 1863, the ore at the Andover Mine was exhausted.

Negotiating for Cooper over the purchase of the Ringwood Iron Works, Hewitt, secretary and business manager of the Trenton Iron Company (formed 1844), was pleased with the quantity and quality of the ore; however, he questioned the economic efficiency of available transportation methods. In addition, the existing furnaces at Ringwood and Long Pond were essentially in ruin. Hewitt had hoped to build a railroad from the iron workings to the Pompton Feeder of the Morris Canal. Potentially 25,000 to 50,000 tons of ore per year could then be floated to the Trenton Iron Company furnaces which had been erected between 1847 and 1848 at Phillipsburg. In a July 19, 1853 letter to Ephraim Marsh, then President of the Morris Canal Company, Hewitt requested that the Pompton feeder be made and maintained as to be navigable for the same class of boats as the rest of the Morris Canal. He also asked for a toll rate for ore which would be shipped down the feeder. After three unsuccessful years of negotiations, Hewitt never got a favorable rate from the Morris Canal Company. Still burdened with transportation problems, he then turned to the Erie Railroad with proposals for a new railroad.

By 1861, without progress on the efficiency of transportation, cessation of the Ringwood operations seemed inevitable. During the enlargement of the canal, the Cooper-Hewitt retained the Morris Canal as one of its customers. Old inclined plane rail iron was sent to the Cooper furnace by canal boat and sold for scrap or reformed into rails for the new inclined planes. Only the demand for iron created by the beginning of the Civil War saved the works. In 1864, Hewitt wrote to the Morris Canal Company offering the business of the Ringwood and Sterling Works as well as the Philadelphia Company for reduced toll rates on the Morris Canal. They were unable to reach an agreement because of strong competition between the Morris Canal and the Morris and Essex Railroad (chartered 1835).

THE DECLINE OF THE MORRIS CANAL

The Morris Canal only enjoyed financial success between 1860 and 1870, with its peak year 1866. The iron industry, which the Morris Canal helped revive, was continuing to thrive on the needs of the developing New Jersey railroad industry. The Morris Canal was contributing to its own destruction as it hauled iron ore and scrap which would ultimately be used to supply its own competition. The railroads would eventually replace the Morris Canal.

Toward the end of 1863, increased labor expenses, decreased tonnage being shipped because of the on-going development of the railroads and the unpredictable and dynamic nature of the coal industry forced the Morris Canal to cater to the iron industry. Concessions were finally made to the iron industry. Specifically, at the request of Cooper-Hewitt, the lift lock at the head of the Pompton Feeder was enlarged to accommodate the larger boats of the main canal. The canal also strived to maintain a full canal prism to allow the maximum tonnage to be shipped. Dredging machinery was purchased in an attempt to offset the spring season labor costs associated with dredging by hand. These actions helped to maintain the iron industry as an ally of the canal rather than the Erie Railroad.

In 1865, the Ogden Mine Railroad Company built a 10 mile long railroad from the Ogden Mines in Jefferson Township to ore docks at Nolan's Point on the east shore of Lake Hopatcong. The ore was then transferred to canal boats and towed approximately 2.6 miles by steamer to the Brooklyn Lock where they entered the Lake Hopatcong Feeder and then the main prism of the Morris Canal.

However, further outreaches of the railroad industry only served harm to the Morris Canal. In 1864, the Morris and Essex Railroad built a branch from Denville to Boonton to service the local iron works and nail factory business. Horse, and later steam railroads serviced the Mount Hope and Hibernia iron mines to landings on the Morris Canal. In 1866, the Morris and Essex Railroad began carrying coal. This railroad was leased in 1868 to the Delaware, Lackawanna and Western Railroad Company. The railroad could carry 70 tons of coal in only three cars and make the trip across New Jersey in 8 hours rather than the 5 days needed for a sectioned canal boat to make the passage. In addition, the railroad could operate throughout the year whereas the navigation season on the canal was limited by the cold weather to approximately seven months. The Morris Canal and Banking Company, conscious of the encroaching railroad competition, attempted to reduce its tolls, however, financial trouble followed.

In response to the Morris Canal being too slow to compete with the railroads, mechanical means of propelling canal boats were attempted. Gasoline and steam powered boats and electrical devices which pulled the boats were designed and experimented with. These methods proved to be useless because the canal banks would be washed out by the wake of a canal boat drawn faster than approximately 3 miles/hour.

The railroads continued to prosper and by 1870 the Morris
Canal had the last of its ten consecutive prosperous years.
By this same year the Sussex Railroad had reached Franklin
Furnace replacing the old method of zinc and iron ore shipment
by wagon from the Sterling Hill and Mine Hill mines to
Woodport, on the northern shores of Lake Hopatcong, where it
could then be transferred to canal boats and hauled by Morris
Canal. In 1871, the Morris Canal was leased by the Lehigh
Valley Railroad for 99 years. The Eastern and Amboy Railroad
was constructed in 1875. This railroad provided a direct
connection between the Pennsylvania anthracite mines and
tidewater. In 1881 the Central Railroad of New Jersey took
over the Ogden Mine Railroad and connected it to its High
Bridge Branch. This branch was extended to Port Oram and
Rockaway. All of these railroad improvements resulted in a
major coal, iron and local freight tonnage loss for the Morris
Canal.

A Legislative Commission was appointed to study the
possible abandonment of the canal. However, in 1903 and again
in 1911, complicated issues which included water, land and
reversion rights brought the abandonment process to all but a
stop. In 1914 the Morris Canal Parkway Association proposed
the abandoned canal and towpath be converted to a continuous
"water parkway" for recreational purposes such as canoeing,
fishing, swimming, picnicking, bicycle and horseback riding,
and skating. This idea was knocked down and on November 29,
1922, and the Morris Canal was transferred to the State of New
Jersey.

The formal abandonment of the Morris Canal began with New
Jersey State legislature, known as the "Morris Canal
Abandonment Acts", passed on March 12, 1924. On April 7,
1924, Cornelius C. Vermeule was appointed as the State
Consulting and Directing Engineer in charge of surveys, plans
and estimates for the abandonment of the Morris Canal. After
his resignation on April 15, 1928, he was replaced by his son.

The abandonment would include demolition and
reconstruction of some existing structures, draining of
selected sections and refilling and regrading portions of the
canal bed in order to "put [the canal] in a condition safe to
life and limb"and "make proper provision to prevent future
obstruction of highways, roads or water courses through the
decay and fall of culverts, aqueducts or other structures, and
to provide the proper drainage of the canal" (Vermeule, 1929).
The abandonment modifications to the Morris Canal were
completed in June of 1929. Unfortunately, there was no clause
for preserving the canal for the sake of history. Therefore,
only small, disjunct portions of the Morris Canal can be
recognized today.

REFERENCES
Baum, J.L., 1973, Three Hundred Years of Mining in Sussex
        County, New Jersey, 14 pp.
Bayley, W.S., 1910, Iron Mines and Mining in New Jersey,
        Geological Survey of New Jersey, 512 pp.
Kalata, B.N., 1983, A Hundred Years, A Hundred Miles, New
        Jersey's Morris Canal, Compton Press Inc., 711 pp.
Lee, J., 1979, The Morris Canal: A Photographic History,
        Delaware Press, 136pp.
Neu, I.D., 1979, Hudson valley extractive industries before
        1815, *in* J.R. Frese and J. Judd eds., Business
        Enterprise in Early New York, Sleepy Hollow Press, pp.
        133-165.
Puffer, J.H., 1980, Iron ore deposits of the New Jersey
        Highlands, *in* Manspeizer ed., Field Studies of New
        Jersey Geology and Guide to Field Trips, 52 Annual
        Meeting of the New York State Geological Association, p.
        202-208.
Ransom, J.M., 1966, Vanishing Ironworks of the Ramapos,
        Rutgers University Press, 382 pp.
Shuster, E.D., 1927, Historical Notes of the Iron and Zinc
        Mining Industry in Sussex County, New Jersey, 48 pp.
Simon, R.C., 1992, The Morris Canal: New Jersey's Mountain-
        Climbing Waterway, Macculloch Hall Historical Museum, 60
        pp.
Vermeule, C.C., 1894, Final Report of the State Geologist,
        Volume III, Water Supply, Geological Survey of New
        Jersey, p. 190-196.
Vermeule, C.C Jr., 1929, Morris Canal and Banking Company
        Final Report of Consulting and Directing Engineer, June
        29, 1929, 80 pp.
Widmer, K., 1969, Topographic and geologic mapping in New
        Jersey, *in* Subitsky ed., Geology of Selected Areas in
        New Jersey and Eastern Pennsylvania, Rutgers University
        Press, p. 48-50.

PLATE 4

Plate 4: Photomicrographs and SEM backscatter image of textures and reactions in rocks from the Reservoir fault zone, New Jersey Highlands. A) Photomicrograph of mildly deformed granitic gneiss showing reaction from plagioclase (p) to fluoro-hastingsite (h) bearing assemblages. Scale bar = 2 mm. B) Photomicrograph of cataclasite with subangular xenoclasts and xenocrysts (x) of granitic gneiss within a matrix of fine-grained, randomly oriented actinolite, biotite, chlorite, albite, epidote, apatite, titanite, and pyrite. Scale bar = 1 cm. C) Photomicrograph of S-C mylonite composed primarily of hastingsite (h) and ferro-actinolite (a). C planes (C) are crossed by late C' planes (C'), both of which show consistent dextral (top of photo to the right) movement. Scale bar = 6 mm. D) SEM backscatter image of the edge of a shear plane. Early fluoro-hastingsite (f) is progressively fractured and microbrecciated and subsequently indurated (epitaxial overgrowths) with chloro-hastingsite (c) and finally ferro-actinolite (a) and actinolite. Scale bar = 50 um.

PLATE 5

Chapter 7 (Costa and Gates)
Ramapo Fault system, northern New Jersey.

Figure 2:   Photomicrograph of mafic dike which intruded the
            Proterozoic basement is subsequently sheared.
            This sheared dike contains chlorite (ch) "fish".
            Arrows indicate top to the north-northeast reverse
            shear.   Scale bar = 1.0 mm.

Figure 3:   Photomicrograph of southeast-dipping Taconic S-C
            mylonite contains δ-type porphyroclast of
            plagioclase feldspar.   Porphyroclast tails and
            edges of core are dynamically recrystallized.
            Porphyroclast rotation is counterclockwise.
            Arrows indicate top to the northwest reverse
            shear.   Scale bar = 0.5 mm.

Figure 4:   Photomicrograph of southeast-dipping Taconic S-C
            mylonite contains a hornblende porphyroclast with
            two generations of antithetic shears.   Chlorite
            and tremolite-actinolite are present on the edges
            of and in between some hornblende fragments.
            Large arrows indicate the sense for early (1) and
            parallel but oppositely directed late (2)
            movements.   The early Proterozoic Z fabric was the
            result of top to the southeast extension.   The
            late Taconic fabric was the result of top to the
            northwest reverse shear.   Small arrows indicate
            the direction of antithetic shearing of a
            hornblende porphyroclast for the early (1) and
            late (2) movements.   The early generation of
            antithetic shears are crosscut by the later
            antithetic shears and are often rotated and opened
            on one side to form a "V" shape as a result of the
            parallel but oppositely directed reactivation.
            Scale bar = 1.0 mm.

Figure 5:   Photograph of southeast-dipping Taconic
            ultramylonite.   Mylonite foliation is offset by
            conjugate strike-slip faults.   Arrows indicate the
            direction of offset.   Marker = 14 cm.

ACKNOWLEDGEMENT